



**Technische Universität München**

TUM School of Life Sciences

**Spatiotemporal GLP-1 and GIP Receptor Signaling and  
Trafficking/Recycling Dynamics Induced by Selected  
Receptor Mono- and Dual-agonists**

Aaron Novikoff

Vollständiger Abdruck der von TUM School of Life Sciences der Technischen  
Universität München zur Erlangung des akademischen Grades eines

**Doktors der Naturwissenschaften**

genehmigten Dissertation.

Vorsitz:

Prof. Dr. med. Dietmar Zehn

Prüfer\*innen der

1. Prof. Dr. Martin Klingenspor

Dissertation:

2. PD Dr. rer. nat. Timo Müller

Die Dissertation wurde am 03.01.2021 bei der Technischen Universität  
München eingereicht und durch die TUM School of Life Sciences am 24.05.2022  
angenommen.

---

## Acknowledgments

---

Looking out at the city of Munich as my flight was halfway through its descent 5 years ago, it was as if I could see the projection of everything I needed to achieve the dream I'd set out 9,601 km for. From the start of my Master's degree to the end of my Doctorate, it has been an absolutely surreal experience to have lived it. Therefore, I am humbled and proud to express my gratitude.

First, I'd like to express my appreciation, if that word can do it justice, to God that makes it all possible. We do not choose the choices from which we get to choose, so I want to thank Him for opening the doors.

My parents, Ivan and Mary Novikoff, your unconditional love, your understanding, and willingness to tell me I am being an idiot if I really am, has brought me from the depths to the surface. To both of you, and Allie, thank you.

I would like to express my upmost gratitude to Dr. Timo Müller. You gave me a real opportunity here in Munich to learn and develop, and provided the resources and connections that allowed true growth in the field of Molecular Pharmacology. The knowledge and professionalism I have learned from you along the way are too numerous to count, so I would like to express my appreciation as a genuine thank you.

To Prof. Dr. Matthias Tschöp, my highest appreciation for setting the underlying infrastructure to make this opportunity possible. To Prof. Dr. Martin Klingenspor and PD Dr. Anja Zeigerer, thank you for your valuable input, understanding, and guidance during the thesis committee meetings. To Prof. Dr. Davide Calebiro, your hospitality and expertise have set the foundations for how I approach science. Thank you, and to Dr. Shannon O'Brien, for hosting me at the University of Birmingham (U.K.) and for allowing me to work alongside you. To Prof. Dr. Hannelore Daniel, during my Master's degree, your input, passion, and the opportunities you provided, have shaped the way I see science, thank you.

I would like to thank all of my colleagues, at and through the IDO, for treating me at eye-level from the first day. To Dr. Maximillian Kleinert, Dr. Alexandra Hager, Dr. Gustav Collden, Dr. Qian Zhang, Dr. Gerald Grandl, Dr. Gandhari Maity, Dr. Stephan Sachs, Dr. Brian Finan, Dr. Sebastian Parlee, and Dr. Jon Douros, thank you all for your scientific input and friendship over the years. Additionally, I would like to thank Dr. Sigrid Jall and Dr. Katrin Fischer for passing down knowledge, you were a pleasure to work with. Most importantly, a very large thank you to Laura Sehrer, Luisa Müller, Emilija Malogajski, Xenia Leonhardt, and Cassie Hollerman. Besides single-handedly keeping the lab functional, and your day-to-day help resulting in an inconceivable amount of benefit, none of this would be possible without you. I also want to personally thank all of you for your patience and willingness to teach a former bioinformatic master student the ways of the *in vitro* and *in vivo* laboratory. To Callum Coupland and Seun Akindehin, thank you for your openness and unparalleled teamwork within developing projects, I can't wait to see where they go.

Lastly, but definitely not least, I would like to express my appreciation to all my new friends, my friends back home, and all the people that make life feel normal and good, thank you. Rest in peace, Ryan Tornell, #47.

## Table of Contents

Glossary .....	6
Figure Index .....	9
Table Index .....	17
Abstract .....	18
CHAPTER 1: Introduction.....	23
The Epidemic of Obesity and Type II diabetes .....	24
Insulin Resistance and Development of T2D .....	26
Regulation of Food Intake and Energy Expenditure .....	27
The GLP-1 and GIP Receptors: The Incretin System in Glucoregulation and Satiety.....	30
GIP and GLP-1 Secretion .....	30
Systemic GIP actions.....	32
Systemic GLP-1 actions.....	32
The Effect of Obesity and Diabetes on Incretin Action.....	33
Insulin and Glucagon Secretion.....	35
Basic Anatomy of the Pancreas .....	35
Processing and Maturation of Insulin.....	36
Insulin Secretion .....	36
Glucagon Secretion.....	38
G-protein Coupled Receptors .....	38
Background.....	38
GPCR: Class Categorization.....	39
GPCR: Ligand Binding and Receptor Activation.....	39
GPCR: G $\alpha$ Subunits and GPCR Signal Termination .....	40
Structure of the GLP-1R and GIPR.....	41
Commonalities.....	41
GLP-1R Structure .....	43
GIPR Structure .....	43
GPCR Signaling .....	44
Commonalities.....	44
The GLP-1R and GIPR: $\beta$ -cell Adenylate Cyclase .....	47
The GLP-1R and GIPR: PKA and EPAC2 in $\beta$ -cells .....	48
The GLP-1R and GIPR: PKA and EPAC2 in the CNS.....	49
The GLP-1R and GIPR: $\beta$ -arrestin Recruitment and Signaling.....	50
The GLP-1R and GIPR: G $\alpha_q$ Signaling .....	52
The GLP-1R and GIPR: G $\alpha_s$ Signal Amplification .....	53
GPCR Internalization .....	53
Background.....	53
Clathrin-mediated Endocytosis.....	54
$\beta$ -arrestin-dependent CME of GPCRs .....	57
Caveolin-dependent internalization of GPCRs .....	59
The Endolysosomal Network .....	61
Plasma Membrane Nanodomain “Hotspots” .....	61
Early Endosomes.....	61
Recycling Endosomes .....	62
Late Endosomes/Lysosomes.....	63

## Table of Contents

Endosomal $G\alpha_s$ Signaling .....	65
<b>Pharmacology .....</b>	<b>68</b>
Efficacy and Potency .....	68
Dose-Response Curve .....	68
Spare Receptor Effect .....	69
Signal Amplification .....	70
Principles of Bioluminescence Resonance Energy Transfer (BRET) .....	72
<b>GLP-1 and GIP Pharmacological Development .....</b>	<b>74</b>
Background and Historical Development of GLP-1 based Pharmacology .....	74
Optimization of GLP-1R Mono-agonists .....	75
Co-administration of GLP-1 Mono-agonists with Complementary Peptides .....	76
Development of Unimolecular Dual-Agonists .....	79
<b>CHAPTER 2: Methodology .....</b>	<b>84</b>
<b>Materials .....</b>	<b>85</b>
Peptide Ligands.....	85
Small Molecule Agonists and Inhibitors .....	85
Plasmid Constructs .....	85
<b>Methods .....</b>	<b>86</b>
Generation and Amplification of Plasmid Constructs.....	86
Cell Culture .....	87
Cell-based Temporal Assays .....	88
Gene Expression Analysis .....	92
<b>CHAPTER 3: Spatiotemporal GLP-1 and GIP Receptor Signaling and Trafficking/Recycling Dynamics Induced by Selected Receptor Mono- and Dual-Agonists.....</b>	<b>93</b>
Introduction .....	94
Implications of Signaling and Trafficking at the GLP-1R and GIPR.....	95
Biased Signaling.....	97
MAR709 and Tirzepatide (Dual-agonists) .....	98
Select Mono- and Dual-Agonists for Characterization.....	100
Objective .....	102
<b>Results.....</b>	<b>103</b>
MAR709 and Tirzepatide Differ from Mono-Agonists in Ligand-induced $G\alpha_s$ -subunit Recruitment to the GLP-1R and GIPR .....	103
Constitutive Activity at the GIPR is Not Responsible for Reduced Efficacy of GIP (1-42) Relative to GLP-1 (7-36 Amide) at the GLP-1R .....	106
MAR709 and Tirzepatide are Characterized as Partial $G\alpha_s$ Agonists with Full Efficacy within the cAMP Pathway at the GLP-1R .....	109
The Full cAMP Agonism Profile of MAR709 and Tirzepatide at the GLP-1R is Preserved Through Downstream PKA Activity.....	113
MAR709 and Tirzepatide Stimulate Minimal Internalization of the GLP-1R in HEK293T and Min6 Cell Lines .....	115
GIP Receptor Exhibits Unique Assay-Dependent Ligand-Induced Internalization Dynamics .....	118
Ligand-induced GLP-1R Internalization Strongly Correlates with Ligand-specific $G\alpha_s$ Recruitment Efficacy .....	123
MAR709 and Tirzepatide Differentially Recruit $\beta$ -arrestin 1/2 to the Plasma Membrane via the GLP-1R, but is Not A Determinant of Receptor Internalization.....	126
The GIP Receptor Does Not Actively Recruit $\beta$ -arrestin 2 Following Ligand Stimulation .....	132

---

## Table of Contents

---

MAR709 and Tirzepatide Induce Weak Partial $G\alpha_q$ Recruitment at the GLP-1R but Strong Partial $G\alpha_q$ Recruitment at the GIPR.....	135
The Internalized GLP-1R is Primarily Trafficked Through Rab5 <sup>+</sup> , Rab7 <sup>+</sup> , and Rab11 <sup>+</sup> Endosomes.....	138
Rab5-associated Endosomal GLP-1R and GIPR Trafficking and Signaling are Uniquely Modulated by MAR709 and Tirzepatide.....	142
Differential GLP-1R Endosomal Colocalization and Signaling Within Rab7 <sup>+</sup> Endosomes By MAR709 and Tirzepatide, but Not at the GIPR.....	145
MAR709 and Tirzepatide Direct Less Terminal Lysosomal Colocalization of the GLP-1R.....	149
MAR709 Comparatively Incorporates the GLP-1R into Rab11 <sup>+</sup> Endosomes to that of GLP-1R Mono-agonists .....	150
Maximally-induced GLP-1R Rab11 Colocalization by MAR709 Does Not Enhance Physical Recycling.....	153
GLP-1R Population at Endosomal Compartments is Positively Associated with the Degree of Endosomal $G\alpha_s$ Recruitment.....	156
The Transcriptional Response to GLP-1R Activation is Linked to the Degree of Receptor Internalization and Endosomal $G\alpha_s$ Recruitment but not Global cAMP production .....	158
CHAPTER 4: Discussion .....	161
References .....	177
Letter of Approval – Molecular Metabolism, Volume 49, July 2021, 101181 .....	203
List of Publications.....	204
Bibliometrics:.....	204
Presentations: .....	204
Curriculum Vitae.....	205
Affidavit .....	207

## Glossary

---

7TM	Seven Transmembrane
AC	Adenylate Cyclase
AGRP	Agouti-related Peptide
Akt	Protein Kinase B
AMPK	Adenosine Monophosphate Protein Kinase
AP2	Adaptor Protein 2
AT	Adipose Tissue
$\beta$ arr1	$\beta$ -arrestin 1
$\beta$ arr2	$\beta$ -arrestin 2
Ca <sup>2+</sup>	Calcium
cAMP	cyclic AMP
CCK	Cholecystokinin
CICR	Ca <sup>2+</sup> -induced Ca <sup>2+</sup> release
CLASPS	Clathrin-associated Sorting Proteins
CME	Clathrin-mediated Endocytosis
CNS	Central Nervous System
CRE	cAMP Response Element
CREB	cAMP Response Element Binding Protein
DAG	Diacylglycerol
DIO	Diet-induced Obesity
EAA1	Early Endosome Autoantigen 1
ECE1	Endothelin-converting Enzyme-1
ECL	Extracellular Loop
EPAC2	Exchange Protein Activated by Cyclic AMP 2
ER	Endoplasmic Reticulum
ERK 1/2	Extracellular Signal-Regulated Protein Kinase
ESCRT	Endosomal Sorting Complex Required for Transport
EX4	Exendin-4
FACS	Fluorescence-activated Cell Sorting
GAPDH	Glyceraldehyde-3-Phosphate Dehydrogenase
GASP1	GPCR-associated Binding Protein-1
GDP	Guanosine diphosphate
GEF	Guanine nucleotide exchange factor
GIP	Gastric Inhibitory Peptide
GIPR	Gastric Inhibitory Peptide Receptor
GLP-1	Glucagon-like Peptide-1
GLP-1R	Glucagon-like Peptide-1 Receptor
GLUT	Glucose Transporter

---

## Glossary

---

GPCR	G-protein coupled receptor
GRK	GPCR kinase
GRPP	Glicentin-related Pancreatic Polypeptide
GSIS	Glucose-stimulated Insulin Secretion
GTP	Guanosine triphosphate
GWAS	Genome-wide Association Studies
I.P.	Intraperitoneal Administration
IBMX	3-isobutyl-1-methylxanthine
ICL	Intracellular Loop
ICV	Intracerebroventricular
IL-18	Interleukin-18
IL-6	Interleukin-6
ILV	Intraluminal Vesicles
IP1	Intervening Peptide 1
IP2	Intervening Peptide 2
IP3	Phosphatidylinositol (3,4,5)-trisphosphate
IR	Insulin Receptor
IRS-1	Insulin Receptor Substrate 1
K <sub>ATP</sub>	ATP-dependent K-channels
K <sub>d</sub>	Dissociation Constant
LepR	Leptin Receptor
MAPK	Mitogen Activated Protein Kinases
MC4R	Melanocortin 4 Receptor
MEK	Mitogen-activated Protein Kinase Kinase
NPY	Neuropeptide Y
PC	Proprotein Convertase
PCK1	Phosphoenolpyruvate Carboxykinase 1
PDE	Phosphodiesterase
PDX1	Pancreatic Duodenal Homeobox-1
PI3K	Phosphoinositide 3-kinases
PIP2	Phosphatidylinositol 4,5-bisphosphate
PIP3	Phosphatidylinositol 3-phosphate
PKA	Protein Kinase A
PKAcat	PKA Catalytic Subunit
Prkar1a KO	PKA regulatory subunit KO
PKC	Protein Kinase C
PLC-β:	β-isoforms of phospholipase C
PNS	Peripheral Nervous System
POI	Protein of Interest
POMC	Pro-opiomelanocortin
PTH	Parathyroid Hormone

---

## Glossary

---

PTH1R	Parathyroid Hormone 1 Receptor
PTHrP	Parathyroid Hormone-related Protein
PYY	Peptide YY
qPCR	Quantitative Real-time PCR
Rab	Ras-associated Binding Proteins
RGS	Regulator of G-protein signaling
T2D	Type 2 Diabetes
TMD	Transmembrane Spanning Domain
TNF	Tumor Necrosis Factor
V2R	Vasopressin Type 2 Receptor



## Figure Index

- Figure 1: Classification of obesity status by BMI according to the World Health Organization (WHO)**..... 24
- Figure 2: Dynamic regulation of MC4R<sup>+</sup> PVN neurons according to the interplay between AGRP/NPY and POMC neural activation or inhibition.** AGRP/NPY and POMC neurons localized within the arcuate nucleus respond to endocrine stimuli and mediate orexigenic (AGRP/NPY) or anorexigenic (POMC) status via regulation of downstream MC4R activity and AGRP/NPY to POMC communication. This figure was created using Sevier medical art and was inspired from Cone et al., 2001..... 28
- Figure 3: Tissue-specific processing of proglucagon.** The proglucagon precursor protein is cleaved from preproglucagon following enzymatic removal of the signal peptide (PS). Within L-cells of the small intestine, prohormone convertase 1/3 (PC1/3) cleaves and breaks down proglucagon into separate proteins consisting of GLP-1, GLP-2, oxyntomodulin, IP2, and glicentin. The resultant GLP-1 is predominantly found in the form of GLP-1 (7-37) and GLP-1 (7-36 amide). Within  $\alpha$ -cells of the pancreas, the proglucagon precursor is instead cleaved and broken down by prohormone convertase 2 (PC2) resulting in glucagon, glicentin-related pancreatic polypeptide (GRPP), IP1, and a major proglucagon fragment. .... 31
- Figure 4: Structure of human GLP-1R and GIPR.** The GLP-1R and GIPR consist of an extracellular N-terminal domain, seven  $\alpha$ -helical transmembrane segments (1-7) connected via three intracellular (ICL<sub>1</sub>-ICL<sub>3</sub>) and extracellular loops (ECL<sub>1</sub>-ECL<sub>3</sub>), and an intracellular C-terminal domain. Common to class B GPCRs, the extracellular N-terminal domain is stabilized by six cysteine residues (highlighted in green). The cleavable signal peptide (highlighted in red), located at the N-terminus, is required for processing and cell-surface expression of both the GLP-1R and GIPR. Specific amino acids targeted for post-translational modifications are highlighted in purple and may influence receptor cell surface expression and receptor degradation. PTM: Post-translational modification. This figure was created using the Protter Software. .... 42
- Figure 5: Schematic of G $\alpha$ s/G $\alpha$ q activation and signaling.** Steps following ligand binding at the GPCR: 1) The heterotrimeric G-protein complex consisting of a GDP-bound G $\alpha$  subunit, the G $\beta$  subunit, and G $\gamma$  subunit, are recruited to the ligand-bound GPCR. 2) The G $\alpha$  subunit interacts with the intracellular loops of the GPCR forming a high-affinity complex that opens the G $\alpha$  subunit to binding GTP. The GPCR acts as a guanine nucleotide exchange factor (GEF) replacing GDP with GTP at the G $\alpha$  subunit. 3) The GTP-bound G $\alpha$  subunit dissociates from the G $\beta$  and G $\gamma$  subunits. 3a) The liberated GTP-bound G $\alpha$ s subunits interact with adenylate cyclase (AC) to convert ATP into cAMP. The rise in intracellular cAMP results in the activation of multiple downstream targets including PKA, EPAC2, and cyclic nucleotide-gated channels. 3b) The liberated GTP-bound G $\alpha$ q subunits activate the membrane-bound  $\beta$ -isoform of phospholipase C (PLC- $\beta$ ). The activated PLC- $\beta$  converts membrane-localized PIP<sub>2</sub> into membrane-localized DAG and cytosol-localized IP<sub>3</sub>, in which DAG activates membrane-bound PKC while the cytosol-diffused IP<sub>3</sub> induces calcium release via IP<sub>3</sub> receptors on the ER. 4) Intrinsic GTPase activity of the G $\alpha$  subunits hydrolyses GTP to GDP thus inactivating the G-protein subunit and increasing its affinity for G $\beta$  and G $\gamma$  subunit binding. G-protein hydrolysis of GTP to GDP can be accelerated by complementary proteins such as RGS, increasing GTPase activity by as much as 1,000 fold. .... 46
- Figure 6: Formation and liberation of endosomes containing internalized receptors.** Clathrin (black) recruitment to the inner leaflet of the plasma membrane promotes bending and

invagination of the membrane. Plasma membrane associated proteins, including GPCRs, heterotrimeric G-protein subunits, and downstream effector proteins (i.e. adenylate cyclase) are directed into the budding formation. Dynamin-dependent scission (light blue) of the formed neck of the invaginated bud liberates the endosome and its contents from the plasma membrane, in which the newly formed endosome can then shed the endocytic machinery (i.e. clathrin) and continue trafficking within the cell and signaling within the endosomal compartment..... 57

**Figure 7:  $\beta$ -arrestin facilitation of  $G\alpha$  signaling inhibition and GPCR movement into clathrin-coated pits.** Steps following ligand binding at the GPCR: 1)  $G\alpha$  subunits are recruited to the GPCR to swap GDP for GTP. 2) In parallel to  $G\alpha$  subunit recruitment, GRK is recruited to the C-terminal tail of the GPCR resulting in the phosphorylation of serine and threonine residues. 3) The C-terminal serine/threonine phosphorylation sites on the GPCR act as an interaction point for  $\beta$ -arrestin binding which sterically inhibits further  $G\alpha$  subunit recruitment and connects the GPCR to the AP2 endocytic machinery facilitating accumulation within the clathrin-coated pits. .... 59

**Figure 8: Schematic of endolysosomal trafficking and the mosaic of overlapping Rab domains.** Rab proteins facilitate endosomal trafficking and define distinct endosomal domains within a network of cargo transport. Rab5 is the immediate destination for internalized cargo via clathrin coated pits and represents the early endosomal compartment. Following Rab5 colocalization, Rab4 and Rab11 represent the primary routes for receptor recycling via receptor resensitization and return to the plasma membrane. Cargo can be rapidly recycled back to the plasma membrane by sorting through Rab4<sup>+</sup> endosomes, or recycled through the perinuclear region to the plasma membrane via Rab11<sup>+</sup> endosomes. The Rab5, Rab4, and Rab11 domains are not distinctly separate but are dynamically interconnected. Alternatively, Rab5 endosomes can be trafficked to accomplish cellular desensitization through the Rab7 late endosomal pathway which ultimately leads to cargo to incorporation into LAMP1<sup>+</sup> terminal lysosomes. .... 65

**Figure 9: The Hill Equation.** .... 69

**Figure 10: Ligand potency as a product of intracellular signal amplification.** Comparison of ligand potency within subsequent steps of the signaling cascade in which a leftward shift in each dose-response curve is attributed to an intracellular amplification of signal. Immediate G-protein signaling as measured by mini $G\alpha_s$  recruitment, also viewed as ‘receptor activation’, is the first step within the cascade. Quantification of direct cAMP production (as measured by unimolecular cAMP sensors or cAMP antibody sandwich assays) represents a step downstream that is subject to a degree of signal amplification. Indirect cAMP measurements using nuclear cAMP CRE-luciferase reporters, which are dependent on PKA phosphorylation of CREB, represent quantitative readouts most effected by amplification of signal. .... 71

**Figure 11: Examples of “gain in signal” and “loss in signal” BRET assays by Mini $G\alpha_s$  recruitment to the GPCR and GPCR dissociation from the plasma membrane.** Protein-protein interactions can be quantified through bioluminescent resonance energy transfer (BRET) when a donor lumiphore is brought into close vicinity (< 10 nm) to a suitable acceptor fluorophore. BRET assays can be grouped into “gain in signal” or “loss in signal” assays. Mini $G\alpha_s$ -Nluc recruitment assays, in which a lumiphore-tagged truncated version of  $G\alpha_s$  resides within the cytosol at baseline and is recruited to a fluorophore-tagged GPCR upon ligand stimulation, is representative of a gain in signal assay as BRET is established. In a loss in signal assay, in which baseline BRET is dissipated by the lumiphore moving away from its fluorophore counterpart, is exemplified with receptor internalization assays as the

internalizing lumiphore-tagged GPCR moves to a distance > 10 nm relative to the fluorophore-tagged plasma membrane marker..... 73

**Figure 12: Amino acid sequence homology of GIP (1-42) and Glucagon (1-29) to GLP-1 (7-36 amide).** Amino acids within the GIP (1-42) sequence highlighted in blue are unique relative to GLP-1 (7-36 amide). Amino acids within the Glucagon (1-29) sequence highlighted in red are unique relative to GLP-1 (7-36 amide)..... 80

**Figure 13: Unimolecular hybridization of GLP-1 (7-36 amide) and GIP (1-42).** High sequence similarity between GLP-1 and GIP within the N-terminal region of the peptides, the necessity of Tyr1 for GIPR activation, and the functional exchangeability of Tyr1His in maintaining GLP-1R potency, had allowed for the iterative development of the balanced GLP-1/GIP dual-agonist MAR709 (NNC0090-2746, Novo Nordisk, Copenhagen, Denmark). Tirzepatide (LY3298176; Eli Lilly, Indianapolis, IN, USA), an unbalanced GLP-1/GIP dual-agonist, was similarly modeled to the MAR709 sequence however with specific amino acid substitutions conferring greater preference to the GIPR over the GLP-1R..... 82

**Figure 14: Amino acid sequence and structure of the tested GLP-1R and GIPR ligands.** GLP-1R mono-agonists used within this thesis are comprised of GLP-1 (7-36 amide), Semaglutide, and Acyl-GLP-1 (a pharmacokinetically-matched His1 and Val10 mutant of MAR709) (left panel, green). Comparative GIPR mono-agonists included are GIP (1-42) and Acyl-GIP (a pharmacokinetically matched Ile7 mutant of MAR709) (middle panel, blue). GLP-1/GIP dual-agonists investigated are MAR709 and Tirzepatide (right panel, orange). Amino acid sequences, in paper abbreviations, and external identifiers of the GLP-1 and GIP-derived compounds used (bottom table). ..... 101

**Figure 15: Ligand-induced  $G\alpha$  subunit recruitment at the GLP-1R.** Ligand-induced (1  $\mu$ M) recruitment of Nluc-tagged Mini-  $G\alpha_s$  (A),  $G\alpha_q$  (B),  $G\alpha_i$  (C),  $G\alpha_{12/13}$  (D), to a GFP-tagged GLP-1R in HEK293T cells. The positive iAUC (+iAUC) representation of vehicle- and baseline-corrected 30 min response to each agonist is expressed as mean  $\pm$  SEM. Bonferroni's test, \*p < 0.05, \*\*p < 0.005, and \*\*\*p < 0.0005 using one-way ANOVA vs GLP-1 (7–36 amide), Semaglutide, and Acyl-GLP-1. Three independent experiments were performed with at least two technical replicates per group. Figure adapted from . ..... 104

**Figure 16: Ligand-induced  $G\alpha$  subunit recruitment at the GIPR.** Ligand-induced (1  $\mu$ M) recruitment of Nluc-tagged Mini-  $G\alpha_s$  (A),  $G\alpha_q$  (B),  $G\alpha_i$  (C),  $G\alpha_{12/13}$  (D), to a GFP-tagged GIPR in HEK293T cells. The +iAUC representation of vehicle- and baseline-corrected 30 min response to each agonist is expressed as mean  $\pm$  SEM. Bonferroni's test, \*p < 0.05, \*\*p < 0.005, and \*\*\*p < 0.0005 using one-way ANOVA vs GIP (1-42) and Acyl-GIP. Three independent experiments were performed with at least two technical replicates per group..... 105

**Figure 17: Baseline constitutive activity of  $G\alpha_s$  and  $G\alpha_q$  subunits at the GLP-1R and the GIPR.** Normalized comparison of maximal Mini $G\alpha$ -Nluc recruitment to GFP-tagged GLP-1R or GIPR following 1  $\mu$ M stimulation of either GLP-1 (7-36 amide) or GIP (1-42) (A). Mini $G\alpha_s$ -Nluc recruitment to GFP-tagged GLP-1R or GIPR following vehicle (PBS) administration without statistical normalization to baseline values (B). Mini $G\alpha_q$ -Nluc recruitment to GFP-tagged GLP-1R or GIPR following vehicle (PBS) administration without statistical normalization to baseline starting values (C). Three independent experiments were performed with at least two technical replicates per group..... 107

**Figure 18: Dose-dependent and temporal effects of ligands on  $G\alpha_s$  recruitment and cAMP production at the GLP-1R.** Dose-response curves (A) and temporal resolution (1  $\mu$ M stimulation) (B) of ligand-induced BRET between Mini $G\alpha_s$ -Nluc and GFP-tagged GLP-1R in HEK293T cells. Dose-response curves of ligand-induced cAMP production in GLP-1R<sup>+</sup> HEK293T cells (C). +iAUC representation of vehicle- and baseline-corrected 60 min ( $G\alpha_s$  recruitment) or

25 min (cAMP generation) temporal responses to each agonist is expressed as mean $\pm$ SEM. Three independent experiments were performed with at least two technical replicates per group. ....	109
<b>Figure 19: Saturation of unimolecular CAMYEL cAMP sensor is not achieved following 10 <math>\mu</math>M ligand stimulation at the GLP-1R.</b> Time course (A) and fitted dose-response curve (100 pM – 100 $\mu$ M) (B) of the cAMP positive control forskolin in GLP-1R <sup>+</sup> HEK293T cells. Stimulation with 10 $\mu$ M of agonist or forskolin in GLP-1R <sup>+</sup> HEK293T cells (C). The +iAUC representation of vehicle- and baseline-corrected 60 min response to each agonist is expressed as mean $\pm$ SEM. Three independent experiments were performed with at least two technical replicates per group. ....	111
<b>Figure 20: Dose-dependent and temporal effects of ligands on G<math>\alpha_s</math> recruitment and cAMP production at the GIPR.</b> Dose-response curves (A) and temporal resolution (1 $\mu$ M stimulation) (B) of ligand-induced BRET between MiniG $\alpha_s$ -Nluc and GFP-tagged GIPR in HEK293T cells. Dose-response curves of ligand-induced cAMP production in GIPR <sup>+</sup> HEK293T cells (C). +iAUC representation of vehicle- and baseline-corrected 60 min (G $\alpha_s$ recruitment) or 25 min (cAMP generation) temporal responses to each agonist is expressed as mean $\pm$ SEM. Three independent experiments were performed with at least two technical replicates per group. ....	112
<b>Figure 21: PKA activity at the GLP-1R.</b> Temporal resolution (A) and AUC (B) of ligand-induced PKA activity as measured by the unimolecular circularly permuted ExRai-AKAR2 sensor in GLP-1R <sup>+</sup> HEK293T cells. The AUC representation of vehicle- and baseline-corrected 40 min response to each agonist is expressed as mean $\pm$ SEM. Bonferroni's test, *p < 0.05, **p < 0.005, and ***p < 0.0005 using one-way ANOVA vs GLP-1 (7-36 amide). Three independent experiments were performed with at least two technical replicates per group. ....	114
<b>Figure 22: Ligand-induced GLP-1R internalization.</b> Dose-response (A) and temporal resolution (1 $\mu$ M) (B) of ligand-induced hGLP-1-Rluc8 internalization as measured by loss of BRET with plasma membrane marker Venus-KRAS. Live HILO imaging of hGLP-1R-GFP internalization in HEK293T cells at baseline and 15 minutes after 1 $\mu$ M ligand treatment (C). The -AUC representation of vehicle- and baseline-corrected 40 min response to each agonist is expressed as mean $\pm$ SEM. Three independent experiments were performed with at least two technical replicates per group. ....	115
<b>Figure 23: Ligand-induced GLP-1R internalization in hGLP-1R<sup>+</sup> Min6 cells.</b> Temporal resolution (1 $\mu$ M ligand stimulation) (A), AUC (B) and % normalized AUC to GLP-1 (7-36 amide) (C), of hGLP-1R-Rluc8 internalization as measured by loss of BRET with plasma membrane marker Venus-KRAS in HEK293T cells. The -AUC representation of vehicle- and baseline-corrected 60 min response to each agonist is expressed as mean $\pm$ SEM. Bonferroni's test, *p < 0.05, **p < 0.005, and ***p < 0.0005 using one-way ANOVA vs GLP-1 (7-36 amide). Three independent experiments were performed with at least two technical replicates per group. ....	117
<b>Figure 24: Ligand-induced GIPR internalization.</b> Dose-response (A) and temporal resolution (1 $\mu$ M) (B) of ligand-induced hGIPR-Rluc8 internalization as measured by loss of BRET with plasma membrane marker Venus-KRAS. Live HILO imaging of hGIPR-GFP internalization in HEK293T cells at baseline and 15 minutes after 1 $\mu$ M ligand treatment (C). The -AUC representation of vehicle- and baseline-corrected 20 min response to each agonist is expressed as mean $\pm$ SEM. Three independent experiments were performed with at least two technical replicates per group. ....	119
<b>Figure 25: Ligand-induced GIPR internalization and GIPR recruitment to the plasma membrane.</b> Temporal resolution (1 $\mu$ M) of ligand-induced hGIPR-Rluc8 movement toward	

and away from the plasma membrane marker GFP-CAAX (A), in which the +iAUC is represented as ligand-stimulated net GIPR movement towards the plasma membrane (B) and -iAUC represented as ligand-stimulated net GIPR departure away from the plasma membrane (C). Temporal resolution (D) and +iAUC (E) of ligand-induced (1  $\mu$ M) GIPR movement toward the plasma membrane following 30 min pretreatment with 0.43 M sucrose to inhibit receptor internalization. The iAUC representation of vehicle- and baseline-corrected 30 min response to each agonist is expressed as mean  $\pm$  SEM. Bonferroni's test, \*p < 0.05, \*\*p < 0.005, and \*\*\*p < 0.0005 using one-way ANOVA vs GIP (1-42). Three independent experiments were performed with at least two technical replicates per group. .... 121

**Figure 26: XY relationship of ligand  $G\alpha_s$  recruitment and cAMP production efficacy, to GLP-1R internalization.** Linear regression demonstrating relationship of ligand-specific receptor internalization  $E_{max}$  (X-axis) to  $G\alpha_s$  recruitment  $E_{max}$  (Y-axis) (A) and cAMP production  $E_{max}$  (Y-axis) (B). .... 123

**Figure 27: The influence of GLP-1R receptor inhibition on  $G\alpha_s$  recruitment.** Dose-response curves of ligand-induced hGLP-1R-Rluc8 internalization without (A) or with (B) 30 min pretreatment of 10 mM M $\beta$ CD in HEK293T cells to inhibit receptor internalization as measured by dissipation of BRET signal with plasma membrane marker Venus-KRAS. Dose-response curves of ligand-induced mini $G\alpha_s$ -Nluc recruitment to GFP-tagged hGLP-1R without (C) or with (D) 30 min pretreatment of 10 mM M $\beta$ CD. Dose-response curves of ligand-induced mini $G\alpha_s$ -Nluc recruitment to the plasma membrane marker Venus-KRAS without (E) or with (F) 30 min pretreatment of 10 mM M $\beta$ CD. The iAUC representation of vehicle- and baseline-corrected 30 min response to each agonist is expressed as mean  $\pm$  SEM. Three independent experiments were performed with at least two technical replicates per group. .... 124

**Figure 28: Ligand-induced  $\beta$ -arrestin 1/2 recruitment to the GLP-1R.** Dose-response curves (A) and temporal resolution (1  $\mu$ M stimulation) (B) of ligand-induced BRET resulting from  $\beta$ arr1-Rluc8 recruitment to the GFP-tagged hGLP-1R. Dose-response curves (C) and temporal resolution (1  $\mu$ M stimulation) (D) of ligand-induced BRET resulting from  $\beta$ arr2-Rluc8 recruitment to the GFP-tagged hGLP-1R. +iAUC representation of vehicle- and baseline-corrected 30 min temporal responses to each agonist is expressed as mean  $\pm$  SEM. Three independent experiments were performed with at least two technical replicates per group. .... 127

**Figure 29: Ligand-induced  $\beta$ -arrestin 2 recruitment to the plasma membrane and endosomal compartments as mediated by GLP-1R.** Temporal resolution (1  $\mu$ M stimulation) (A) and +iAUC (B) of ligand-induced BRET resulting from  $\beta$ arr2-Rluc8 recruitment to the plasma membrane marker Venus-KRAS as mediated by the untagged hGLP-1R. Temporal resolution (1  $\mu$ M stimulation) of  $\beta$ arr2-Rluc8 recruitment to hGLP-1R<sup>+</sup> Venus-Rab5<sup>+</sup> (C) and Venus-Rab7<sup>+</sup> (D) endosomes. +iAUC representation of vehicle- and baseline-corrected 30 min temporal responses to each agonist is expressed as mean  $\pm$  SEM. Three independent experiments were performed with at least two technical replicates per group. .... 129

**Figure 30: Ligand-induced GLP-1R internalization within the context of  $\beta$ -arrestin inhibition.** Temporal resolution (1  $\mu$ M stimulation) (A) and -iAUC (B) of loss in BRET signal resulting from hGLP-1R-Rluc8 internalization and movement away from the plasma membrane marker Venus-KRAS within the context of barbadin pretreatment (100  $\mu$ M). -iAUC representation of vehicle- and baseline-corrected 30 min temporal responses to each agonist is expressed as mean  $\pm$  SEM. Three independent experiments were performed with at least two technical replicates per group. .... 131

- Figure 31: The presence of  $\beta$ -arrestin recruitment to the GIPR is dependent on assay type.** Dose-response (A) and temporal resolution (1  $\mu$ M) (B) of the ligand-induced  $\beta$ arr2-Rluc8 response as measured by a gain in BRET signal following recruitment to the GFP-tagged hGIPR. Relative difference in the extent of ligand-induced (1  $\mu$ M)  $\beta$ arr2-Rluc8 recruitment to either GFP-tagged hGLP-1R or hGIPR by the respective native ligands GLP-1 (7-36 amide) or GIP (1-42) (C). Amino acid sequence of synthetic linker connecting hGIPR to the GFP fluorophore with serine residues highlighted in bold red (D). Untagged hGIPR-mediated  $\beta$ arr2-Rluc8 colocalization with plasma membrane marker Venus-KRAS following ligand stimulation (1  $\mu$ M) (E).  $\beta$ arr2-Rluc8 colocalization with plasma membrane marker Venus-KRAS as mediated by the untagged endogenous GLP-1R or GIPR sequences following ligand stimulation (1  $\mu$ M) (F). +iAUC representation of vehicle- and baseline-corrected 30 min temporal responses to each agonist is expressed as mean  $\pm$  SEM. Three independent experiments were performed with at least two technical replicates per group..... 134
- Figure 32:  $G\alpha_q$  subunit recruitment to the GLP-1R or the GIPR.** Dose-response (A, C) and temporal resolution (1  $\mu$ M) (B, D) for MiniG $\alpha_q$ -Nluc recruitment to the GFP-tagged hGLP-1R or hGIPR. +iAUC representation of vehicle- and baseline-corrected 60 min temporal responses to each agonist is expressed as mean  $\pm$  SEM. Three independent experiments were performed with at least two technical replicates per group..... 136
- Figure 33: Screen of ligand-induced hGLP-1R colocalization into various endolysosomal/biosynthetic pathways.** Temporal resolution of hGLP-1R-Rluc8 colocalization into Venus-tagged Rab1 (A), Rab4 (B), Rab 5 (C), Rab6 (D), Rab7 (E), Rab8 (F), Rab9 (G), Rab11a (H) -positive endosomal compartments following GLP-1 (7-36 amide) stimulation (1  $\mu$ M) over the course of 60 minutes. Three independent experiments were performed with at least two technical replicates per group..... 139
- Figure 34: Schematic of GLP-1R  $G\alpha$  subunit signaling and subsequent endosomal trafficking.** ..... 141
- Figure 35: GLP-1R colocalization and signaling within Rab5<sup>+</sup> early endosomes.** Temporal resolution, +iAUC, and % +iAUC normalized to GLP-1 (7-36 amide), of ligand-induced (1  $\mu$ M) hGLP-1R-Rluc8 colocalization into Venus-Rab5<sup>+</sup> endosomes in HEK293T (A-C) and Min6 (D-F) cell lines. MiniG $\alpha_s$  recruitment to Venus-Rab5<sup>+</sup> endosomes as mediated by the untagged hGLP-1R (G-I). The +iAUC representation of vehicle- and baseline-corrected 60 min response to each agonist is expressed as mean  $\pm$  SEM. Bonferroni's test, \* $p$  < 0.05, \*\* $p$  < 0.005, and \*\*\* $p$  < 0.0005 using one-way ANOVA vs GLP-1 (7-36 amide), Semaglutide, and Acyl-GLP-1. Three independent experiments were performed with at least two technical replicates per group. .... 143
- Figure 36: GIPR colocalization and signaling within Rab5<sup>+</sup> early endosomes.** Temporal resolution, +iAUC, and % +iAUC normalized to GIP (1-42), of ligand-induced (1  $\mu$ M) hGIPR-Rluc8 colocalization into Venus-Rab5<sup>+</sup> endosomes in HEK293T cells (A-C). MiniG $\alpha_s$  recruitment to Venus-Rab5<sup>+</sup> endosomes as mediated by the untagged hGIPR (D-F). The +iAUC representation of vehicle- and baseline-corrected 60 min response to each agonist is expressed as mean  $\pm$  SEM. Bonferroni's test, \* $p$  < 0.05, \*\* $p$  < 0.005, and \*\*\* $p$  < 0.0005 using one-way ANOVA vs GIP (1-42) and Acyl-GIP. Three independent experiments were performed with at least two technical replicates per group..... 144
- Figure 37: GLP-1R colocalization and signaling within Rab7<sup>+</sup> late endosomes.** Temporal resolution, +iAUC, and % +iAUC normalized to GLP-1 (7-36 amide), of ligand-induced (1  $\mu$ M) hGLP-1R-Rluc8 colocalization into Venus-Rab7<sup>+</sup> endosomes in HEK293T (A-C) and Min6 (D-E) cell lines. MiniG $\alpha_s$  recruitment to Venus-Rab7<sup>+</sup> endosomes as mediated by the untagged hGLP-1R (F-H). The +iAUC representation of vehicle- and baseline-corrected 60 min response

to each agonist is expressed as mean  $\pm$  SEM. Bonferroni's test, \* $p$  < 0.05, \*\* $p$  < 0.005, and \*\*\* $p$  < 0.0005 using one-way ANOVA vs GLP-1 (7-36 amide), Semaglutide, and Acyl-GLP-1. Three independent experiments were performed with at least two technical replicates per group. .... 146

**Figure 38: GIPR colocalization and signaling within Rab7<sup>+</sup> late endosomes.** Temporal resolution and +iAUC of ligand-induced (1  $\mu$ M) hGIPR-Rluc8 colocalization into Venus-Rab7<sup>+</sup> endosomes in HEK293T cells (A-B). MiniG $\alpha_s$  recruitment to Venus-Rab7<sup>+</sup> endosomes as mediated by the untagged hGIPR (C-D). The +iAUC representation of vehicle- and baseline-corrected 60 min response to each agonist is expressed as mean  $\pm$  SEM. Bonferroni's test, \* $p$  < 0.05, \*\* $p$  < 0.005, and \*\*\* $p$  < 0.0005 using one-way ANOVA vs GIP (1-42) and Acyl-GIP. Three independent experiments were performed with at least two technical replicates per group. .... 148

**Figure 39: GLP-1R colocalization into LAMP1<sup>+</sup> terminal lysosomes.** Temporal resolution, +iAUC, and % +iAUC normalized to GLP-1 (7-36 amide), of ligand-induced (1  $\mu$ M) hGLP-1R-Rluc8 colocalization into LAMP1-mNeonGreen<sup>+</sup> terminal lysosomes in HEK293T cells (A-C). The +iAUC representation of vehicle- and baseline-corrected 60 min response to each agonist is expressed as mean  $\pm$  SEM. Bonferroni's test, \* $p$  < 0.05, \*\* $p$  < 0.005, and \*\*\* $p$  < 0.0005 using one-way ANOVA vs GLP-1 (7-36 amide), Semaglutide, and Acyl-GLP-1. Three independent experiments were performed with at least two technical replicates per group. .... 149

**Figure 40: GLP-1R colocalization and signaling within Rab11<sup>+</sup> recycling endosomes.** Temporal resolution, +iAUC, and % +iAUC normalized to GLP-1 (7-36 amide), of ligand-induced (1  $\mu$ M) hGLP-1R-Rluc8 colocalization into Venus-Rab11<sup>+</sup> recycling endosomes in HEK293T (A-C) and Min6 (D-E) cell lines. MiniG $\alpha_s$  recruitment to Venus-Rab11<sup>+</sup> endosomes as mediated by the untagged hGLP-1R (F-H). The +iAUC representation of vehicle- and baseline-corrected 60 min response to each agonist is expressed as mean  $\pm$  SEM. Bonferroni's test, \* $p$  < 0.05, \*\* $p$  < 0.005, and \*\*\* $p$  < 0.0005 using one-way ANOVA vs GLP-1 (7-36 amide), Semaglutide, and Acyl-GLP-1. Three independent experiments were performed with at least two technical replicates per group. .... 151

**Figure 41: GIPR colocalization and signaling within Rab11<sup>+</sup> recycling endosomes.** Temporal resolution and +iAUC of ligand-induced (1  $\mu$ M) hGIPR-Rluc8 colocalization into Venus-Rab11<sup>+</sup> endosomes in HEK293T cells (A-B). MiniG $\alpha_s$  recruitment to Venus-Rab11<sup>+</sup> endosomes as mediated by the untagged hGIPR (C-D). The +iAUC representation of vehicle- and baseline-corrected 60 min response to each agonist is expressed as mean  $\pm$  SEM. Bonferroni's test, \* $p$  < 0.05, \*\* $p$  < 0.005, and \*\*\* $p$  < 0.0005 using one-way ANOVA vs GIP (1-42) and Acyl-GIP. Three independent experiments were performed with at least two technical replicates per group. .... 153

**Figure 42: Physical reappearance of GLP-1R at the plasma membrane following receptor internalization.** Temporal resolution of ligand-induced (1  $\mu$ M) changes in hGLP-1R-Rluc8 colocalization with the plasma membrane marker Venus-KRAS. Following 20 minutes of ligand-incubation, ligands were washed out and either re-administered ligands (A) or administered the GLP-1R antagonist Jant4 (9-39) (B), in which the resulting positive increases in BRET signal, indicative of hGLP-1R-Rluc8 return to the plasma membrane from the intracellular space, was measured over the course of the next 30 minutes. Pertaining to all data points following JANT4 (9-39) administration, the rate of GLP-1R recycling was quantified using the +iAUC which had been normalized to the respective immediate post-washout measurement of each agonist (C). Again pertaining to all data points following JANT4 (9-39) administration, total GLP-1R presence at the plasma membrane was quantified via +AUC (not iAUC) by normalizing all ligand post-washout responses to a common minimal value (D). The

iAUC and AUC representation of vehicle- and baseline-corrected 50 min response to each agonist is expressed as mean  $\pm$  SEM. Bonferroni's test, \*p < 0.05, \*\*p < 0.005, and \*\*\*p < 0.0005 using one-way ANOVA vs GLP-1 (7-36 amide), Semaglutide, and Acyl-GLP-1. Three independent experiments were performed with at least two technical replicates per group.

..... 154

**Figure 43: Association of Rab-specific GLP-1R colocalization with the degree of GLP-1R mediated endosomal  $G\alpha_s$  recruitment.** Linear regression between Mini $G\alpha_s$ -Nluc recruitment and the physical colocalization of the hGLP-1R-Rluc8 into the Venus-tagged Rab endosomal compartments for Rab5 early endosomes (A), Rab7 late endosomes (B), and Rab11 recycling endosomes (C)..... 157

**Figure 44: The relationship of ligand-stimulated PCK1 transcription with GLP-1R internalization, Rab5<sup>+</sup> endosomal  $G\alpha_s$  signaling, and global cAMP production.** Ligand-induced hGLP-1R-mediated transcription of the cAMP-responsive gene PCK1 as normalized to vehicle (A). Linear regression between ligand-induced PCK1 transcription and hGLP-1R-Rluc8 internalization (B), hGLP-1R-mediated recruitment of mini $G\alpha_s$ -Nluc to Venus-Rab5<sup>+</sup> endosomal compartments (C), and cAMP production (D). Data is expressed as mean  $\pm$  SEM. Bonferroni's test, \*p < 0.05, \*\*p < 0.005, and \*\*\*p < 0.0005 using one-way ANOVA vs GLP-1 (7-36 amide). Four independent experiments were performed. .... 160



## Table Index

**Table 1: Characterization of clinically-relevant GLP-1R mono-agonists.** Pharmaceutical GLP-1R mono-agonists with described general modifications relevant to enhancing agonist in vivo half-life. .... 75

**Table 2: Maximal ( $E_{max}$ ) drug effects and potencies ( $EC_{50}$ ) at the GLP-1R or GIPR target receptors.** Data were generated in HEK293T cells transiently transfected to express GLP-1R or GIPR.  $E_{max}$ ,  $pEC_{50}$ , and  $EC_{50}$  values were generated from dose–response values fitted to sigmoidal curves using a three-parameter non-linear logistic regression. The  $E_{max}$  is the maximal response elicited by an agonist and is expressed as % of the maximum response of GLP-1 (7–36 amide) or GIP (1–42). The EC is the molar concentration in which an agonist produced half of the maximal response. The  $pEC_{50}$  is the negative logarithm of the EC. Values are given for  $G\alpha_s$  recruitment, cAMP accumulation, receptor internalization,  $\beta$ -arrestin 1/2, and  $G\alpha_q$  recruitment at the GLP-1R and the GIPR. All of the values were derived from the iAUC of a temporal response for each concentration/agonist and are expressed as mean  $\pm$  SEM from at least 3 independent experiments with at least two technical replicates per group. Statistical significance was determined using one-way ANOVA and corrected with Bonferroni's multiple comparisons test. \*/#/ $\dagger p < 0.05$ . \* vs GLP-1 (7–36 amide) or GIP (1–42). # vs Semaglutide.  $\dagger$  vs fatty acyl-GLP-1 or fatty acyl-GIP. NA = no agonism significantly different than zero observed at 1  $\mu$ M stimulation. Bold red = with significant non-zero agonism at 1  $\mu$ M stimulation but incomplete curve fit, last value at 10  $\mu$ M used..... 108

## Abstract

Obesity, and the often-associated co-morbidity of Type 2 diabetes (T2D), have been exemplified as worldwide health threats due to their high prevalence and physiological burden. The primary driver of obesity is an imbalance between excessive energy intake and minimal caloric expenditure. Strategies designed to “re-balance” energy intake and expenditure, while simultaneously optimizing metabolic glucose handling, primarily consist of lifestyle modification, bariatric surgery, and pharmacotherapy. In recent time, pharmacological targeting of receptors and biological processes involved in food intake and energy expenditure have developed in both efficacy and safety. The endogenous glucagon-like peptide-1 (GLP-1), which is well-known to enhance the insulinotropic response through the ‘incretin’ effect and induce CNS-mediated satiety, has been heavily explored for its therapeutic potential. Liraglutide and Semaglutide, which are GLP-1 analogues with 97% and 94% amino acid sequence homology, have revolutionized peptide-based diabetes and obesity treatment due to exponential improvements in circulating half-life. As GLP-1-based therapeutics have taken center stage despite persistent occurrence of adverse side effects, combinatorial use of GLP-1-based pharmacology with its incretin counterpart, the gastric inhibitory peptide (GIP), has demonstrated synergistic potentiation of the dose-response in improving therapeutic endpoints such as body weight reduction and decreases in food intake. In short, with GLP-1 and GIP co-administration, similar therapeutic endpoints are achieved with less ligand required, thereby improving the tolerability profile. As a result, novel strategies for combining GLP-1 and GIP action have manifested in the development of hybridized unimolecular GLP-1/GIP dual-agonists, which consists of an eclectic positioning of amino acids from both peptides into a single molecule. These unimolecular GLP-1/GIP dual-agonists have exhibited therapeutic superiority to both mono-agonism and co-administration of the individual peptides. However, questions remain pertaining to the novel amino acid sequences that constitute these unimolecular dual-agonists, in particular, if the superior therapeutic benefits observed are attributable solely to dual-agonism at the GLP-1R and GIPR, or if the unique peptide sequences confer specialized signaling, trafficking, and receptor recycling properties at the individual receptors, culminating in what is known as biased agonism. Previous studies have selectively altered or substituted amino acids within the GLP-1 sequence and have highlighted an impact on ligand-induced parameters such as receptor

internalization,  $\beta$ -arrestin 1/2 recruitment, cAMP signaling, and differential cellular desensitization. Sequence-mediated biases in ligand-induced signaling and trafficking have also resulted in differential *in vivo* effects on glucose regulation and food intake.

Therefore, the goal of this presented PhD thesis is to assess the spatiotemporal GLP-1 and GIP receptor signaling, trafficking, and recycling dynamics elicited by the GLP-1/GIP dual-agonists MAR709 and Tirzepatide, relative to select GIPR and GLP-1R mono-agonists. In comparison to the GLP-1 mono-agonists, which include a pharmacokinetically-matched MAR709 mono-agonist control, both MAR709 and Tirzepatide show preserved maximal cAMP production despite partial  $G\alpha_s$  recruitment. The unique signaling dynamics of the dual-agonists were also paralleled by diminished ligand-induced internalization of both target receptors. Despite a lower internalization rate by MAR709, GLP-1R colocalization with Rab11-associated recycling endosomes was not different between MAR709 and GLP-1R specific mono-agonists. However, this did not directly translate to a faster rate of physical receptor reinsertion into the plasma membrane for MAR709. Interestingly at the GLP-1R, we identify agonist-specific differential induction of  $G\alpha_s$  signaling,  $\beta$ -arrestin 1/2 recruitment, receptor internalization, endosomal trafficking and signaling, and ultimately that of cAMP-responsive gene transcription, despite equal efficacy for both cAMP production and PKA activity across all ligands. At the GIPR, Tirzepatide acted as a full agonist at most signaling and trafficking parameters, thereby acting as an equivalent to the GIPR mono-agonists, while MAR709 displayed strong but partial agonism at most parameters aside from cAMP.

The data presented within this PhD thesis support the hypothesis that the structure of GLP-1/GIP dual-agonists confer a biased agonism consisting of unique influences on receptor signaling, endosomal trafficking, and transcriptional responses, that may ultimately underlie *in vivo* efficacy as mediated by the individual GLP-1 and GIP receptors.

## Abstrakt

Fettleibigkeit, und die oft damit einhergehende Begleiterkrankung Typ 2 Diabetes (T2D) werden aufgrund ihrer weiten Verbreitung und der hohen körperlichen Belastung die sie verursachen, als weltweite Bedrohung für das Gesundheitssystem betrachtet. Die Hauptursache für Fettleibigkeit ist ein Ungleichgewicht zwischen übermäßiger Energieaufnahme und minimalem Energieverbrauch. Strategien, um die Balance zwischen Energieaufnahme und Energieverbrauch wieder auszugleichen, wobei auch der Blutzuckerstoffwechsel verbessert wird, sind in erster Linie Anpassungen des Lebensstils, bariatrische Chirurgie und Pharmakotherapie. In den letzten Jahren hat sich sowohl die Wirksamkeit als auch die Sicherheit von Pharmakotherapien, die auf Nahrungsaufnahme oder Energieverbrauch wirken, deutlich verbessert. In diesem Zusammenhang wurde auch das therapeutische Potential des endogenen „glucagon-like peptid-1“ (GLP-1), welches Insulinausschüttung durch den Inkretin-Effekt verstärkt, und im Zentralnervensystem ein Sättigungsgefühl verursacht, intensiv erforscht. Die peptidbasierte Behandlung von Fettleibigkeit und T2D wurde durch die exponentielle Verbesserung der Halbwertszeit der GLP-1 Analoga Semaglutid und Liraglutid, welche 97% bzw. 94% Sequenz-Homologie zu GLP-1 haben, revolutioniert. Während GLP-1 basierte Therapeutika trotz des anhaltenden Auftretens von negativen Nebenwirkungen inzwischen eine zentrale Rolle einnehmen, zeigt die Kombination von GLP-1 mit seinem Inkretin-Gegenüber „gastric inhibitory peptide“ (GIP) eine synergistische Verstärkung und Verbesserung des Dosis-Wirkungs Verhältnisses in wichtigen therapeutischen Endpunkten wie Gewichtsreduktion oder Verringerung der Nahrungsaufnahme. Kurz gesagt, durch Ko-Administration von GLP-1 und GIP werden vergleichbare therapeutische Endpunkte bei niedrigerer Dosis erzielt, wodurch das Verträglichkeitsprofil verbessert wird. Diese neuen Strategien, die Effekte von GLP-1 und GIP zu kombinieren, führten zur Entwicklung von unimolekularen GLP-1R/GIPR Dual-Agonisten, die Aminosäuresequenzen aus beiden Peptiden in einem Molekül vereinen. Diese unimolekularen Agonisten zeigen eine Verbesserung des therapeutischen Potentials sowohl gegenüber den beiden Mono-Agonisten, als auch gegenüber der gemeinsamen Verabreichung dieser. Es gibt jedoch noch viele offene Fragen zu diesen unimolekularen Agonisten. Insbesondere die Frage, ob die beobachteten therapeutischen Verbesserungen nur durch den dualen Agonismus der GLP-1R und GIPR Rezeptoren entstehen, oder aber ob die besonderen Sequenzen spezielle Veränderungen der Signale, des Transportes, oder des intrazellulären

Recyclings der Rezeptoren, und damit sogenannte funktionelle Selektivität verursachen. Bisherige Studien, in denen selektiv verschiedene Aminosäuren von GLP-1 ausgetauscht oder verändert wurden, haben gezeigt, dass dadurch Parameter wie Internalisierung, Rekrutierung von  $\beta$ -arrestin 1/2, cAMP-Signale oder Desensibilisierung verändert werden können. Solche sequenzbasierten Veränderungen des Signalisierens oder des Transportes führten auch zu Unterschieden in den in vivo Effekten auf Regulation der Glukosespiegel und Nahrungsaufnahme.

Das Ziel der hier vorgestellten Doktorarbeit ist es daher, die zeitliche und räumliche Dynamik des Signalisierens, Transportes und Recyclens der GLP-1 und GIP Rezeptoren, die durch die GLP1/GIP Dual-Agonisten MAR709 und Tirzepatid verursacht werden, im Vergleich mit ausgewählten GIPR und GLP1-1R Mono-Agonisten zu untersuchen.

Im Vergleich zu den GLP-1R Agonisten, einschließlich eines Monoagonisten der pharmakokinetisch auf MAR709 abgestimmt ist, zeigen sowohl MAR709 als auch Tirzepatid bestehende maximale cAMP Produktion trotz nur partieller Rekrutierung von  $G\alpha_s$ . Die besondere Signal-Dynamik dieser Dual-Agonisten zeigte sich auch in reduzierter Liganden-induzierter Internalisierung beider Zielrezeptoren. Trotz der niedrigeren Internalisierungsrate durch MAR709, unterschied sich die GLP-1R Ko-Lokalisierung mit dem Rab-11-assoziierten Recycling-Endosom nicht zwischen MAR709 und den GLP1-R Mono-Agonisten. Dennoch führte dies nicht zu einer schnelleren Rate der physischen wieder-Einführung des Rezeptors in die Plasmamembran bei MAR709-Behandlung. Interessanterweise stellten wir eine enge Korrelation zwischen der Liganden-induzierten Aktivierung von  $G\alpha_s$  Signalen,  $\beta$ -arrestin 1/2 Rekrutierung, Rezeptor Internalisierung, Endosomalem Transport und Signalisieren, und letztlich cAMP-abhängiger Gen-Transkription, obwohl die Wirksamkeit für cAMP-Produktion und PKA-Aktivierung bei allen Liganden gleich war. Tirzepatid wirkte als voller Agonist für die meisten Signalisierungs- und Transportparameter und wirkte daher Äquivalent zu den GIPR Mono-Agonisten, während MAR709 einen starken aber partiellen Agonismus in den meisten Parametern außer cAMP zeigte.

Die in dieser Doktorarbeit präsentierten Daten unterstützen die Hypothese, dass die Struktur von GLP-1/GIP Dual-Agonisten funktionelle Selektivität an deren Rezeptoren verursachen, die sich in besonderem Einfluss auf das Signalisieren, den endosomalen Transport, und transkriptionelle Aktivität manifestiert, und der letztlich wahrscheinlich die in vivo

Wirksamkeit zugrunde liegt, die durch die beiden einzelnen GLP-1R und GIP Rezeptoren verursacht wird.

---

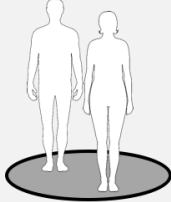
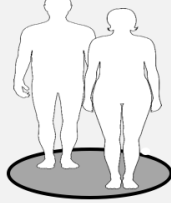
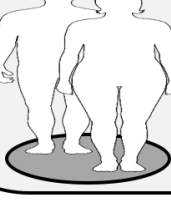
# **CHAPTER 1: Introduction**

---

---

## The Epidemic of Obesity and Type II diabetes

Obesity, and the often-associated Type 2 diabetes (T2D), have been inserted into the world stage due to high prevalence and health burden. By 2030, 50% of the United States adult population is expected to be overweight or obese, while on a global scale the epidemic is expected to reach up to 1.35 billion adult individuals (Kelly et al., 2008; Ward et al., 2019). Obesity is traditionally defined as having a Body Mass Index (BMI) greater than 30 (**Figure 1**) (WHO | Obesity, 2020), which is characterized as abnormal or excessive accumulation of fat relative to lean mass. Specifically, a BMI  $\geq 30$  indicates a substantial deviation away from the normal proportional relationship between weight (kg) and height (m<sup>2</sup>) that is expected on average (Eknoyan, 2021).

	<b>Classification</b>	<b>BMI (Kg/m<sup>2</sup>)</b>
	<i>Underweight</i>	$< 18.5$
	<i>Normal weight</i>	$18.5 - 24.99$
	<i>Overweight</i>	$\geq 25$
	<i>Pre-obese</i>	$25 - 29.99$
	<i>Obese</i>	$\geq 30$
	<i>Obese I</i>	$30 - 34.99$
	<i>Obese II</i>	$35 - 39.99$
	<i>Obese III</i>	$\geq 40$

**Figure 1: Classification of obesity status by BMI according to the World Health Organization (WHO).**

The classical driver of obesity is an imbalance between excessive energy intake and minimal caloric expenditure. This chronic imbalance of nutrient intake predisposes an individual to heightened systemic circulating glucose and fatty acid levels, along with the growth and expansion of adipose tissue (AT) (Zamboni et al., 2014). However, the underlying etiology behind this imbalance is not simple and is often multi-varied and complex. There are a large number of predisposing dietary factors, activity patterns, genetic-lifestyle interactions, and environmental exposures that contribute to the development of obesity (Hruby et al., 2016).



In a meta-analysis, it has been identified that up to 70% of the body weight differences observed between individuals can be attributed to inter-individual differences in genetic and epigenetic landscape (Elks et al., 2012).

Prominent monogenic sources of obesity have been identified as genes encoding for leptin, the leptin receptor (LepR), the melanocortin 4 receptor (MC4R) and pro-opiomelanocortin (POMC) (Myers and Leibel, 2015). However, for the majority of the population, monogenic mutations are rare and the current theory behind the genetic predisposition to obesity is emphasized within a polygenic mutation framework, in which combinations of numerous small-effect genetic variants cohere into an effect size that can be both independent of, and intertwined with, environmental risks (Khera et al., 2019). The interaction of polygenic risk with environmental factors, such as sex, socioeconomic status, race, and food availability, amplifies the effect size and ultimately contributes to the obesity epidemic (Domingue et al., 2014; Lee et al., 2019).

Nonetheless, on the molecular level, pathological changes present in adipose tissue, due to the culminating effect of obesity risk factors, normally precede the development of clinical comorbidities (Longo et al., 2019). The ability of individual white adipocytes to properly metabolize and store energy surplus under conditions of reduced AT oxygenation and blood flow, a context attributable to excess adiposity, is a key determinant in the development of pathological comorbidities (González-Muniesa et al., 2015; Goossens and Blaak, 2012). Impaired metabolism and systemic lipid buffering within white adipocytes can result in a decreased capacity for AT-mediated clearance of circulating triglycerides, which can negatively affect insulin sensitivity, cardiometabolic risk, atherosclerosis, and ectopic fat deposition in the liver and kidneys. In addition, hypertrophied adipocytes can lead to a systemic increase in pro-inflammatory adipokines such as tumor necrosis factor (TNF), interleukin-6 (IL-6), interleukin-18 (IL-18), and resistin, with a concomitant decrease in anti-inflammatory adipokines such as adiponectin, accentuating the risk of obesity-driven comorbidities (Ouchi et al., 2011). Taken together, the metabolic status of AT, as determined by diet, lifestyle, genetic predisposition and social cues, is an integrating influence into the systemic health profile of an individual, in which obesity represents a pathological avenue toward determinantal comorbidities.

## Insulin Resistance and Development of T2D

In 1936, the first noted differentiation between insulin sensitive and insulin insensitive diabetic human types was observed in a first of its kind hyperinsulinemic euglycemic clamp (Himsworth, 1936). Insulin is a peptidic hormone, secreted by pancreatic beta cells, that targets insulin receptor (IR) expressing tissue, where it then primarily enhances the target tissue's immediate uptake of glucose. T2D is characterized as a long-term chronic impairment in glucose regulation that can be either due to reduced insulin secretion (while maintaining systemic insulin sensitivity), or reduced insulin potency at IR-expressing target tissue (manifesting as systemic insulin insensitivity).

Normally, insulin accomplishes its enhancement of glucose uptake in target tissues by binding to the  $\alpha$  subunit of the IR, which consequently initiates IR  $\beta$  subunit-localized tyrosine kinase autophosphorylation and tyrosine phosphorylation of insulin-receptor substrate 1 (IRS-1). Within the target tissues of insulin, phosphorylated IRS-1 provokes a cascade of signals that ultimately lead to the translocation and insertion of glucose transporter type 4 (GLUT4) into the plasma membrane. When present at the plasma membrane, GLUT4 can interact with circulating extracellular glucose and facilitate its diffusion into the cell (Lee and Pilch, 1994). Insulin resistance, or insulin insensitivity, is then the inability of exogenous or endogenous insulin to stimulate an IR-mediated decrease in blood glucose levels through this mechanism. The primary tissues targeted by insulin for enhanced glucose uptake are skeletal myocytes, white adipocytes, hepatocytes and brain neurons, with skeletal muscle contributing to approximately 80% of insulin-stimulated glucose uptake and representing the primary defect of T2D (DeFronzo and Tripathy, 2009; Rask-Madsen and King, 2013).

Within the development and presence of obesity and ectopic fat deposition, increased circulation of AT-derived pro-inflammatory cytokines negatively affect IRS-1 activation (Dresner et al., 1999; Snel et al., 2012). This inhibitory effect can occur via enhanced IRS-1 serine phosphorylation, or through transcriptional reductions in IRS-1 expression (Makki et al., 2013; Tilg and Moschen, 2008). Consequentially, both visceral and muscular ectopic adiposity have been found to negatively correlate with insulin sensitivity (Pan et al., 1997; Zhang et al., 2015).

Generally, the insulin secreting  $\beta$ -cells of the pancreas will respond to chronically elevated peripheral insulin resistance by upregulating insulin secretion (DeFronzo, 2004). However, counterintuitively, chronic elevation of circulating insulin further reduces myocyte insulin

sensitivity, progressively decreases  $\beta$ -cell functionality, and leads to  $\beta$ -cells exhaustion and de-differentiation. Ultimately, the consequence of these developments lead to the induction of severe insulin resistance and the development of T2D (Iozzo et al., 2001; Talchai et al., 2012). Additionally, the prolonged hyperglycemia and high levels of circulating free fatty acids associated with obesity-driven insulin resistance deteriorate  $\beta$ -cell functionality via gluco- and lipotoxic mechanisms, which culminates as an increase in endoplasmic reticulum (ER) stress, alterations in  $\beta$ -cell metabolism, and induction of pro-apoptotic signals (Chang-Chen et al., 2008). The manifestation of insulin resistance, and its association with elevated circulating macronutrients and insulin, represent preceding steps to the deterioration of  $\beta$ -cell functionality, insulin synthesis, and insulin secretion, which when fulfilled, ultimately characterize T2D and reliance on exogenous insulin therapy to cope.

## Regulation of Food Intake and Energy Expenditure

Energy homeostasis represents a robust balance between energy intake and energy expenditure. Energy intake is defined as the amount of energy consumed from food or drink, and energy expenditure is the energy utilized for basal metabolic rate (BMR), the thermic effect of food, and external work (Heaney, 2013). The unit of biological energy is expressed as a calorie, in which a kilocalorie (kcal) equates to the energy required to increase the temperature of 1 kilogram (kg) of water by 1°C. In mice, energy intake is quantified by the consumption of kcal standardized food, while the amount of ingested energy that is then assimilated into metabolism warrants additional considerations and is adjusted using bomb calorimetry. The most commonly used method for measuring energy expenditure is by quantifying and calculating the amount of oxygen consumed and carbon dioxide produced using an indirect calorimeter system (Tschöp et al., 2011). Most healthy adults, in both humans and animals, maintain a steady body weight over years, indicating high conservation and robustness towards equating food intake with energy expenditure.

Several circulating peptides predominantly produced by adipocytes, the gastrointestinal tract, and pancreas influence food intake by modulating neural regions with far reaching regulatory effects such as the hypothalamus, brain stem, and autonomic nervous system (Cone et al., 2001). In particular, the hypothalamic arcuate nucleus, housing both anorexigenic POMC neurons and orexigenic agouti-related peptide (AgRP)/neuropeptide Y (NPY) neurons, acts as

the primary sensor of peripheral metabolic inputs that indicate host energy state (Cone et al., 2001).

From the gastrointestinal tract, the satiety inducing hormones Cholecystikinin (CCK), Glucagon-like peptide-1 (GLP-1), Gastric inhibitory peptide (GIP), and Peptide YY (PYY) all act within the hypothalamic feeding circuit. Most notable of the periphery-originating satiety hormones is the adipose-secreted hormone leptin (Ahima and Antwi, 2008). These anorexigenic hormones can either bind to and inhibit AgRP/NPY neurons, stimulate POMC neurons, or both (**Figure 2**). For example, leptin, via CNS-localized leptin receptors (LepR), simultaneously activates POMC neurons while inhibiting AgRP/NPY neurons, ultimately resulting in a reduction of energy intake (Baver et al., 2014; Cowley et al., 2001). When the POMC neuron is activated, it processes POMC to  $\alpha$ -melanocyte stimulating hormone ( $\alpha$ -MSH), which then acts at the MC4R within the neighboring paraventricular nucleus (PVN), thus inhibiting feeding. Conversely, the orexigenic hormone ghrelin is capable of inhibiting POMC neurons while simultaneously activating AgRP/NPY, therefore inducing strong feeding activity (Tschöp et al., 2000).

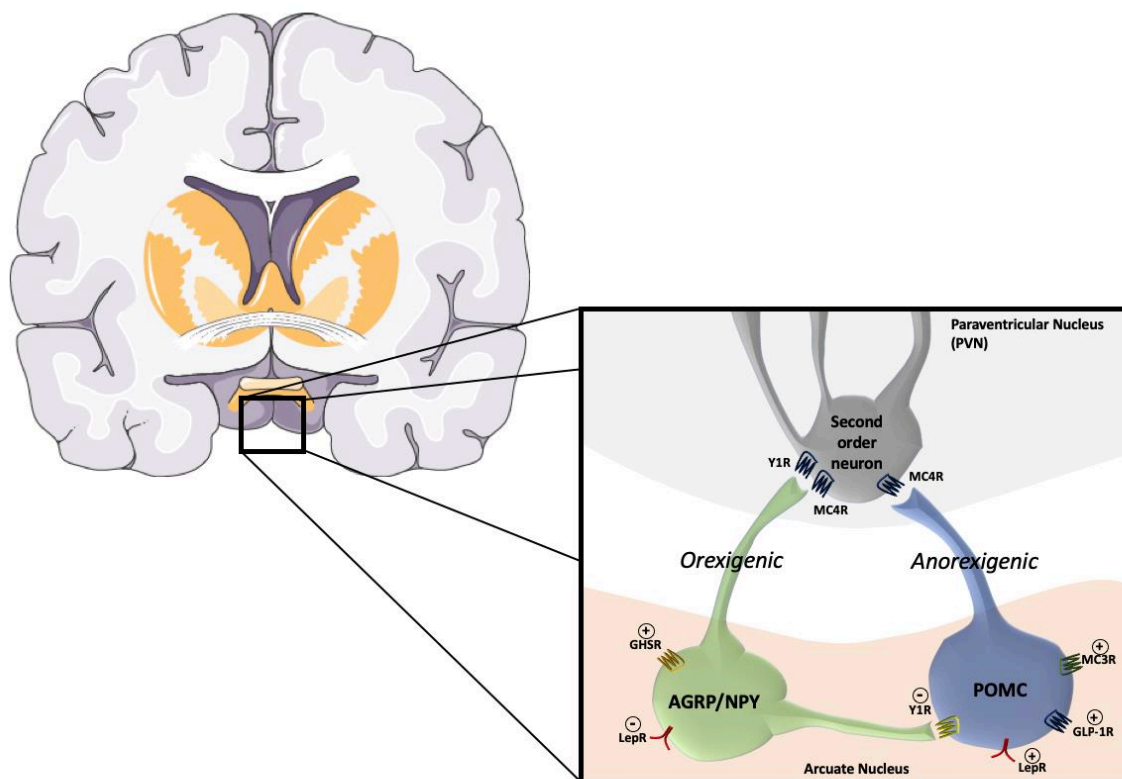


**Figure 2: Dynamic regulation of MC4R<sup>+</sup> PVN neurons according to the interplay between AgRP/NPY and POMC neural activation or inhibition.** AgRP/NPY and POMC neurons localized within the arcuate nucleus respond to endocrine stimuli and mediate orexigenic

(AGRP/NPY) or anorexigenic (POMC) status via regulation of downstream MC4R activity and AGRP/NPY to POMC communication. This figure was created using Sevier medical art and was inspired from Cone et al., 2001.

The mechanism for which ligand-stimulated energy expenditure occurs can be both dependent and independent of the hypothalamic POMC feeding circuit. Leptin, for example, stimulates sympathetic nervous system (SNS) outflow and an increase in energy expenditure by activating PVN-localized MC4R neurons via POMC projections (Haynes et al., 1999; Rahmouni et al., 2003). Although leptin has a moderate effect on increasing energy expenditure, other arcuate nucleus POMC-targeting ligands such as GLP-1 do not have the same energy expenditure effect, indicating ligand specificity for increases in energy expenditure (Bergmann et al., 2019).

Independent of the hypothalamic feeding circuit, brown adipose tissue (BAT) “uncoupling” represents a primary mechanism for increased energy expenditure. BAT has the capacity to induce thermogenesis due to high expression of uncoupling protein 1 (UCP1) on the inner mitochondrial membrane (IMM) (Aquila et al., 1985). Mitochondria without expression of UCP1 establish a competent proton gradient situated on either side of the inner mitochondrial membrane through substrate oxidation, which ultimately drives ATP synthesis. In this way, ATP synthesis is “coupled” to the energetic potential of the proton gradient, which itself is mediated by the availability of oxidizable substrate. In order to “decouple” ATP synthesis from substrate oxidation, UCP1 facilitates a short-circuited flow of protons across the IMM to dissipate the mitochondrial proton gradient, resulting in the conversion of proton gradient potential (as established by substrate oxidation) into heat instead of ATP (Nicholls and Locke, 1984). The thyroid hormone tri-iodothyronine (T3) and the now disbanded 2,4-Dinitrophenol (DNP), of which upregulate UCP1 expression and act as a membrane-penetrable proton ionophore respectively, are examples of molecules that can advantageously capitalize on the BAT uncoupling system for enhancements in energy expenditure. Often, the stimulated energy expenditure effects of a compound can be attributed to both enhanced hypothalamic sympathetic outflow and resulting downstream adrenergic-mediated upregulation of UCP1 in BAT, an effect that exemplifies the classical amphetamine-based mechanism of action in improvements of energy expenditure (Jones et al., 1992; Kong et al., 2003).

## The GLP-1 and GIP Receptors: The Incretin System in Gluoregulation and Satiety

### *GIP and GLP-1 Secretion*

The hormones GIP and GLP-1 are secreted peptides originating from the intestinal tract in response to luminal sensing of nutrients during food ingestion. Both peptides play an important role in stimulating the incretin response. Following GLP-1/GIP binding, the incretin effect is characterized as an amplification of pancreatic  $\beta$  cell insulin secretion during periods of hyperglycemic (Kreymann et al., 1987; McIntyre et al., 1964; Perley and Kipnis, 1967). From the first observation of an unknown intestinal factor whose insulinotropic efficacy was dependent on oral glucose consumption rather than intravenous glucose administration in 1964, to the identification of GIP and GLP-1 as incretin peptides a few years later, it wasn't until 1998 in which the dual-purpose potential of incretins to also simultaneously induce satiety was discovered. (Drucker et al., 1987; Dupre et al., 1973; Elrick et al., 1964; Holst et al., 1987).

Both K-cells and L-cells are enteroendocrine cell-types capable of directly sensing nutrient content in the intestinal lumen. GIP is secreted from K-cells, which are located within the duodenum and jejunum of the small intestine, whereas GLP-1 is secreted from L-cells located at the distal end of the small intestine and colon. Exposure to luminal carbohydrates and fats stimulate the basolateral secretion of GIP and GLP-1 into the hepatic portal system.

The secretion of GLP-1 relies on the apical entry of glucose into the L-cell and its subsequent metabolism into ATP, in which the increase in intracellular ATP concentrations stimulate ATP-sensitive  $K^+$  channel closure resulting in membrane depolarization and GLP-1 exocytosis. Non-metabolizable sugars and unsaturated long-chain free fatty acids can also stimulate GLP-1 secretion, however sodium-glucose co-transporter-dependent mechanisms and G-protein coupled receptor 120 activation respectively facilitate this response (Gribble et al., 2003; Reimann and Gribble, 2002).

The secretion of GIP and GLP-1 is not a straightforward process. Upon nutrient stimulation, bioactive GIP is post-translationally cleaved from a proGIP precursor by proprotein convertase 1/3 (PC1/3) within K-cells. Within L-cells, pro-glucagon is post-translationally cleaved by PC1/3 into GLP-1, GLP-2, oxyntomodulin, intervening peptide-2 (IP2), and glicentin (**Figure 3**). The biologically active GIP and GLP-1 products are secreted out of the basolateral surfaces of the respective cells primarily as GIP (1-42), GLP-1 (7-36 amide) and GLP-1 (7-37). Most active GLP-

1 in circulation appears predominately in the amidated form as mediated by  $\alpha$ -amidating monooxygenase, in which the primary function of the amide group is to enhance the survival and stability of GLP-1 in plasma (Orskov et al., 1994; Wettergren et al., 1998). Immediately following basolateral secretion of GIP and GLP-1, dipeptidyl peptidase-4 (DPP-4), a serine exopeptidase that cleaves X-alanine segments from the N-terminus of peptides, rapidly cleaves between the second and third amino acids to produce GIP (3-42) and GLP-1 (9-36 amide), thereby inactivating the biological activity of both peptides (Kieffer et al., 1995). The short 2-5 minute half-life of GLP-1 and GIP is due to high expression of DPP-4 by multiple tissues, and the adjacent positioning of DPP-4 at the enteric vasculature around K-cells and L-cells, which ultimately allows less than half of the secreted incretins to reach portal circulation (Hansen et al., 1999). However, it appears GIP is less susceptible to DPP-4 inactivation, as exogenous infusion of either incretin demonstrated a retention of 40% active GIP and 20% GLP-1 (Deacon et al., 2000; Deacon et al., 1995b).

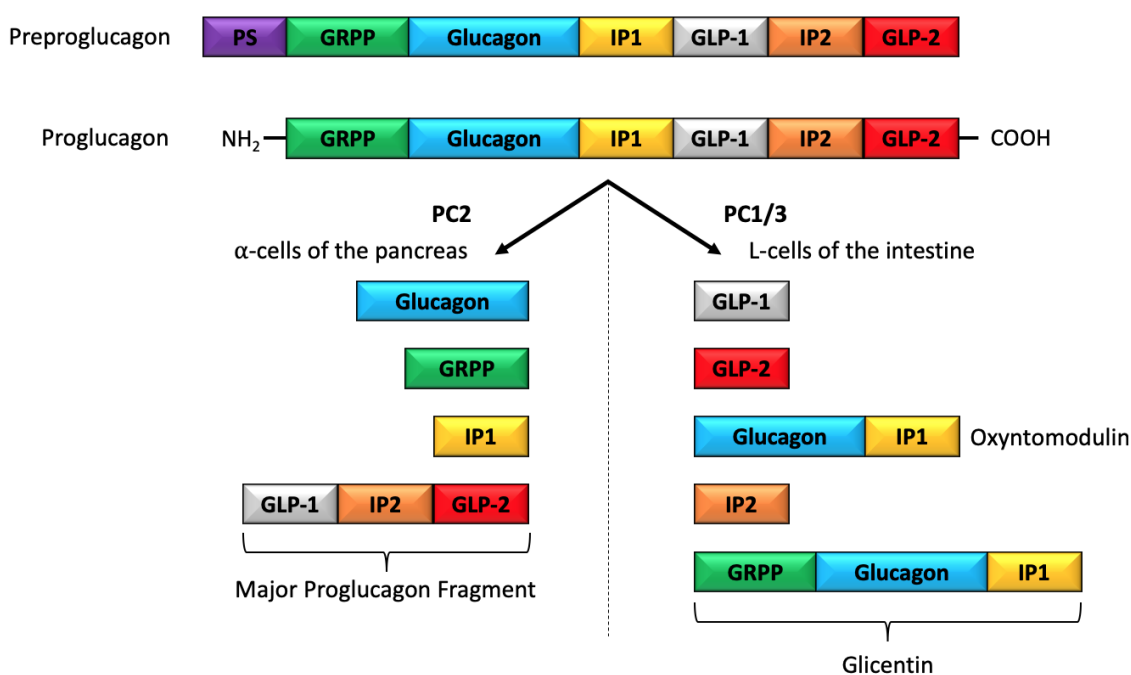


**Figure 3: Tissue-specific processing of preproglucagon.** The proglucagon precursor protein is cleaved from preproglucagon following enzymatic removal of the signal peptide (PS). Within L-cells of the small intestine, prohormone convertase 1/3 (PC1/3) cleaves and breaks down proglucagon into separate proteins consisting of GLP-1, GLP-2, oxyntomodulin, IP2, and glicentin. The resultant GLP-1 is predominantly found in the form of GLP-1 (7-37) and GLP-1 (7-36 amide). Within  $\alpha$ -cells of the pancreas, the proglucagon precursor is instead cleaved and broken down by prohormone convertase 2 (PC2) resulting in glucagon, glicentin-related pancreatic polypeptide (GRPP), IP1, and a major proglucagon fragment.

### *Systemic GIP actions*

GIP, secreted from the intestine, targets pancreatic  $\beta$ -cells to enhance glucose-dependent insulin secretion, increase insulin biosynthesis and  $\beta$ -cells proliferation, and reduce markers of ER stress (Wang et al., 1996; Yusta et al., 2006). Not all GIP effects are located at the  $\beta$ -cell however, GIP also targets extrapancreatic tissues such as the central nervous system (CNS), bone, and adipose tissue. In the CNS, GIPR activation promotes proliferation and differentiation of neural progenitor cells and may ultimately influence the development of behavior (Nyberg et al., 2005). Recent evidence has additionally identified a degree of GIPR expression in the arcuate, dorsomedial, and paraventricular nuclei of the hypothalamus, suggesting that it may regulate energy balance via food intake independently of GLP-1R (Adriaenssens et al., 2019; Zhang et al., 2021b). In WAT, GIP acts as an anabolic agent to: reduce lipolysis, enhance lipid uptake, elicit triglyceride formation to buffer against elevated circulating lipids, increase adipocyte sensitivity to insulin, and promote insulin-stimulated adipocyte GLUT4 translocation (Mohammad et al., 2011; Yip et al., 1998; Yip and Wolfe, 2000). In line with the GIP action at WAT, relatively enhanced GIP secretion upon an oral glucose stimulus has been found within obese individuals in comparison to lean individuals (Salera et al., 1982). Additionally, a genome-wide association study (GWAS) identified GIPR as positively associated with the development of increases in body mass index (Speliotes et al., 2010). However, the GIP receptor is an enigmatic receptor, particularly when it comes to linking directly to obesity. Approaches to GIPR pharmacology have surprisingly evidenced both GIPR antagonism and agonism to protect against diet-induced increases in body weight (Finan et al., 2016; McClean et al., 2007). Paradoxically, both gain-of-function and loss-of-function models of GIPR in mice have also been evidenced to protect against diet-induced obesity (DIO). Altogether, conflicting data from multiple studies makes it difficult to conclude the therapeutic role of GIP in diabetes and obesity (Campbell, 2021).

### *Systemic GLP-1 actions*

Circulating GLP-1 evokes biological action in several tissues via GLP-1R. These tissues include the pancreas, CNS, peripheral nervous system (PNS), and gastrointestinal system. In principle, GLP-1 facilitates the glucose-dependent insulinotropic response. However, it also suppresses glucagon secretion, induces satiety, inhibits gastric motility, and small intestinal transit (MacDonald et al., 2002).



In the pancreas, GLP-1 acts at  $\beta$ -cells to stimulate glucose-dependent insulin release, support the replenishment of insulin storage in  $\beta$ -cells through insulin mRNA upregulation and biosynthesis, increase  $\beta$ -cell proliferation and mass, and prevent cytotoxicity and apoptosis in animal models of diabetes (Drucker, 2003; Drucker *et al.*, 1987; Mojsov *et al.*, 1987). Additionally at the pancreas, GLP-1 is not restricted to only  $\beta$ -cells, but also inhibits glucagon secretion and promote somatostatin secretion via GLP-1R expressed within  $\alpha$ -cells and  $\delta$ -cells (Fehmann and Habener, 1991; Zhang *et al.*, 2019).

The GLP-1R is also expressed within hypothalamus and brain stem of the CNS. In the hypothalamus, the GLP-1R is primarily expressed in the PVN, arcuate nucleus (ARC), and the dorsomedial hypothalamus (DMH), with a greater density of GLP-1R expressed in POMC neurons than in AgRP neurons (van Bloemendaal *et al.*, 2014). GLP-1 is well-known to induce satiety via CNS mechanisms as first evidenced by intracerebroventricular (ICV) injections of GLP-1 (Tang-Christensen *et al.*, 1996; Turton *et al.*, 1996). The CNS-specific effects of GLP-1 on satiety and body weight loss are primarily mediated by hypothalamic activation of GLP-1R+ POMC neurons and indirect inhibition of AgRP/NPY neurons, in both mice and humans (Flint *et al.*, 1998; Secher *et al.*, 2014).

Interestingly, the location of action for GLP-1 mediated suppression of food intake is not only restricted to the CNS. The blood-brain barrier impermeable GLP-1R agonist Albugon (human GLP-1–albumin recombinant protein) also inhibited food intake and induced c-FOS activation in feeding-related CNS nuclei after both ICV and intraperitoneal administration (IP) in mice (Baggio *et al.*, 2004). This finding indicates that activation of peripheral nervous system (PNS) vagal afferents can relay satiety signals to CNS feeding centers in the brain (Baraboi *et al.*, 2011). Additionally, the effect of GLP-1 inhibition on gastric emptying and gastric acid secretion depends on both the direct activity at GLP-1R<sup>+</sup> gastric parietal cells, and GLP-1R vagal afferent transduction to the CNS (Broide *et al.*, 2013; Imeryüz *et al.*, 1997).

### *The Effect of Obesity and Diabetes on Incretin Action*

In obese or T2D individuals, loss in the efficacy of the incretin effect is an early determinant of T2D development, and has occurred despite mostly normal rates of GIP and GLP-1 secretion (Holst *et al.*, 2011; Muscelli *et al.*, 2008). However, the loss in incretin efficacy is not equal between GIP and GLP-1. T2D confers a greater loss, or resistance, in efficacy towards GIP than to GLP-1 (Nauck *et al.*, 1993c). The preserved capacity for GLP-1 to stimulate an effective,

albeit reduced, insulinotropic response within the context of obesity and T2D during exogenous GLP-1 administration has securely placed GLP-1 on the forefront of pharmaceutical development and design. In the context of healthy human subjects, approximately 50-70% of the total insulin released during hyperglycemia is attributed to the incretin effect, in which the effects of both GIP and GLP-1 are additive toward insulin secretion (Nauck and Meier, 2016). Interestingly, when administered at physiological concentrations in healthy individuals, GIP is identified to produce most of the incretin response while GLP-1 adds just a minor contribution (Nauck et al., 1993a).

As mentioned, the incretin effect is largely eliminated in patients with T2D. This suggests that the decrease in systemic efficacy of GIP and GLP-1 plays a role in the pathological development of diabetes and its comorbidities (Meier and Nauck, 2010). However, questions remain whether the loss of the incretin effect is causal or consequential to the development of T2D. Despite the incretin effect accounting for approximately 70% of the postprandial insulin response in healthy individuals, this effect is reduced to approximately 20% in patients with T2D (Nauck et al., 1986). Evidence has pointed to a reduction in incretin efficacy occurring simultaneous to the transient development of hyperglycemia and insulin resistance in healthy subjects on a 12-week experimental trial of steroid treatment, physical inactivity, and a high caloric diet (Hansen et al., 2010). In this way, a decrease in incretin efficacy is at least capable of being mediated by exogenous sources, however the etiology of the reduction in incretin efficacy within obese and T2D patients is not fully understood.

The impairment in GIP action within unhealthy T2D subjects has continuously been shown as a 50% reduction in GIP insulinotropic efficacy relative to healthy subjects (Nauck *et al.*, 1993c). Particularly, relevant to pharmaceutical applications, increasing exogenous GIP dosing past physiologically levels does not make up for the loss in efficacy (Meier et al., 2004). However, not all the efficacy of GIP is lost in T2D, as specific dynamics of the GIP signaling system seem more intact during an immediate bolus of intravenous GIP rather than continuous infusion (Meier et al., 2004). This finding indicates that the GIP receptor system is saturable, and that hyperglycemia-induced downregulation of GIPR mRNA and protein expression may shift the saturable framework of GIPR availability and activity to levels not beneficial pharmacologically within T2D (Grespan et al., 2021; Xu et al., 2007).

Other avenues of GIPR desensitization, and its consequential effect on insulin sensitivity, may be found within altered GIPR trafficking dynamics. WAT-specific GIPR E354Q variant displays

minimal recycling back to the plasma membrane following ligand-induced receptor internalization (Mohammad et al., 2014). While no direct evidence has yet been identified linking the development of systemic T2D to abnormal GIPR trafficking, endogenously occurring truncated splice variants of GIPR in mice have been shown to negatively modulate trafficking and signaling of the co-expressed full-length GIPR at the plasma membrane (Harada et al., 2008). Despite advances, full understanding of the consequential effects of alterations in GIPR expression, trafficking, and regulation on systemic metabolism have yet to be fully elucidated.

The insulinotropic effect of GLP-1 is mostly preserved within T2D, however a reduction in efficacy by 29% compared to healthy subjects has been observed (Nauck *et al.*, 1993c). Despite persistence of GLP-1 efficacy within T2D, hyperglycemia has been shown downregulate the expression of GLP-1R and its presence at the plasma membrane via protein kinase C (PKC) or protein kinase A (PKA) interacting mechanisms as evidenced in perfused and primary mouse islets (Rajan et al., 2015; Xu *et al.*, 2007). However, as GLP-1R downregulation occurs during hyperglycemia, evidence suggests that short-term normalization of fasting glucose can resensitize the GLP-1R system (Højberg et al., 2009; Iizuka et al., 2012). Therefore, despite the minor hyperglycemia-induced decreases in GLP-1R efficacy, the dynamic nature and general persistence of GLP-1R responsiveness make it a useful target in pharmacological approaches to T2D.

## Insulin and Glucagon Secretion

### *Basic Anatomy of the Pancreas*

The pancreas is an essential organ located within the abdomen that is involved in exocrine and endocrine functions critical to digestion and the regulation of systemic blood glucose levels. The exocrine pancreas produces enzymes that are secreted into the intestinal tract to facilitate the digestion of proteins, carbohydrates, and fats. The endocrine pancreas secretes circulating hormones such as glucagon, somatostatin, and insulin, which cooperatively function to maintain proper blood glucose concentrations critical to organ functionality. The endocrine pancreas is primarily populated with three cell types:  $\alpha$ -cells,  $\beta$ -cells, and  $\delta$ -cells, which produce glucagon, insulin, and somatostatin respectively (Da Silva Xavier, 2018). Glucagon functions to increase systemic blood glucose concentrations during bouts of

hypoglycemia, insulin functions to facilitate rapid glucose uptake in insulin-responsive tissues thereby lowering blood glucose during bouts of hyperglycemia, and somatostatin functions to negatively regulate glucagon and insulin secretion (Huising, 2020; Watts et al., 2016).

### *Processing and Maturation of Insulin*

Insulin secretion is a potently activated  $\beta$ -cell response within the context of hyperglycemic conditions during the post-prandial state. Mature insulin is a 5.8-kDa protein consisting of two disulfide-linked peptide chains (Dodson and Steiner, 1998). Before glucose stimulation, insulin mRNA is translated into preproinsulin, which consists of an amino-terminal B chain, a carboxy-terminal A chain, and a connecting chain called the C-peptide. Preproinsulin is directed into the endoplasmic reticulum as a single chain molecule of 110 amino acids, where its signal peptide is removed to form proinsulin. Subsequent vesicular transfer of multiple proinsulin molecules to the Golgi facilitates the formation of zinc proinsulin hexamers. Following, the C-peptide chains are cleaved away, resulting in a precipitated crystalized mature zinc insulin hexamer and an independent C-peptide. Ultimately, the insulin-containing vesicles are directed to a plasma membrane-associated pool to be readily available for the event of glucose-stimulated exocytosis (Dodson and Steiner, 1998; Fu et al., 2013)

### *Insulin Secretion*

The secretion of insulin follows two phases, a first phase consisting of an acute release of stored insulin, and a second phase of sustained continuation of insulin secretion at a lower rate and amplitude. Upon post-prandial increases in blood glucose, glucose is shuttled across the  $\beta$ -cell plasma membrane via the glucose transporter 2 (GLUT2) in mice, and GLUT1 and GLUT3 in humans (McCulloch et al., 2011). The incoming glucose is directly metabolized to modulate intracellular ATP/ADP ratios. The resulting increase in ATP triggers closing of the Kir and Sur subunits of the ATP-dependent K-channels ( $K_{ATP}$ ), which results in the depolarization of the plasma membrane (Fu *et al.*, 2013). To compliment, activated voltage-gated  $Ca^{2+}$  channels induce an influx of  $Ca^{2+}$  further depolarizing the plasma membrane (Koster et al., 2005). The resulting increase in intracellular  $Ca^{2+}$  triggers the exocytosis of the available pre-synthesized pool of insulin-containing vesicles, which have been previously localized to the plasma membrane by a complex of proteins. This complex of proteins also initiates the formation of a membrane fusion pore, from which the insulin is then released into the

extracellular space (Koster *et al.*, 2005). This first phase of insulin release is characterized as a sharp increase in circulating insulin following the initial increase of glucose, in which a subsequent decline in insulin secretion is eminent over the next 10-20 minutes (Campbell and Newgard, 2021).

The initiation of the second phase of insulin secretion allows for sustained release of insulin over time, albeit with a lower magnitude. The second phase begins within the wake of the declining output of the first phase response. The second phase typically spans 2-3 hours, and is largely driven by  $K_{ATP}$ -independent mechanisms, as at this point the  $\beta$ -cell is maximally saturated with  $Ca^{2+}$  (Campbell and Newgard, 2021). The first phase insulin response is associated with the release of approximately 1% of the pre-synthesized plasma-membrane associated pool of insulin-containing vesicles, while the second phase causes the continued release of the remaining membrane-localized primed vesicles and recruitment of insulin-containing vesicles from the intracellular space to the plasma membrane (Campbell and Newgard, 2021).

The intracellular machinery primarily regulating the catabolism of the incoming glucose is glucokinase, which is the rate-limiting step facilitating the phosphorylation of glucose to glucose-6-phosphate. In the  $\beta$ -cell of mice and man, glucokinase is expressed as opposed to other hexokinase subtypes. The expression of glucokinase is advantageous to the  $\beta$ -cell as it has a low sensitivity  $K_m$  ( $\sim 10$  mM) and a high  $V_{max}$ , meaning that it allows for excess glucose uptake capacity relative to the metabolic rate so that glucose transport across the  $\beta$ -cell plasma membrane is not a rate-limiting step in the sensing of extracellular glucose (Matschinsky, 2002). Hexokinase subtypes, on the other hand, typically have a high sensitivity  $K_m$  ( $\sim 0.2$  mM) and low  $V_{max}$ , lending themselves capable of sensing and metabolizing dynamic ranges of glucose flux. (Matschinsky, 2002). The high  $V_{max}$  of glucokinase is due to a lack of a specific N-terminal domain present on hexokinase, which is an allosteric site for inhibiting activity during exposure to excess levels of glucose-6-phosphate (Campbell and Newgard, 2021). With the glycolytic rate-limiting step of glucose to glucose-6-phosphate conversion performed by a high  $V_{max}$  glucokinase, the resulting increased capacity in glycolytic throughput and conversion to ATP allows for a proportional insulinotropic response against sharp increases in blood glucose.

## Glucagon Secretion

Glucagon is typically seen as antithetical to insulin and its glucose-lowering attributes. Glucagon is a 3.5-kDa peptide cleaved from the precursor peptide proglucagon by prohormone convertase 2 (PC2) in pancreatic  $\alpha$ -cells (Habegger et al., 2010; Mojsov et al., 1986). Glucagon secretion is regulated through several endocrine and paracrine mechanisms. Namely, the most potent stimulus for  $\alpha$ -cell glucagon secretion is hypoglycemia, whereas elevated amino acids and GIP (in low glucose-conditions) also facilitate glucagon secretion (Müller et al., 2017). Alternatively, hyperglycemia is a potent inhibitor of glucagon secretion. In addition, intestinal-derived GLP-1 at the  $\alpha$ -cell acts as an endocrine inhibitor of glucagon secretion, as do the paracrine actions of somatostatin, insulin, zinc, and potentially amylin. Interestingly, glucagon may influence its own regulation through insulinotropic feedback from glucose-stimulated  $\beta$ -cells (Müller *et al.*, 2017).

In  $\alpha$ -cells, the principle mechanism behind glucagon secretion is opposite to the paradigm of insulin secretion. During hypoglycemic conditions, the lack of glucose uptake across the  $\alpha$ -cell plasma membrane via GLUT-1 results in a low intracellular ATP:ADP ratio (Gromada et al., 2007). The low ATP:ADP ratio initiates  $\alpha$ -cell  $K_{ATP}$  closure, which subsequently elicits membrane depolarization and opening of voltage-gated  $Ca^{2+}$  and  $Na^{+}$  channels. In a similar fashion to  $\beta$ -cell insulin secretion, these depolarization and calcium-influx promoting events ultimately lead to the exocytic release of glucagon (Müller *et al.*, 2017). Oppositely, during hyperglycemia, the high ATP:ADP ratio in  $\alpha$ -cells does not cause  $K_{ATP}$  closure, therefore no depolarization and hence no glucagon secretion occurs (Müller *et al.*, 2017).

## G-protein Coupled Receptors

### Background

G-protein coupled receptors (GPCRs) are the largest protein family in the human proteome and are a key mediator in the transduction of signals across membranes to initiate coordinated cascades of intracellular responses (Heng et al., 2013). GPCRs are characterized as membrane-bound structures that, despite having a relatively generalizable structure, diversely recognize a wide variety of ligands, which can include photons, ions, small molecules, and peptides. Due to the high number of GPCRs, and their collective ability to recognize a variety of ligands with tractability over multiple intracellular signaling cascades, a critical role is attributed to these

receptor in regulating outcomes on both intracellular and systemic scales (Katritch et al., 2012). These attributes make GPCRs a premier target in pharmacological intervention and drug discovery (Sriram and Insel, 2018). In recent years, GPCR drug discovery research for major disease indications has shifted toward diabetes and obesity, and has recently represented approximately 10% of total agents put through clinical trials, with approximately 34% of all clinically approved drugs targeting GPCRs (Hauser et al., 2017).

### *GPCR: Class Categorization*

GPCRs are categorized by class. This designation is based on sequence, structure, and function. These designations consist of Class A (rhodopsin-like), Class B (secretin family), Class C (metabotropic glutamate), Class D (fungal mating pheromone receptors), Class E (cAMP receptors), and Class F (frizzled and smoothed receptors). Between these classes, all GPCR members share an N-terminal extracellular domain, and a common seven transmembrane (7TM) spanning domain (TMD), which has 3 corresponding intra- and extra- cellular loops, and an intracellular carboxyl (C)-terminal domain. The N-terminal extracellular domain typically consists of 100-150 amino acids that form a secondary structure consisting of an  $\alpha$ -helix and four  $\beta$ -strands held together by three conserved disulfide bonds (Lee et al., 2015). Despite the common GPCR base architecture, the N-terminal domains and core ligand binding pockets between GPCRs share low amino acid sequence homology, which confers the diversity of class and function. Class A receptors recognize ligands at their 7TM spanning core domain, facilitate transient recruitment of  $\beta$ -arrestin 2, and generally lack the capacity for sustained endosomal signaling. Class B receptor ligand recognition occurs at two sites, via the peptide's N-terminal interactions with the GPCR core TMD, and the peptide's C-terminal interaction with the GPCR's large N-terminal extracellular domain. Generally, class B GPCRs bind both  $\beta$ -arrestin isoforms equally and promote stable GPCR- $\beta$ -arrestin interactions (Basith et al., 2018; Jean-Charles et al., 2017; Oakley et al., 2000).

### *GPCR: Ligand Binding and Receptor Activation*

In principle, ligand binding to a GPCR's transmembrane extracellular-facing pocket induces a conformational change of the TMD at both the outer and inner membrane leaflets. The ligand-induced structural shift of the GPCR facilitates its interaction with a variety of cytosolic and membrane-bound proteins. The initial proteins recruited to and interacting with the ligand-

bound GPCR are the heterotrimeric G proteins. The heterotrimeric G proteins represent the mediating signal transduction channel between ligand binding at the GPCR and intracellular events.

Heterotrimeric G-proteins are guanine nucleotide binding proteins composed of three subunits,  $\alpha$  ( $G\alpha$ ),  $\beta$  ( $G\beta$ ), and  $\gamma$  ( $G\gamma$ ) (Milligan and Kostenis, 2006). The phosphate status of the guanine nucleotide bound to the G-protein dictates its activity, in which guanosine diphosphate (GDP) and guanosine triphosphate (GTP)-bound  $G\alpha$  subunits represent the inactive and active state, respectively. In the inactive state, the  $G\alpha$  subunit is also bound to the  $G\beta$  and  $G\gamma$  subunits. Upon ligand binding, the GPCR assumes a conformational status that increases the affinity for G-protein binding. This G-protein interaction with the receptor causes the G-protein to release its GDP molecule (Calebiro et al., 2021). When GDP is released, the receptor and the heterotrimeric G-proteins form a stable high-affinity complex that opens the  $G\alpha$  subunit to binding GTP. The concentration of GTP is approximately 10 times higher than GDP within the cytosol, which allows for the ready replacement of GDP by GTP, and thus characterizes the GPCR as a guanine nucleotide exchange factor (GEF) (Bos et al., 2007; Calebiro *et al.*, 2021). When GTP binds to the  $G\alpha$  subunit, the heterotrimeric complex is disrupted, which allows for dissociation of the  $G\alpha$  subunit from the  $G\beta$  and  $G\gamma$  complex. The liberated catalytic  $G\alpha$  subunit is able to act on downstream effector proteins, while the non-catalytic  $G\beta\gamma$  complex can modulate other downstream protein-protein interactions (Oldham and Hamm, 2008; Smrcka, 2008). GTP-bound  $G\alpha$  subunits are intrinsic, however weak, GTPases (Ross, 2008). Therefore, over a course of seconds to minutes, GTP will be hydrolyzed to GDP deactivating the  $G\alpha$  subunit. This attribute of slow intrinsic GTPase activity of the G-protein may act as a control on signal amplitude, as new signaling information cannot be integrated until GTP hydrolysis occurs. However, regulators of G-protein signaling (RGS), which stimulate intrinsic  $G\alpha$  GTPase activity by as much as 1,000 fold, can accelerate GTP hydrolysis (Calebiro *et al.*, 2021).

### ***GPCR: $G\alpha$ Subunits and GPCR Signal Termination***

The  $G\alpha$  subunit is most broadly categorized into 4 different subtypes, which are defined by their downstream interaction with effector proteins and unique cellular response. The 4  $G\alpha$  subtypes are:  $G\alpha_s$ , which directly interacts with adenylate cyclase (AC) and raises cyclic AMP (cAMP) thus stimulating Protein Kinase A (PKA) among several other downstream kinases;



$G\alpha_{i/0}$ , which inhibits AC activity and is counteractive to  $G\alpha_s$ ;  $G\alpha_{q/11}$ , which activates phospholipase C  $\beta$  thus increasing intracellular inositol triphosphate (IP3) and membrane-localized diacylglycerol (DAG) which together modulate a unique set of downstream kinases; and  $G\alpha_{12/13}$ , which is involved in the activation of Rho GTPases (Wettschreck and Offermanns, 2005). Following GPCR-ligand binding and subsequent  $G\alpha$  activation, signal termination is initiated by GPCR kinase (GRK) phosphorylation of specific serine/threonine residues on the C-terminal domain of the activated GPCR. These phosphorylated residue patterns encode motifs for  $\beta$ -arrestin binding to the receptor C-terminal domain.  $\beta$ -arrestins, when bound to the GPCR, sterically inhibit further G-protein activation, effectively terminating the GEF capacity of the GPCR- $G\alpha$  interaction (Calebiro *et al.*, 2021). However, although  $\beta$ -arrestin binding terminates canonical GPCR signaling, recruited  $\beta$ -arrestin can also confer additional G-protein-independent signaling such as inducing specific transcriptomic profiles, mitogen activated protein kinases (MAPK) activity, and anti-inflammatory actions by inhibition of NF $\kappa$ B activation (van Gastel *et al.*, 2018).

## Structure of the GLP-1R and GIPR

### *Commonalities*

The GLP-1 and GIP receptors are characterized as class B secretin family GPCRs. These receptors are predominantly  $G\alpha_s$  coupled with varying, and sometimes debatable, degrees of  $G\alpha_q$  activity (Iyengar *et al.*, 1988; Montrose-Rafizadeh *et al.*, 1999a; Xu and Xie, 2009; Yip *et al.*, 1998). As these receptors are class B, ligand binding follows a two-domain model in which the C-terminal region of the ligand binds to the N-terminal GPCR extracellular domain thus determining affinity and specificity, while the N-terminal region of the ligand binds to the TMD to activate the receptor. Specifically, the GPCR N-terminal extracellular domain and the TMD work in concert to facilitate ligand binding into the 7TM binding pocket, in which the initial movement of the ligand-bound N-terminal extracellular domain facilitates optimal orientation of the ligand into the TMD (Yang *et al.*, 2016). When GLP-1 is exposed to an experimental GLP-1 receptor containing a denatured and alternatively renatured N-terminal extracellular domain, GLP-1 loses almost complete affinity to the receptor (Bazarsuren *et al.*, 2002). In compliment, GLP-1 binds with less affinity to an isolated GLP-1R N-terminal extracellular domain than it does to the native full length receptor, indicating that both the GPCR

extracellular N-terminal domain and the TMD work in concert to establish ligand affinity and stability (Bazarsuren *et al.*, 2002).

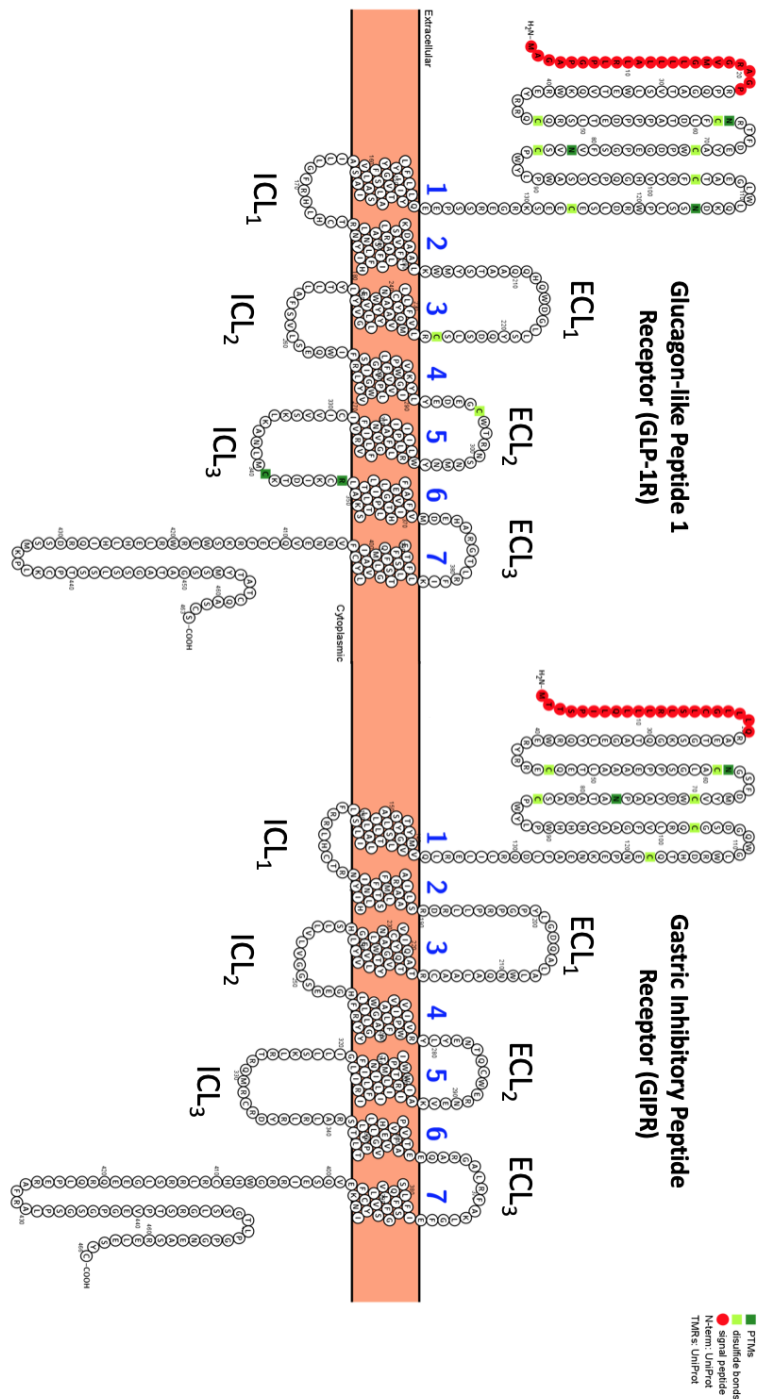


**Figure 4: Structure of human GLP-1R and GIPR.** The GLP-1R and GIPR consist of an extracellular N-terminal domain, seven  $\alpha$ -helical transmembrane segments (1-7) connected via three intracellular (ICL<sub>1</sub>-ICL<sub>3</sub>) and extracellular loops (ECL<sub>1</sub>-ECL<sub>3</sub>), and an intracellular C-terminal domain. Common to class B GPCRs, the extracellular N-terminal domain is stabilized by six cysteine residues (highlighted in green). The cleavable signal peptide (highlighted in red), located at the N-terminus, is required for processing and cell-surface expression of both

the GLP-1R and GIPR. Specific amino acids targeted for post-translational modifications are highlighted in purple and may influence receptor cell surface expression and receptor degradation. PTM: Post-translational modification. This figure was created using the Protter Software.

### *GLP-1R Structure*

The GLP-1R is a 463 amino acid transmembrane protein (**Figure 4**). The first clone of the GLP-1 receptor was generated from rat pancreatic islet cDNA isolated in 1992, while the first human GLP-1R clone was successfully generated in 1993 (Dillon et al., 1993; Graziano et al., 1993; Thorens, 1992). The human GLP-1R shares conserved amino acid homology to the chimp, cynomolgus monkey, pig, rat, mouse, and rabbit GLP-1R, of 100%, 98%, 93%, 91%, 92%, and 91% respectively (Knudsen et al., 2012). General structures include a cleavable signal peptide at the GLP-1R N-terminus required for biosynthetic processing and trafficking toward the plasma membrane, conserved N-terminal cysteine residues critical to the secondary structure of the extracellular domain, and glycosylation sites critical for GLP-1R insertion into the plasma membrane (Bazarsuren *et al.*, 2002; Huang et al., 2010; Whitaker et al., 2012). In principal, the third intracellular loop of GLP-1R has been identified as the sight for  $G\alpha_s$  localization at the GLP-1R (Hällbrink et al., 2001).

### *GIPR Structure*

The human GIP receptor is 466 amino acids in length and has approximately 40% sequence homology to the human GLP-1R (**Figure 4**) (Al-Sabah, 2016). Sequence homology between species of the human GIPR is 92% and 87% to that of rhesus monkeys and cattle, and 82% in both rats and mice. Despite a relatively high sequence homology between the GLP-1R and GIPR, the GIPR is not as markedly conserved across humans and mice (92% for GLP-1R, 82% for GIPR). As a consequence, and due to species-specific differences in endogenous GIP sequence, the human GIP loses a degree of potency at the mouse and rat GIP receptors (Sparre-Ulrich et al., 2016). GIP is a 42 amino acid long peptide. The mouse GIP (1-42) differentiates itself from human GIP (1-42) via two arginine substitutions at position 18 and 30. GIPR activation requires the binding of the central 8-30 amino acids of GIP to the N-terminal extracellular domain for specificity and affinity, and the first 7 amino acids of GIP for activation of the GIPR through the TMD (Yaqub et al., 2010). Rather than inertly sitting at the plasma membrane in the unstimulated state, the ligand-free GIPR is evidenced to have

constitutive basal activity almost 3x greater than that of GLP-1R, and is constitutively trafficked and recycled between the plasma membrane and cytosolic space. A naturally occurring variant of the GIPR (E354Q) shifts the constitutive internalization/recycling equilibrium toward increased receptor degradation resulting in reduced presence of the GIPR at the plasma membrane, an effect which has been associated with insulin resistance and T2D (Al-Sabah et al., 2014; Mohammad *et al.*, 2014). The GIPR also contains site-specific glycosylation sites that are important for its proper folding and insertion into the plasma membrane (Whitaker *et al.*, 2012), while other segments of the GIPR are responsible for heterodimerization with GLP-1R following GLP-1 administration (Schelshorn et al., 2012).

## GPCR Signaling

### *Commonalities*

Despite a generalizable structure between GPCRs within the individual classes, GPCRs demonstrate remarkable specificity for ligands and uniquely differentiated signaling responses. For class B GPCRs, the majority of ligands insert their N-terminal domain between TM5 and TM6, in which the ligand body interacts with all GPCR TM segments and extracellular loops (ECL) with the exception of TM4 (Krumm and Roth, 2020). Additionally, the C-terminal end of the bound ligand extends out of the TM core as it interacts with the N-terminal extracellular domain of the receptor. In particular, when comparing multiple class B peptide-receptor interactions, ligand binding commonly induces an upward movement of TM4/TM5 and repositioning of both the ECL2 and intracellular loop 2 (ICL2). The ligand interaction with ECL2 repositions the ICL2 into an orientation critical for  $G\alpha$  subunit coupling (Krumm and Roth, 2020). The binding characteristics of a  $G\alpha$  subunit to the GPCR is generally conserved between both class A and class B receptors, in which the  $G\alpha$  C-terminal end is inserted into the cavity established by TM outward movement. However, subtle differences in the angle of accessibility in which the  $G\alpha$  heterotrimeric subunit is capable to bind may confer unique signaling profiles attributable to different GPCRs (Krumm and Roth, 2020). GPCRs can be promiscuous or restrained in which G-protein they are selective for. In principal, universally conserved elements within the GPCR facilitate the potential interaction with a diverse set of  $G\alpha$  subunit subtypes (Flock et al., 2015). However, additional levels of specificity within the GPCR structure either act as a “master key” for activating multiple  $G\alpha$  subunit subtypes

through common interaction sites shared between different  $G\alpha$  subtypes, or as a specified key in which the GPCR is highly selective for an interaction point unique to a certain  $G\alpha$  subunit (Flock et al., 2017).

As mentioned before, there are four primary well-defined  $G\alpha$  subunit subtypes and pathways:  $G\alpha_s$ ,  $G\alpha_{q/11}$ ,  $G\alpha_i$ , and  $G\alpha_{12/13}$ .

Regarding  $G\alpha_s$ , GTP-bound  $G\alpha_s$  dissociates from the  $G\beta\gamma$  complex and interacts with AC to convert ATP into cyclic AMP (**Figure 5**). A single GTP-bound  $G\alpha_s$  is capable of stimulating the production of 100-1000 soluble cAMP molecules. Elevated cAMP can activate PKA, cyclic nucleotide-gated channels, and Exchange Protein Activated by Cyclic AMP 2 (EPAC2) (Moorthy et al., 2011). For the cAMP to activate PKA, cAMP binds to the regulatory subunits of PKA, which causes the release and activation of the catalytic PKA subunits (PKAcat) (Syrovatkina et al., 2016). The liberated PKAcat is then free to phosphorylate intracellular targets to alter functionality, and nuclear targets to induce transcriptional events. Degradation of the cAMP is performed by phosphodiesterase (PDE) which is a cytosolic enzyme that catalyzes the hydrolysis of cAMP into 5' adenosine monophosphate (Moorthy et al., 2011).

GTP-bound  $G\alpha_q$  is known to activate the  $\beta$ -isoforms of phospholipase C (PLC- $\beta$ ). PLC- $\beta$  is responsible for hydrolyzing the phosphoester bond of phosphatidylinositol 4,5-bisphosphate (PIP2) resulting in 1,4,5-trisphosphate (IP3) and diacylglycerol (DAG) (**Figure 5**) (McCudden et al., 2005). IP3 is capable of diffusing into the cytosol and binding to IP3 receptors on the endoplasmic reticulum (ER) which triggers the intracellular release of calcium ( $Ca^{2+}$ ). While IP3 diffuses into the plasma membrane, DAG remains membrane-bound and is used to facilitate protein kinase C (PKC) translocation from the cytosol to the plasma membrane and its activation. Within the PKC, the two regulatory domains C1 and C2 bind DAG and  $Ca^{2+}$  respectively. Therefore, when sufficient intracellular concentrations of both DAG and  $Ca^{2+}$  are achieved by  $G\alpha_q$ -dependent activation, PKC is activated and can affect a number of downstream effectors (Mizuno and Itoh, 2009).

GTP-bound  $G\alpha_i$  is known to inhibit the cAMP pathway, and act as an antithesis to GTP-bound  $G\alpha_s$  (Taussig et al., 1993). Following GTP binding,  $G\alpha_i$  dissociates from the  $G\beta\gamma$  complex and interacts directly with AC. It has been suggested that complex interaction between  $G\alpha_i$  and AC lead to the resulting inhibition of cAMP production. The interactions induced by  $G\alpha_i$  onto AC include: relocation of the  $\beta 7$ - $\beta 8$  loop (of AC5) which is found to be critical to inhibiting the stimulatory activity of  $G\alpha_s$ ; rearrangement of the C2 domain which further deconstructs the

$G\alpha_s$  active site, and lastly a conformational rearrangement that minimizes AC affinity for  $G\alpha_s$ . Through these interactions,  $G\alpha_i$  may both terminate and prevent reactivation of the  $G\alpha_s$ -activated AC complex (van Keulen and Rothlisberger, 2017).

Lastly, GTP-bound  $G\alpha_{12/13}$  subunits are known to link GPCR activity to the regulation of actin cytoskeleton dynamics through Rho GTPases. The  $G\alpha_{12/13}$ -mediated regulation of actin cytoskeleton remodeling is involved in cellular movement, migration, and metastasis. Additionally,  $G\alpha_{12/13}$  subunits can regulate nuclear dynamics such as Jun N-terminal kinase signaling,  $Na^+/H^+$  exchangers, focal adhesion assemblies, and transcriptional action of specific genes (Dhanasekaran and Dermott, 1996).

As mentioned prior (Structure of the GLP-1R and GIPR – Commonalities), the GLP-1 and GIP receptors are primarily coupled to  $G\alpha_s$ , with the GLP-1R additionally coupled to  $G\alpha_q$  albeit to a lesser degree (Oduori et al., 2020).

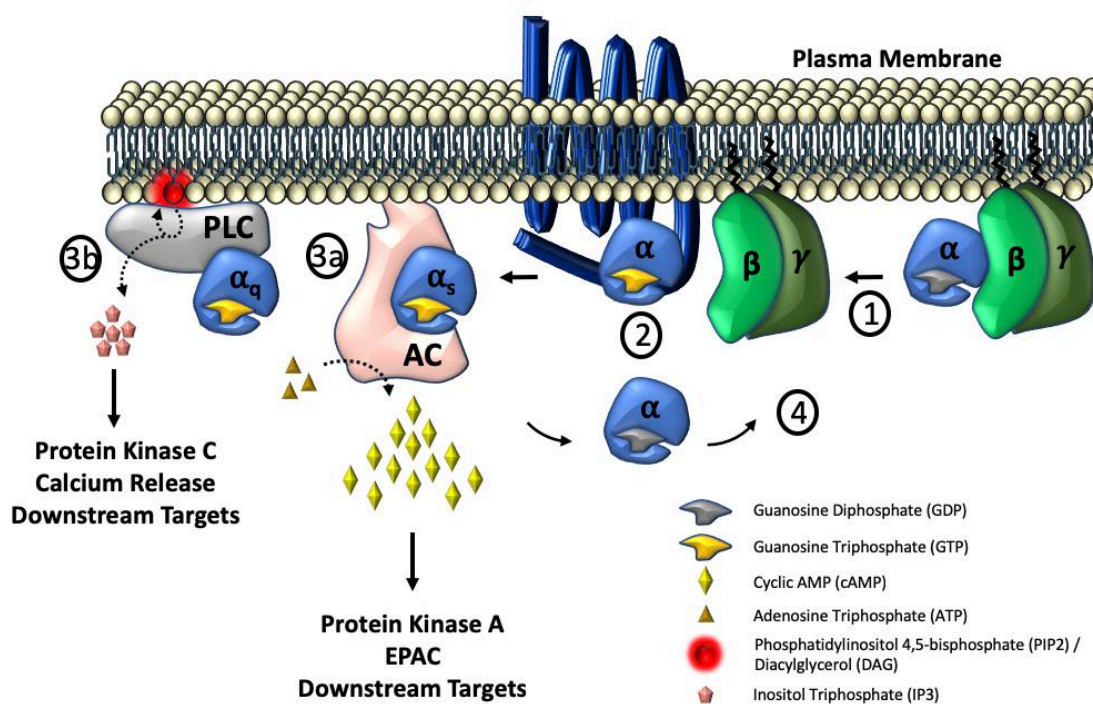


**Figure 5: Schematic of  $G\alpha_s/G\alpha_q$  activation and signaling.** Steps following ligand binding at the GPCR: 1) The heterotrimeric G-protein complex consisting of a GDP-bound  $G\alpha$  subunit, the  $G\beta$  subunit, and  $G\gamma$  subunit, are recruited to the ligand-bound GPCR. 2) The  $G\alpha$  subunit interacts with the intracellular loops of the GPCR forming a high-affinity complex that opens the  $G\alpha$  subunit to binding GTP. The GPCR acts as a guanine nucleotide exchange factor (GEF) replacing GDP with GTP at the  $G\alpha$  subunit. 3) The GTP-bound  $G\alpha$  subunit dissociates from the  $G\beta$  and  $G\gamma$  subunits. 3a) The liberated GTP-bound  $G\alpha_s$  subunits interact with adenylate cyclase (AC) to convert ATP into cAMP. The rise in intracellular cAMP results in the activation of multiple downstream targets including PKA, EPAC2, and cyclic nucleotide-gated channels. 3b) The liberated GTP-bound  $G\alpha_q$  subunits activate the membrane-bound  $\beta$ -isoform of

phospholipase C (PLC- $\beta$ ). The activated PLC- $\beta$  converts membrane-localized PIP<sub>2</sub> into membrane-localized DAG and cytosol-localized IP<sub>3</sub>, in which DAG activates membrane-bound PKC while the cytosol-diffused IP<sub>3</sub> induces calcium release via IP<sub>3</sub> receptors on the ER. 4) Intrinsic GTPase activity of the G $\alpha$  subunits hydrolyses GTP to GDP thus inactivating the G-protein subunit and increasing its affinity for G $\beta$  and G $\gamma$  subunit binding. G-protein hydrolysis of GTP to GDP can be accelerated by complementary proteins such as RGS, increasing GTPase activity by as much as 1,000 fold.

### *The GLP-1R and GIPR: $\beta$ -cell Adenylate Cyclase*

The binding of GLP-1 and GIP to their respective receptor induces intracellular cAMP signaling cascades that are primarily responsible for the physiological effects of  $\beta$ -cell insulin biosynthesis and glucose-stimulated secretion,  $\beta$ -cell proliferation,  $\beta$ -cell survival, and hypothalamus-mediated reductions in food intake. GLP-1 or GIP binding to their respective receptor leads to recruitment and activation of G $\alpha_s$ , which then interacts with the membrane-bound AC to increase localized intracellular cAMP levels using the substrate ATP. Human and rodent  $\beta$ -cells express multiple AC isoforms, which include the Ca<sup>2+</sup> and calmodulin activated isoforms AC1, AC3, and AC8 (Delmeire et al., 2003; Kitaguchi et al., 2013; Roger et al., 2011; Seed Ahmed et al., 2012).

G $\alpha_s$  and Ca<sup>2+</sup> together synergistically co-activate the AC1 and AC8 isoforms, inducing greater cAMP production than if G $\alpha_s$  and Ca<sup>2+</sup> interacted alone (Cali et al., 1994; Wayman et al., 1994). However, an important differentiating factor between AC1 and AC8 lies within the capacity for G $\alpha_i$  to inhibit Ca<sup>2+</sup>-mediated synergism at AC1, while the stimulatory effect of Ca<sup>2+</sup> on AC8 remains unaffected to G $\alpha_i$  (Nielsen et al., 1996). The synergism between G $\alpha_s$  and Ca<sup>2+</sup>, along with the insensitivity to G $\alpha_i$ , positions AC8 to be a source point for cAMP-induced transcriptional changes that require prolonged elevation of cAMP. Additionally, the enhanced capacity for synergistic cAMP production by AC8 may provoke a concept similar to the high capacity V<sub>max</sub> of glucokinase within the  $\beta$ -cell, in which the proportional response of AC8 to sharp increases in concomitant inputs of extracellular glucose and GLP-1/GIP stimulation is not capped by negative feedback regulation (Cali *et al.*, 1994; Lønsmann and Bak, 2020; Nielsen *et al.*, 1996).

Interestingly, AC8 has been linked to the glucose-dependent synergistic insulinotropic response of GLP-1 in  $\beta$ -cell models, in that cAMP generation, calcium signaling, and activation of downstream cAMP response element (CRE) transcription were decidedly suppressed upon AC8 knockout (Delmeire *et al.*, 2003; Roger *et al.*, 2011). Therefore, upon elevation of

circulating levels of glucose, the resulting  $\beta$ -cell plasma membrane depolarization and  $\text{Ca}^{2+}$  influx due to glucose metabolism activate AC8. Following, as the respective ligands bind to the GLP-1R (or potentially GIPR), the resulting activated  $\text{G}\alpha_s$  interacts and synergizes with the  $\text{Ca}^{2+}$ -activated AC8. In this way, the  $\text{Ca}^{2+}$ - $\text{G}\alpha_s$  synergism at AC8 may provide the amplifying response for insulin release typically associated with the incretin effect. Interestingly, AC8 has been shown to be upregulated in rat INS-1E and human pancreatic islets exposed to chronic hyperglycemia, as well as in diabetic Goto-Kakizaki rat pancreas (Guenifi et al., 2000; Roger et al., 2011). Additionally, a recent finding has discovered that the lack of substantial decrease in therapeutic GLP-1R agonism efficacy within the context of T2D is due to the GLP-1R's ability to switch from  $\text{G}\alpha_s$  to  $\text{G}\alpha_q$  signaling (Oduori et al., 2020). Therefore, it may be the case that within the context of T2D,  $\text{G}\alpha_q$ -mediated increases in  $\text{Ca}^{2+}$  facilitate the continued incretin action via AC8. Nonetheless, the importance of other AC isoforms involved within the GLP-1R/GIPR response have not been ruled out.

### *The GLP-1R and GIPR: PKA and EPAC2 in $\beta$ -cells*

Within  $\beta$ -cells, GLP-1R and GIPR signaling have been shown to acutely enhance glucose-stimulated insulin secretion. This enhancement is accomplished in part by increases in intracellular  $\text{Ca}^{2+}$  concentrations as mediated through PKA and EPAC2-dependent mechanisms (Kaihara et al., 2013). The cAMP-activated PKA subunit is capable of phosphorylating the Kir6.2 and SUR1 subunits of the  $\text{K}_{\text{ATP}}$  channels as well as the  $\beta_2$  subunit of the L-type voltage-gated  $\text{Ca}^{2+}$  channels, which together ultimately results in further cell membrane depolarization, voltage-dependent channel opening, and  $\text{Ca}^{2+}$  influx into the cell. Additionally, PKA also stimulates ER  $\text{Ca}^{2+}$ -induced  $\text{Ca}^{2+}$  release (CICR) through its phosphorylating activity at the inositol-1,4,5-trisphosphate receptors (IP3R) (Bünemann et al., 1999; Chaloux et al., 2007; Ehses et al., 2002; MacDonald et al., 2003; Trümper et al., 2001). In a similar manner, GLP-1R or GIPR-mediated increases in cAMP also activate Epac2, which induces further  $\text{K}_{\text{ATP}}$  channel closure and CICR through the ryanodine receptors (RyR) (Doyle and Egan, 2007; Harada and Inagaki, 2017; Seino et al., 2010).

PKA and Epac2 activation work in concert to increase intracellular calcium concentrations which in turn facilitates the plasma membrane-fusion and exocytosis of insulin-containing granules (Seino et al., 2010). The docking of insulin granules at the plasma membrane and their eventual  $\text{Ca}^{2+}$ -mediated exocytosis is regulated by a complex of proteins called SNARE



proteins. This complex holds the insulin granules at the membrane until elevation in intracellular  $\text{Ca}^{2+}$  allows for  $\text{Ca}^{2+}$  binding to synaptogamin, a modulator of the SNARE complex. The  $\text{Ca}^{2+}$ -bound synaptogamin binds to the SNARE complex initiating the fusion of the insulin vesicles through the plasma membrane. Interestingly, GLP-1R activation elicits a PKA-mediated phosphorylation of synaptogamin. This phosphorylation enhances the efficacy of  $\text{Ca}^{2+}$  in mediating synaptogamin-associated insulin granule exocytosis. GLP-1R activation does not induce the same degree of glucose-stimulated insulin secretion in synaptogamin mutants lacking the PKA phosphorylation sites as compared to the wildtypes (Wu et al., 2015).

Interestingly, the inhibition of PKA in isolated islets and  $\beta$ -cell lines has evidenced suppression of GLP-1- and glucose-mediated insulin secretion. In a mouse model in which PKA activity was disinhibited via a PKA regulatory subunit KO (Prkar1a KO), improved glucose tolerance and glucose-stimulated insulin secretion (GSIS) were evident during GLP-1R agonist exposure (Song et al., 2011). When both Prkar1a and EPAC2a were knocked out, a marked reduction in GSIS during GLP-1R agonist exposure was evident, indicating a reliance of PKA on EPAC2a for an enhancement of insulin secretion (Song et al., 2013). EPAC2a KO mice on chow diet displayed slightly reduced efficacy in glucose clearing following intraperitoneal administration of GLP-1R agonist Exendin-4. Within a DIO context, EPAC2a KO significantly reduced the functional response of Exendin-4, indicating a reliance of GLP-1R agonism on intact EPAC2a signaling in a diet-specific manner (Song *et al.*, 2013). Both PKA and EPAC2 bind cAMP with differing affinities, in which the dissociation constant ( $K_d$ ) of PKA is in the range of 0.12-1  $\mu\text{M}$ , while the  $K_d$  of EPAC2a is 87  $\mu\text{M}$ . This lower cAMP binding affinity likely allows EPAC2a to remain sensitive to further elevations in cAMP, which may be useful when PKA activation is already saturated by elevated levels of cAMP, such as during chronic GLP-1R or GIPR agonism (Doyle and Egan, 2007). Altogether, these results indicate a dynamic interplay between PKA and EPAC in mediating the GLP-1R and GIPR-mediated amplification of insulin release.

### *The GLP-1R and GIPR: PKA and EPAC2 in the CNS*

The physiological effects of the GLP-1R and GIPR on food intake and body weight are mediated by their activity within the interconnected regions of the CNS (Baggio and Drucker, 2014; Samms et al., 2021). Within the hindbrain and hypothalamus, these anorectic effects are primarily attributed to the regulation of neuronal excitability through a  $G\alpha_s$ -cAMP-PKA mediated pathway not dissimilar to that found in the  $\beta$ -cell, particularly in terms of facilitating

Ca<sup>2+</sup> entry. The neural intracellular mechanism that mediates the inhibition of food intake by GLP-1R activation, involves the dual-action of activated PKAcat in suppressing the activity adenosine monophosphate protein kinase (AMPK) through phosphorylation, and activating Extracellular Signal-Regulated Protein Kinase 1/2 (ERK 1/2)/ mitogen-activated protein kinase kinase (MEK) signaling (Hayes, 2012). Each of these responses leads to increased firing of GLP-1R+ neurons via Ca<sup>2+</sup>-dependent depolarization. In the pre-synapse, PKA and Epac2-mediated increases in intracellular Ca<sup>2+</sup> mediate neurotransmitter release. In the post-synaptic neuron, increases in PKA activity may allow for phosphorylation of receptors which may regulate receptor trafficking to the plasma membrane (Liu and Pang, 2016; Ohtake et al., 2014).

An additional neural intracellular pathway for GLP-1R-mediated anorectic effect further involves the activated cAMP/PKA cascade, which subsequently activates PI3K/PIP3-dependent translocation of Protein Kinase B (Akt) to the plasma membrane, which results in the subsequent suppression of Akt activity (Rupprecht et al., 2013; Yang et al., 2017).

Altogether, following GLP-1R activation, the aforementioned cAMP-PKA-mediated AMPK suppression and ERK/MEK activation peak in activity within 10 minutes following ICV hindbrain injection of EX-4, and returns to baseline within 30 minutes. However, behavioral food intake suppression effects are not evident until 3 hours post-injection. Therefore, it is hypothesized that the PKA-activated AMPK/ERK/MEK effects and the PKA-activated PI3K/PI3-dependent suppression of Akt activity work together to encode for a prolonged resilient translational signal for food intake reduction (Hayes, 2012; Rupprecht *et al.*, 2013).

### *The GLP-1R and GIPR: $\beta$ -arrestin Recruitment and Signaling*

$\beta$ -arrestin recruitment to an activated GPCR terminates continuous G $\alpha_s$  activation by binding within a region at the GPCR that sterically inhibits further G $\alpha_s$  binding. However,  $\beta$ -arrestin recruitment has also been implicated in its own G $\alpha_s$ -independent signaling profile attributable to GLP-1R agonism.  $\beta$ -arrestins are expressed in all cell types, and their recruitment and binding to a GPCR depends on GRK phosphorylation of serine/threonine residues on the C-terminal tail of the GPCR. This serine/threonine-site phosphorylative barcode on the GPCR directs  $\beta$ -arrestin binding and specificity (Liggett, 2011; Moore et al., 2007). There are two isoforms of non-visual  $\beta$ -arrestin, these are  $\beta$ -arrestin 1 ( $\beta$ arr1) and  $\beta$ -arrestin 2 ( $\beta$ arr2), which share an approximate 78% homology (Smith and Rajagopal, 2016). Despite non-trivial homology, the two isoforms have been evidenced to differ in specificity, expression, and

downstream effects involving  $\beta$ arr signaling, intracellular receptor trafficking, and transcriptional responses.

In terms of signaling,  $\beta$ -arrestins facilitate activation of ERK1/2 by acting as a scaffold for ERK 1/2. Although the  $G\alpha_s$ -cAMP-PKA cascade also activates ERK1/2, there are differences between source activation; in that ERK1/2 as activated by the  $G\alpha_s$ -cAMP-PKA cascade tends to facilitate nuclear translocation of ERK1/2, while ERK1/2 activation facilitated by  $\beta$ -arrestins tends to remain cytosolic (Quoyer et al., 2010). Using an *in vitro* model of HEK293 cells, deletion or inhibition of  $G\alpha$  subunits eliminated the effect of  $\beta$ -arrestins on ERK 1/2 despite  $\beta$ -arrestins still binding to and trafficking the receptor. This indicates the reliance of  $\beta$ -arrestins on  $G\alpha$  activation to stimulate ERK1/2, and indicates that  $\beta$ -arrestins are not solely responsible for ERK1/2 activation (Grundmann et al., 2018).

Ligand-stimulated  $\beta$ -arrestin 1 and 2 recruitment to the GIPR has been a center of controversy due several studies with conflicting results. In particular, ligand stimulation of the GIPR has been evidenced to induce no GRK phosphorylation and only minimal subsequent  $\beta$ arr1/2 recruitment (Al-Sabah *et al.*, 2014; Ismail et al., 2015; Jones et al., 2021). In contrast, other studies have evidenced substantial ligand-induced  $\beta$ -arrestin recruitment to the GIPR (Gabe et al., 2018; Willard et al., 2020). An illuminating recent study has identified that common linkers connecting the GIPR to tagged molecules used for ratiometric quantification or colorimetric models may contain potential GRK phosphorylation motifs capable of facilitating the quantification of artificial  $\beta$ -arrestin recruitment. When these phosphorylation sites on the linker are removed, all residual  $\beta$ -arrestin recruitment is eliminated at the GIPR (Al-Sabah et al., 2020). Therefore, it is suggested  $\beta$ -arrestin recruitment to the GIPR is an artificial phenomenon and not implicative of GIPR biology.

Ligand-stimulated recruitment of  $\beta$ -arrestin to the GLP-1R is robust for both  $\beta$ -arrestin isoforms. In one study, GLP-1R stimulation in high glucose conditions within a  $\beta$ -arrestin 1 KO INS-1 cell model resulted in a 60% reduction in insulin secretion compared to the WT, with ERK1/2 phosphorylation reduced by 50% (Sonoda et al., 2008). This finding indicates a  $\beta$ -arrestin-mediated signaling dynamic that mediates the amplitude of insulin secretion. However, the effects of  $\beta$ arr on insulin secretion have been contradictory between studies. The development of GLP-1R agonists that are biased toward  $\beta$ arr recruitment, meaning they recruit less  $\beta$ arr to the GLP-1R, has demonstrated enhanced insulin secretion likely due to a lack of  $\beta$ arr-mediated desensitization of the GLP-1R (Jones *et al.*, 2021). Additionally, acute

enhancement in both glucose-stimulated insulin secretion and subsequent GLP-1R agonism-driven insulin secretion was evidenced in perfused islets of  $\beta$ arr1 KO mice. Interestingly however, the differential effect of  $\beta$ arr1 KO on insulin secretion was not present during stimulation with GIP, suggesting a minimal role for  $\beta$ arr1 at the GIPR (Willard *et al.*, 2020). Altogether, evidence suggests that ligand-induced  $\beta$ arr recruitment to the GLP-1R influences the magnitude of insulin secretion, and that engineered ligands demonstrating minimal  $\beta$ arr recruitment may be useful in providing a superior insulinotropic effect.

### *The GLP-1R and GIPR: $G\alpha_q$ Signaling*

In terms of  $G\alpha$  activation, the extent of  $G\alpha_q$  activation by the GLP-1R is secondary compared to  $G\alpha_s$  (Wheeler *et al.*, 1993). Interestingly, GIPR does not seem to be  $G\alpha_q$  coupled (Oduori *et al.*, 2020). The  $G\alpha_q$  subunit activates a number of pathways mostly independent to that of the canonical  $G\alpha_s$  pathways. The primary pathway mediated by  $G\alpha_q$  is the initiation of calcium- and lipid-dependent signaling as mediated by PLC- $\beta$ . A GTP-bound  $G\alpha_q$  can generate important intracellular second messengers by interacting with PLC- $\beta$  which stimulates the conversion of PIP2 into IP3 and DAG. Downstream PKC is targeted and activated by DAG and IP3-IP3R-mediated increases in ER intracellular calcium (Sánchez-Fernández *et al.*, 2014). While there are several non-canonical pathways activated downstream of  $G\alpha_q$ , which includes  $G\alpha_q$ -mediated Rho activation, PI3K/Akt pathway modulation, and inhibition of cold-activated TRMP8 channel, most literature around GLP-1R- $G\alpha_q$ -mediated physiological effects is seen as attributable to PKC phosphorylation (Marzook *et al.*, 2021). Within normoglycemic conditions, both  $\beta$ -cell GLP-1R and GIPR seem to exclusively couple to  $G\alpha_s$ , while under chronic hyperglycemia  $\beta$ -cell GLP-1R additionally couples to  $G\alpha_q$  (Oduori *et al.*, 2020). Interestingly, the alternative capacity for  $G\alpha_q$  activation by the GLP-1R seems to be a defining reason as to why the GLP-1R retains its therapeutic activity within diabetic conditions while the GIPR does not.

It was stated that  $K_{ATP}$  channel closure, as mediated by the products of intracellular glucose metabolism, is an important aspect of the  $\beta$ -cell membrane depolarization and  $Ca^{2+}$  entry process. This process is critical to stimulating the exocytosis of insulin. A chronic hyperglycemic state is associated with prolonged membrane depolarization and excess influx of  $Ca^{2+}$  into the  $\beta$ -cell. A chronic hyperglycemic state can be modeled within  $\beta$ -cells through persistent membrane depolarization as engineered by a partial loss of  $\beta$ -cell  $K_{ATP}$  channels or

prolonged pharmacological sulfonylurea treatment. These representative models lead to a switch in  $\beta$ -cell GLP-1R  $G\alpha$  coupling from  $G\alpha_s$  to  $G\alpha_q$ , while the GIPR remains persistently coupled to  $G\alpha_s$  (Oduori *et al.*, 2020). Within either model of chronic  $\beta$ -cell depolarization, the resulting cAMP/PKA activity induced by GLP-1R or GIPR activation was comparatively reduced to the matched control, largely due to a loss of  $G\alpha_s$  efficacy at the respective receptors. Additionally, within these models,  $G\alpha_q$  inhibition abrogated any GLP-1R insulinotropic response confirming the lack of efficacy in the  $G\alpha_s$  pathway in conditions of chronic hyperglycemia. Therefore, through a yet unknown mechanism, the switch from  $G\alpha_s$  to  $G\alpha_q$  at the GLP-1R seems to facilitate a resilient insulinotropic response in conditions of chronic hyperglycemia (Oduori *et al.*, 2020).

### *The GLP-1R and GIPR: $G\alpha_s$ Signal Amplification*

Plasma membrane-bound GPCRs are lowly expressed, and therefore the  $G\alpha_s$  signal needs to be amplified to produce a global intracellular effect. Signal amplification is defined as the exponential increase in signal intensity as the signal travels through multiple networks of intracellular reactions that contain an increasingly greater number of downstream effectors. In this way, the signal amplification mechanisms following GLP-1 or GIP binding amplify the reach of the initial  $G\alpha_s$  signal, thereby saturating intracellular microcompartments with cAMP resulting in maximal PKA activation. Therefore, stimulation of a relatively few GPCRs at the plasma membrane is capable of evoking a maximal global cellular response. An example of this phenomenon is the GLP-1R/GIPR interaction with AC8, in which GTP- $G\alpha_s$  and  $Ca^{2+}$  can synergize at AC8 to elicit an exponentially higher degree of cAMP production relative to  $G\alpha_s$  input. This exponentially greater cAMP output as stimulated by  $G\alpha_s$  is capable of initiating numerous downstream pathways (Buenaventura *et al.*, 2019; Buenaventura *et al.*, 2018b; Gao *et al.*, 2002; Tengholm, 2012). However, not much is known about the prevailing mechanisms mediating signal amplification.

## GPCR Internalization

### *Background*

When a ligand binds to its respective GPCR, most receptors will undergo endocytosis. The process of endocytosis, in which an extracellular-facing plasma membrane-bound GPCR is

internalized within the cell, serves multiple purposes including regulating cell surface GPCR expression, adjusting cell responsiveness and accessibility to chronic ligand exposure, and providing a systematic trafficking utility to move the active receptor within various intracellular compartments (Ferguson, 2001). A trafficked GPCR can be shuttled into receptor degrading pathways to achieve long-term desensitization, or it can enter into recycling pathways for the continuation of signaling by cellular resensitization (Maxfield and McGraw, 2004).

The schematic of the endocytic pathway is a continuous chain of intracellular vesicular compartments, starting from the initial endocytosis of the receptor to the gradual maturation across multiple compartments that serve specific functionalities. The primary branches of the endocytic pathway start with the early endosomes containing a newly internalized receptor, in which from there the GPCR can be trafficked either back to the plasma membrane within recycling endosomes, or into late endosomes eventually meeting terminal entry into lysosomes. Within these primary branches of trafficking there are several side branches that create an interconnected network capable of shuttling a GPCR between multiple intracellular organelle sites, including the Golgi apparatus, the endoplasmic reticulum, nucleus, and mitochondria (Benmerah, 2004; English and Voeltz, 2013; Todkar et al., 2019; Tu et al., 2020). There are a number of cytosolic proteins that transiently interact with endosomes to regulate processes such as endocytic sorting, compartment identification, and the dynamic fusion and fission events underlying endosome departure from the plasma membrane or re-entry (Elkin et al., 2016). Endocytic markers called Ras associated binding proteins (Rab), which interact with the internalized vesicles, generally define the identity and stage of the vesicle. Due to the quality-assurance nature intrinsic to degradation or recycling processes, the intact endocytic trafficking of cellular components is essential for maintaining expression of cell surface proteins and membrane composition (Cullen and Steinberg, 2018). Improper execution of the endocytic machinery has been implicated in several metabolic pathologies including T2D, hypercholesterolemia, and non-alcoholic fatty liver disease (Gilleron et al., 2019).

## *Clathrin-mediated Endocytosis*

### *Background*

The initial steps in the formation of an endosome consists of several overlapping steps that ultimately result in the invagination of a plasma membrane segment containing the target

transmembrane protein cargo. Intracellular scission of the budded invagination finalizes the form of a liberated endosome. This common principle is shared between divergent classifications of endocytosis type. Clathrin-dependent and clathrin-independent classifications make up the primary eukaryotic endocytic internalization routes. Clathrin-independent pathways include the dynamin-dependent caveolin and RhoA internalization pathways; however the primary mammalian endocytic route that has been most often characterized is clathrin-mediated endocytosis (Kaksonen and Roux, 2018; Mayor et al., 2014). Less is known about the GIPR, but both the GLP-1R and GIPR have been evidenced to be dependent on clathrin-mediated endocytosis (CME) (Ismail *et al.*, 2015; Marzook *et al.*, 2021). Multiple studies have identified GLP-1R CME in various cell types, including  $\beta$ -cells, HEK293, min6, CHO, and CHL cell lines (Buenaventura *et al.*, 2019; Roed et al., 2015; Widmann et al., 1997).

#### *Initial Clathrin Coat Assembly*

The initiation of CME following ligand binding at the GPCR begins with the recruitment and clustering of cytosolic proteins at the intracellular side of the plasma membrane. Over 50 cytosolic proteins cluster at the target plasma membrane site within a highly ordered manner. However, the first to cluster are clathrin, and clathrin adaptor proteins such as adaptor protein 2 (AP2) (Kaksonen and Roux, 2018). Free clathrin in the cytosol is found in the form of trimers, and is composed of three heavy and three light clathrin chains. These clathrin trimers ultimately self-assemble into a polyhedral lattice outlining the future endocytic site. AP2 is a complex of four subunits  $\alpha$ ,  $\beta$ 2,  $\mu$ 2, and  $\sigma$ 2, and is localized to the plasma membrane by binding to PIP2-abundant microdomains using the  $\alpha$  and  $\beta$ 2 subunits (Kovtun et al., 2020; Mettlen et al., 2018). This initial coordinated clustering forms the 'pioneer module', and represents the earliest stage of endocytosis which is mostly conserved between species (Kaksonen and Roux, 2018; Traub, 2011). This pioneer module will be developed further with additional endocytic accessory and regulatory proteins involved in each step of the maturation of a clathrin-coated pit (CCP).

#### *Transmembrane Receptor Recruitment into Clathrin Coated Pits*

A CCP is the matured assembly of clathrin and associated proteins, which ultimately manifest as bending or invagination of the plasma membrane. Following CCP formation, specific

cytosolic-facing binding motifs on the transmembrane cargo are used for lateral recruitment into the CCP (Kaksonen and Roux, 2018). AP2 interacts with the cytosolic-facing binding motifs of the transmembrane receptor to facilitate cargo sorting and concentrative accumulation into CCPs. The most well-known binding motif for AP2 within transmembrane protein amino acid sequences is a tyrosine-based YXX $\emptyset$  sequence (X is any amino acid,  $\emptyset$  is an aromatic amino acid), in which the C-terminus of AP2's  $\mu$ 2 subunit binds. An alternative binding motif is the dileucine sequence [DE]XXXL[LIM], which the  $\alpha$ - $\sigma$ 2 subunit hemicomplex of AP2 binds (Marks et al., 1996; Owen and Evans, 1998). There are an additional number of clathrin-associated sorting proteins (CLASPs) that function to sort transmembrane proteins by binding site recognition (Traub, 2009). AP2 and other adaptor proteins FCHO1, EPS15, and the CALM family, facilitate or directly interact with target transmembrane protein cargo to facilitate their site-directed accumulation and CCP maturation (Traub, 2009).

#### *Membrane Curvature and Scission*

Site-specific plasma membrane bending and invagination involve clathrin, the complex interactions of additional cytosolic proteins, and actin polymerization (Kaksonen and Roux, 2018). Membrane bending is first initiated with clathrin recruitment, while actin polymerization finalizes the budded shape by interacting with scission and coat proteins. Following the recruitment of GPCR cargo into the CCP and membrane invagination, dynamin-dependent scission of the formed neck of the invaginated bud liberates the clathrin-coated vesicle from the plasma membrane (**Figure 6**). Within the intracellular space, the liberated vesicle sheds its endocytic machinery, allowing the GPCR-containing endosome to be trafficked further (Kaksonen and Roux, 2018).



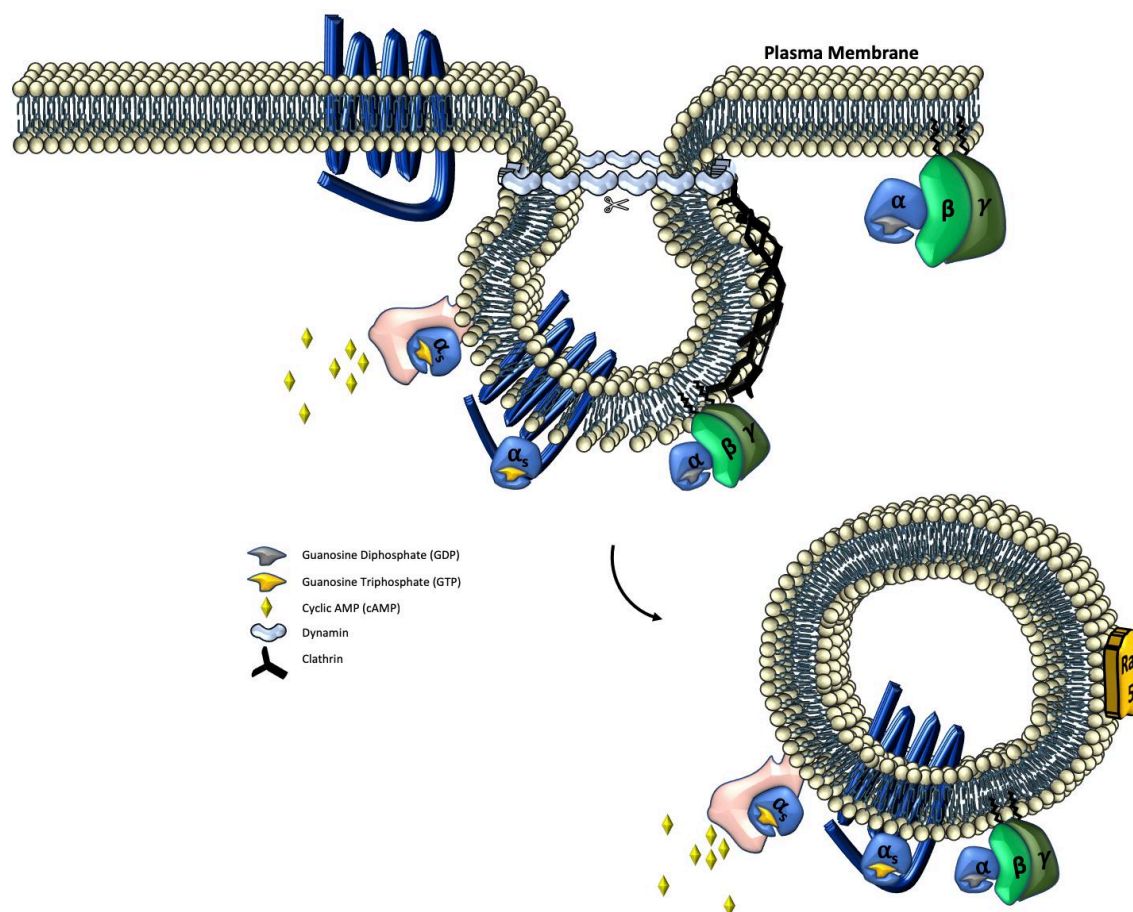


**Figure 6: Formation and liberation of endosomes containing internalized receptors.** Clathrin (black) recruitment to the inner leaflet of the plasma membrane promotes bending and invagination of the membrane. Plasma membrane associated proteins, including GPCRs, heterotrimeric G-protein subunits, and downstream effector proteins (i.e. adenylate cyclase) are directed into the budding formation. Dynamin-dependent scission (light blue) of the formed neck of the invaginated bud liberates the endosome and its contents from the plasma membrane, in which the newly formed endosome can then shed the endocytic machinery (i.e. clathrin) and continue trafficking within the cell and signaling within the endosomal compartment.

### *$\beta$ -arrestin-dependent CME of GPCRs*

The internalization of GPCRs typically revolve around processes that congregate the receptor into clathrin-coated pits (CCP) or caveolin-rich nanodomains, in which a subsequent endosomal bud forms protruding into the intracellular space from the plasma membrane, where then dynamin-mediated scission of the bud liberates an independent endocytic vesicle (Cocucci et al., 2014; Henley et al., 1998).  $\beta$ -arrestins act as a connecting partner to the CCP protein machinery thereby facilitating GPCR internalization. Here,  $\beta$ -arrestins act as both a regulator of endocytic processes and GPCR desensitization (Figure 7).

Within vertebrates, 4 arrestin genes expressed, there are Arrestin-1 and Arrestin-4, which are referred to as visual arrestins due to their exclusive role of desensitizing the photoactivated transduction cascade of the retina, and Arrestin-2 and Arrestin-3, which are near ubiquitous non-visual arrestins and have been renamed  $\beta$ -arrestin 1 and  $\beta$ -arrestin 2. Outside of acting as steric inhibitors for  $G\alpha$  activation,  $\beta$ -arrestin are multifunctional scaffold proteins that bind both AP2 and a respective GPCR. Similar to AP2,  $\beta$ -arrestin mediates endosomal trafficking, vesicle sorting and signal modulation of the GPCR. The aforementioned tyrosine and dileucine-based binding motifs for AP2 are not generally seen as the primary means for facilitating GPCR endocytosis (Spillmann et al., 2020). While not ruling out the presence of direct AP2 binding sequence motifs on the C-terminal portion of GPCRs, the canonical GPCR internalization route is typically associated with the N-terminal end of  $\beta$ -arrestin binding to phosphorylated serine/threonine motifs on the C-terminal tail of the GPCR while simultaneously forming a tripartite interaction with the clathrin heavy chain and  $\beta 2$  subunit of AP2 (Marzook *et al.*, 2021; Traub, 2009).

The initiation of  $\beta$ -arrestin binding at the GPCR is dependent on preceding GRK phosphorylation of the GPCR C-terminal tail, in which the presented phosphorylation barcode specifies  $\beta$ -arrestin binding (Hausdorff et al., 1991; Liggett, 2011; Xiao and Sun, 2018). Class B GPCR's bind both  $\beta$ -arrestin isoforms with equal affinity, yet despite an approximate 80% homology in amino acid sequence, the ability for  $\beta$ -arrestin 1 and 2 to facilitate GPCR internalization is dependent on their own phosphorylation status. This phosphorylation status of  $\beta$ -arrestin itself is differentially regulated, in that  $\beta$ -arrestin 1 is phosphorylated by ERK and  $\beta$ -arrestin 2 phosphorylated by casein kinase 2 (Lin et al., 2002; Lin et al., 1999).

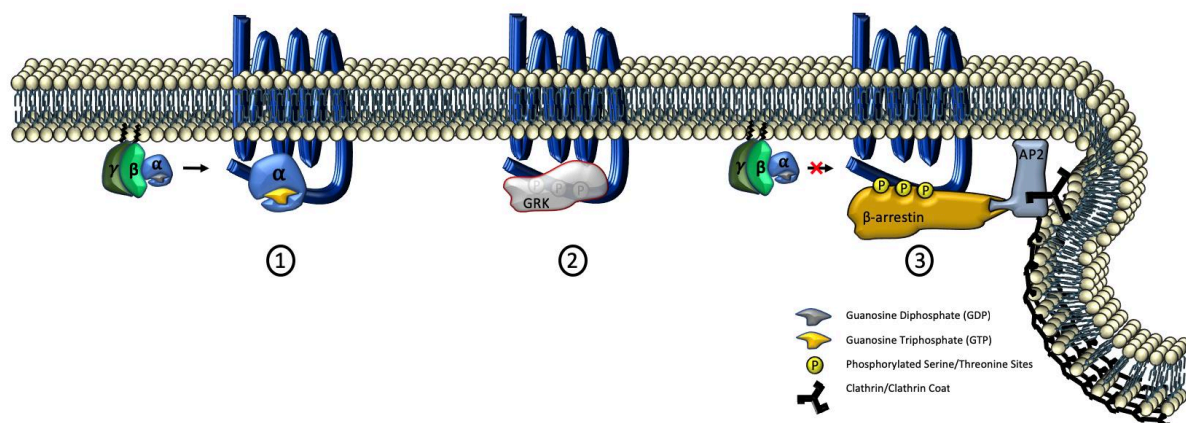


**Figure 7:  $\beta$ -arrestin facilitation of  $G\alpha$  signaling inhibition and GPCR movement into clathrin-coated pits.** Steps following ligand binding at the GPCR: 1)  $G\alpha$  subunits are recruited to the GPCR to swap GDP for GTP. 2) In parallel to  $G\alpha$  subunit recruitment, GRK is recruited to the C-terminal tail of the GPCR resulting in the phosphorylation of serine and threonine residues. 3) The C-terminal serine/threonine phosphorylation sites on the GPCR act as an interaction point for  $\beta$ -arrestin binding which sterically inhibits further  $G\alpha$  subunit recruitment and connects the GPCR to the AP2 endocytic machinery facilitating accumulation within the clathrin-coated pits.

Class B GPCRs allow highly stable interactions with  $\beta$ -arrestin due to increased clusters of serine and threonine phosphorylation sites at the receptors C-terminal tail. This enhanced stability confers endosomal co-internalization of both GPCR and  $\beta$ -arrestin (Drake et al., 2006). This is opposed to class A GPCRs, which only transiently interact with  $\beta$ -arrestin at the plasma membrane and do not co-internalize. Class A receptors recycle rapidly, undergoing the entire desensitization process and reappearance at the plasma membrane within 30 minutes, while class B GPCRs recycle slowly and are found to co-localize with  $\beta$ -arrestin up to an hour after ligand stimulation (Pierce and Lefkowitz, 2001). Interestingly, this stable co-internalization of  $\beta$ -arrestin with the GPCR may facilitate a signalosome scaffold, allowing for transient spatial compartmentalization of ERK signaling. Unphosphorylated ERK normally resides in the cytoplasm with the core signaling complex of Raf, MEK, and ERK. Via  $\beta$ -arrestin acting as a stabilizing scaffold to ERK, it has been demonstrated that ERK can colocalize at GPCR/ $\beta$ -arrestin-occupied internalizing endosomes (Eichel and von Zastrow, 2018). The co-internalization of a GPCR and  $\beta$ -arrestin, and the  $\beta$ -arrestin-facilitated colocalization of endosomal ERK has been demonstrated to regulate downstream ERK activity (Eichel and von Zastrow, 2018; Lin et al., 1998; Luttrell et al., 1997). While ERK's signaling relation with GPCR/ $\beta$ -arrestin internalization has been assessed using binary off or on receptor internalization inhibitors, the effect of ligand biases in receptor trafficking that target a GPCR to specific intracellular compartments has yet to be explored.

### *Caveolin-dependent internalization of GPCRs*

An alternative to clathrin-mediated GPCR internalization is caveolin-dependent internalization, which utilizes the cell-surface protein caveolin. Lipid rafts are low-density membrane microdomains rich in cholesterol and sphingolipids, known to function as an organizational hub for signaling protein assembly and membrane protein trafficking. Caveolae are smooth invaginations of the lipid raft fraction associated with the presence of integral

membrane protein caveolin-1. Caveolins are proteins inserted to form hairpin loops within the plasma membrane, which ultimately oligomerize to facilitate inward membrane curvature (Kurzchalia and Parton, 1999).

Caveolar budding is a process regulated by kinases and phosphatases. Caveolin-1, in addition to its co-localized isoform caveolin-2, are phosphorylated by Src, which promotes the caveolar budding and internalization (Lee et al., 2002). Src phosphorylation-induced caveolin internalization is inhibited by the presence of protein phosphatase 1 and 2, thereby representing a potential path for negative regulation on caveolin-mediated internalization (Botos et al., 2007).

GPCRs are internalized through either clathrin-dependent or clathrin-independent processes. Clathrin-independent pathways relative to GPCR internalization includes the dynamin-dependent caveolin, and RhoA internalization pathways. Specific GPCRs typically favor either a clathrin-dependent or clathrin-independent internalization process. However, some GPCRs have also been shown to be flexible in route of intracellular entry, and may internalize through both clathrin-dependent and clathrin-independent processes. For example, the GLP-1R has been found to internalize via clathrin-dependent endocytosis in pancreatic  $\beta$ -cells, but is caveolin-dependent in the  $\beta$ -cell min6 cell line and HEK293 cells (Buenaventura et al., 2018a; Syme et al., 2006). Interestingly, certain GPCRs have been evidenced to switch from caveolin-dependent endocytosis to CME within the same cell type, depending on context (Okamoto et al., 2000). However, there is a degree of intracellular overlap between clathrin-dependent and -independent endocytic trafficking, as membrane lipids from caveolin-dependent internalization processes have been found to be rapidly incorporated into clathrin-associated early endosomes, indicating an almost immediate merging of endosomal content from both internalization pathways at the sub-membrane level (Sharma et al., 2003).

Within intracellular loop 2, GLP-1R contains a classical caveolin binding motif. Mutating this motif inhibits all GLP-1R signaling (Syme et al., 2006). Interestingly,  $G\alpha_q$ , but not  $G\alpha_s$  or  $G\alpha_i$ , is evidenced to exclusively co-localize within caveolar pits rather than the surrounding lipid raft. Caveolin acts as a scaffold to stably trap and concentrate  $G\alpha_q$  into microdomains both at the plasma membrane and internalized cytosolic caveosomes (Oh and Schnitzer, 2001). The internalization of GLP-1R has been shown to be dependent on  $G\alpha_q$  presence and activation through an unknown mechanism (Thompson and Kanamarlapudi, 2015). As a CRISPR knockout model of  $\beta$ -arrestin, and a separate knockdown of clathrin via small interfering RNA,

both failed to inhibit GLP-1R internalization, the GLP-1R-caveolin-G $\alpha_q$  dynamic remains a reputable route for GLP-1R internalization (Jones et al., 2018b; Thompson and Kanamarlapudi, 2015). Nonetheless, GLP-1R may be able to use multiple internalization pathways, as accumulated evidence also support clathrin-dependent internalization (Marzook *et al.*, 2021). It is not clear if the GIP receptor internalizes via a caveolin-dependent process, but supporting evidence has instead pointed to its internalization process being clathrin-dependent. However, due to a lack of  $\beta$ -arrestin recruitment to the GIPR, the mediating factors of GIPR internalization are not fully understood (Ismail *et al.*, 2015).

## The Endolysosomal Network

### *Plasma Membrane Nanodomain “Hotspots”*

Ligand-induced activation of GPCRs can lead to dynamic compartmentalization of both receptor and effector proteins within plasma membrane domains rich in sphingolipids and cholesterol. These compartmentalized “hotspots” house the G $\alpha_s$  through its interaction within the cholesterol-rich regions of the domain (Buenaventura *et al.*, 2019; Sungkaworn et al., 2017)). Depletion of plasma membrane cholesterol by using methyl- $\beta$ -cyclodextrin reduces signaling efficacy and eliminates internalization of both GLP-1R and GIPR in  $\beta$ -cells. Therefore, lipid- and cholesterol-rich nanodomain compartmentalization of these receptors is critical for both clathrin-dependent and -independent receptor internalization (Buenaventura *et al.*, 2019). Additionally, C-terminal palmitoylation of the GLP-1R, and potential cholesterol interaction sites at the GLP-1R TMD, may play a role in concentrating the active receptor into these nanodomain hotspot and may facilitate additional conformational stability following ligand binding (Ansell et al., 2020; Buenaventura *et al.*, 2018b; Taghon et al., 2021).

### *Early Endosomes*

The endolysosomal system is the interconnected network of both biosynthetic and endocytic intracellular vesicular transport processes (Cullen and Steinberg, 2018). Endosomes are highly dynamic organelles capable of sorting and merging into specific compartments of the endosomal network through a process termed homotypic fusion. Additionally, endosomal

compartment are generated following morphological and endosomal maturation of early endosomes (Woodman, 2000).

Following dynamin-dependent scission of the budded plasma membrane, the first compartmental identity following either clathrin-dependent or -independent internalization is the early endosome, also known as a sorting endosome. Early endosomes have a hollow-type central vacuole that is approximately 100-500 nm in diameter from which tubular structures and intraluminal vesicles form. Early endosomes are identified by the key marker Rab5, which is a small monomeric GTPase involved in the biogenesis and sorting of early endosomes (Koo et al., 2010). Rab5 primarily facilitates homotypic fusion of sorting endosomes, and secondarily orchestrates endosome trafficking and function.

In terms of Rab5 functionality, at the early endosomes, the inactive cytosolic GDP-bound Rab5 is recruited to the initial endosomal membrane upon GTP binding, where it is then stabilized and clustered by the Rabaptin-5/Rabex-5 complex. Rab5-GTP facilitates p150/hVps34 PI3-kinase localized production of phosphatidylinositol 3-phosphate (PI3P) which then acts as a scaffold for recruitment of the early endosome autoantigen 1 (EAA1) (Woodman, 2000). This Rab5-mediated complex, in addition to the recruitment of proteins with PI3P-binding domains to the endosomal surface, facilitate the tethering and docking of early endosomes to other endosomal compartments such as recycling endosomes, late endosomes, and organelles.

### *Recycling Endosomes*

Despite Rab5<sup>+</sup> endosomes described as an initial sorting hub, live-cell imaging has detected that there are two distinct populations of early endosomes, a highly mobile microtubule-interacting population and a static population. The highly dynamic, quickly maturing early endosome population is preferentially targeted toward pathways destined for degradation, while endosomal cargo destined for recycling pathways is enriched within static slowly maturing endosomes (Lakadamyali et al., 2006).

Leading up to and within the endosomal recycling pathway are three endosomal populations. There are the initial Rab5<sup>+</sup> early endosomes, Rab4<sup>+</sup> early recycling endosomes, and the Rab11<sup>+</sup> recycling endosomes (Zerial and McBride, 2001). Rather than these endosomal populations co-localizing exclusively with the respective Rab proteins, the populations are identified by a mosaic of the Rab proteins that can interact, but also maintain stable endosomal organization. Therefore, the three primary recycling endosomal populations consist of Rab5<sup>+</sup> early

endosomes, Rab4<sup>+</sup> and Rab5<sup>+</sup> co-localized early recycling endosomes, and Rab4<sup>+</sup> and Rab11<sup>+</sup> recycling endosomes (**Figure 8**) (Sönnichsen et al., 2000). Rab5<sup>+</sup> endosomes represent entry into the endocytic network, while Rab4 and Rab11 colocalization direct and regulate endocytic recycling (Sönnichsen *et al.*, 2000). Two different kinetics have been attributed to recycling pathways. There is a quick pathway, which results in rapid cargo return to the plasma membrane by endosomes with Rab5 and Rab4 co-localized (Sheff et al., 1999). There is also a comparatively slower recycling pathway, which occurs following segregation of cargo away from Rab5<sup>+</sup> endosomes into a separate endosomal population that co-localizes both Rab4 and Rab11 (Sheff *et al.*, 1999).

### *Late Endosomes/Lysosomes*

Endosomal maturation, which involves preferential targeting of the highly dynamic Rab5<sup>+</sup> vesicles toward endosomal degradation, is distinguished by Rab7 colocalization. Rab7 is the most important marker for late endosomes destined for maturation into lysosomes. Within the early endosomal compartment, the formation of intraluminal vesicles (ILV) separates cargo destined for degradation from that which will be recycled. These ILVs are subsets of the early endosomal compartment that have been segregated from the original starting material. Within the endosomal membrane, sorting of the internalized cargo (i.e. GPCRs), membrane dynamics, and sub-vesicle scission is mediated by the endosomal sorting complex required for transport (ESCRT). The ESCRT machinery is made up of the subcomplexes ESCRT-0, -I, -II, and -III, and ATPase VPS4 (Wenzel et al., 2018). The formation of ILVs begins when the endosomal cargo destined for degradation is ubiquitinated at its lysine residues and is sorted by ESCRT-0 into spatially restricted areas within the endosomal membrane (Wenzel *et al.*, 2018). Following, a highly orchestrated recruitment of ESCRT (I-III) and ATPase VPS4 ensures the sequestered cargo is scissioned into distinct smaller ILVs within the lumen of the original endosome (Wenzel *et al.*, 2018).

Early endosomes enriched in ILV following multiple rounds of sub-endosomal fusion and fission by ESCRT machinery, are remodeled to form globular late endosomes. As these ILV acidify, lose colocalization with Rab5, and gain colocalization with Rab7, the globular late endosome moves from the cell periphery to the cell center (**Figure 8**) (Trivedi et al., 2020). Rab7 is a key mediator in the maturation and fusion of late endosome and lysosome structures and is important for sustaining the lysosomal compartment (Bucci et al., 2000). An additional

requirement for the early to late endosome transition is the presence of the endosomal proton pump v-ATPase, which acidifies the late endosome and lysosome to a pH of approximately 5 (Trivedi *et al.*, 2020).

The acidification of early and late endosomes allow for a ligand's dissociative release from an internalized receptor, thus allowing for receptor resensitization and recycling (Trivedi *et al.*, 2020). However, various ligands specific for a single receptor may exhibit differential ligand-receptor stability within an acidic environment, and this may act as a determinant to the ligand's dissociative rate from the receptor. Consequently, the more stable the ligand-GPCR interaction is at the early endosome, the greater the continued endosome-localized signaling activity will be at the GPCR (Sutkeviciute and Vilardaga, 2020). Interestingly, as a ligand stays bound to a  $G\alpha_s$ -coupled GPCR that is co-localized within the Rab5<sup>+</sup> endosomal compartment, the resulting  $G\alpha_s$  activity localized at the endosomal membrane may be a determinant of GPCR incorporation into ILVs. It has previously been evidenced that endosomal  $G\alpha_s$  subunits directly interact with GPCR-associated binding protein-1 (GASP1) and dysbindin, which act as a linkage between GPCR and ESCRT machinery for sequestering the GPCR into ILV/Rab 7<sup>+</sup> late endosomes (Roscioglione *et al.*, 2014). Therefore, continued endosomal  $G\alpha_s$  signaling due to a strong ligand-GPCR interaction, may facilitate a trafficking bias of the receptor toward Rab7<sup>+</sup> endosomes and terminal lysosomes.

Additionally, different ligands for the same receptor may be more or less susceptible to being inactivated and degraded by proteolytic cleavage. For example, GLP-1R agonists GLP-1 (7-36 amide) and Exendin-4 (EX-4) are differentially susceptible to proteolytic degradation by metalloprotease endothelin-converting enzyme-1 (ECE1). GLP-1 (7-36 amide) is a target for ECE1-mediated degradation, which may enhance recycling of the receptor due to ligand deactivation. However, EX-4 is not a substrate for ECE1, which results in the preferential targeting of the GLP-1R to the lysosome (Fang *et al.*, 2020; Lu and Willars, 2019).



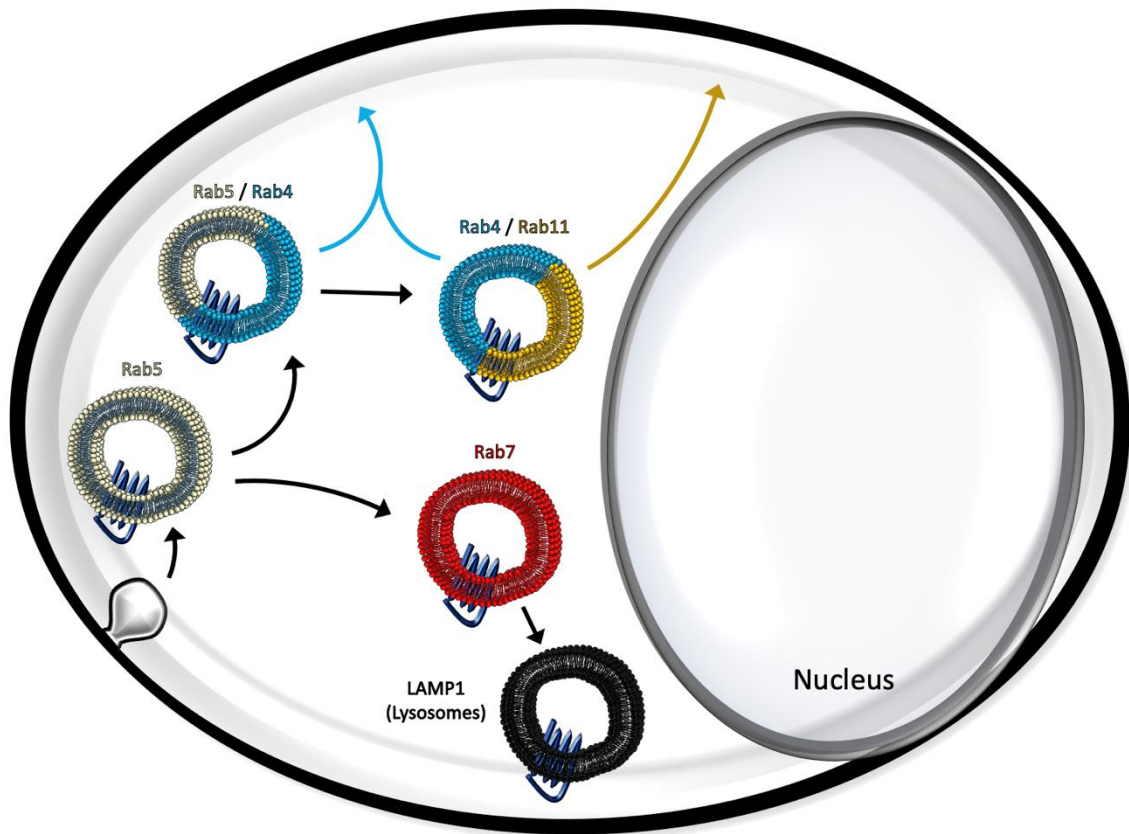


**Figure 8: Schematic of endolysosomal trafficking and the mosaic of overlapping Rab domains.** Rab proteins facilitate endosomal trafficking and define distinct endosomal domains within a network of cargo transport. Rab5 is the immediate destination for internalized cargo via clathrin coated pits and represents the early endosomal compartment. Following Rab5 colocalization, Rab4 and Rab11 represent the primary routes for receptor recycling via receptor resensitization and return to the plasma membrane. Cargo can be rapidly recycled back to the plasma membrane by sorting through Rab4<sup>+</sup> endosomes, or recycled through the perinuclear region to the plasma membrane via Rab11<sup>+</sup> endosomes. The Rab5, Rab4, and Rab11 domains are not distinctly separate but are dynamically interconnected. Alternatively, Rab5 endosomes can be trafficked to accomplish cellular desensitization through the Rab7 late endosomal pathway which ultimately leads to cargo to incorporation into LAMP1<sup>+</sup> terminal lysosomes.

### *Endosomal G $\alpha_s$ Signaling*

GPCR G $\alpha$  activation had once been thought to be isolated exclusively to the plasma membrane, in which following, GRK/ $\beta$ arr-facilitated rapid termination of signaling would coincide with receptor internalization. However, recently accumulated evidence has indicated an alternative mode of GPCR signaling, in which GPCR signaling by G $\alpha$  can occur at the membrane of endosomes localized to various intracellular compartments such as the nucleus, mitochondria, Golgi, and endoplasmic reticulum. G $\alpha_s$ , G $\alpha_q$ , and G $\alpha_i$  endosomal recruitment and signaling have been evidenced to occur within early endosomes (Kuna et al., 2013;

Mullershausen et al., 2009; Wright et al., 2021; Yarwood et al., 2017). The advantage of continued G $\alpha$  signaling at the endosome is the resulting persistence in sustained signaling regardless of changes in extracellular ligand concentrations (Calebiro et al., 2009). Additionally, the mobility of GPCR signaling conferred by endocytic trafficking alters the spatial landscape of downstream effectors that can be activated (Peng et al., 2021; Tsvetanova and von Zastrow, 2014).

Determinants of ligand-induced endosomal GPCR signaling are complex and not fully understood. However, it has been implicated that the stability of the ligand-GPCR complex may be a key element in resisting ligand release during endosomal acidification, and thus may be a determinant in sustaining the receptor conformational active state at the endosome (Sutkeviciute and Vilardaga, 2020).

For example, parathyroid hormone (PTH) at the parathyroid hormone 1 receptor (PTH1R) is known to induce sustained cAMP production at the internalized endosomal, while the alternative ligand parathyroid hormone-related protein (PTHrP) at the PTH1R exhibits cAMP signaling restricted to the plasma membrane (Ferrandon et al., 2009). Therefore, ligand-specific effects may influence the spatiotemporal signaling and localization behavior of a receptor. At the PTH1R, an alternative long-acting PTH analog, which exhibits more ligand-receptor residue interactions in comparison to native PTH, prolongs endosomal cAMP production more so than PTH, sustains the receptor in its active state, and consequently decreases receptor recycling (Sutkeviciute and Vilardaga, 2020; Zhao et al., 2019). Therefore, characteristics of the ligand sequence, and how it interacts with the target GPCR, may influence both the spatiotemporal attributes of receptor signaling and the receptors propensity to be recycled or degraded.

Both the lipid composition of the plasma membrane at the site of GPCR internalization, and endosomal membrane composition, may play a role in facilitating continued endosomal signaling. Membrane lipid composition can affect GPCR function. Membrane lipid composition can modulate orthosteric ligand binding, GPCR oligomerization, and GPCR access to downstream effectors (Sutkeviciute and Vilardaga, 2020). For example, an increased presence of phosphatidylglycerol and phosphatidylethanolamine within the local membrane space promotes agonist binding to the  $\beta_2$ AR. Additionally, elevated phosphoinositide composition within the plasma membrane has been evidenced to bind directly to GPCRs and modulate their functional capacity (Dawaliby et al., 2016; Yen et al., 2018). This effect is demonstrated

with enhanced stabilization of  $G\alpha_s$ -specific coupling facilitated by PIP2 binding at the  $\beta 1AR$ , and increased GTP turnover within  $G\alpha_i$  coupling at the neurotensin receptor (Yen *et al.*, 2018). Internalized GPCR signaling has demonstrated distinct physiological relevance. The spatial and temporal elements of endosome-produced cAMP have been shown to mediate PKA nuclear localization and PKA-dependent gene transcription (Calebiro *et al.*, 2009; Peng *et al.*, 2021; Tsvetanova and von Zastrow, 2014). In particular, as internalized endosomes dynamically move within the intracellular space, they may “bump” into metastable pools of PKA, which facilitate amplified downstream signaling over a spatial scale, and promote translocation of the PKA catalytic subunits into the nucleus. Inhibition of receptor internalization, and thus endosomal signaling, has been shown to diminish the cAMP-mediated nuclear transcriptional response of an upstream ligand-GPCR interaction (Peng *et al.*, 2021).

An example relevant to functional outcomes of endocytic signaling bias is seen with the ligands vasopressin and oxytocin at the vasopressin type 2 receptor (V2R). Both ligands activate cAMP/PKA signaling, yet only vasopressin induces an antidiuretic effect within the kidneys. Oxytocin binds to the V2R and easily dissociates from the receptor during internalization, which results in a primarily plasma membrane-localized cAMP signal. Vasopressin binds much more tightly to the V2R, and prolongs receptor internalization and induces endosomal  $G\alpha$  signaling (Zalyapin *et al.*, 2008). Interestingly, the translocation of aquaporin water channels and epithelial sodium channels from the cytosol to the plasma membrane, which thereby induces the anti-diuretic effect, is reliant on the sustained endosomal  $G\alpha_s$  signaling attributed to the vasopressin-V2R complex (Zalyapin *et al.*, 2008). Taking advantage of ligands that induce, or bias, temporal and spatial organization of GPCR signaling toward cellular outcomes that are therapeutically beneficial, is a lucrative endeavor for drug exploration (Thomsen *et al.*, 2018).

## Pharmacology

### *Efficacy and Potency*

The agonist-induced stimulation of a plasma membrane-bound GPCR will initiate a cascade of intracellular signaling events. This chain of events will ultimately lead to a physiological response. This physiological response, as well as the intermediate steps within the intracellular signaling cascade, can be measured to obtain information about the ligand-receptor interaction. Therefore, common receptor ligand pharmacology has been centered around mathematical models of stimulus and response to relatively compare “efficacy” and “potency” (Vauquelin and Mentzer, 2008). The most common model used to pharmacologically describe ligands is the  $E_{max}$  model. It is an empirical model primarily used for interpretation of concentration-response data. The  $E_{max}$  model does not convey mechanical interpretation, but instead describes the observational relationship of the agonist to a target response (Finlay et al., 2020). The two key parameters of intracellular pharmacodynamics are the maximal response ( $E_{max}$ , also efficacy) and the concentration of the ligand that produces 50% of the  $E_{max}$  ( $EC_{50}$ , also potency) (Holford, 2017). Analyses on pharmacological time course data using these parameters depend on the assumption that drug effects are immediately related to concentration in the specified compartment. These dose-response relationships are central to identifying safe and efficacious dosages for ligands (Holford, 2017).

### *Dose-Response Curve*

A coordinate graph that relates the concentration of a ligand to the magnitude of the receptor response is called a dose-response curve. Typically, the logarithmic molar concentration of a ligand is plotted on the X-axis while the measured event response is plotted on the Y-axis. Due to the desired logarithmic increase in ligand concentration, the lowest concentrations typically produce no signal and the highest of concentrations produce the maximal signal, resulting in a sigmoid curve with the steepest portion of the curve representing the dosages attributable to signal escalation.

The  $E_{max}$  model, which is most often used to describe dose-response relationships, describes the non-linear relationship of log-transformed agonist concentrations to the response using four parameters. In this fundamental equation,  $E$  is the response magnitude, and the four

parameters are the *basal* response,  $E_{max}$ ,  $EC_{50}$ , and *hill slope* (**Figure 9**). The basal response is the baseline constitutive activity of the receptor.  $E_{max}$  is the maximal Y-axis magnitude of the response.  $EC_{50}$  is the concentration eliciting 50% of the maximal response, and the hill slope is a factor that improves fitting of the curve (Finlay *et al.*, 2020). The hill slope in GPCR pharmacology, in particular, is usually constrained to 1 and thus simplified to a three parameter system due to the hill slope factor representing a ligand-dependent parameter and not a system parameter. GPCRs are represented as having one orthosteric site for ligand binding, therefore a hill slope equal to 1 is demonstrative of a 1:1 ratio constraint of one ligand activating one receptor, thereby remaining in accordance with the law of mass action. A hill slope >1 would indicate that a single ligand-receptor interaction could activate more than one receptor (Finlay *et al.*, 2020).

$$E = \frac{basal + (Emax - basal)}{1 + \left(\frac{EC50}{[agonist]}\right)^{hill\ slope}}$$

**Figure 9: The Hill Equation.**

Generally, the data derived from the dose-response curve ( $E_{max}$ ,  $EC_{50}$ ) allow for characterization of ligands as “full agonists”, “partial agonists”, and “antagonists”. A full agonist produces the maximal response ( $E_{max}$ ) regardless of the degree of ligand receptor occupancy. Despite potential variability in  $EC_{50}$  values, a full agonist will nonetheless produce a full response at some escalated concentration. Therefore, a partial agonist will produce an  $E_{max}$  that is a degree lower than the full agonist regardless of stimulated concentration, while an antagonist will produce an effect 0% to that of a full agonist at all concentrations (Wacker *et al.*, 2017).

### *Spare Receptor Effect*

In 1926, the pharmacological “occupation theory” was developed, in which it proposed that an agonist-mediated response is proportional to the number of ligand-occupied receptors at a cell. This theory was based on the principle of a ligand’s equilibrium dissociation constant ( $K_d$ ), which characterizes a ligand’s structural binding affinity to the receptor (Finlay *et al.*, 2020). Therefore, at a concentration in which 50% of available receptors are occupied by a ligand, the  $EC_{50}$  would be the expected result. However, as various full agonist ligands with

equivalent receptor binding affinities for a single receptor were developed, it was identified that the concentration required to reach the half maximal effect was variable between agonists. Due to this phenomenon of full agonist ligands with similar binding affinities yet different EC values, the concept of “receptor reserve” or “spare receptor” was established (Vauquelin and Mentzer, 2008). The spare receptor concept explained that a measured ligand binding event could achieve a maximal measurable response ( $E_{max}$ ) without full occupation of all available receptors. In this case, full agonist ligands with similar receptor binding affinities were characterized by differential potencies, in that “high potency” full agonists needed to only bind a fraction of the total number of receptors in order to achieve the saturable maximal response, while “lower potency” full agonists required higher ligand-receptor occupancy to achieve a maximal response. The spare receptor capacity between ligands with matched binding affinities describes shifts in the EC of full agonists, however it must be taken care that the  $K_d$  of comparative ligands are considered (Vauquelin and Mentzer, 2008).

### *Signal Amplification*

The spare receptor effect, in which differential degrees of ligand-receptor occupancy can achieve maximal intracellular responses, is facilitated by an effect called signal amplification. Very often, the relationship between consecutive intracellular events tends to be non-linear (Vauquelin and Mentzer, 2008). In which, the signal magnitude of a second event in a signal chain becomes maximally saturated before the magnitude of the first event can reach its maximum. Therefore, within generated dose-response curves, the EC of a ligand shifts to the left (decreases) at each event downstream of ligand binding within the intracellular signaling cascade (**Figure 10**) (Vauquelin and Mentzer, 2008). This increase in potency is due to cascading signal amplification occurring within the metabolic network (Ross, 2014). Of consequence, ligands with partial agonism for an upstream target such as  $G\alpha_s$  may be classified as full agonists for downstream events such as cAMP or pERK. The non-linearity underlying the effect of signal amplification is not fully understood but likely involves synergistic actions within the number of available effectors at each step of the signaling pathway (See: The GLP-1R and GIPR:  $G\alpha_s$  Signal Amplification).

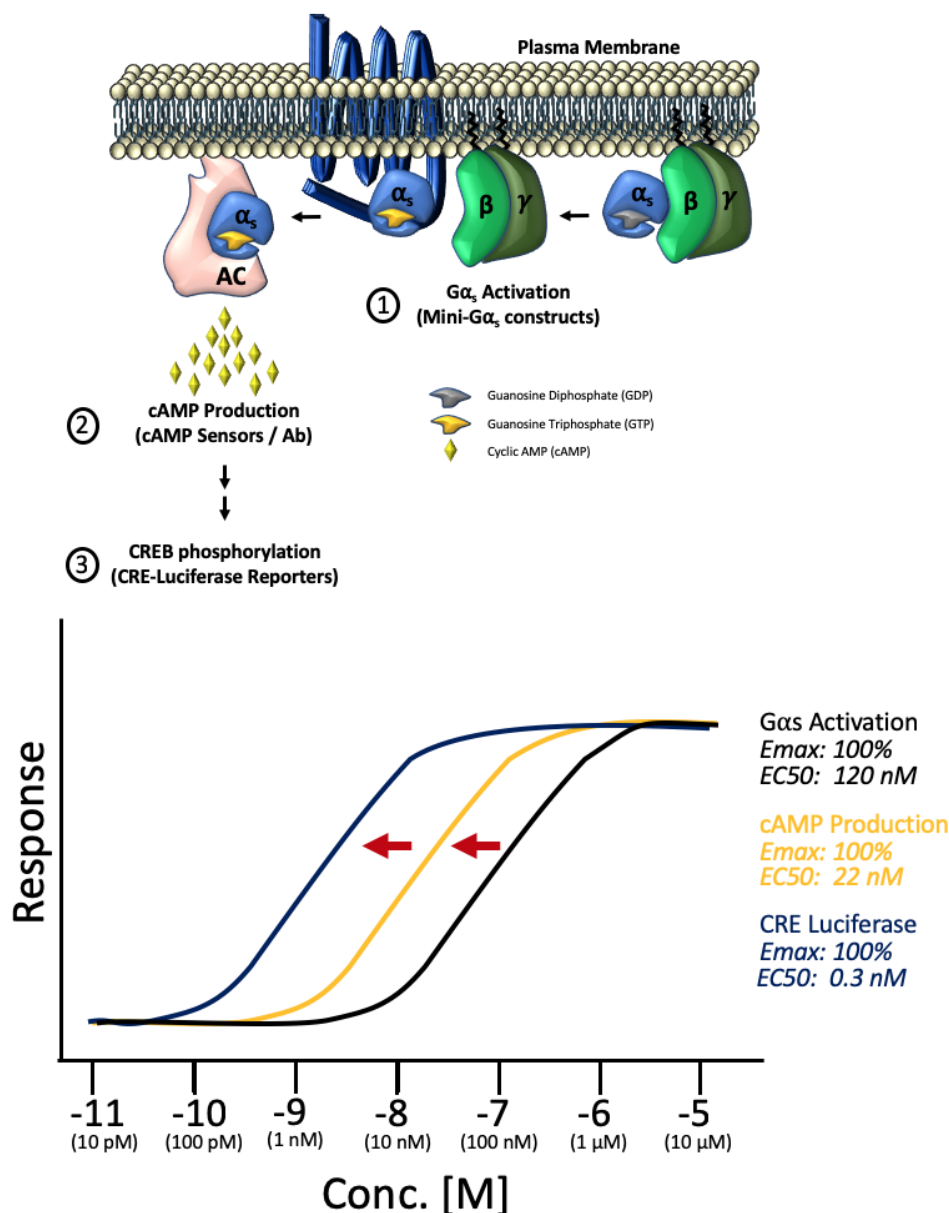


**Figure 10: Ligand potency as a product of intracellular signal amplification.** Comparison of ligand potency within subsequent steps of the signaling cascade in which a leftward shift in each dose-response curve is attributed to an intracellular amplification of signal. Immediate G-protein signaling as measured by mini $G\alpha_s$  recruitment, also viewed as ‘receptor activation’, is the first step within the cascade. Quantification of direct cAMP production (as measured by unimolecular cAMP sensors or cAMP antibody sandwich assays) represents a step downstream that is subject to a degree of signal amplification. Indirect cAMP measurements using nuclear cAMP CRE-luciferase reporters, which are dependent on PKA phosphorylation of CREB, represent quantitative readouts most effected by amplification of signal.

## *Principles of Bioluminescence Resonance Energy Transfer (BRET)*

A primary live-cell technique used within this thesis to quantify the differential relationship between each ligand and multiple intercellular signaling pathway targets, is bioluminescent resonance energy transfer (BRET). Similar to fluorescence resonance energy transfer (FRET), BRET allows for the quantification of proximal protein-protein interactions between lumiphore-tagged and fluorophore-tagged proteins of interest (POI) through non-radiative energy transfer (Salahpour et al., 2012). Luminescent substrate is utilized and degraded by the lumiphore to produce luminescence. Therefore if the lumiphore- and fluorophore-tagged POI move within a distance  $< 10\text{nm}$  of each other, which is considered sufficient distance to facilitate a biological interaction, quantifiable resonance energy transfer occurs, thus distilling details both about constitutive and dynamic protein interactions (Salahpour *et al.*, 2012). The separation in emission spectra between the lumiphore and fluorophore, and lumiphore-mediated energy transfer into the fluorophore, allow for ratiometric quantitation in assessing changes in fluorophore emission due to the presence or lack of energy transfer. One of the primary benefits of BRET over FRET is the minimization of fluorophore photobleaching and noise attributable to a lack of external laser excitation. Due to the minimal photobleaching and noise, BRET provides an opportunity to temporally quantify pharmacological induction of protein-protein interactions over an extended period of time (approximately 1 hour). In addition, BRET assays can be performed in live-cell environments that more closely relate to that of living systems (Salahpour *et al.*, 2012).

Strategic lumiphore/fluorophore tagging allows for the implementation of either gain in- or loss in- resonance energy assays. For example, a lumiphore-tagged  $G\alpha_s$  subunit paired with a C-terminal fluorophore-tagged GLP-1R can quantify the degree of ligand-induced  $G\alpha_s$  recruitment to the GLP-1R via gain in resonance-mediated signal intensity (Liu et al., 2019). Here, the tagged  $G\alpha_s$  subunit establishes resonance by translocating to the GPCR following ligand binding at the GPCR. Oppositely, a C-terminal lumiphore-tagged GLP-1R paired with a fluorophore-tagged marker of the inner plasma membrane leaflet can quantify the disappearance of a plasma membrane-bound GPCR as mediated by receptor internalization (Tiulpakov et al., 2016b). Here, ligand stimulated GLP-1R internalization dissociates the baseline resonance occurring between the plasma membrane-bound GPCR and plasma membrane marker, resulting in a loss in signal (**Figure 11**).



In addition to quantifying the interaction between two separate proteins to elucidate an event within a metabolic pathway, unimolecular sensors are capable of quantifying ligand-induced changes of intracellular signaling molecules and kinase activity (i.e. cAMP, PKA) (Jiang et al., 2007; Mehta et al., 2018). Here, a unimolecular sensor with either a lumiphore and fluorophore present on opposing ends, or a single fluorophore split to both sides, is conformationally adjusted following an interaction with the target (cAMP binding, PKA phosphorylation) ultimately leading to a gain or loss in signal.

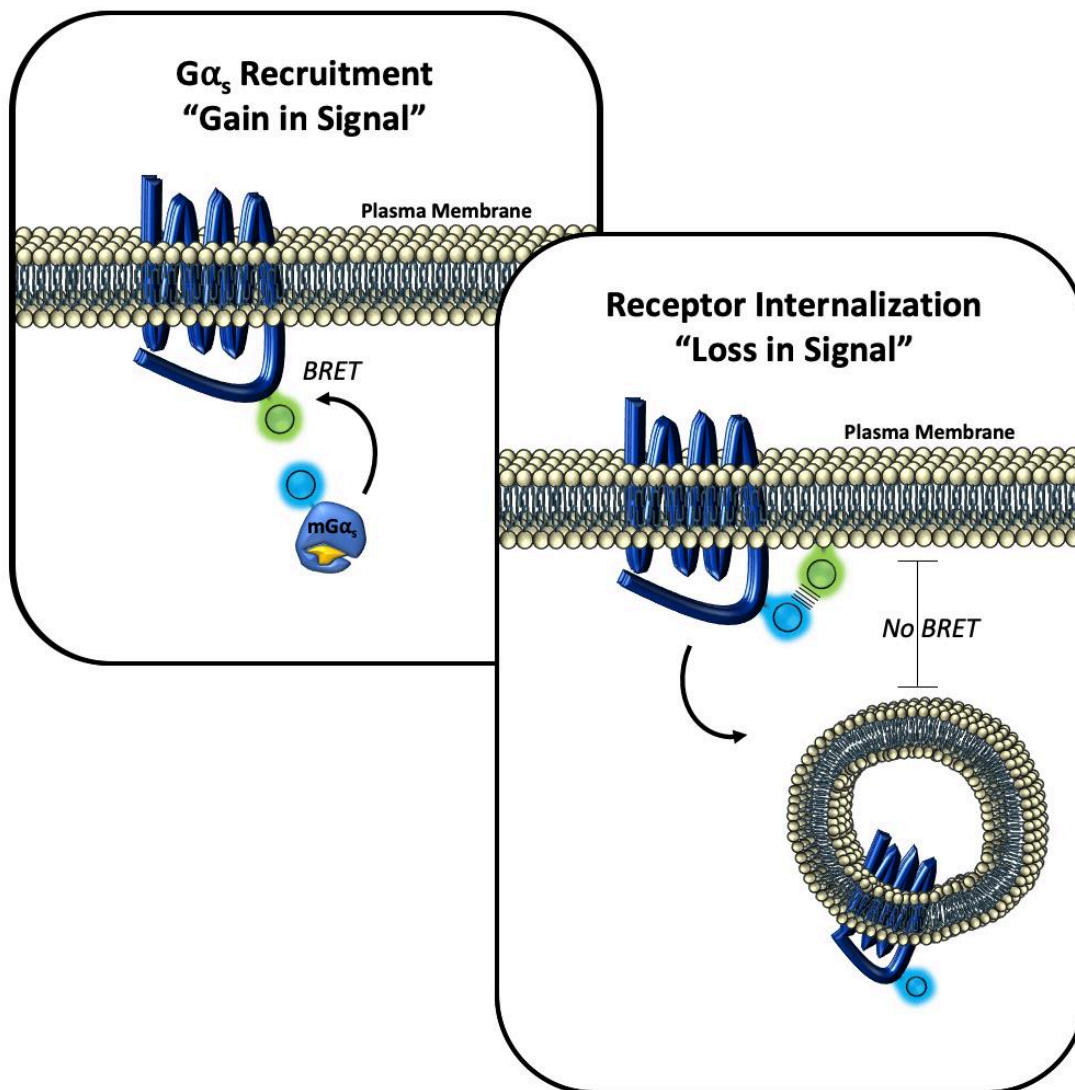


**Figure 11: Examples of "gain in signal" and "loss in signal" BRET assays by MiniGα<sub>s</sub> recruitment to the GPCR and GPCR dissociation from the plasma membrane.** Protein-protein interactions can be quantified through bioluminescent resonance energy transfer (BRET) when a donor lumiphore is brought into close vicinity (< 10 nm) to a suitable acceptor fluorophore. BRET assays can be grouped into "gain in signal" or "loss in signal" assays. MiniGα<sub>s</sub>-Nluc recruitment assays, in which a lumiphore-tagged truncated version of Gα<sub>s</sub> resides within the cytosol at baseline and is recruited to a fluorophore-tagged GPCR upon ligand stimulation, is representative of a gain in signal assay as BRET is established. In a loss in

signal assay, in which baseline BRET is dissipated by the lumiphore moving away from its fluorophore counterpart, is exemplified with receptor internalization assays as the internalizing lumiphore-tagged GPCR moves to a distance > 10 nm relative to the fluorophore-tagged plasma membrane marker.

## GLP-1 and GIP Pharmacological Development

### *Background and Historical Development of GLP-1 based Pharmacology*

The GLP-1R has been extensively explored over the past decades as a lucrative target for the treatment of diabetes in part due to its preserved therapeutic potential within the context of metabolic syndrome (Nauck et al., 1993b). GLP-1, and its counterpart GIP, make up the incretin hormone family, which is a set of gut-derived peptides that enhance glucose-dependent insulin secretion following the ingestion of nutrients. Expression of the GLP-1R within key hypothalamic regions known for appetite regulation and within pancreatic  $\beta$ -cells confers dual purpose therapeutic benefit by simultaneously targeting both appetite satiation and enhancing hyperglycemia-stimulated insulin secretion. However, the efficacy of GLP-1 within therapeutic settings has been limited due to its short circulating half-life (1.5-5 minutes), resulting from an inactivating cleavage at amino acid position 2 of the “active” GLP-1 (7-36 amide) by the ubiquitous enzyme DPP-4. Since the establishment of the first amino acid sequence of GLP-1 in the early 1980s, to the discovery of the “active” N-terminally truncated form GLP-1 (7-37) and GLP-1 (7-36 amide) in 1987, and the identification of the structure-function relationship of each amino acid within active GLP-1 in 1994, biochemical GLP-1 peptide sequence optimization has been intrinsic to the development of therapeutic efficacy (Adelhorst et al., 1994; Holst *et al.*, 1987; Mojsov *et al.*, 1987). In parallel, the isolation and sequencing of the GLP-1 homolog EX-4 from *Heloderma suspectum* has lent further insight into improving the half-life stability of circulating GLP-1 analogs (Eng et al., 1992). The commonly used EX-4 inspired modifications to improve half-life stability of the active GLP-1 sequence include a glycine or aminoisobutyric acid (Aib) substitution to the alanine at position 2 to protect against DPP-4 inactivation, and an addition of the EX-4 GPSSGAPPPS C-terminal extension (CEX) to stabilize the secondary structure of the peptide and potentially improve affinity to the GLP-1R (Doyle et al., 2003; Simonsen et al., 2013).

## Optimization of GLP-1R Mono-agonists

The primary therapeutic endpoints for GLP-1-based treatments are, the healthy control of post-prandial dysglycemic excursions, reductions in fasted Hb1Ac, and either a reduction or no change in body weight. The therapeutic potential of GLP-1 agonists on these parameters is predominately linked to engineered improvements in the circulating half-life of the peptide (Prasad-Reddy and Isaacs, 2015). The aforementioned EX-4 inspired modifications to the GLP-1 peptide sequence is capable of prolonging plasma half-life of up to 2-4 hours. However, developments in application and linkage technologies have allowed for greater achievement in therapeutic endpoints through the creation of “long-acting” GLP-1 agonists, which present half-lives ranging between 12 hours and several days (**Table 1**). A primary extra-sequence modification contributing to long-acting effects is peptide acylation, which confers non-covalent binding of the peptide to larger circulating albumin proteins resulting in DPP-4 protection and reduced renal clearance (Knudsen and Lau, 2019). The increased molecular weight of the acylated peptide-albumin complex pushes the complex past the renal threshold for renal clearance (60-70 kda) extending the peptide’s circulating half-life (Knudsen and Lau, 2019). Liraglutide demonstrates the half-life enhancing properties of fatty acid acylation, in which despite a 97% sequence homology to human GLP-1 and a lack of sequence-mediated protection from DPP-4, a C16 fatty acid acylation increases the circulating plasma half-life of liraglutide to 11-13 hours from the 1.5-5 minutes of human GLP-1 (Knudsen and Lau, 2019).

**Table 1: Characterization of clinically-relevant GLP-1R mono-agonists.** Pharmaceutical GLP-1R mono-agonists with described general modifications relevant to enhancing agonist in vivo half-life.

Agonist	General Modification	In vivo half-life	Company
<b>Endogenous GLP-1</b>	• none	1.5 - 5 min	
<b>Exenatide</b>	• Glycine substitution (Pos2) • CEX tail	2 -3 hours	AstrazZeneca
<b>Lixisenatide</b>	• Glycine substitution (Pos2) • CEX tail • Poly-lysine C-terminal addition	3 - 4 hours	Sanofi
<b>Albiglutde</b>	• Glycine substitution (Pos2) • Sequential fusion of two GLP-1 analogs covalently bound to human albumin	5 - 8 days	GlaxoSmithKline
<b>Dulaglutide</b>	• Glycine substitution (Pos2) • Two identical GLP-1 analogs covalently bound to an IgG4 Fc fragment to form a disulfide-bonded homodimer	5 days	Eli Lilly
<b>Liraglutide</b>	• Arginine Substitution (Pos27) to confer acylation • C16 monoacid acylation (Pos20)	11 - 13 hours	Novo Nordisk
<b>Semaglutide</b>	• Aminoisobutyric acid substitution (Pos2) • Arginine substitution (Pos27) to confer acylation • C18 diacid acylation (Pos20)	7 days	Novo Nordisk
<b>Taspoglutide</b>	• Aminoisobutyric acid substitution (Pos2 and Pos29) • Formulated with zinc chloride for sustained release	Unknown half-life Once-weekly administration	Roche
<b>Exenatide-LAR</b>	• Exenatide-containing biodegradable poly(lactide-co-glycolide) microspheres for sustained release	2 - 3 hours (exenatide) Once-weekly administration	AstraZeneca, Amylin

Other molecular weight-increasing modifications to reduce renal clearance have achieved similar therapeutic profiles due to their extended half-lives, including the synthetic fusion of GLP-1 to albumin prior to injection (Albiglutide), or the linkage of two individual GLP-1 molecules within a disulfide-bridged Fc fragment (Dulaglutide) (Madsbad, 2016). Other methods to establish stable circulating GLP-1 agonist concentrations over a prolonged period of time include developments in formulation application, in which a GLP-1 analog has either been co-infused with zinc chloride to delay the absorption of the peptide from subcutaneous tissue (Taspoglutide), or has been infused into biodegradable microspheres for sustained release in circulation (Madsbad, 2016). However in total, despite the extensive success of long-acting GLP-1 agonists in treating dysglycemia, the body weight lowering success of these compounds has been relatively modest with an average 2.6 kg BW loss over 24-30 weeks between all agonists in humans (Madsbad, 2016; Owens et al., 2013). The best-in-class GLP-1 agonist Semaglutide (1.0mg) demonstrated a mean BW loss of 6 kg following at least 30 weeks of treatment through multiple clinical trials, an effect that was not mediated by the appearance of gastrointestinal side effects (Ahmann et al., 2018; Capehorn et al., 2020; Lingvay et al., 2020; Pratley et al., 2018). However, GLP-1-based treatment complications, such as nausea and gastrointestinal adverse effects, have limited the escalation of dosing to achieve greater weight loss. While GLP-1 analogs of varying modifications have been successful in treating dysglycemia, it has become clear that targeting body weight reduction solely by GLP-1R agonism has intrinsic limitations. Therefore, pharmaceutical activation of additional receptors in parallel to GLP-1R has been investigated for potential synergies that can improve GLP-1 agonist efficacy while limiting the side-effect profile.

### *Co-administration of GLP-1 Mono-agonists with Complementary Peptides*

Targeting additional receptors to accentuate GLP-1R agonism via synergistic or additive mechanisms has been a goal founded on improving both the efficacy and tolerability profile of GLP-1 agonists. Cooperative peptide enhancement of insulinotropic efficacy, satiation, and energy expenditure are the ideal functional targets to achieve these optimized therapeutic endpoints. GIP administration, for example, has demonstrated to elicit a consistent insulinotropic response in healthy subjects (Dupre *et al.*, 1973). GIP, GLP-1, glucagon, CCK, PYY, and amylin have all been evidenced to exhibit varying degrees of food intake reduction and satiation promotion (Geary, 1990; Karra et al., 2009; Lutz, 2005; Moran and Kinzig, 2004;

Zhang *et al.*, 2021b). Glucagon has been proven potent at increasing energy expenditure through its lipolytic and thermogenic properties (Galsgaard *et al.*, 2019; Salem *et al.*, 2016). Thereby, the physiological benefits of these various peptides in conjunction with GLP-1 is a lucrative combinatorial approach that either reinforces effects already found with GLP-1 (insulinotropism, satiety) or adds a novel element of therapeutic benefits to GLP-1-based treatments (energy expenditure).

The co-administration of GLP-1 and GIP has proven to provide an additive benefit above that of GLP-1 alone with regard to stimulating insulin secretion (Elahi *et al.*, 1994; Nauck *et al.*, 1993a). Regarding satiety, low-dose administration of either GLP-1 (0.3 nmol) or GIP (1 and 3 nmol) alone fail to decrease food intake and body weight using ICV injections in mice, while separate higher doses of ICV GLP-1 (1 and 3 nmol) or GIP (6 nmol respectively) alone effectively achieve significant reductions in food intake and body weight. Interestingly, ICV co-administration of both GLP-1 and GIP at subeffective doses (0.3 nmol and 1 nmol, respectively) significantly decreased food intake and body weight demonstrating synergistic action between GLP-1 and GIP co-administration in promoting satiety (NamKoong *et al.*, 2017). Similarly, subcutaneous injection of an acylated GIP (3 nmol) failed to significantly reduce body weight and food intake in DIO mice over a 14 day period, however when the acylated GIP (3 nmol) was co-administered with an acylated GLP-1 (3 nmol) the body weight and food intake reductions were significantly greater than the effects elicited by acylated GIP or acylated GLP-1 alone (Finan *et al.*, 2013). These findings together point toward a lucrative synergism between GLP-1 and GIP to not only improve the efficacy of GLP-1R-mediated decreases in food intake and body weight, but also to improve the therapeutic tolerability profile by reducing the dosage of GLP-1 agonist required to achieve the same body weight and food intake reductions seen with GLP-1 agonism alone.

At first glance, glucagon seems to be on the opposing side of GLP-1's biological functionality due to its stimulation of hyperglycemia-promoting processes such hepatic and renal glycogenolysis and gluconeogenesis. Interestingly, co-administration of glucagon with GLP-1 has been demonstrated to suppress glucagon-mediated increases in blood glucose in nonhuman primates. The blood glucose excursion during an IVGTT within the context of co-administration of GLP-1 and Gcg agonists was non-significantly different relative to an IVGTT performed without administration of any agonists. Similarly, 30 days co-administration with GLP-1 and Gcg agonists achieved approximately 40% of the reduction in HbA1c to that of the

GLP-1 agonist-only group (Elvert et al., 2018). Despite the suppressing effect of GLP-1 agonism on the hyperglycemia-promoting effects of glucagon agonism, GLP-1R agonism spares the glucagon-mediated effects on energy expenditure, satiety, and lipolytic activity. GcgR-mediated body weight reductions are minimal in nonhuman primates, and during GLP-1R/GcgR co-agonism in GLP-1R KO DIO mice (Day et al., 2009; Elvert *et al.*, 2018). However, when a glucagon agonist is co-administered with a GLP-1 agonist, or when the GcgR agonism of a GLP-1R/GcgR co-agonist is stabilized by a lactam-bridge side chain and administered into WT DIO mice, the body weight lowering effect is amplified to a greater extent than is seen with GLP-1R or GcgR agonism alone (Day *et al.*, 2009; Elvert *et al.*, 2018). Food intake is similarly affected by peripheral co-administration of GLP-1 and glucagon in mice, which results in reduced food intake over the course of 30 minutes and a greater induction of c-fos expression in the area postrema and central nucleus of the amygdala relative to the saline or mono-treatment controls (Parker et al., 2013). Additionally, in obese humans, both glucagon mono-treatment and co-administration of GLP-1 and glucagon significantly increase resting energy expenditure to a similar extent, while GLP-1 alone fails to do so. However, the usefulness of GLP-1 within glucagon co-administration, in comparison to glucagon treatment alone, achieves the same rapid rise in energy expenditure without the accompanying rise in plasma glucose levels (Tan et al., 2013). The complementation of GLP-1R and GcgR co-agonism demonstrates synergy in terms of body weight loss and satiety, while the added component of GcgR agonism expands the therapeutic functionality to include an increase in energy expenditure that is absent the GcgR-mediated hyperglycemia.

Synergistic effects between GLP-1 agonists and other peptide targets have not been limited to only the GIPR and GcgR. Co-administration of the GLP-1 analog exenatide with a CCK1 (but not CCK2) agonist induced synergistic reductions in both body weight and food intake in DIO mice (Trevaskis et al., 2015). Co-administration of liraglutide and the amylin analog salmon calcitonin in DIO rats synergistically reduced food intake and body weight over 24 hours, however chronic co-administration over the course of 32 days produced a stronger, but not synergistically greater, effect than liraglutide and the amylin analog alone (Liberini et al., 2019). Co-administration of GLP-1 (7-36 amide) and PYY (3-36), which are known to co-originate from L-cells upon nutrient exposure, synergistically decreased body weight and food intake despite the matched mono-treatment dosage of GLP-1 and PYY (1 nmol and 10 nmol, respectively) having no effect on food intake or body weight in genetically obese mouse

models. Interestingly, when GLP-1 and PYY were co-administered in humans, a 27% reduction in food intake during a buffet meal was observed, noting an additive benefit between GLP-1 and PYY on reducing energy intake (Neary et al., 2005). Taken together, the additive and synergistic benefits of multiple peptides in combination with GLP-1 have provided an opportunity to shift from a pure mono-agonist approach toward a multi-agonism approach capable of improving efficacy and tolerability of GLP-1 based pharmaceutical intervention.

### *Development of Unimolecular Dual-Agonists*

GLP-1 (7-36 amide), GIP, and glucagon are secreted peptides that are 30, 42, and 29 amino acids in length. Interestingly, the GIP and glucagon peptides share high sequence homology with GLP-1 of 36% and 48% (**Figure 12**). The first 14 and 15 N-terminal amino acids of the GIP and glucagon sequence are of predominant importance to the activation of their respective receptors. GIP and glucagon share 53% and 67% sequence homology within the first 15 amino acids to GLP-1 (Chabenne et al., 2014; Hinke et al., 2004).

This tri-directional sequence homology between ligands and receptors presents a lucrative opportunity to hybridize the sequences of two or more ligands into a unimolecular peptide with the purpose of simultaneously activating two or more target receptors. By combining these ligands into unimolecular dual- and tri- agonists it may be possible to provide complementary and potentially synergistic pharmacological action within a single molecule. The facilitating factor of pharmacological action of the unimolecular dual- or tri-agonists lies within the capacity to act at spatially separated biological structures that express one or more of the target receptors. The goal is to not only improve the combinatorial efficacy of biological endpoints (i.e. superior insulinotropism, satiation, energy expenditure) for therapeutic benefit, but also to potentially decrease the dosing regimen and minimize the probability of adverse side effect appearance attributable to high dose GLP-1 treatment.

The unimolecular approach provides distinct advantages in comparison to loose adjunct administration of multiple mono-agonists. In particular, the key benefit is in eliminating differences in pharmacokinetic profile of individual agonists (Finan et al., 2015). The loose combination of peptides is subject to individual profiles of absorption, distribution, metabolism, and excretion. The unimolecular hybrids however have a single pharmacokinetic profile, allowing for optimal dosing and a higher likelihood of potential regulatory approval.

Compound	Sequence
GLP-1 (7-36 amide) 100% homology	HAEGTFTSDVSSYLEGQAAKEFIAWLVKGR-NH <sub>2</sub>
GIP (1-42) 36% homology	YAEGTFI SDYSIAMDKIHQQDFVNWLLAQKGGKNDWKHNITQ
Glucagon (1-29) 48% homology	HSQGTFTSDYSKYLD SRRRAQDFVQWLMNT

**Figure 12: Amino acid sequence homology of GIP (1-42) and Glucagon (1-29) to GLP-1 (7-36 amide).** Amino acids within the GIP (1-42) sequence highlighted in blue are unique relative to GLP-1 (7-36 amide). Amino acids within the Glucagon (1-29) sequence highlighted in red are unique relative to GLP-1 (7-36 amide).

### *GLP-1/Gcg Dual-agonists*

Oxyntomodulin, an endogenously secreted 37 amino acid peptide originating from the same proglucagon fragment as GLP-1 and glucagon (Gcg), and presenting activity at both the GLP-1R and GcgR, can lay claim as the first GLP-1/Gcg dual-agonist. However, the first clinically-relevant template of a unimolecular GLP-1/Gcg dual-agonist was developed in 2009, with the goal of engineering GLP-1 agonism into a glucagon core sequence (Day *et al.*, 2009). The N-terminal sequences between both GLP-1 and glucagon are highly conserved. Interestingly the GLP-1R transmembrane domain does not differentiate in recognizing and binding the GLP-1 and glucagon N-terminal sequences (Hjorth *et al.*, 1994). As amino acid positions 2, 3, 10, and 12 of glucagon are of critical importance to GcgR activation, and as this N-terminal sequence does not negatively impact binding to the GLP-1R, the first 15 amino acids were left unmodified in the GLP-1/Gcg dual-agonist's development. The remaining mid to C-terminal amino acid sequence of GLP-1 and Gcg is where the majority divergence occurs and where receptor selectivity is mediated. Ligand specificity of the GLP-1R and GcgR is primarily determined by the ligand's C-terminal sequence interaction with the receptor's N-terminal extracellular domain (Runge *et al.*, 2003). Therefore, adhering to the critical importance of the first 15 amino acids of glucagon in mediating glucagon receptor activation, an opportunity is provided to engineer in specificity to the GLP-1R within the glucagon C-terminal sequence. C-terminal amidation and substitution of seven GLP-1-specific amino acids into the last 14 amino acid stretch of the glucagon sequence conferred GLP-1R activity through enhanced C-terminal helical stability and N-terminal ECD recognition. An additional Aib substitution at position 2 conferred DPP-IV resistance, and the addition of a lactam bridge within the middle of the peptide enhanced glucagon activity by promoting secondary structure stabilization. With this



particular GLP-1/Gcg peptide, pre-clinical studies in DIO mice have evidenced a strong weight lowering effect compared to the vehicle, which is largely mediated by a decrease in food intake and an increase in energy expenditure (Day *et al.*, 2009). Interestingly, the GLP-1/Gcg dual-agonist conferred greater glycemic control than the vehicle, demonstrating the protective effect of GLP-1 against Gcg-induced hyperglycemia. This same molecule was seen to restore leptin sensitivity in DIO mice, which may contribute the weight lowering responsiveness of the dual-agonist.

### *GLP-1/GIP Dual-Agonists*

Due to the higher sequence homology between GLP-1 and glucagon, development of the GLP-1/GIP dual-agonist has relatively lagged behind that of the GLP-1R/GcgR dual-agonists. Given the co-expression of GLP-1R and GIPR in some tissues, the principle of the GLP-1/GIP dual-agonist is to allow for a peptide that binds to one or the other receptor, but that does not simultaneously link the two local receptors as may be the case with a GLP-1/GIP fusion peptide (two individual peptides connected by a linker). By creating a unimolecular GLP-1/GIP co-agonist, the rationale was that GLP-1 would reduce body weight and improve glycemic control which would then facilitate the metabolic benefits of GIP sensitivity (Finan *et al.*, 2013).

The first clinical template for a balanced GLP-1/GIP dual-agonist was engineered from the earlier GLP-1/Gcg dual-agonist and was designed to provide balanced agonism between both the GLP-1R and GIPR while minimizing activity at the GcgR, as measured by a cell-based CRE luciferase assay in HEK293 cells (Day *et al.*, 2009; Finan *et al.*, 2013). It is known that the first and seventh amino acids of the GLP-1 (7-36 amide) and GIP (1-42) sequences are primarily responsible for conferring differential receptor selectivity, as a Tyr1His and Ile7Thr substitution to the GIP sequence diverts its selectivity away from the GIPR to the GLP-1R (Moon *et al.*, 2012). To invoke GIPR selectivity and conserve GLP-1R activity within the GLP-1/Gcg dual-agonist, a His1Tyr substitution was made while the threonine at position 7 shared between glucagon and GLP-1 was retained. Additional GIP-specific substitutions were made at position 3, 12, 16, 20, 23, 24, and 27 to increase GIPR activity, while the lactam bridge present from the GLP-1/Gcg molecule was removed to minimize GcgR cross-reactivity. Unlike the GLP-1R and GcgR, the C-terminal sequence of GIP does not mediate ligand selectivity or activity at the GIPR, so the EX-4 CEX tail was added to confer peptide stability and promote enhanced GLP-1R selectivity. Lastly, a lysine was added at position 40 to facilitate fatty acid

acylation for albumin binding and prolongment of half-life (Finan *et al.*, 2013). This particular compound, MAR709 (NNC0090-2746) of Novo Nordisk made it to phase 2 clinical trials but was later discontinued.

A current leader in the GLP-1/GIP dual-agonist clinical field is the Eli Lilly compound Tirzepatide (LY3298176). The sequence of Tirzepatide is an imbalanced agonist favoring the GIPR over GLP-1R in terms of cAMP potency (Coskun *et al.*, 2018). The sequence of Tirzepatide is relatively similar to MAR709, however a few alterations consist of substituting in GIP-specific, or substituting out GLP-1-specific amino acids, at position 13, 17, 19, 20, 21, 24, and 27. Additionally, a GLP-1 specific lysine at position 20 was employed so that the peptide can be acylated with a C20 unsaturated diacid chain.

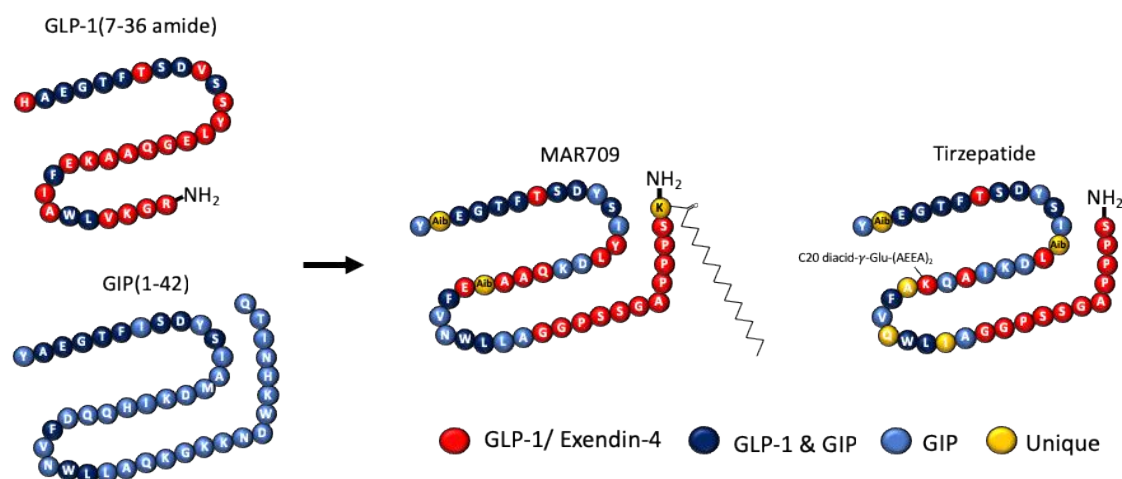


**Figure 13: Unimolecular hybridization of GLP-1 (7-36 amide) and GIP (1-42).** High sequence similarity between GLP-1 and GIP within the N-terminal region of the peptides, the necessity of Tyr1 for GIPR activation, and the functional exchangeability of Tyr1His in maintaining GLP-1R potency, had allowed for the iterative development of the balanced GLP-1/GIP dual-agonist MAR709 (NNC0090-2746, Novo Nordisk, Copenhagen, Denmark). Tirzepatide (LY3298176; Eli Lilly, Indianapolis, IN, USA), an unbalanced GLP-1/GIP dual-agonist, was similarly modeled to the MAR709 sequence however with specific amino acid substitutions conferring greater preference to the GIPR over the GLP-1R. *Figure adapted from Novikoff et al. 2021 (Mol. Met.).*

Both MAR709 and Tirzepatide have both had pre-clinical and clinical success. MAR709 was evidenced to improve glucose tolerance in WT DIO mice comparably to that of co-administration of matched GLP-1 and GIP mono-agonists, but failed to do so in a GLP-1R/GIPR KO model indicating a lack of off-target effects (Finan *et al.*, 2013). MAR709 was also proven to reduce body weight, food intake, decrease fat mass, ad-libitum blood glucose, and cholesterol in WT DIO mice, diabetic ZDF mice, and db/db mice. In diabetic ZDF mice, MAR709 administration reduced HOMA-IR, improved pancreatic islet cytoarchitecture, and improved

HOMA- $\beta$  scores (indicative of  $\beta$ -cell functionality). In cynomolgus monkeys, MAR709 was superior compared to liraglutide in inducing an insulinotropic and blood glucose clearing response during graded dextrose infusion (Finan *et al.*, 2013). These effects translated into first proof-of-concept in patients with T2D inadequately controlled by metformin, in which a superior reduction in body weight, HbA1c, and cholesterol was observed compared to the vehicle in human subjects (Frias *et al.*, 2017). Tirzepatide has demonstrated similar therapeutic benefits in mice which were successfully translated to phase 1 clinical trials (Coskun *et al.*, 2018). Additionally, in further human clinical trials, Tirzepatide demonstrated better efficacy on weight loss and glycemic parameters compared to vehicle, dulaglutide, and semaglutide, with additional unpublished clinical trials (SURPASS-3 and SURPASS-5) reporting Tirzepatide as superior to insulin degludec or insulin glargine, with or without metformin (Dahl *et al.*, 2021; Frías *et al.*, 2021; Frias *et al.*, 2018; Ludvik *et al.*, 2021; Min and Bain, 2021; Rosenstock *et al.*, 2021).

---

# CHAPTER 2: Methodology

---

---

## Materials

### *Peptide Ligands*

Semaglutide and GLP-1R antagonists JANT-4 (9-39) were provided by Novo Nordisk (Bagsværd, Denmark). All of the other peptides were prepared via standard automated Fmoc/tBu solid-phase peptide synthesis on Rink Amide ChemMatrix resin. An orthogonal protecting group strategy was used to incorporate the protraction moiety onto the appropriate lysine side chain. Following synthesis, crude compounds were cleaved from the resin with 95:2.5:2.5 trifluoroacetic acid/water/triisopropylsilane. The crude compounds were purified by reversed-phase high-performance liquid chromatography (RP-HPLC) on a Luna C8 (2) preparative column with a gradient of water/acetonitrile containing 0.1% trifluoroacetic acid, then lyophilized to produce the desired compounds as white powders. Compound identity was confirmed via RP-HPLC-mass spectrometry. hGLP-1 (7–36 amide) was purchased from Anaspec (Cat#: AS-22463, Fremont, CA, USA). hGIP (1–42) was purchased from Anaspec (Cat#: AS-61226-1, Fremont, CA, USA).

### *Small Molecule Agonists and Inhibitors*

Barbadin was purchased from Toronto Research Chemicals (Cat#: B118250, North York, Ontario, Canada) (Beautrait et al., 2017). Methyl- $\beta$ -Cyclodextrin was purchased from Sigma–Aldrich (Cat#: 332615, St. Louis, MO, USA). Sucrose was purchased from Thermo Fisher Scientific (Cat#: 15456759, Waltham, MA, USA). Forskolin was purchased from Sigma Aldrich (Cat#: 93049, St. Louis, MO, USA).

### *Plasmid Constructs*

Untagged human GLP-1R was purchased from Sino Biological Inc. (Cat#: HG13944-UT, Beijing, China) and untagged human GIPR and human GIPR-turbo GFP were purchased from OriGene Technologies Inc. (Cat#: SC110906 and RG210811, Rockville, MD, USA). Human GLP-1R-GFP was a gift from Professor David Hodson (University of Birmingham, Birmingham, UK). Human GLP-1R-Rluc8 (hGLP-1R-Rluc8) was a gift from Professor Patrick Sexton (Monash University, Melbourne, Australia). Human CMV-GIPR-Rluc8 (hGIPR-Rluc8) with VSLGSSG residues was constructed and purchased from VectorBuilders Inc. (Neu-Isenburg, Germany). cAMP sensor pcDNA3L-His-CAMYEL (ATCC MBA-277TM) was purchased from ATCC (Manassas, VA, USA)

(Jiang *et al.*, 2007). NES-Nluc-MiniG plasmids (denoted as MiniG-  $\alpha_s$ ,  $\alpha_q$ ,  $\alpha_i$ , and  $\alpha_{12/13}$ ) and subcellular/endosomal markers Rab GTPase makers Venus-Rab5a (early endosomes), Venus-Rab7a (late endosomes/lysosomes), Venus-Rab11a (recycling endosomes), and Venus-KRAS (plasma membrane) were gifts from Kevin Pflieger (Harry Perkins Institute of Medical Research, Nedlands, WA, Australia) as originally published by Professor Nevin Lambert (Augusta University, Augusta, GA, USA) (Lan *et al.*, 2011).  $\beta$ -arrestin 1/2-Rluc8 plasmids were a gift from Professor Terry Hébert (McGill University, Montreal, Canada) (Fillion *et al.*, 2019). EGFP-CAAX was a gift from Lei Lu (Addgene plasmid # 86056) (Madugula and Lu, 2016). The unimolecular PKA sensor ExRai-AKAR2 was a gift from Jin Zhang (Addgene plasmid # 161753) (Zhang *et al.*, 2021a).

## Methods

### *Generation and Amplification of Plasmid Constructs*

#### *Transformation of Bacterial Cells*

DH5 $\alpha$  competent cells (Cat#: 18265017, Life Technologies, Carlsbad, CA, USA) cells were thawed on ice, and 20  $\mu$ L of cells were mixed with 2  $\mu$ L of plasmid previously constituted in sterile water. The bacterial cells and DNA were incubated for 15 minutes on ice. Cells were then heat-shocked at 42 °C for 30 seconds, returned to ice for 2 minutes, and followed with the subsequent addition of 800  $\mu$ L of Luria Bertani (LB) media without antibiotic. Cells were incubated at 37 °C for 1 hours shaking at approximately 200 rpm. 100  $\mu$ L of bacteria were then plated on an LB agar plate with either 100  $\mu$ g/mL of ampicillin or 40  $\mu$ g/mL of kanamycin. Agar plates were incubated overnight at 37 °C.

#### *Bacteria Colony Selection*

Following overnight incubation, a single bacterial colony was selected from the agar plate with a sterilized pipette tip and added to 200 mL of LB media with either 100  $\mu$ g/mL of ampicillin or 40  $\mu$ g/mL of kanamycin added. The bacteria-containing broth was then incubated overnight at 37 °C with shaking at approximately 200 rpm.

#### *DNA Extraction*

To extract DNA, the Plasmid Plus Maxi Kit (Cat#: 12963, Qiagen, Hilden, DE) was used according to the manufacturer's protocol. In short, 200 ml of the overnight culture was

centrifuged for 30 min at 4 °C at 4000 x g to generate a pellet of cells. The supernatant was then discarded and the cell pellet re-suspended in Buffer P1 containing RNase A. Lysis buffer P2 was added to lyse the cells. Neutralization buffer P3 was added to stop the lysis reaction and precipitate genomic DNA and cell debris. The precipitate-containing fluid was filtered using a Qiagen cartridge to remove non-soluble debris. The filtrate was passed through a Qiagen-tip by vacuum suction, and plasmid DNA was finally eluted using distilled H<sub>2</sub>O. Purity and plasmid concentration were measured using the NanoDrop 2000 Spectrophotometer (Cat#: ND-2000, Waltham, MA, USA). The resulting H<sub>2</sub>O containing DNA was frozen at 37 °C and stored.

## *Cell Culture*

All processes related to cell culture were performed in laminar flow hoods under sterile conditions.

### *Culture of Human Embryonic Kidney 293 Cell Line*

Human Embryonic Kidney 293 cells were chosen as the primary *in vitro* model due to their lack of endogenous GLP-1R and GIPR expression, and their general acceptance as a sufficient model to investigate GPCR signaling. HEK293T cells lacking endogenous GLP-1R and GIPR were cultured in Dulbecco's Modified Eagle Medium (DMEM, Cat#: 11995073, Life Technologies, Carlsbad, CA, USA) with 10% heat-inactivated fetal bovine serum (FBS, Cat#: 10500064, Life Technologies, Carlsbad, CA, USA), 100 IU/mL of penicillin, and 100 µg/mL of streptomycin solution (Pen-Strep, Cat#: P4333, Sigma–Aldrich, St. Louis, MO, USA). Upon cells reaching approximately 80% confluency in tissue culture flasks, cells were washed with phosphate buffered saline (PBS) (Cat#: 10010056, Gibco, Carlsbad, CA, USA) and harvested using Trypsin-EDTA (0.05%). Centrifugation of the harvested cells at 400 g x 4 min was performed to form a pellet, which was then resuspended in media. The resuspended cells were either transferred into a flask to maintain the cell line or plated into 6-well plates for future transfection and assays.

### *Culture of Min6 Cell Line*

Min6 cells were cultured in Dulbecco's Modified Eagle Medium with 15% heat-inactivated fetal bovine serum, 100 IU/mL of penicillin, 100 µg/mL of streptomycin solution, 20 mM of HEPES, and 50 µM of β-mercaptoethanol. All cells were maintained at 37 °C in 5% CO<sub>2</sub>.

### *Freezing and Thawing Cells*

Cells were cultured in T175 flasks (Cat#: 83.3912.302, Sarstedt, Hildesheim, Germany) and when approximately 80% confluency was reached, cells were washed with PBS, harvested with trypsin, and centrifuged at 400 g x 4 min to form a cell pellet. The cell pellet was resuspended in a freezing solution (80% v/v sterile FBS, 10% dimethylsulphoxide (DMSO), and 10% DMEM) at a concentration of  $1 \times 10^6$  cells/ml, in which 1 mL of resuspended cells were aliquoted into 1.5 mL cryo-tubes. Cells were stored at  $-80^\circ\text{C}$  before they were transferred to a nitrogen storage system. To defrost and revitalize the frozen cells, cells were defrosted within a  $37^\circ\text{C}$  water bath and gently added to pre-warmed media in a falcon tube. Cells were pelleted via centrifugation, in which the freezing solution and pre-warmed media supernatant were discarded and cells resuspended with fresh media. Cells were then transferred to a culture flask to adhere and proliferate.

### *Transient Transfection of Cells*

The cells were seeded (700,000 cells/well) in 6-well plates and incubated to ~70% confluency in complete media supplemented with 10% FBS and 1% Pen-Strep. Twenty-four hours after seeding, overexpression of target proteins was performed under transient transfection conditions using Lipofectamine 2000 (Cat#: 11668019, Invitrogen, Carlsbad, CA, USA) according to the manufacturer's protocol without including additional carrier DNA.

## *Cell-based Temporal Assays*

### *Bioluminescent Resonance Energy Transfer Assays*

Twenty-four hours after transfection, cells were washed with PBS then detached and resuspended in FluoroBrite phenol red-free complete media (Cat#: A1896701, Life Technologies, Carlsbad, CA, USA) containing 5% FBS and 2 mM of l-glutamine (Cat#: 25030081, Life Technologies, Carlsbad, CA, USA). Then 100,000 cells/well were plated into poly-d-lysine-coated (Cat#: P6403, Sigma–Aldrich, St. Louis, MO, USA) 96-well white polystyrene LumiNunc microplates (Cat#: 10072151, Thermo Fisher Scientific, Waltham, MA, USA). After 24 hours of cell incubation, the media was replaced with PBS containing 10  $\mu\text{M}$  of coelenterazine-h (Cat#: S2011, Promega, Madison, WI, USA) or 1:500 NanoGlo substrate (Cat#: N1110, Promega,



Madison, WI, USA). BRET<sup>1</sup> measurements were taken every 30 seconds - 2 minutes at 37 °C using a PHERAstar FS multi-mode microplate reader with 430–485 nm and 505–590 nm dual filters. Following 5 minutes of incubation with coelenterazine-h or NanoGlo, baseline measurements used for normalization were taken. Following, the cells were then treated with a vehicle or the respective agonists. The resulting increase or decrease in ratiometric BRET signal between the interacting fluorophore and lumiphore was normalized by subtracting the ratio (505–590 nm emission over 430–485 nm) of the vehicle-treated wells with the matched agonist-treated wells producing a signal defined as the “ligand-induced BRET ratio” (Porrello et al., 2011). The temporal data of the vehicle-corrected agonist measurement was then additionally normalized to the baseline reading of the same well to control for any discrepancy in cell number between wells at time of readout. Within the temporal data sets, the first BRET reading following treatment with agonist/vehicle is visualized as the subsequent measurement after time point zero. Positive or negative incremental areas under the curves (+iAUC/-iAUC) were calculated where noted, indicating the AUC for each ligand to be calculated in reference to its own baseline values. Each experiment was independently performed at least three times, with at least two technical replicates for each group.

#### *G-protein Recruitment Assays*

HEK293T cells were plated into 6-well plates at a plating density of 700,000 cells/well. MiniG protein probes (MiniG $\alpha$ -Nluc) translocate to ligand-bound active receptors retaining their specificity (Wan et al., 2018). To measure the ligand-induced recruitment of the G $\alpha_s$ , G $\alpha_q$ , G $\alpha_i$ , and G $\alpha_{12/13}$ , 50 ng DNA of the respective Nluc-tagged miniG $\alpha$  plasmid was co-transfected with 500 ng DNA of hGLP-1R-GFP or hGIPR-GFP per well of a 6-well plate. MiniG $\alpha$ -Nluc probes are localized to the cytosol at baseline, and upon ligand GPCR activation translocate within spatial proximity of the GFP-tagged GPCR.

#### *cAMP assays*

CAMYEL, a cAMP sensor using YFP-Epac-RLuc8 was utilized to quantify cAMP accumulation with temporal resolution (Jiang *et al.*, 2007). 500 ng of CAMYEL plasmid DNA was co-transfected with 300 ng of untagged GLP-1R or GIPR plasmid DNA per well in a 6-well plate. The experiments were performed in the absence of 3-isobutyl-1-methylxanthine (IBMX). Within the unstimulated baseline state, the CAMYEL protein sensor assumes a configuration

that allow for resonance transfer between the lumiphore and fluorophore, while in the stimulated state in which intracellular cAMP levels rise, a cAMP-mediated reconfiguration of the sensor consequentially dissipates the baseline resonance energy transfer represented as a “loss in signal” assay.

#### *Receptor Internalization and Receptor Recycling Assays*

A GPCR internalization assay was established by measuring the loss of baseline resonance energy transfer between an intracellular plasma membrane marker Venus-KRAS and hGLP-1R-RLUC8 or hGIPR-RLUC8. 500 ng of Venus-KRAS or GFP-CAAX DNA and 300 ng of the respective RLUC8-tagged GPCR DNA were used per well in a 6-well plate (Lan *et al.*, 2011). While the degree of internalization is measured by the loss in colocalization of the lumiphore-tagged GPCR with the fluorophore-tagged plasma membrane, it is also possible to measure the return of the receptor back to the plasma membrane via re-colocalization following ligand washout and receptor antagonism. For receptor recycling assays, following 20 minutes of receptor internalization, media was removed, cells were washed multiple times with PBS, and lumiphore substrate in PBS along with receptor antagonist (JANT-4 (9-39), 10  $\mu$ M) were then added. Reconstitution of the BRET signal over time was then indicative receptor recycling. To quantify rate of receptor recycling and the total presence of receptor localized to membrane following antagonist administration, the +iAUC was normalized to the respective immediate post-washout measurement of each agonist to quantify the rate of GLP-1R recycling, while total GLP-1R presence at the plasma membrane was quantified via +AUC (not iAUC) by normalizing all ligand post-washout responses to a common minimal value. In separate experiments, to inhibit GLP-1R or GIPR internalization, 30 minute pretreatment with either sucrose (0.43 M) or methyl- $\beta$ -cyclodextrin (M $\beta$ CD) (10 mM) in PBS was used.

#### *$\beta$ -arrestin 1/2 Recruitment Assays*

Colocalization of  $\beta$ -arrestin 1/2-RLUC8 with hGLP-1R-GFP or hGIPR-GFP was assessed (Fillion *et al.*, 2019). 50 ng of  $\beta$ -arrestin1-RLUC8 or  $\beta$ -arrestin2-RLUC8 DNA and 300 ng of GLP-1R-GFP, GIPR-GFP, or Venus-KRAS DNA were co-transfected into each well in a 6-well plate. The  $\beta$ -arrestin 1/2-RLUC8 proteins are localized within the cytosol at baseline, in which upon ligand stimulation translocate to the GPCR at the plasma membrane. Inhibition of the  $\beta$ -arrestin/AP2

complex formation was achieved by 30 minute pretreatment of cells with 100  $\mu$ M barbadin diluted in PBS.

#### *Endosomal Trafficking Assays*

GPCR endosomal trafficking was assessed by measuring the ligand-stimulated gain in resonance energy transfer between Venus-Rab5/7/11 and hGLP-1R-RLUC8 or hGIPR-RLUC (Tiulpakov et al., 2016a). 500 ng of the respective Venus-Rab subtype DNA and 300 ng of hGLP-1R-RLUC8 or hGIPR-RLUC8 DNA were co-transfected into each well in a 6-well plate.

#### *Endosomal Signaling Assays*

Endosomal G-protein recruitment was assessed by bystander BRET via GPCR-induced colocalization of MiniG $\alpha_s$ -NLuc with Venus-Rab5/7/11. 300 ng of GLP-1R-untagged or GIPR-untagged DNA, 500 ng of Venus-Rab5/7/11 DNA, and 50 ng of MiniG $\alpha_s$ -NLuc DNA were co-transfected per well in a 6-well plate.

#### *PKA Activity Assays*

Protein Kinase A (PKA) activity was measured using the ratiometric, circularly permuted fluorophore-based activity sensor ExRai-AKAR2 (Zhang *et al.*, 2021a). This particular sensor has a LRRATLVD PKA substrate sequence and a phosphoamino acid-binding forkhead-associated 1 domain, which when bound together following substrate phosphorylation by PKA, dictates peak excitation wavelengths of the circularly permuted fluorophore. 1000 ng of ExRai-AKAR2 and 500 ng of GLP-1R-untagged per well were co-transfected into HEK293T cells on a 6-well plate.

#### *HILO Microscopy*

HEK293T cells were seeded onto 24 mm coverslips (Cat #: 631–1584, VWR, Radnor, PA, USA) and transfected with 500 ng of hGLP-1R-GFP or hGIPR-GFP over 24 h. HILO image sequences were acquired with a custom-built TIRF microscope (Cairn Research) based on an Eclipse Ti2 (Nikon, Tokyo, Japan) equipped with an EMCCD camera (iXon Ultra, Andor), a 488 nm diode laser, a hardware Perfect Focus System, a TIRF iLas2 module, and a 100 $\times$  oil-immersion objective (NA 1.49, Nikon). Coverslips were mounted onto metal imaging chambers with a plastic seal and filled with imaging medium (HBSS supplemented with 10 mM of HEPES). The objective and samples were maintained at 37  $^{\circ}$ C in a heated enclosure. Images were acquired

on MetaMorph software (Molecular Devices) using a frame exposure of 50–200 ms with an image acquired before ligand stimulation and a subsequent image taken every 30 s thereafter, up to 20 min. All of the images were analyzed using ImageJ.

### *Data Analysis*

Data are represented as means  $\pm$  S.E.M. Each experiment was independently conducted at least three times, each with at least two technical replicates.  $E_{\max}$  values were normalized to GLP-1 (7–36 amide) or GIP (1–42). Dose responses were fitted using non-linear regression.  $pEC_{50}$  and  $EC_{50}$  values were calculated using GraphPad Prism 8.0 (GraphPad, San Diego, CA, USA). Statistical analyses were calculated in GraphPad 8.0 using one-way analysis of variance (ANOVA) and corrected with Tukey's or Bonferroni's multiple comparison test. Differences are considered significant with an adjusted p value  $< 0.05$ .

### *Gene Expression Analysis*

*In vitro* expression profiling of ligand-induced Phosphoenolpyruvate Carboxykinase 1 (PCK1) upregulation was measured in HEK293T cells transiently transfected with hGLP-1R-untagged DNA at 300 ng/well of a 6-well plate. Cells were plated on a 6-well plate at 700,000 cells per well, transfected following 24 hours, and then after an additional 24 hours were incubated in with 1  $\mu$ M of ligand for 3 hours. Following ligand incubation, cells were washed with ice cold PBS and immediately frozen on dry ice. RNA was extracted using QIAzol<sup>®</sup> Lysis Reagent (Cat#: 79306, Qiagen, Hilden, Germany) and synthesis of cDNA was performed using a QuantiTect Reverse Transcription Kit (Cat#: 205311, Qiagen, Hilden, Germany). Gene expression was profiled using quantitative real-time PCR (qPCR) using SYBR<sup>®</sup> Green Real-Time PCR master mix (Cat#: 4364344, Life Technologies, Carlsbad, CA, USA). The relative expression of the human PCK1 gene (forward primer 5' CTGCCCAAGATCTTCCATGT '3; reverse primer 5' CAGCACCTGGAGTTCTCTC '3) was measured (Peng *et al.*, 2021). PCK1 expression was normalized to the reference gene Glyceraldehyde-3-Phosphate Dehydrogenase (GAPDH) (forward primer 5' CTGCCCAAGATCTTCCATGT '3; reverse primer 5' GACAAGCTTCCCGTTCTCAG '3). The threshold cycle method ( $2^{-\Delta\Delta CT}$ ) of comparative PCR was used to analyze the results.

---

## **CHAPTER 3:**

# Spatiotemporal GLP-1 and GIP Receptor Signaling and Trafficking/Recycling Dynamics Induced by Selected Receptor Mono- and Dual-Agonists

---

---

## Introduction

GPCRs are, by number, the largest class of plasma membrane-associated proteins in the human genome. The physiological efficacy and tractability of pharmacologically agonizing these receptors have made them important targets for drug discovery (Wacker *et al.*, 2017). The GLP-1 and GIP receptors are class B/secretin family GPCRs, and represent lucrative targets for the treatment of T2D and obesity. Pharmaceutical strategy revolving around GLP-1 receptor activation has been notably advanced due to the preserved therapeutic potential of GLP-1 agonism within the context of metabolic syndrome (Nauck *et al.*, 1993b). The preservation of therapeutic activity at the GLP-1R has been suggested to be due to a switch in G-protein signaling, in which the primary  $G\alpha_s$  coupling of GLP-1R is swapped for  $G\alpha_q$  coupling during conditions of chronic hyperglycemia (Oduori *et al.*, 2020). GIP receptor agonism is more enigmatic. While GIP action accounts for 70% of the incretin effect in healthy individuals, its insulinotropic efficacy in individuals with T2D is predominantly impaired (Gasbjerg *et al.*, 2019; Nauck *et al.*, 1993c). Interestingly, the inability of GIPR to switch its  $G\alpha_s$ -coupling to  $G\alpha_q$  seems to be the driving force behind the loss of therapeutic power within the context chronic hyperglycemia (Oduori *et al.*, 2020).

GLP-1 (7-36 amide), and to a lower extent GLP-1 (7-37), are the primary active forms of circulating GLP-1, however these peptides are subject to rapid proteolytic degradation and fast renal elimination (Deacon *et al.*, 1995a; Deacon *et al.*, 1995b; Kieffer *et al.*, 1995). Long acting GLP-1 analogs with biochemical modifications to the peptide sequence have been designed to overcome half-life limitations and establish therapeutic value for the treatment of T2D. Despite molecular enhancements in circulating half-life, dose-dependent appearance of adverse effects limit maximal efficacy and therapeutic value (Meier, 2012; Muller *et al.*, 2018).

Co-administration of GLP-1 and GIP has proven to synergistically enhance reductions in food intake and body weight. This synergism produces pronounced physiological effects when combining sub-effective dosages for either peptide, pointing towards an ability for GLP-1/GIP synergism to not only improve the efficacy of GLP-1R-mediated decreases in food intake and body weight, but also to improve the therapeutic tolerability profile by reducing the dosage of GLP-1 agonist required (Finan *et al.*, 2013; NamKoong *et al.*, 2017).

Single chimeric molecules with dual agonism at the GLP-1 and GIP receptors have been demonstrated to improve body weight and glucose handling with superior potency relative to

GLP-1R mono-agonists in preclinical and clinical studies (Coskun *et al.*, 2018; Finan *et al.*, 2013; Frias *et al.*, 2017; Frías *et al.*, 2021; Frias *et al.*, 2018). Chronic simultaneous agonism of the GLP-1R and GIPR through the use of unimolecular GLP-1/GIP dual-agonists has been suggested to facilitate synergistic action in DIO models of obesity through step-wise sensitization, in which the hypoglycemic effects of GLP-1R agonism over time facilitate resensitization of GIPR agonism (Finan *et al.*, 2013).

Depending on engineered variations to the peptide sequence, specific ligands can engage in unique receptor signaling, trafficking, and/or recycling dynamics, a phenomenon referred to as biased agonism. Biased agonism at the GLP-1R has been implicated in differential cellular desensitization capacities via alterations in receptor internalization and  $\beta$ -arrestin recruitment (Jones, 2021). It is suggested that certain ligand biases at the GLP-1R facilitate enhanced therapeutic efficacy, as has been shown for the Phe1-substituted EX-4 in which limited receptor internalization and enhanced recycling was associated with higher insulinotropic efficacy *in vivo* (Jones *et al.*, 2018b). Additionally, certain  $\alpha/\beta$  amino acid substitutions to the GLP-1 backbone have been evidenced to confer a degree of engineered control in inducing differential signaling, while naturally-occurring GLP-1 agonists oxyntomodulin and EX-4 are intrinsically biased toward  $\beta$ -arrestin recruitment (Hager *et al.*, 2017; Wootten *et al.*, 2016). The GLP-1/GIP dual-agonist Tirzepatide (LY3298176; Eli Lilly, Indianapolis, IN, USA) was recently discovered to favor ERK 1/2 phosphorylation relative to  $\beta$ -arrestin recruitment at both target receptors (Yuliantie *et al.*, 2020).

## Implications of Signaling and Trafficking at the GLP-1R and GIPR

GPCR signaling and endocytic internalization are intertwined processes bidirectionally linked (Sorkin and von Zastrow, 2009). GPCR internalization is associated with the attenuation of ligand-induced receptor activation through multiple mechanisms. The binding of  $\beta$ -arrestin 1/2 to the GRK-phosphorylated C-terminal tail of the GPCR sterically inhibits further  $G\alpha$  activation and subsequently acts as linkage to the clathrin adaptor AP2 residing at clathrin-coated pits mediating receptor internalization (Spillmann *et al.*, 2020). Subsequently, the colocalization of the GPCR at the internalized endosome, with emphasis on the N-terminal end of the GPCR residing in the endosomal lumen, facilitates the dissociative release of the ligand via early and late endosomal acidification (Trivedi *et al.*, 2020). Additionally, receptor

internalization can further attenuate cell signaling by pulling the receptor away from signaling mediators or substrate that are bound or localized to the plasma membrane (Sorkin and von Zastrow, 2009). Therefore, regarding immediate plasma-membrane localized signal transduction of an activated GPCR, internalization acts as a primary modulator of its efficacy. Separately, receptor internalization can also modify global cellular signaling by isolating the receptor from the plasma membrane and limiting continued access of the GPCR to extracellular ligand in a process called cellular desensitization (Rajagopal and Shenoy, 2018). Ligand-induced cellular desensitization of the GPCR can occur in both acute and prolonged phases. Acute short-term desensitization of the GPCR can occur within minutes, and is accomplished through  $\beta$ -arrestin-mediated processes, ligand dissociation, and physically removing the GPCR from the plasma membrane and thus from access to extracellular ligands (Smith and Rajagopal, 2016). However, long-term ligand-induced GPCR desensitization, which predominates over hours to days, acts when a portion of the activated receptor population is trafficked away from recycling endosomes and toward lysosomal compartments for degradation (Rajagopal and Shenoy, 2018). Targeting the desensitization process using biased ligands that favor either reduced GPCR internalization or enhanced recycling may prove to be of pharmacological value within the class B GPCR family (Jones *et al.*, 2018b)

GPCR internalization is however not entirely about attenuation of signal transduction and desensitization. While  $G\alpha$  activation had been classically thought of as a process isolated exclusively to the plasma membrane, recent evidence has highlighted the presence and utility of continued GPCR-mediated  $G\alpha$  activation at intracellular endosomal compartments. The stable interaction of a ligand-GPCR complex is the most well-known determinant of continued endosomal signaling due to the facilitation of improved resistance against  $\beta$ -arrestin/acidification-induced ligand dissociation (Sutkeviciute and Vilardaga, 2020). In terms of functionality, continued GPCR-mediated  $G\alpha_s$  activation at Rab5<sup>+</sup> and Rab7<sup>+</sup> endosomes produce an advantageous mechanism of prolonged intracellular signaling regardless of extracellular ligand clearance, a process which may prove as a critical amplifier for the physiological action of ligands with short circulating plasma half-lives (Calebiro *et al.*, 2009). Additionally, intracellular GPCR mobility through the endosomal network allows for alternative spatial regulation of downstream effectors, which may result in compartment-specific signaling patterns marked by differentially internalized ligand-receptor complexes. Therefore, the presence or absence of endocytic GPCR trafficking and endosomal signaling,



specific to a ligand, may confer unique signaling characteristics, such as the stimulated import of PKA catalytic subunits into the nucleus, or induced translocation of functional proteins relevant to an immediate physiological response (as with vasopressin at the V2R) (Peng *et al.*, 2021; Zalyapin *et al.*, 2008). Interestingly, the degree of Rab5<sup>+</sup> endosome-localized GPCR G $\alpha_s$  recruitment may determine the re-direction of the GPCR away from recycling endosomes into Rab7<sup>+</sup> late endosomes by interacting with GASP1 and dysbindin, which physically link the GPCR to the late endosome-specific ESCRT machinery (Roscioglione *et al.*, 2014). Therefore, a ligand-receptor complex with strong stability in an acidic pH, that induces a high-degree of endosomal G $\alpha_s$  recruitment, may preferentially target GPCR trafficking into the degradative pathway (Roscioglione *et al.*, 2014; Sutkeviciute and Vilardaga, 2020; Trivedi *et al.*, 2020). By engineering ligands with partial agonism for G $\alpha_s$  recruitment, it may be possible to limit lysosomal degradation of the GPCR by avoiding late endosome incorporation, while also simultaneously capitalizing on the saturating effects of cAMP signal amplification.

## Biased Signaling

The majority of GPCRs are capable of coupling to multiple G $\alpha$  subunit types, allowing for parallel activation of multiple intracellular pathways. Distinct ligands specific for the same receptor may, upon binding, initiate differential receptor conformations through complex interactions between ligand and receptor amino acid residues. Through the distinct receptor conformations that various ligands confer on a GPCR, the accessibility of the GPCR to signaling proteins that mediate the initiation of various intracellular signaling cascades may become selective. Endogenous or engineered ligands can take advantage of the induced conformational profile of the GPCR, and predominantly amplify one signaling pathway over another in what is termed 'biased agonism'. While not all of the elements that contribute to a ligand's bias are understood, the stability of a unique interaction between ligand and GPCR is generally evidenced to facilitate biased agonism, which is likely accomplished through ligand-induced alternative adjunct subtle movements within the extracellular and intracellular loops of the GPCR. The bias of a ligand can effect multiple intracellular parameters including G $\alpha$  recruitment and G $\alpha$ -associated downstream effectors,  $\beta$ -arrestin recruitment, receptor trafficking and endosomal signaling dynamics, among others (Costa-Neto *et al.*, 2016).

Biased agonism at the GLP-1 receptor, such as with a Phe1 substituted EX-4 molecule, has been attributed to differential outcomes both *in vitro* and *in vivo* regarding receptor trafficking, cellular desensitization, and prolonged insulinotropic properties (Jones et al., 2018a). Oxyntomodulin, an endogenous unimolecular GLP-1R/GcgR dual-agonist, has been evidenced to be biased away from cAMP and toward  $\text{Ca}^{2+}$ , pERK, and  $\beta$ -arrestin recruitment at the GLP-1R in comparison to the native GLP-1 (7-36 amide) (Koole *et al.*, 2010; Wootten *et al.*, 2016). In addition, some  $\alpha/\beta$  amino acid modifications within the GLP-1 backbone sequence have been demonstrated to bias ligands toward  $\beta$ -arrestin recruitment, while the GLP-1/GIP dual-agonist Tirzepatide (LY3298176; Eli Lilly, Indianapolis, IN, USA) was recently demonstrated to be biased towards phosphorylation of ERK due to reductions in  $\beta$ -arrestin efficacy (Hager et al., 2016; Yuliantie *et al.*, 2020).

As mentioned prior, GIPR engagement for the therapeutic treatment of T2D and obesity has been enigmatic. Despite potent effects of GIPR agonism in healthy individuals, mice with GIPR deletion are protected from DIO while GIPR antagonizing antibodies also improve blood glucose parameters and body weight in obese rodents and non-human primates (Killion et al., 2018). To reconcile the discrepancies between findings, it has been hypothesized that GIPR agonists may act as functional GIPR antagonists, or that bias agonism underlies unique GIP benefits (Holst and Rosenkilde, 2020). GIPR biased agonists have not been developed to the same extent as that of GLP-1R agonists, however Phe1 and dGln3 N-terminal substitutions within the GIP sequence have been shown to negatively impact both cAMP potency and  $\beta$ -arrestin recruitment efficacy (Jones et al., 2020a). These findings indicate potential for GIPR biased agonism that has yet to be explored *in vivo*.

## MAR709 and Tirzepatide (Dual-agonists)

GLP-1 and GIP co-administration has demonstrated an additive benefit above that of GLP-1 alone in regards to stimulating insulin secretion in human subjects (Elahi *et al.*, 1994; Nauck *et al.*, 1993a). ICV co-administration of GLP-1 and GIP, at concentrations ineffective when given separately, significantly decreased food intake and body weight in DIO mice indicating synergistic action between GLP-1 and GIP (NamKoong *et al.*, 2017). Additionally, chronic subcutaneous injections of an acylated GIP mono-agonist (3 nmol) failed to reduce body weight and food intake in DIO mice, however co-administration of the acylated GIP (3 nmol)

and an acylated GLP-1 (3 nmol) significantly decreased body weight and food intake to an extent greater than that of the acylated GLP-1 alone (Finan *et al.*, 2013). Together, these findings indicated a synergism between GLP-1 and GIP, to not only improve the efficacy of the food intake and body weight reductions attributable to GLP-1R agonism, but also suggests an improved tolerability profile.

The first proof-of-principle for combining GLP-1 and GIP pharmacology into a unimolecular dual-agonist that demonstrated high efficacy on body weight and glycemic control across rodents, non-human primates, and clinical trials was with MAR709 (NNC0090-2746, Novo Nordisk, Copenhagen, Denmark) (Finan *et al.*, 2013; Frias *et al.*, 2017). MAR709, which was derived from the sequence of a previously engineered GLP-1/Gcg dual-agonist, was designed as a balanced dual-agonist, meaning it has equal activity at both respective receptors as quantified indirectly by a cAMP-response element (CRE) luciferase assay in HEK293 cells (Day *et al.*, 2009; Finan *et al.*, 2013). Of the specific substitutions within the GLP-1/Gcg molecule: a His1Tyr substitution, an Aib placement at position 2, removal of a lactam bridge within the center of the molecule, the inclusion of a C-terminal CEX tail, and the addition of Lys40 for C16 fatty acid acylation – respectively facilitated GIP activity, protected against DPP-IV degradation, eliminated GcgR cross-reactivity, enhanced circulating compound stability, and prolonged circulating half-life via albumin binding (Finan *et al.*, 2013). However, despite its success, MAR709 was discontinued following phase 2 clinical trials.

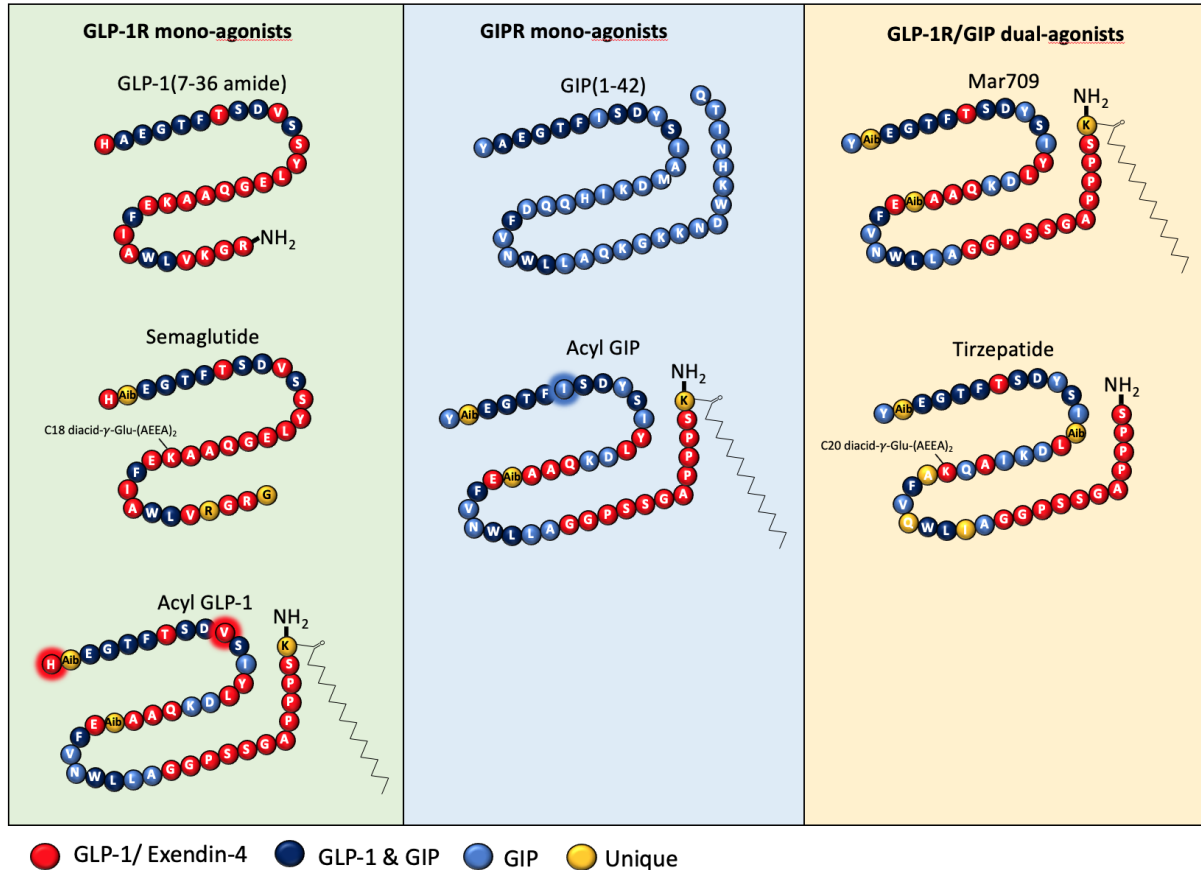
Another clinically relevant GLP-1/GIP dual-agonist is Tirzepatide. Tirzepatide, unlike MAR709, was engineered with the base GIP (1-42) sequence in mind to create an imbalanced agonist that favors GIPR activity. The amino acid sequence between MAR709 and Tirzepatide is relatively similar, however Tirzepatide contains a number of additional GIP-specific substitutions designed to emphasize GIPR potency over GLP-1R (Coskun *et al.*, 2018). In addition to the GIP-specific substitutions, a GLP-1 specific lysine was inserted at position 20 to allow for acylation with a C20 unsaturated diacid side chain. Tirzepatide has continued on to multiple phase 2 and phase 3 clinical trials where it has successfully competed against dulaglutide (SURPASS-1), Semaglutide (SURPASS-2), insulin degludec (SURPASS-3), and insulin glargine (SURPASS-5) (Dahl *et al.*, 2021; Frías *et al.*, 2021; Frias *et al.*, 2018; Ludvik *et al.*, 2021; Min and Bain, 2021; Rosenstock *et al.*, 2021).

## Select Mono- and Dual-Agonists for Characterization

While much of the work characterizing MAR709 and Tirzepatide was accomplished *in vivo*, the early *in vitro* intracellular characterization of these agonists has been limited to cAMP production. It has been previously understood that co-activation of the GLP-1R and GIPR facilitates much of the benefits seen with the dual-agonists. However, the effect that these highly unique amino acid sequences of MAR709 and Tirzepatide have on signal bias at the individual receptor has not been fully understood, or excluded as a point of enhanced therapeutic value. It was not until recently that Tirzepatide was understood to have a GLP-1R bias toward pERK and that its induced GLP-1R internalization was muted in comparison to GLP-1 (7-36 amide) (Willard *et al.*, 2020; Yuliantie *et al.*, 2020). However, within these studies, large sequence divergences between Tirzepatide and that of the comparators GLP-1 (7-36 amide) and GIP (1-42) may highlight caveats to interpretability as they lack matched mono-agonist controls that account for (1) ligand modifications not intrinsic to receptor specificity (i.e. Aib at position 2 and 20, C-terminal CEX tail, acylation) and (2) which particular GLP-1 or GIP amino acid substitutions are responsible for gating any bias if found. Importantly, another aspect not covered within the recent publications was that of quantifying receptor endosomal trafficking within receptor degradation or recycling pathways,  $G\alpha$  signaling within different endosomal compartments, and that of cohesively quantifying the chain of GPCR dynamics from  $G\alpha$  signaling down to receptor colocalization within terminal lysosomes.

Within this study, a total of seven agonists specific for either GLP-1R, GIPR, or both will be utilized. The native peptides GLP-1 (7-36 amide) and full-length GIP (1-42) will be used as reference agonists and positive controls at their respective receptors. The clinically relevant GLP-1R mono-agonist Semaglutide will be utilized. Semaglutide (NNC 0113-0217, Novo Nordisk, Copenhagen, Denmark) was developed as a once-weekly long-acting GLP-1R agonist through its Aib substitution at position 2 to protect against DPP-IV deactivation, Arg27Lys substitution to allow for post-peptide synthesis acylation at Lys20, and a C18 diacid acylation at Lys20 via an L- $\gamma$ -glutamic acid linker to facilitate reversible albumin binding for enhanced protection against DPP-IV degradation and renal clearance (Lau *et al.*, 2015). Both unimolecular GLP-1/GIP dual-agonist MAR709 and Tirzepatide will be examined. Lastly, two pharmacokinetically matched mono-agonist controls of MAR709 specific for either the GLP-

1R or GIPR will be used. The matched GLP-1-specific MAR709 control “Acyl-GLP-1” (NN 0441-1746) is a His1 and Val10 mutant of MAR709. The matched GIP-specific MAR709 control “Acyl-GIP” (NN 0441-1745) is a matched Ile7 mutant of MAR709.



Identifier	Abbreviation	Structure
	native GLP-1	HAEGT FTSDV SSYLE GQAAK EFLAW LVKGR-NH <sub>2</sub>
	native GIP	YAEGT FISDY SIAMD KIHQQ DFNWV LLAQK GKND WKHNI TQ
NNC 0441-1745	acyl-GIP	YXEGT FISDY SIYLD KQAAX EFNWV LLAGG PSSGA PPPSK(C16)-NH <sub>2</sub>
NNC 0441-1746	acyl-GLP-1	HXEGT FTSDV SIYLD KQAAX EFNWV LLAGG PSSGA PPPSK(C16)-NH <sub>2</sub>
NNC 0090-2746	MAR709	YXEGT FTSDY SIYLD KQAAX EFNWV LLAGG PSSGA PPPSK(C16)-NH <sub>2</sub>
NNC 0113-0217	Semaglutide	HXEGT FTSDV SSYLE GQAAK((AEEA) <sub>2</sub> -γGlu-C18 diacid) EFLAW LVRGR G
LY3298176	Tirzepatide	YXEGT FTSDY SIXLD KIAQK((AEEA) <sub>2</sub> -γGlu-C20 diacid) AFWQV LIAGG PSSGA PPPS-NH <sub>2</sub>

**Figure 14: Amino acid sequence and structure of the tested GLP-1R and GIPR ligands.** GLP-1R mono-agonists used within this thesis are comprised of GLP-1 (7-36 amide), Semaglutide, and Acyl-GLP-1 (a pharmacokinetically-matched His1 and Val10 mutant of MAR709) (left panel, green). Comparative GIPR mono-agonists included are GIP (1-42) and Acyl-GIP (a pharmacokinetically matched Ile7 mutant of MAR709) (middle panel, blue). GLP-1/GIP dual-agonists investigated are MAR709 and Tirzepatide (right panel, orange). Amino acid sequences, in paper abbreviations, and external identifiers of the GLP-1 and GIP-derived compounds used (bottom table). *Figure adapted from Novikoff et al. 2021 (Mol. Met.).*

## Objective

To evaluate the spatiotemporal GLP-1 and GIP receptor signaling, trafficking, and recycling dynamics of GIPR mono-agonists, GLP-1R mono-agonists including Semaglutide, and GLP-1/GIP dual-agonists MAR709 and Tirzepatide.

## Results

### *MAR709 and Tirzepatide Differ from Mono-Agonists in Ligand-induced G $\alpha$ -subunit Recruitment to the GLP-1R and GIPR*

The capacity for ligand-induced G protein recruitment was measured using bioluminescence resonance energy transfer (BRET)-based technology within HEK293T cells transiently transfected with NanoLuc-tagged MiniG constructs (miniG-Nluc) (Wan *et al.*, 2018). NanoLuc-tagged MiniG $\alpha$  constructs, which are cytosol-localized synthetic G-protein surrogates, contain: a truncated N-terminus eliminating plasma membrane anchoring and  $\beta\gamma$  subunit binding, deletion of the  $\alpha$ -helical domain, specific mutations to improve stability *in vitro*, and importantly, a mutation in the C-terminal  $\alpha 5$  helix that promotes miniG $\alpha$ -Nluc stable binding to the GPCR by uncoupling its dissociation from GTP release (Wan *et al.*, 2018). The miniG-Nluc is capable of reporting receptor activation within the most upstream position of the subsequent cellular cascade, making it indispensable for assessing direct ligand effects without the complication of signal amplification. In HEK293T cells, expression of either hGLP-1R-GFP or hGIPR-GFP with one of the MiniG $\alpha$ -Nluc subgroup variants respective to either G $\alpha_s$ , G $\alpha_q$ , G $\alpha_i$ , or G $\alpha_{12/13}$ , allow for systemic profiling of each ligand, and assessment if the unique amino acid sequences of MAR709 or Tirzepatide induce novel coupling to G-protein subgroups.

In GLP-1R<sup>+</sup> HEK293T cells, stimulation with 1  $\mu$ M GLP-1 (7-36 amide) primarily recruited G $\alpha_s$  to the GLP-1R, with a minor recruitment of G $\alpha_q$  (**Figure 15, A-B**). GLP-1 (7-36 amide) demonstrated no meaningful recruitment for both G $\alpha_i$  and G $\alpha_{12/13}$  (**Figure 15, C-D**). These findings align with GLP-1 (7-36 amide) agonism profiles in previous literature (Oduori *et al.*, 2020). 1  $\mu$ M stimulation of GIP (1-42) and Acyl-GIP evidenced no significant effect at the GLP-1R among any of the G-protein subunits (**Figure 15, A-D**). The negative findings between GIP (1-42) and Acyl-GIP demonstrate the specificity of the GLP-1R-mediated assay, as well as confirm the lack of GLP-1R activity imbued in the Acyl-GIP MAR709 control.

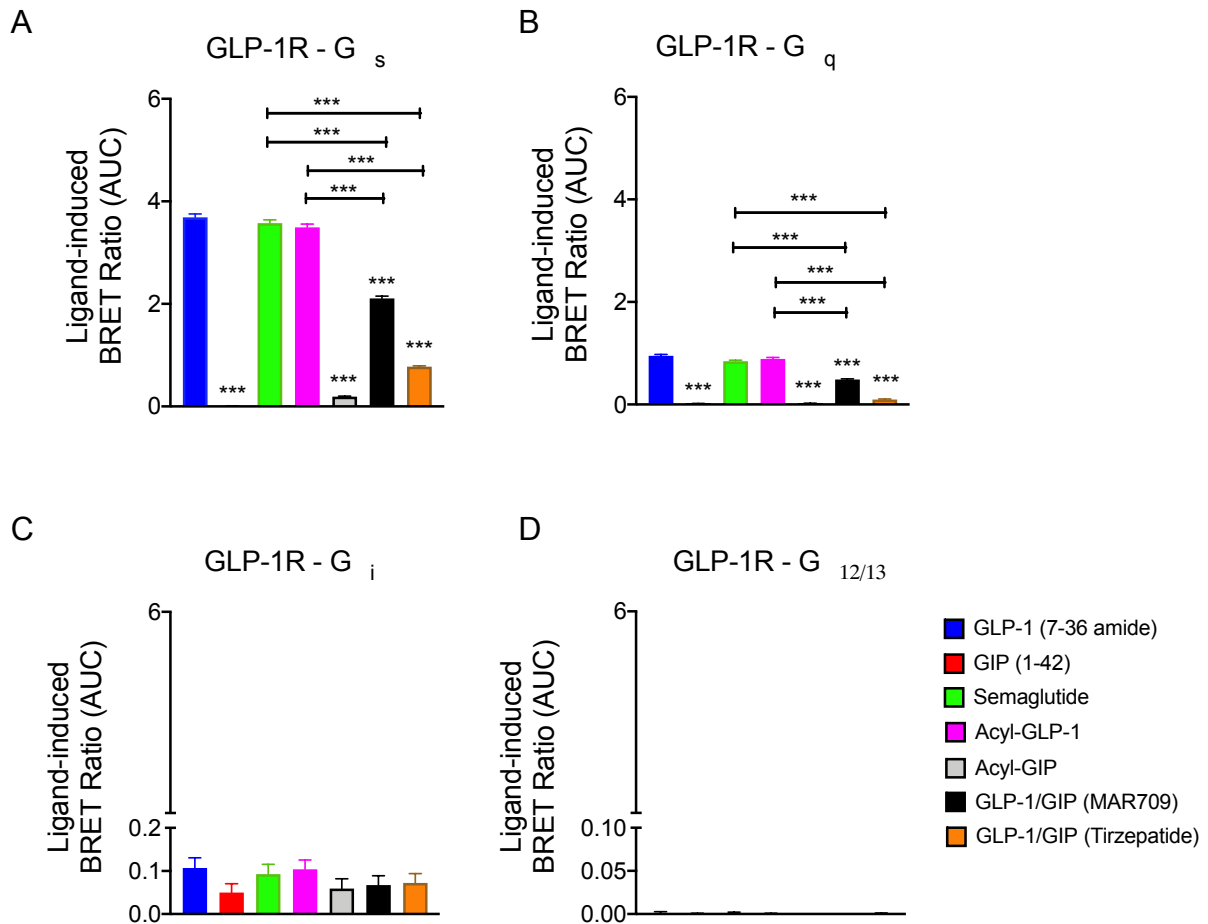


**Figure 15: Ligand-induced  $G\alpha$  subunit recruitment at the GLP-1R.** Ligand-induced ( $1 \mu\text{M}$ ) recruitment of Nluc-tagged Mini-  $G\alpha_s$  (A),  $G\alpha_q$  (B),  $G\alpha_i$  (C),  $G\alpha_{12/13}$  (D), to a GFP-tagged GLP-1R in HEK293T cells. The positive iAUC (+iAUC) representation of vehicle- and baseline-corrected 30 min response to each agonist is expressed as mean  $\pm$  SEM. Bonferroni's test, \* $p < 0.05$ , \*\* $p < 0.005$ , and \*\*\* $p < 0.0005$  using one-way ANOVA vs GLP-1 (7–36 amide), Semaglutide, and Acyl-GLP-1. Three independent experiments were performed with at least two technical replicates per group. *Figure adapted from Novikoff et al. 2021 (Mol. Met.).*

Both GLP-1R mono-agonists Semaglutide and Acyl-GLP-1 similarly recruited  $G\alpha_s$  and  $G\alpha_q$  and were not significantly different from each other, nor from GLP-1 (7-36 amide). Both Semaglutide and Acyl-GLP-1 did not differentially affect  $G\alpha_i$  or  $G\alpha_{12/13}$  recruitment relative to GLP-1 (7-36 amide), which therefore indicates a ligand-induced selectivity for  $G\alpha_s$  and  $G\alpha_q$ . Interestingly, relative to the GLP-1 mono-agonists, both MAR709 and Tirzepatide exhibited reduced capacity to recruit both  $G\alpha_s$  and  $G\alpha_q$  at the GLP-1R. However, MAR709 exhibited a greater ability to recruit  $G\alpha_s$  and  $G\alpha_q$  than Tirzepatide at the GLP-1R. It was of question whether the unique chimeric sequences of MAR709 and Tirzepatide allow for novel coupling of different G-protein subtypes to the GLP-1R. However, recruitment of both  $G\alpha_i$  and  $G\alpha_{12/13}$  were notably absent and non-significantly different compared to the GLP-1R mono-agonist.



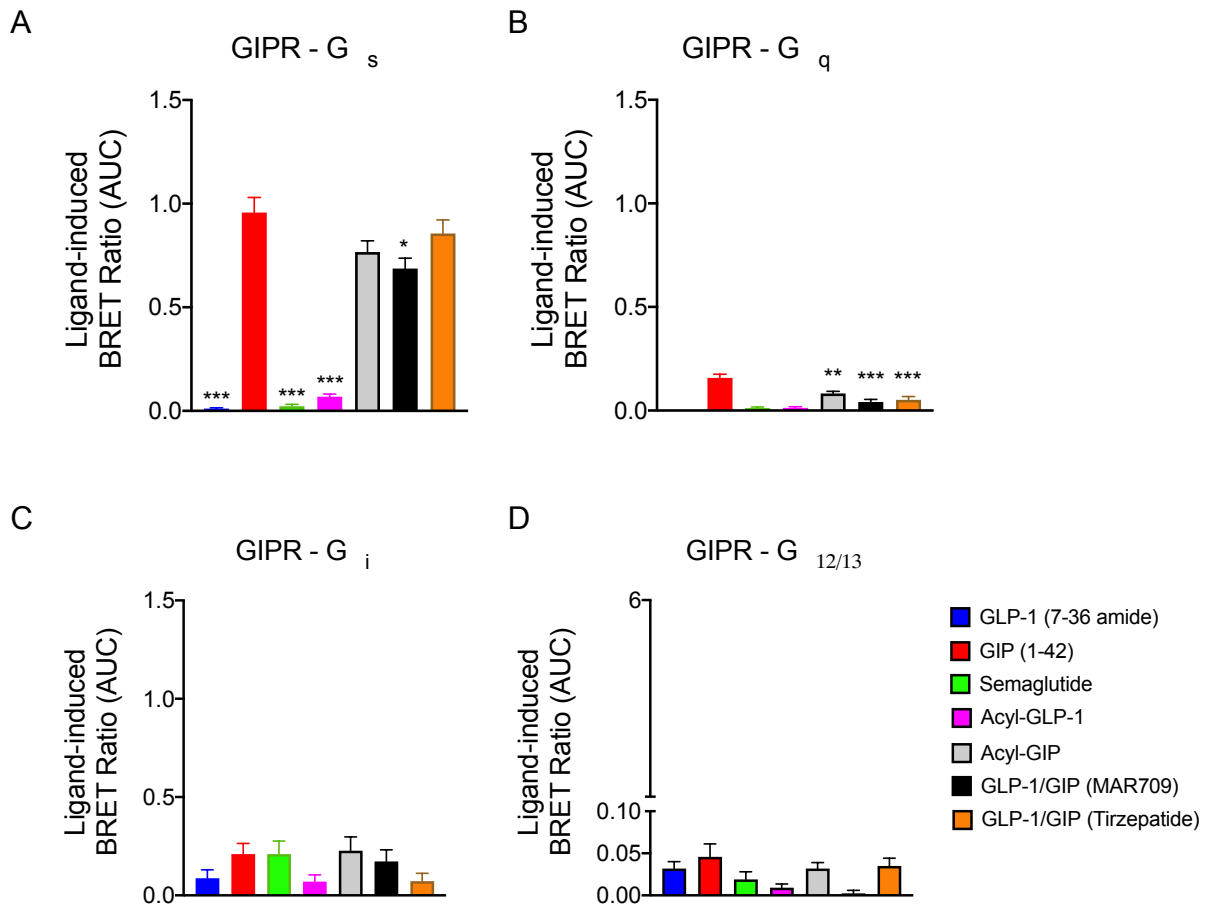


**Figure 16: Ligand-induced  $G\alpha$  subunit recruitment at the GIPR.** Ligand-induced (1  $\mu$ M) recruitment of Nluc-tagged Mini-  $G\alpha_s$  (A),  $G\alpha_q$  (B),  $G\alpha_i$  (C),  $G\alpha_{12/13}$  (D), to a GFP-tagged GIPR in HEK293T cells. The +iAUC representation of vehicle- and baseline-corrected 30 min response to each agonist is expressed as mean  $\pm$  SEM. Bonferroni's test, \* $p$  < 0.05, \*\* $p$  < 0.005, and \*\*\* $p$  < 0.0005 using one-way ANOVA vs GIP (1-42) and Acyl-GIP. Three independent experiments were performed with at least two technical replicates per group. *Figure adapted from Novikoff et al. 2021 (Mol. Met.).*

In GIPR<sup>+</sup> HEK293T cells, 1  $\mu$ M stimulation of GIP (1-42) primarily recruited  $G\alpha_s$ , but did not recruit with any meaningful impact  $G\alpha_q$ ,  $G\alpha_i$ , or  $G\alpha_{12/13}$  (**Figure 16, A-D**). These results align with previous literature stating GIPR to be coupled exclusively to  $G\alpha_s$  (Oduori *et al.*, 2020). However, it should be considered that recent literature has implicated a role for  $G\alpha_q$  at the GIPR (Harris *et al.*, 2021). Likewise to the negative controls within the GLP-1R<sup>+</sup> model, GLP-1 (7-36 amide), Semaglutide, and Acyl-GLP-1 did not elicit a substantial signal within GIPR<sup>+</sup> HEK293T cells for any of the G-protein subunits. This indicates the specificity and lack of cross-reactivity of GLP-1 mono-agonists at the GIPR at 1  $\mu$ M concentrations. Acyl-GIP stimulated full  $G\alpha_s$  recruitment, in which the extent was non-significantly different compared to the native GIP (1-42) (**Figure 16, A**). Stimulation with MAR709 and Tirzepatide both resulted in substantial recruitment of  $G\alpha_s$  to the GIPR, thus in conjunction with the results at the GLP-1R

(**Figure 15, A**), validates the dual-agonistic profile of MAR709 and Tirzepatide at both receptors. In agreement with the GIP-based design of Tirzepatide,  $G\alpha_s$  recruitment by Tirzepatide was non-significantly different in comparison GIP (1-42) and tended to produce a greater response than the “balanced” dual-agonist MAR709. There were no additional significant differences between MAR709 or Tirzepatide and GIP (1-42) for either  $G\alpha_q$ ,  $G\alpha_i$ , or  $G\alpha_{12/13}$  recruitment (**Figure 16, B-D**).

*Constitutive Activity at the GIPR is Not Responsible for Reduced Efficacy of GIP (1-42) Relative to GLP-1 (7-36 Amide) at the GLP-1R*

When contrasting the 1  $\mu$ M ligand-induced response for  $G\alpha$  recruitment to the GLP-1R and GIPR, the native GIP (1-42) peptide at the GIPR stimulates only 26% and 16% of the  $G\alpha_s$  and  $G\alpha_q$  recruitment response elicited by the native GLP-1 (7-36 amide) at the GLP-1R (**Figure 17, A**). This brought up the question whether the reduced response of  $G\alpha$  recruitment by GIP (1-42) at the GIPR, relative to GLP-1 (7-36 amide) at the GLP-1R, represents a real difference in receptor capacity for  $G\alpha$  recruitment, or if it is an artifact of the assay.

Typical ligand-induced ratiometric BRET responses are normalized to both baseline and vehicle to correct for differences in cell population and signal drift. These corrections provide values represented as a ligand-induced fold-change in signal normalized to vehicle. When normalizing ligand-induced activity at a receptor to baseline activity present before ligand stimulation, it is possible for artificial ligand-induced differences to occur when contrasting multiple receptors. This is particularly true if there are large differences in preceding baseline activity at the individual receptors. For example, if a pair of receptors exhibit similar maximal capacities to recruit  $G\alpha$  subunits, yet one receptor displays greater preceding constitutive baseline recruitment of  $G\alpha$  subunits, the ligand-induced fold change in signal required to reach maximal signaling capacity will be reduced relative to the ligand-induced fold change needed to reach maximal signaling capacity at an alternative receptor with lower constitutive baseline recruitment. Indeed, the GIPR has been previously evidenced to display higher basal activity than that of GLP-1R in HEK293T cells as measured by an indirect CRE luciferase assay (Al-Sabah *et al.*, 2014).

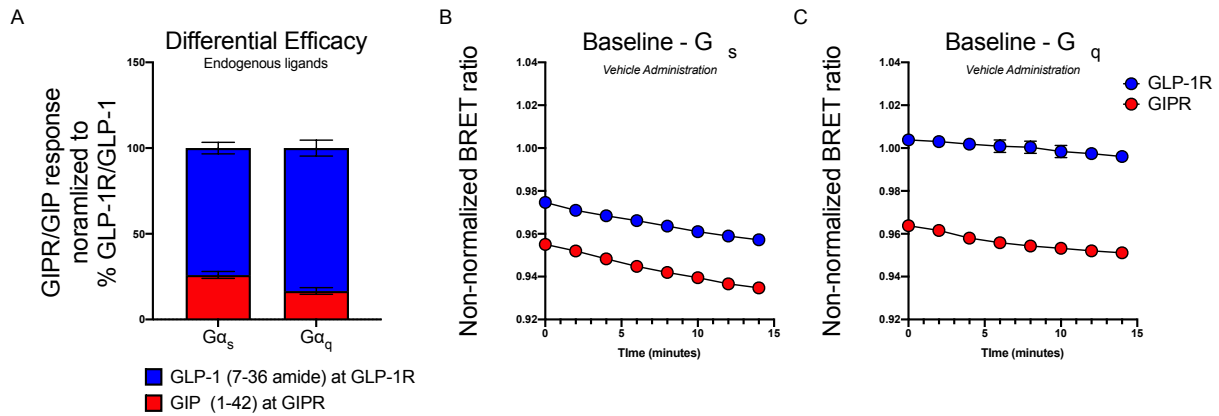


**Figure 17: Baseline constitutive activity of  $G\alpha_s$  and  $G\alpha_q$  subunits at the GLP-1R and the GIPR.** Normalized comparison of maximal Mini $G\alpha$ -Nluc recruitment to GFP-tagged GLP-1R or GIPR following 1  $\mu$ M stimulation of either GLP-1 (7-36 amide) or GIP (1-42) (A). Mini $G\alpha_s$ -Nluc recruitment to GFP-tagged GLP-1R or GIPR following vehicle (PBS) administration without statistical normalization to baseline values (B). Mini $G\alpha_q$ -Nluc recruitment to GFP-tagged GLP-1R or GIPR following vehicle (PBS) administration without statistical normalization to baseline starting values (C). Three independent experiments were performed with at least two technical replicates per group.

Therefore, the difference in degree of GLP-1R/GIPR  $G\alpha$  recruitment as stimulated by the respective ligands may be due to either (**Figure 17, A**): (1) a greater inherent maximal capacity for ligand-induced  $G\alpha$  recruitment at the GLP-1R, or (2) greater constitutive baseline  $G\alpha$  recruitment at the GIPR, leading to a lesser requirement for ligand-induced fold change to achieve maximal recruitment capacity. We tracked and analyzed non-stimulated  $G\alpha_s$  and  $G\alpha_q$  recruitment to the GLP-1R or GIPR within HEK293T cells following vehicle (PBS) administration without normalization to baseline (**Figure 17, B-C**). Over the course of 15 minutes following vehicle administration an expected loss-in-signal was observed, which is in line with the dynamics of lumiphore substrate utilization and decay. However, it is found that the GLP-1R demonstrates higher constitutive baseline activity relative to the GIPR independent of time, as measured by  $G\alpha_s$  and  $G\alpha_q$  recruitment elicited by vehicle administration. This suggests that the differential extent of ligand-induced  $G\alpha$  subunit recruitment to the GLP-1R and GIPR by the respective native peptides is attributable to a greater inherent capacity for ligand-induced  $G\alpha$  recruitment at the GLP-1R, and is not a product of a minimized fold-change at the GIPR due to higher baseline activity (**Figure 17, A**).

**Table 2: Maximal ( $E_{max}$ ) drug effects and potencies ( $EC_{50}$ ) at the GLP-1R or GIPR target receptors.** Data were generated in HEK293T cells transiently transfected to express GLP-1R or GIPR.  $E_{max}$ ,  $pEC_{50}$ , and  $EC_{50}$  values were generated from dose–response values fitted to sigmoidal curves using a three-parameter non-linear logistic regression. The  $E_{max}$  is the maximal response elicited by an agonist and is expressed as % of the maximum response of GLP-1 (7–36 amide) or GIP (1–42). The EC is the molar concentration in which an agonist produced half of the maximal response. The  $pEC_{50}$  is the negative logarithm of the EC. Values are given for  $G\alpha_s$  recruitment, cAMP accumulation, receptor internalization,  $\beta$ -arrestin 1/2, and  $G\alpha_q$  recruitment at the GLP-1R and the GIPR. All of the values were derived from the iAUC of a temporal response for each concentration/agonist and are expressed as mean  $\pm$  SEM from at least 3 independent experiments with at least two technical replicates per group. Statistical significance was determined using one-way ANOVA and corrected with Bonferroni's multiple comparisons test. \*/#/+p < 0.05. \* vs GLP-1 (7–36 amide) or GIP (1–42). # vs Semaglutide. † vs fatty acyl-GLP-1 or fatty acyl-GIP. NA = no agonism significantly different than zero observed at 1  $\mu$ M stimulation. Bold red = with significant non-zero agonism at 1  $\mu$ M stimulation but incomplete curve fit, last value at 10  $\mu$ M used. *Table adapted from Novikoff et al. 2021 (Mol. Met.).*

	cAMP			$G\alpha_s$ Recruitment			Receptor Internalization		
	$E_{max}$ (% GLP-1)	$pEC_{50}$	$EC_{50}$ (nM)	$E_{max}$ (% GLP-1)	$pEC_{50}$	$EC_{50}$ (nM)	$E_{max}$ (% GLP-1)	$pEC_{50}$	$EC_{50}$ (nM)
<b>GLP-1R</b>									
Native GLP-1 (7-36 amide)	100 $\pm$ 3	9.28 $\pm$ 0.11	.5229	100 $\pm$ 6	6.44 $\pm$ 0.12	361.8	100 $\pm$ 7	6.37 $\pm$ 0.15	422.5
GIP (1-42)	NA	NA	NA	NA	NA	NA	NA	NA	NA
Semaglutide	101 $\pm$ 3 [+1]	9.44 $\pm$ 0.12	.3613	95 $\pm$ 2 [-5]	6.90 $\pm$ 0.05	130.3	107 $\pm$ 5 [+7]	6.27 $\pm$ 0.09	528.1
Acyl GLP-1	106 $\pm$ 3 [+6]	9.44 $\pm$ 0.11	.3602	101 $\pm$ 5 [-1]	6.52 $\pm$ 0.10	304.5	108 $\pm$ 4 [+8]	6.41 $\pm$ 0.08	391.6
Acyl GIP	NA	6.74 $\pm$ 0.14	181.2	NA	NA	NA	NA	NA	NA
Dual Agonist (Mar709)	100 $\pm$ 3 [+0]	9.44 $\pm$ 0.10	.3613	59 $\pm$ 1 [-41]* # †	6.88 $\pm$ 0.04	131.2	51 $\pm$ 2 [-49]* # †	6.14 $\pm$ 0.06	728.8
Dual Agonist (Tirzepatide)	110 $\pm$ 4 [+10]	8.42 $\pm$ 0.11 * # †	3.766	31 $\pm$ 1 [-69]* # †	6.29 $\pm$ 0.05 #	514.5	13 $\pm$ 1 [-87]* # †	6.21 $\pm$ 0.13	623.7
<b>GIPR</b>									
Native GLP-1 (7-36 amide)	NA	NA	NA	NA	NA	NA	NA	NA	NA
GIP (1-42)	100 $\pm$ 2	8.45 $\pm$ 0.07	3.573	100 $\pm$ 2	6.65 $\pm$ 0.10	219.2	100 $\pm$ 3	7.43 $\pm$ 0.07	37.23
Semaglutide	NA	NA	NA	NA	NA	NA	NA	NA	NA
Acyl GLP-1	NA	NA	NA	NA	NA	NA	NA	NA	NA
Acyl GIP	97 $\pm$ 2 [-3]	8.87 $\pm$ 0.07 *	1.342	93 $\pm$ 3 [-7]	6.61 $\pm$ 0.15	247.2	11 $\pm$ 2 [-89] *	8.54 $\pm$ 0.04	2.854
Dual Agonist (Mar709)	100 $\pm$ 3 [+0]	9.05 $\pm$ 0.10 *	.8991	81 $\pm$ 2 [-19]*	6.77 $\pm$ 0.09	171.3	4 $\pm$ 2 [-96]*	9.99 $\pm$ 0.03 * †	0.103
Dual Agonist (Tirzepatide)	103 $\pm$ 5 [+3]	7.88 $\pm$ 0.13 * †	13.07	97 $\pm$ 6 [-3]	6.39 $\pm$ 0.28	405	18 $\pm$ 1 [-82]*	8.33 $\pm$ 0.03 * †	4.665
	$\beta$ -arr1 Recruitment			$\beta$ -arr2 Recruitment			$G\alpha_q$ Recruitment		
	$E_{max}$ (% GLP-1)	$pEC_{50}$	$EC_{50}$ (nM)	$E_{max}$ (% GLP-1)	$pEC_{50}$	$EC_{50}$ (nM)	$E_{max}$ (% GLP-1)	$pEC_{50}$	$EC_{50}$ (nM)
<b>GLP-1R</b>									
Native GLP-1 (7-36 amide)	100 $\pm$ 6	6.37 $\pm$ 0.12	427.4	100 $\pm$ 3	6.64 $\pm$ 0.06	231.6	100 $\pm$ 6	6.38 $\pm$ 0.39	420.9
GIP (1-42)	NA	NA	NA	NA	NA	NA	NA	NA	NA
Semaglutide	67 $\pm$ 4 [-33] *	6.58 $\pm$ 0.13	264.5	78 $\pm$ 3 [-22]*	6.78 $\pm$ 0.09	164.4	98 $\pm$ 5 [-2]	6.41 $\pm$ 0.33	389.5
Acyl GLP-1	95 $\pm$ 6 [-5] #	6.42 $\pm$ 0.13	383.6	86 $\pm$ 3 [-14]*	6.72 $\pm$ 0.07	187.7	98 $\pm$ 7 [-2]	6.37 $\pm$ 0.43	423.8
Acyl GIP	NA	NA	NA	NA	NA	NA	NA	NA	NA
Dual Agonist (Mar709)	35 $\pm$ 1 [-65]* # †	6.52 $\pm$ 0.08	301.7	24 $\pm$ 1 [-76]* # †	6.92 $\pm$ 0.12	119.2	48 $\pm$ 3 [-52]* # †	6.36 $\pm$ 0.21	432.2
Dual Agonist (Tirzepatide)	NA	NA	NA	NA	NA	NA	17 $\pm$ 1 [-83]* # †	6.23 $\pm$ 0.06	587.5
<b>GIPR</b>									
Native GLP-1 (7-36 amide)	NA	NA	NA	NA	NA	NA	NA	NA	NA
GIP (1-42)	NA	NA	NA	<b>100 <math>\pm</math> 18 (10<math>\mu</math>M)</b>	<b>6.77 <math>\pm</math> 0.39</b>	NA	100 $\pm$ 5	6.55 $\pm$ 0.04	283.3
Semaglutide	NA	NA	NA	NA	NA	NA	NA	NA	NA
Acyl GLP-1	NA	NA	NA	NA	NA	NA	NA	NA	NA
Acyl GIP	NA	NA	NA	NA	NA	NA	90 $\pm$ 3 [-10]	6.99 $\pm$ 0.03 *	101.4
Dual Agonist (Mar709)	NA	NA	NA	<b>36 <math>\pm</math> 25 [-64]*</b>	<b>7.41 <math>\pm</math> 0.23 *</b>	NA	68 $\pm$ 3 [-32]* †	6.82 $\pm$ 0.03 * †	152.7
Dual Agonist (Tirzepatide)	NA	NA	NA	<b>35 <math>\pm</math> 14 [-65]*</b>	<b>7.49 <math>\pm</math> 0.40 *</b>	NA	85 $\pm$ 3 [-15]*	6.48 $\pm$ 0.03 †	328.7

*MAR709 and Tirzepatide are Characterized as Partial  $G\alpha_s$  Agonists with Full Efficacy within the cAMP Pathway at the GLP-1R*

$G\alpha_s$  is the primary G-protein subunit acting at both the GLP-1R and GIPR following 1  $\mu$ M of ligand-induced stimulation (Figure 15-16, A). The  $G\alpha_s$ -cAMP pathway has been extensively characterized as a primary mediator of GLP-1 and GIP action (Seino, 2012). In order to examine ligand dose-dependency toward a  $G\alpha_s$  temporal response, hGLP-1R-GFP<sup>+</sup> or hGIPR-GFP<sup>+</sup> HEK293T cells were incubated with ligands for 60 minutes, in which the AUC resulting from the temporal span between baseline and the 60-minute endpoint was quantified. cAMP measurements were performed by incubating ligands over the course of 30 minutes with GLP-1R<sup>+</sup> or GIPR<sup>+</sup> HEK293T cells co-expressing the unimolecular cAMP BRET sensor CAMYEL (Jiang *et al.*, 2007).

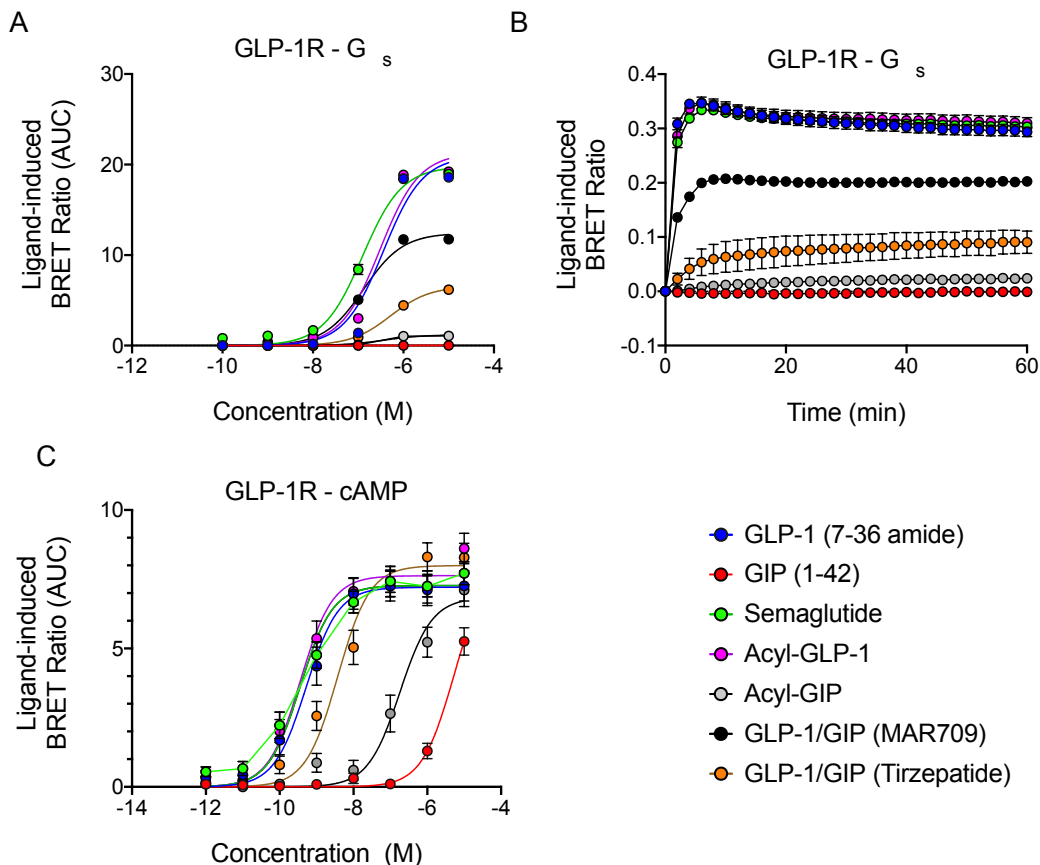


**Figure 18: Dose-dependent and temporal effects of ligands on  $G\alpha_s$  recruitment and cAMP production at the GLP-1R.** Dose-response curves (A) and temporal resolution (1  $\mu$ M stimulation) (B) of ligand-induced BRET between Mini $G\alpha_s$ -Nluc and GFP-tagged GLP-1R in HEK293T cells. Dose-response curves of ligand-induced cAMP production in GLP-1R<sup>+</sup> HEK293T cells (C). +iAUC representation of vehicle- and baseline-corrected 60 min ( $G\alpha_s$  recruitment) or 25 min (cAMP generation) temporal responses to each agonist is expressed as mean  $\pm$  SEM. Three independent experiments were performed with at least two technical replicates per group. *Figure adapted from Novikoff et al. 2021 (Mol. Met.).*

Ranking ligand-induced  $G\alpha_s$  recruitment dose-response efficacy ( $E_{max}$ ) at the GLP-1R followed a similar pattern with the previous G-protein screening data at 1  $\mu$ M. In GLP-1R<sup>+</sup> HEK293T cells, both Semaglutide and Acyl-GLP-1 displayed a similar efficacy (95% and 101%) to that of GLP-1 (7-36 amide) (**Figure 18, A; Table 2**). The pEC50, which is the negative log value of the EC, was not significantly different between these GLP-1R mono-agonists, however Semaglutide hinted at a slightly superior potency of 130 nM as opposed to 361 nM and 304 nM for GLP-1 (7-36 amide) and Acyl-GLP-1 respectively.

Interestingly, both MAR709 and Tirzepatide acted as partial agonists for  $G\alpha_s$  recruitment as demonstrated by a significant reduction in  $G\alpha_s$  recruitment  $E_{max}$  capacity, which is evident as achieving a relative 59% and 31% response to that of GLP-1 (7-36 amide) (**Table 2**). The agonism profile for MAR709 and Tirzepatide remained partial up to a ligand concentration of 10  $\mu$ M, which was the highest achievable dose. This effect was independent of time after drug exposure, as evidenced by the 60 minute temporal response at a concentration of 1  $\mu$ M (**Figure 18, B**). The reduced  $G\alpha_s$  recruitment  $E_{max}$  of both MAR709 and Tirzepatide indicative of partial agonism was unexpected, as the extent of *in vitro* characterization in previous literature had been limited to demonstrations of full agonism via indirect CRE-luciferase reporter assays (Coskun *et al.*, 2018; Finan *et al.*, 2013).

Regarding potency, MAR709 exhibited a slight enhancement in potency with an EC of 131 nM in comparison to the 514 nM of Tirzepatide (**Table 2**). There were no significant differences in pEC50 between the relevant GLP-1R mono-agonists and MAR709. These  $G\alpha_s$  recruitment EC data agree with the engineering intent behind the development of the “balanced” MAR709 and the GIPR-favoring Tirzepatide.

Despite the reduced GLP-1R  $G\alpha_s$  recruitment  $E_{max}$  of MAR709 and Tirzepatide, interestingly, both dual-agonists did not differ in cAMP  $E_{max}$  when compared against the relevant GLP-1 mono-agonists (**Figure 18, C**). In detail, MAR709 and Tirzepatide simulated a maximal cAMP response of 100% and 110% relative to GLP-1 (7-36 amide) (**Table 2**). Therefore, despite MAR709 and Tirzepatide acting as partial agonists for  $G\alpha_s$  recruitment, both remained full agonists for cAMP. Both Semaglutide and Acyl-GLP-1 exhibited similar cAMP  $E_{max}$  capacity of 101% and 106% to that of GLP-1 (7-36 amide). In terms of potency at the GLP-1R, all GLP-1R relevant agonists exhibited similar cAMP pEC50 values indicating a common level of potency with the exception of Tirzepatide, which was significantly decreased relative to all GLP-1R

mono-agonists. The reduction in potency of Tirzepatide for cAMP production was reflected with the prior reduction in potency for  $G\alpha_s$  recruitment.

It was unexpected that MAR709 and Tirzepatide, acting as partial agonists for  $G\alpha_s$  recruitment, remained full agonists for cAMP. It has been previously noted that intracellular cAMP biosensors for use in live cell quantification are susceptible to ligand-induced signal saturation, and that a supersaturating positive control is required to assure that ligand responses are falling within a subsaturatable range (Willoughby and Cooper, 2008). Therefore, we investigated whether cAMP sensor saturation was producing an artifact of equal  $E_{max}$  between agonists.

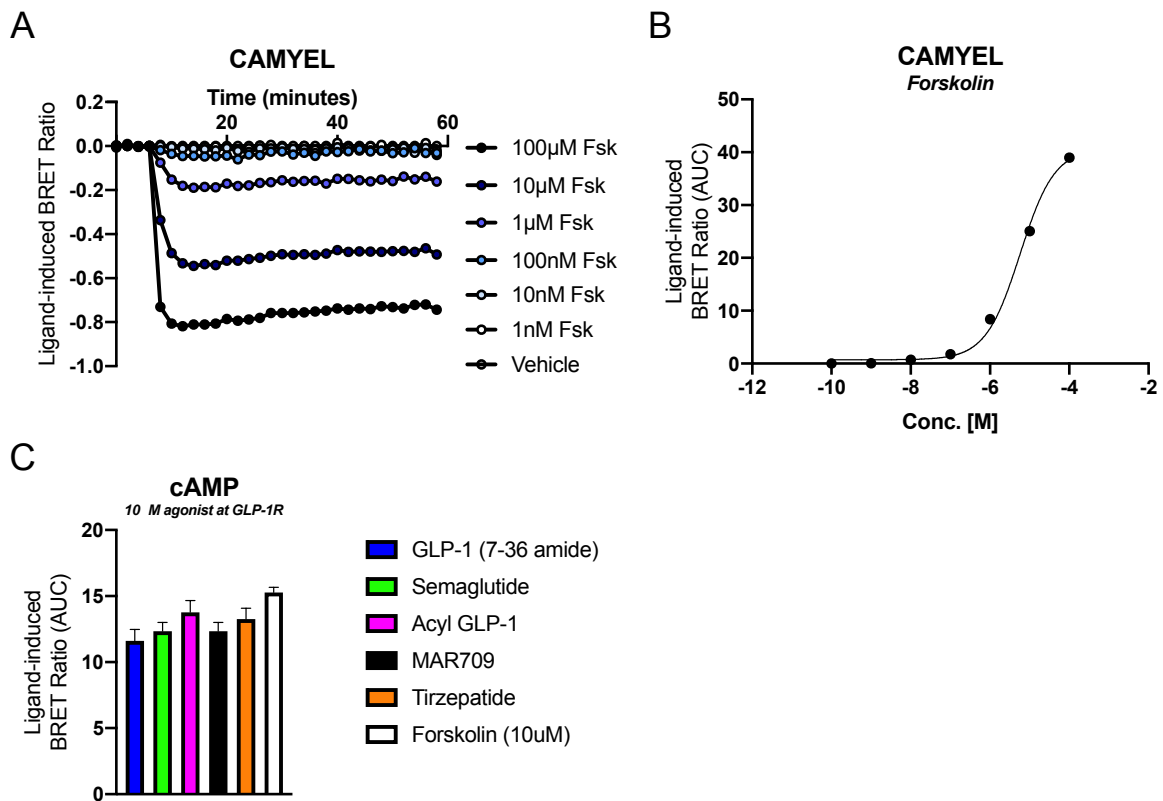


**Figure 19: Saturation of unimolecular CAMYEL cAMP sensor is not achieved following 10  $\mu$ M ligand stimulation at the GLP-1R.** Time course (A) and fitted dose-response curve (100 pM – 100  $\mu$ M) (B) of the cAMP positive control forskolin in GLP-1R<sup>+</sup> HEK293T cells. Stimulation with 10  $\mu$ M of agonist or forskolin in GLP-1R<sup>+</sup> HEK293T cells (C). The +iAUC representation of vehicle- and baseline-corrected 60 min response to each agonist is expressed as mean  $\pm$  SEM. Three independent experiments were performed with at least two technical replicates per group. *Figure adapted from Novikoff et al. 2021 (Mol. Met.).*

A dose-response of the cAMP activator and positive control forskolin demonstrated a progressive increase in cAMP production between the concentrations of 100 nM and 100  $\mu$ M, indicating a lack of forskolin-mediated sensor saturation at 10  $\mu$ M (Figure 19, A-B). Within

GLP-1R<sup>+</sup> HEK293T, a comparison was made between 10  $\mu$ M of forskolin and 10  $\mu$ M of relevant GLP-1R agonists. Forskolin exhibited the highest signal relative to the GLP-1R agonists (**Figure 19, C**). Therefore, as 10  $\mu$ M forskolin eclipsed the cAMP signal produced by 10  $\mu$ M of GLP-1R agonists acting the GLP-1R, and as 100  $\mu$ M forskolin relative to 10  $\mu$ M provided a further increase in CAMYEL signal, it was concluded that sensor saturation had not been reached within the dose-response experiment, and that indeed MAR709 and Tirzepatide are equally efficacious as the mono-agonists at the GLP-1R despite partial  $G\alpha_s$  agonism.

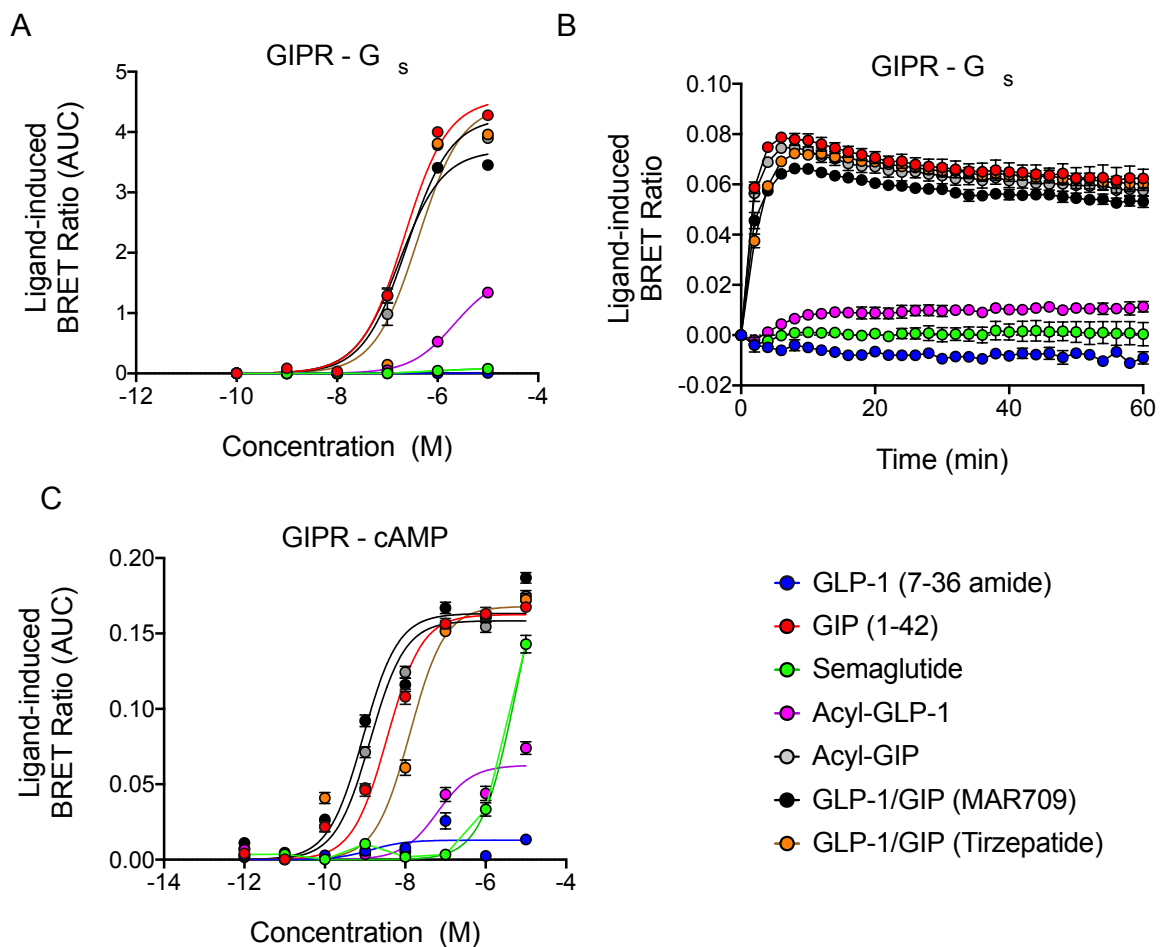


**Figure 20: Dose-dependent and temporal effects of ligands on G $\alpha_s$  recruitment and cAMP production at the GIPR.** Dose-response curves (A) and temporal resolution (1  $\mu$ M stimulation) (B) of ligand-induced BRET between MiniG $\alpha_s$ -Nluc and GFP-tagged GIPR in HEK293T cells. Dose-response curves of ligand-induced cAMP production in GIPR<sup>+</sup> HEK293T cells (C). +iAUC representation of vehicle- and baseline-corrected 60 min (G $\alpha_s$  recruitment) or 25 min (cAMP generation) temporal responses to each agonist is expressed as mean  $\pm$  SEM. Three independent experiments were performed with at least two technical replicates per group. *Figure adapted from Novikoff et al. 2021 (Mol. Met.).*

In GIPR<sup>+</sup> HEK293T cells, Acyl-GIP and both dual-agonists recruited G $\alpha_s$  with comparable potency to that of GIP (1-42) (**Figure 20, A; Table 2**). However in terms of efficacy, MAR709



displayed a slight but significant reduction in  $G\alpha_s$  recruitment efficacy at the GIPR, eliciting 81% of the  $G\alpha_s$  recruitment  $E_{max}$  of GIP (1-42), while Acyl-GIP and Tirzepatide stimulated 93% and 97% respectively (**Figure 20, A-B; Table 2**). This data is in line with previous literature and the  $G\alpha$  subunit screen at 1  $\mu$ M (**Figure 16, A**) (Coskun *et al.*, 2018; Finan *et al.*, 2013).

Translating  $G\alpha_s$  recruitment into cAMP production efficacy, no significant differences were noted as Acyl-GIP stimulated 97% of the GIP (1-42) cAMP  $E_{max}$ , while MAR709 and Tirzepatide achieved 100% and 103% respectively (**Figure 20, C; Table 2**). Regarding cAMP potency at the GIPR, both Acyl-GIP and MAR709 exhibited a significantly superior pEC50 to that of GIP (1-42), however Tirzepatide surprisingly demonstrated a significant 3-fold reduction in potency. The reduced potency of Tirzepatide relative to GIP (1-42) was not expected as previous literature had demonstrated a superior cAMP EC for Tirzepatide in comparison to GIP (1-42) (Coskun *et al.*, 2018). However, the previous study had used an indirect CRE-luciferase reporter to quantify cAMP production, which is a method subject to undue influence by both downstream signal amplification and receptor localization. A potential explanation for this discrepancy is the direct interaction of the CAMYEL sensor with cAMP molecules, which may provide a readout less diluted by signal amplification than an indirectly-associated nuclear reporter assay based on CREB phosphorylation and activity. Previous literature that has utilized assays based on direct cAMP quantification have also aligned with our demonstrated findings, in which an equivalent decrease in cAMP potency relative to GIP (1-42) was evidenced with Tirzepatide at the GIPR (Yuliantie *et al.*, 2020).

Collectively, both MAR709 and Tirzepatide have demonstrated unique agonism properties at their target receptors. At the GLP-1R, both dual-agonists displayed partial agonism properties for  $G\alpha_s$  yet retained full cAMP efficacy, which is likely due to the equalizing effects of signal amplification. This phenomenon may translate to a unique impact on other downstream measurable intracellular events, in which ligand efficacy at an event may either be reflective of immediate receptor activation ( $G\alpha_s$  recruitment) or fall within the signal amplification pathway (cAMP production).

#### *The Full cAMP Agonism Profile of MAR709 and Tirzepatide at the GLP-1R is Preserved Through Downstream PKA Activity*

The unique signaling profile of MAR709 and Tirzepatide at the GLP-1R, in which both dual-agonists demonstrate differential yet partial  $G\alpha_s$  agonism, and maintain full cAMP agonism,

raised the questions if the equalizing signal amplification necessitated for full cAMP agonism persisted through cAMP-activated downstream kinases such as PKA. This was suggested to be an important event in GLP-1R signaling as activated PKA catalytic subunits may mediate the phosphorylation of the Kir6.2 and SUR1 subunits of  $K_{ATP}$  channels driving plasma membrane depolarization, which in turn facilitates  $Ca^{2+}$  influx through voltage-gated channels, resulting in subsequent enhanced insulin release (Holz, 2004).

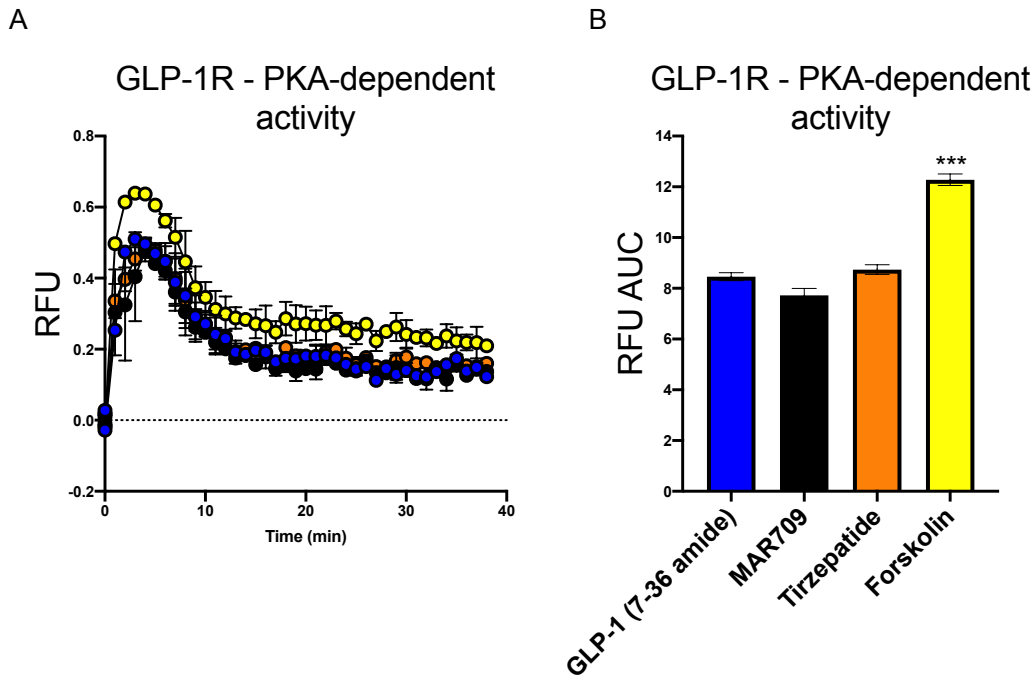


**Figure 21: PKA activity at the GLP-1R.** Temporal resolution (A) and AUC (B) of ligand-induced PKA activity as measured by the unimolecular circularly permuted ExRai-AKAR2 sensor in GLP-1R<sup>+</sup> HEK293T cells. The AUC representation of vehicle- and baseline-corrected 40 min response to each agonist is expressed as mean  $\pm$  SEM. Bonferroni's test, \* $p < 0.05$ , \*\* $p < 0.005$ , and \*\*\* $p < 0.0005$  using one-way ANOVA vs GLP-1 (7-36 amide). Three independent experiments were performed with at least two technical replicates per group.

The ratiometric unimolecular protein-based PKA sensor ExRai-AKAR2, which produces a quantifiable change in signal when phosphorylated by PKA, was used to assess the temporal dynamics of PKA activity in live cells (Zhang *et al.*, 2021a). GLP-1 (7-36 amide) was used as a  $G\alpha_s$  full agonist control, while MAR709 and Tirzepatide represented ligands with decreasing  $G\alpha_s$  efficacy, albeit with full cAMP efficacy. Following 1  $\mu$ M agonist administration over the course of 40 minutes, an initial peak between 0 and 10 minutes was observed for all agonists, followed by a tapering of signal that is characteristic of partial kinase feedback inhibition (Gervasi *et al.*, 2007). Interestingly, no significant differences between GLP-1 (7-36 amide) and the dual-agonists, MAR709 and Tirzepatide, were observed for induced PKA activity via the

GLP-1R (**Figure 21, A-B**). The positive control forskolin (10  $\mu$ M) stimulated the strongest prolonged activation of PKA, which was significantly greater than any GLP-1R relevant agonist. Altogether, this indicates that the partial agonism profiles of MAR709 and Tirzepatide for  $G\alpha_s$  recruitment are restricted to the first steps of the  $G\alpha_s$ -cAMP-PKA pathway, while the full agonism properties attributed to these dual-agonists persist through cAMP and PKA activity, largely due to signal amplification mechanisms.

### *MAR709 and Tirzepatide Stimulate Minimal Internalization of the GLP-1R in HEK293T and Min6 Cell Lines*

Next assessed was the dose-dependent and temporal analysis of ligand-induced GLP-1 receptor internalization. HEK293T or Min6 cells co-expressing hGLP-1R-Rluc8 with the plasma membrane marker Venus-KRAS were incubated with ligands over the course of 60 minutes, in which the magnitude of physical dissociation of the receptor moving away from the plasma membrane was measured.

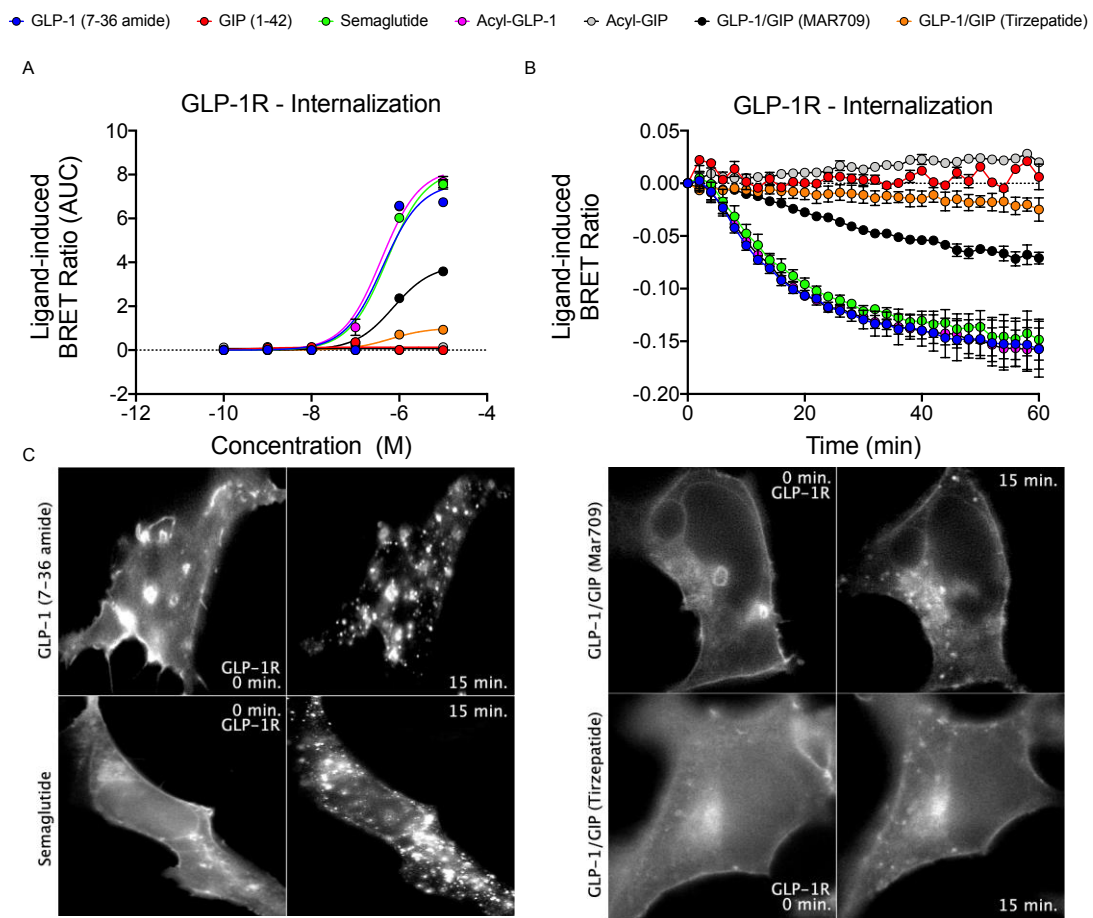


**Figure 22: Ligand-induced GLP-1R internalization.** Dose-response (A) and temporal resolution (1  $\mu$ M) (B) of ligand-induced hGLP-1-Rluc8 internalization as measured by loss of BRET with plasma membrane marker Venus-KRAS. Live HILO imaging of hGLP-1R-GFP internalization in

HEK293T cells at baseline and 15 minutes after 1  $\mu$ M ligand treatment (C). The -AUC representation of vehicle- and baseline-corrected 40 min response to each agonist is expressed as mean  $\pm$  SEM. Three independent experiments were performed with at least two technical replicates per group. *Figure adapted from Novikoff et al. 2021 (Mol. Met.).*

In hGLP-1R-RLuc8<sup>+</sup> HEK293T cells, Semaglutide, and Acyl-GLP-1 acted as full agonists for GLP-1R internalization, maximally stimulating 107% and 108% of the receptor internalization  $E_{max}$  of GLP-1 (7-36 amide) (**Figure 22, A-B; Table 2**). This effect was found to be independent of time length of ligand incubation. The differences in  $E_{max}$  between the GLP-1R mono-agonists and GLP-1 (7-36 amide) were non-significant. The potencies of the GLP-1R mono-agonists were similar, with an  $EC_{50}$  of 422 nM, 526 nM, and 391 nM for GLP-1 (7-36 amide), Semaglutide, and Acyl-GLP-1, respectively (**Table 2**). Surprisingly, both MAR709 and Tirzepatide exhibited drastic reductions in the capacity to stimulate receptor internalization, in which relative to GLP-1 (7-36 amide), the maximal ligand-induced GLP-1R internalization  $E_{max}$  of MAR709 and Tirzepatide were 51% and 13%, respectively. The potencies of MAR709 and Tirzepatide, however, were not significantly different in comparison to any of the GLP-1R mono-agonists.

The differential agonist-induced GLP-1R internalization effects were validated with live hGLP-1R-GFP<sup>+</sup> HEK293T cells using HILO microscopy (**Figure 22, C**). At baseline (0 minutes), the fluorescent tag of the GLP-1R outlines the HEK293T cell as it is co-localized with the plasma membrane. It is of note that residual GLP-1R-GFP localized to the cytosol at baseline is likely due to either constitutive activity, or intracellular trafficking of newly translated GLP-1R-GFP. Following 15 minutes of ligand administration, GLP-1 (7-36 amide) and Semaglutide induced marked reductions in the defined fluorescent signal localized to the plasma membrane, indicating a high degree of GLP-1R-GFP internalization. As the GLP-1R is trafficked from the plasma membrane, the GFP-tagged receptors congregate to form numerous intracellular punctate structures. These punctate structures represent sites of intracellular receptor accumulation, which may be involved in the compartmentalization of endosomal signaling or receptor degradation. In line with the BRET results, stimulation with the GLP-1/GIP dual-agonists MAR709 and Tirzepatide did not induce the same loss in fluorescent signal localized to the plasma membrane as the GLP-1R mono-agonists, which is therefore viewed as a ligand-specific retention of the receptor at the plasma membrane (**Figure 22, C**). The formation of numerous intracellular puncta of internalized GLP-1R was also notably absent for both dual-agonists. Taken altogether, visual representation of ligand-induced GLP-1R internalization via

HILO microscopy in GLP-1R-GFP<sup>+</sup> HEK293T cells confirmed the full agonism properties of GLP-1R mono-agonists, while MAR709 and Tirzepatide are validated in their lack of efficacious induction of receptor internalization.

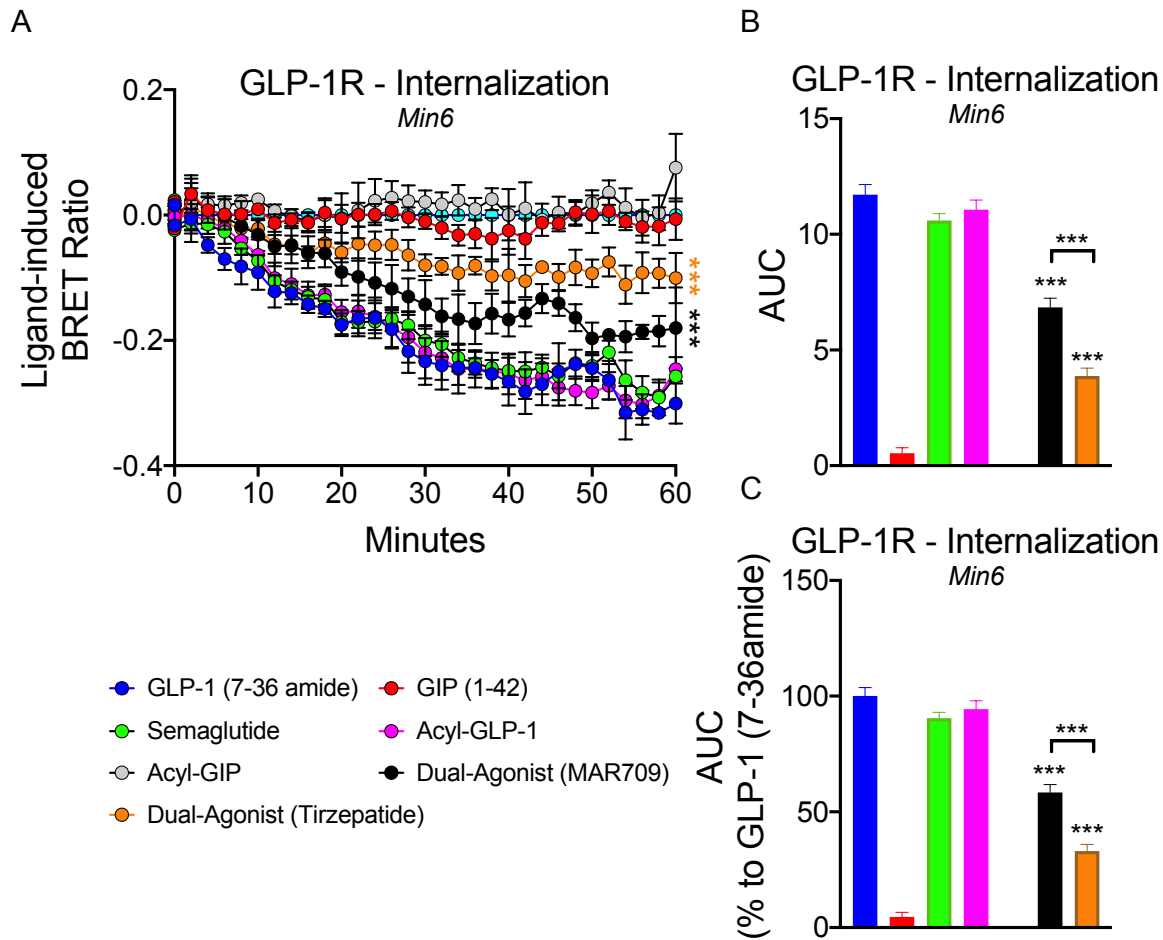


**Figure 23: Ligand-induced GLP-1R internalization in hGLP-1R<sup>+</sup> Min6 cells.** Temporal resolution (1  $\mu$ M ligand stimulation) (A), AUC (B) and % normalized AUC to GLP-1 (7-36 amide) (C), of hGLP-1R-Rluc8 internalization as measured by loss of BRET with plasma membrane marker Venus-KRAS in HEK293T cells. The -AUC representation of vehicle- and baseline-corrected 60 min response to each agonist is expressed as mean  $\pm$  SEM. Bonferroni's test, \* $p$  < 0.05, \*\* $p$  < 0.005, and \*\*\* $p$  < 0.0005 using one-way ANOVA vs GLP-1 (7-36 amide). Three independent experiments were performed with at least two technical replicates per group. *Figure adapted from Novikoff et al. 2021 (Mol. Met.).*

Min6 cells are an immortalized pancreatic mouse  $\beta$ -cell line, and represent a physiologically-relevant *in vitro* model. Ligand stimulation, within the context of hGLP-1R-Rluc8/Venus-KRAS co-expression in Min6 cells, exhibited similar ligand-induced receptor internalization dynamics to that observed in HEK293 cells. Semaglutide and Acyl-GLP-1 induced non-significant differences in Min6 GLP-1 receptor internalization relative to that of GLP-1 (7-36 amide) (**Figure 23, A-C**). Likewise, MAR709 and Tirzepatide demonstrated significant

reductions in ligand-induced GLP-1R internalization over the course of 60 minutes, in which MAR709 and Tirzepatide elicited 58% and 33% of the GLP-1 (7-36 amide) response. Of note, Tirzepatide-induced receptor internalization generally seemed more pronounced in Min6 cells than that observed in HEK293T cells (33% Min6 vs. 13% HEK293T). This may highlight subtle differences and limitations between biological models.

### *GLP Receptor Exhibits Unique Assay-Dependent Ligand-Induced Internalization Dynamics*

In hGIPR-Rluc8<sup>+</sup> HEK293T cells, GIP (1-42) was evidenced to induce sustained receptor internalization over the course of 20 minutes with an EC of 37 nM. However, neither Acyl-GIP nor the dual-agonists MAR709 and Tirzepatide elicited a meaningful internalization response, and this was independent of time (**Figure 24, A-B**). In particular, MAR709 and Tirzepatide respectively stimulated just 4% and 18% of the GIP (1-42) receptor internalization E<sub>max</sub> (**Table 2**).

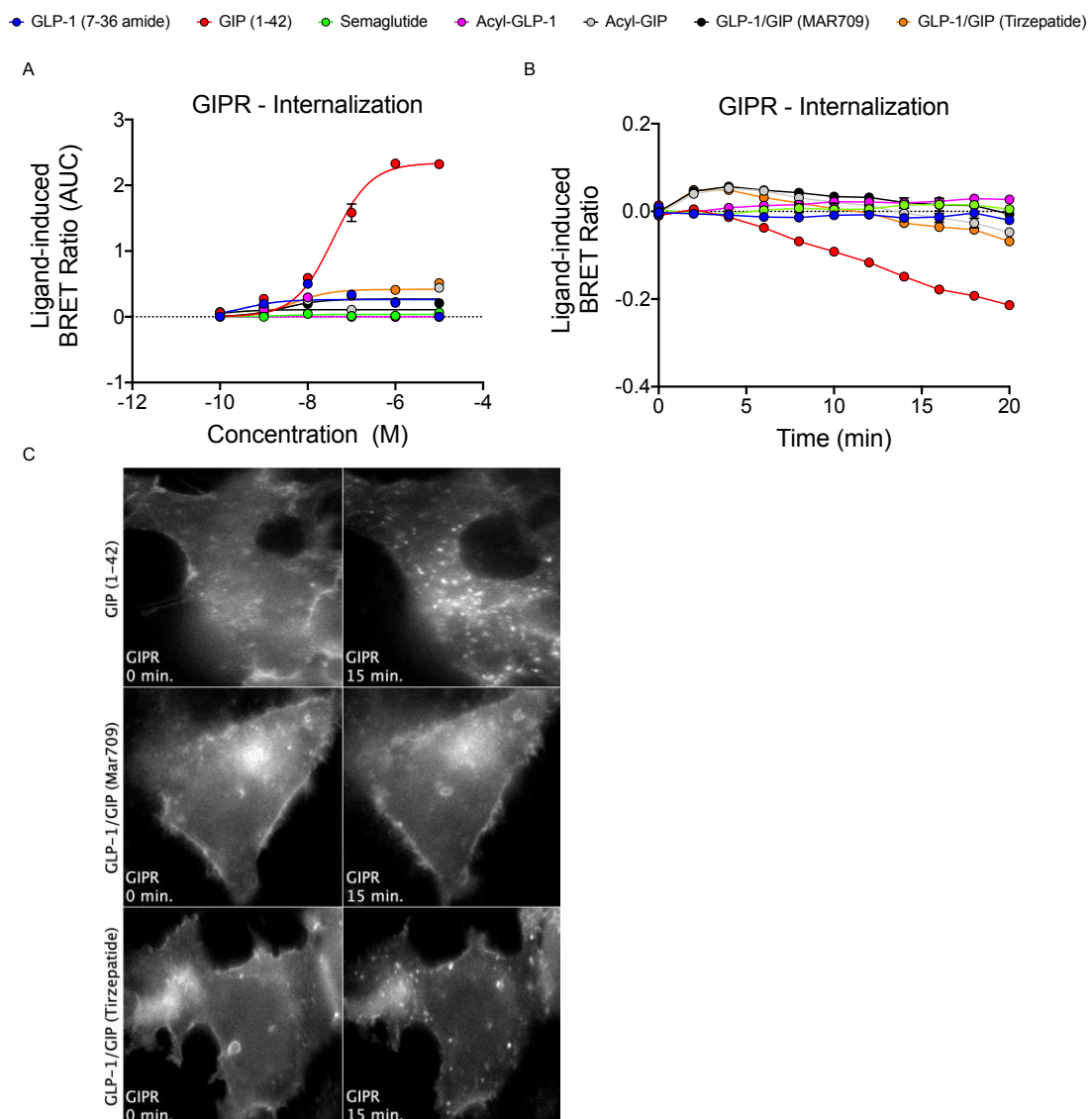


**Figure 24: Ligand-induced GIPR internalization.** Dose-response (A) and temporal resolution (1  $\mu$ M) (B) of ligand-induced hGIPR-Rluc8 internalization as measured by loss of BRET with plasma membrane marker Venus-KRAS. Live HILO imaging of hGIPR-GFP internalization in HEK293T cells at baseline and 15 minutes after 1  $\mu$ M ligand treatment (C). The -AUC representation of vehicle- and baseline-corrected 20 min response to each agonist is expressed as mean  $\pm$  SEM. Three independent experiments were performed with at least two technical replicates per group. *Figure adapted from Novikoff et al. 2021 (Mol. Met.).*

Using live-cell HILO microscopy with hGIPR-GFP<sup>+</sup> HEK293T cells, following 15 minutes of ligand administration, GIP (1-42) elicited high dissolution of the GIPR-GFP defined plasma membrane and formation of punctate structures within the cytosol (**Figure 24, C**). In line with the BRET data, lack of ligand-induced GIPR receptor internalization by both MAR709 and Tirzepatide was confirmed by minimal departure of GIPR-GFP from the plasma membrane and a lack of punctate structure formation (**Figure 24, C**).

Interestingly, within previous literature, conflicting results have been presented regarding the occurrence of ligand-induced GIP receptor internalization. In one study, a SNAP-tag GIPR, which is constructed as a SNAP-tag addition to the N-terminus of the GIPR capable of binding small molecule fluorescent substrate without affecting ligand binding to the GIPR, was expressed and used within a FRET-based internalization assay. The SNAP-tag substrate SNAP-Lumi4-Tb (donor) and fluorescein (acceptor) were administered, in which SNAP-Lumi4-Tb would bind to the extracellular facing N-terminal GIPR SNAP-tag and FRET with the non-membrane permeable extracellular fluorescein at baseline. When GIP (1-42) was then administered, there was no loss in FRET signal attributable to internalization, indicating that the Lumi4-Tb-bound SNAP-tag localized on the N-terminus of GIPR was still at the plasma membrane facing the extracellular space. With this same method, both GLP-1 (7-36 amide) and glucagon elicited internalization of their respective SNAP-tag receptor upon agonism (Roed *et al.*, 2015).

In a separate study using HEK293T cells, an untagged GIPR was expressed and internalization was measured by quantifying the amount of fluorophore-bound GIP (1-42) localized to the intracellular space following ligand administration using fluorescence-activated cell sorting (FACS). Robust internalization of the GIPR was evidenced by a high degree of internalized AlexaF647-GIP (Ismail *et al.*, 2015). Importantly, in another study utilizing the Lumi4-Tb FRET technique within Roed. *et al.*, 2015, Tirzepatide was found to robustly and rapidly internalize

SNAP-tag GIPR in HEK293T cells (Willard *et al.*, 2020). This finding is in contrast to the lack of Tirzepatide-induced GIPR internalization that was evidenced here (**Figure 24, A-C**).

Therefore, due to the highly conflicting conclusions throughout previous literature regarding the presence and ligand-specific effects on GIPR internalization, we set out to better understand the discrepancy between our findings and previous literature.

The most intriguing difference between the GPCR-Rluc8/Venus-KRAS BRET assay and the aforementioned SNAP-tag Lumi4-Tb FRET assay is at the point of baseline quantification. In the BRET assay, all GPCRs actively tagged with an Rluc8 are capable of resonance energy transfer with the Venus-KRAS plasma membrane marker, given close interactive proximity is achieved. Therefore, ligand-induced quantitative changes can be relevant to both plasma membrane-bound GIPR-Rluc8, which automatically resonates with Venus-KRAS at baseline, and cytosol-localized GIPR-Rluc8, which do not resonate with Venus-KRAS at baseline. Oppositely, within the aforementioned FRET assay, SNAP-tag Lumi4-Tb is a cell-membrane impermeable substrate, therefore only SNAP-tagged GIPR present at the plasma membrane at the time of labeling will be utilized within the FRET quantification of ligand-induced receptor internalization. In short, the BRET method purely measures changes in receptor colocalization at the plasma membrane, whether it be from the receptors internalizing away from the plasma membrane inducing a loss in BRET signal, or cytosol-localized receptors shuttling towards and integrating into the plasma membrane inducing an increase in BRET signal. In the FRET method, Lumi4-Tb binding is restricted to only the SNAP-tag receptors localized at the plasma membrane at baseline, therefore quantifications of receptor internalization can only possibly account for a ligand-induced lack of change, or alternatively, a decrease in receptor presence at the plasma membrane, but cannot measure ligand-induced recruitment of non-labeled receptor to the plasma membrane.

Using an alternative but similarly principled BRET plasmid pairing as our earlier approach to allow for higher resolution, HEK293T cells co-expressing hGIPR-Rluc8 and the plasma membrane marker GFP-CAAX were stimulated with 1  $\mu$ M of GIP (1-42) or Tirzepatide (Madugula and Lu, 2016). Surprisingly, it was found that GIPR internalization underwent a parabolic kinetic, in which upon ligand administration, an immediate increase in receptor density at the plasma membrane was observed followed by a gradual internalization of the receptor marked as a loss in BRET signal (**Figure 25, A**). GIP (1-42) induced a rate of internalization that overcame the initial spike in GIPR movement toward the plasma



membrane, and concluded with a net decrease in signal relative to baseline, indicating more receptor was internalized than was recruited to the plasma membrane following 30 minutes of ligand incubation. However, Tirzepatide induced a greater initial increase in GIP receptor density at the plasma membrane, in which the following rate of receptor internalization did not overcome the buffering of receptor recruitment to the plasma membrane (**Figure 25, A**). Therefore, no meaningful difference in net receptor density at the plasma membrane, relative to baseline, was provoked by Tirzepatide at the end of 30 minutes of agonist incubation, despite a legitimate degree of receptor internalization occurring. It is technically challenging to quantify differences in kinetics when both positive and negative values are included in the same temporal data set, therefore GIPR net movement to and away from the plasma membrane was quantified separately, in which Tirzepatide produced a significantly greater degree of net GIPR recruitment to the plasma membrane, while GIP (1-42) induced a greater degree of net GIPR movement away from the plasma membrane (**Figure 25, B-C**).

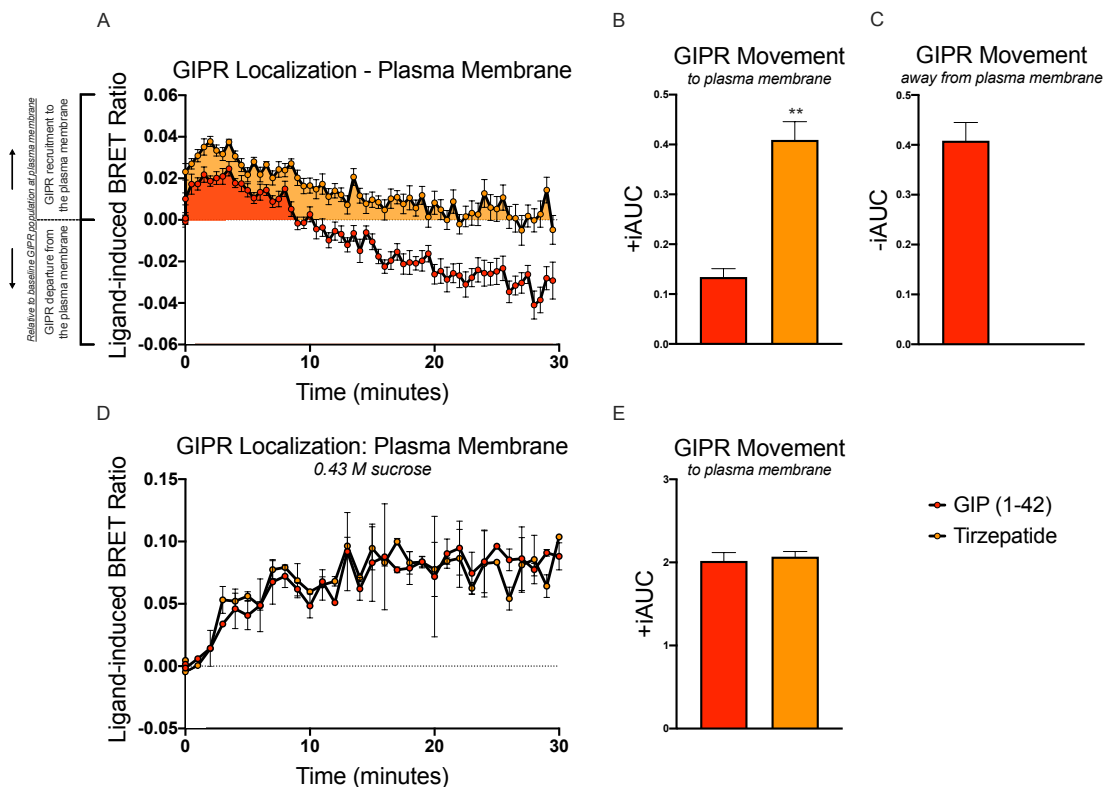


**Figure 1: Ligand-induced GIPR internalization and GIPR recruitment to the plasma membrane.** Temporal resolution (1  $\mu$ M) of ligand-induced hGIPR-Rluc8 movement toward and away from the plasma membrane marker GFP-CAAX (A), in which the +iAUC is represented as ligand-stimulated net GIPR movement towards the plasma membrane (B) and -iAUC represented as ligand-stimulated net GIPR departure away from the plasma membrane (C). Temporal resolution (D) and +iAUC (E) of ligand-induced (1  $\mu$ M) GIPR movement toward the plasma membrane following 30 min pretreatment with 0.43 M sucrose to inhibit receptor internalization. The iAUC representation of vehicle- and baseline-corrected 30 min response

to each agonist is expressed as mean  $\pm$  SEM. Bonferroni's test, \* $p < 0.05$ , \*\* $p < 0.005$ , and \*\*\* $p < 0.0005$  using one-way ANOVA vs GIP (1-42). Three independent experiments were performed with at least two technical replicates per group.

The observation of ligand-induced GIPR recruitment to the plasma membrane is a novel observation that has not yet been reported, and is capable of explaining the discrepancy between methods for quantifying GIPR internalization. To further validate the phenomenon of GIPR recruitment to the plasma membrane, first GIP receptor internalization was inhibited by pre-incubation with 0.43 M sucrose, and was followed with ligand stimulation over the course of 30 minutes (**Figure 25, D**) (Guo et al., 2015). The mechanism behind hypertonic sucrose-mediated inhibition of receptor internalization is not completely understood, but is thought to impact clathrin polymerization (Lefkowitz, 1998). By inhibiting receptor internalization, the gain in signal due to ligand-induced receptor recruitment to the plasma membrane can be quantified without competing against internalization-induced loss in signal. 1  $\mu$ M of either GIP (1-42) or Tirzepatide both similarly induced marked increases in GIP recruitment to the plasma membrane under the context of internalization inhibition, with no significant differences between ligands observed (**Figure 25, D-E**). The high similarity between GIP (1-42) and Tirzepatide in evoking GIPR recruitment to the plasma membrane when receptor internalization is inhibited suggests that, without sucrose inhibition, GIP (1-42) overcame the initial spike in recruited receptor density by evoking a higher rate of receptor internalization than Tirzepatide. Both agonists displayed similar capacity to localize GIPR to the plasma membrane, but only GIP (1-42) stimulation evoked a net decrease in signal without sucrose inhibition. A caveat to these results that has yet to be excluded is that the initial ligand-induced increase in GIPR recruitment to the plasma membrane could be an artifact of receptor overexpression, although this caveat would be unique to the GIPR as GLP-1R overexpression utilizing identical methodology did not show such a phenomenon. Altogether, these results find: common ground between previous literature and different methodologies by evidencing the lack and presence of ligand-induced GIPR internalization, a first-of-its-kind characterization of the differential rate of GIPR internalization rate induced by Tirzepatide, and new avenues of research into ligand-induced biases in influencing GIPR density at the plasma membrane.

### Ligand-induced GLP-1R Internalization Strongly Correlates with Ligand-specific $G\alpha_s$ Recruitment Efficacy

As mentioned, the degree of ligand-induced  $G\alpha_s$  recruitment does not translate proportionally to the degree of cAMP production due to the phenomenon of signal amplification. However,  $G\alpha_s$  is associated with more biological roles than only evoking cAMP production, and therefore partial agonism of  $G\alpha_s$  recruitment may find therapeutic utility in a cAMP-independent manner. Interestingly, in hGLP-1R<sup>+</sup> HEK293 cells, the degree of ligand-induced receptor internalization is found to mirror the degree of ligand-induced  $G\alpha_s$  recruitment, a correlation seen with all associated agonists at 1  $\mu$ M concentration. This is exemplified in an XY plot of  $G\alpha_s$  recruitment and receptor internalization, in which a strong positive linear correlation manifests (**Figure 26, A**).

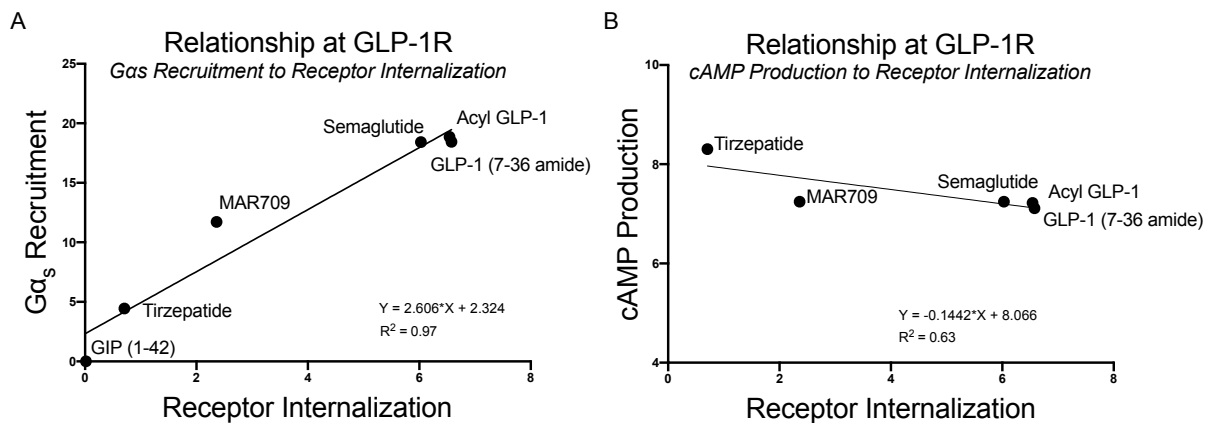


**Figure 26: XY relationship of ligand  $G\alpha_s$  recruitment and cAMP production efficacy, to GLP-1R internalization.** Linear regression demonstrating relationship of ligand-specific receptor internalization  $E_{max}$  (X-axis) to  $G\alpha_s$  recruitment  $E_{max}$  (Y-axis) (A) and cAMP production  $E_{max}$  (Y-axis) (B).

Consequently, cAMP production was not observed to produce a coherent correlation to GLP-1 receptor internalization, as cAMP production was observed to be steadily elevated despite variability in receptor internalization (**Figure 26, B**). These observations represent a GLP-1R specific phenomenon, in which the degree of receptor internalization is observed to be associated with the extent of  $G\alpha_s$  recruitment, and independent of influence from intracellular elements within the signal amplification cascade such as cAMP and cAMP-activated downstream kinases.

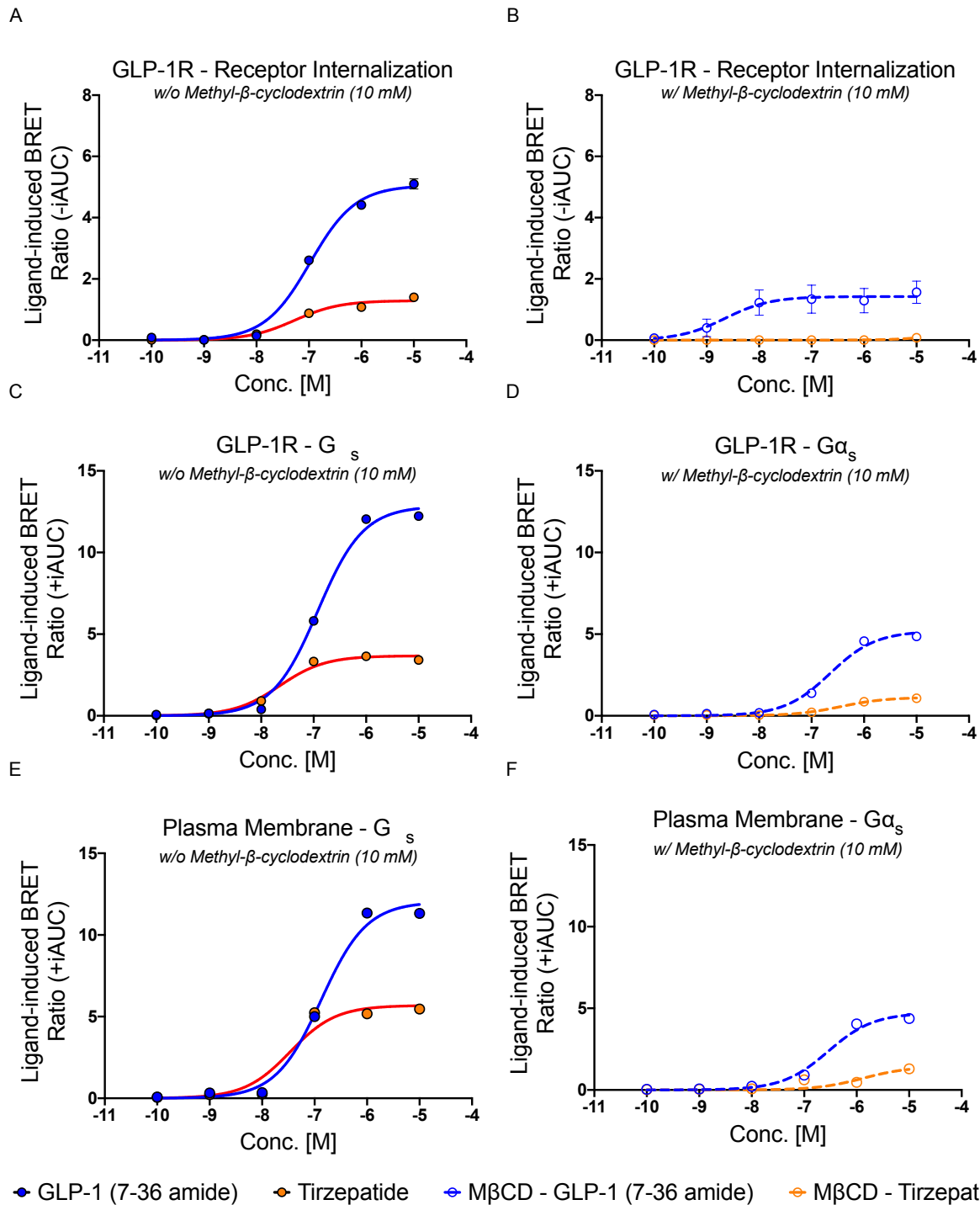


**Figure 27: The influence of GLP-1R receptor inhibition on G $\alpha_s$  recruitment.** Dose-response curves of ligand-induced hGLP-1R-Rluc8 internalization without (A) or with (B) 30 min pretreatment of 10 mM M $\beta$ CD in HEK293T cells to inhibit receptor internalization as measured by dissipation of BRET signal with plasma membrane marker Venus-KRAS. Dose-response curves of ligand-induced miniG $\alpha_s$ -Nluc recruitment to GFP-tagged hGLP-1R without (C) or with (D) 30 min pretreatment of 10 mM M $\beta$ CD. Dose-response curves of ligand-induced miniG $\alpha_s$ -Nluc recruitment to the plasma membrane marker Venus-KRAS without (E) or with (F) 30 min pretreatment of 10 mM M $\beta$ CD. The iAUC representation of vehicle- and baseline-corrected 30 min response to each agonist is expressed as mean  $\pm$  SEM. Three independent experiments were performed with at least two technical replicates per group.

Due to the associative relationship between ligand-stimulated  $G\alpha_s$  recruitment and that of receptor internalization, it was hypothesized that inhibition of GLP-1R internalization may facilitate an equalizing effect on the degree of  $G\alpha_s$  recruitment stimulated by ligands.

Pretreatment of hGLP-1R<sup>+</sup> HEK293T cells with 10mM methyl- $\beta$ -cyclodextrin (M $\beta$ CD), a commonly used caveolin-dependent receptor internalization inhibitor, predominantly inhibited GLP-1R internalization, in which the maximal GLP-1 (7-36 amide)-induced internalization was inhibited by approximately 70% and Tirzepatide-induced internalization was inhibited by 100% (**Figure 27, A-B**).

Subsequently, ligand-induced  $G\alpha_s$  recruitment to the GLP-1R was measured with and without the presence of M $\beta$ CD (**Figure 27, C-D**). Interestingly, the maximal degree of ligand-induced  $G\alpha_s$  recruitment in the presence of M $\beta$ CD by GLP-1 (7-36 amide) and Tirzepatide was also reduced by approximately 60% and 70% to their respective maximal values in the non-M $\beta$ CD control. Notably, no equalizing effect was observed between GLP-1 (7-36 amide) and Tirzepatide within both conditions of M $\beta$ CD pretreatment and without, as the relationship between the agonists retained their proportional differences of approximately 2-2.5 fold. M $\beta$ CD pretreatment depletes membrane-localized cholesterol content, which therefore interrupts the formation of the lipid nanodomains required to confer proper lateral movement of the GPCR across the membrane for optimal signaling and internalization (Kwik et al., 2003; Mahammad and Parmryd, 2015). Therefore, it seems that M $\beta$ CD-mediated cholesterol depletion not only reduces receptor internalization, but also influences ligand potency at the GLP-1R, a finding not only previously demonstrated with cAMP, but now demonstrated at the G-protein level (Buenaventura *et al.*, 2019). Mini $G\alpha_s$ -Nluc proteins are cytosol-localized and translocate to the plasma membrane upon GPCR-ligand interaction (Wan *et al.*, 2018). It may be possible that the reason M $\beta$ CD inhibition of receptor internalization does not create an equalizing effect on  $G\alpha_s$  recruitment between ligands is due to the M $\beta$ CD-mediated lack of GPCR lateral mobility to enter into the signaling hotspots that facilitate direct  $G\alpha_s$  interaction with the GLP-1R (Buenaventura *et al.*, 2019; Buenaventura *et al.*, 2018b; Calebiro and Jobin, 2019). Without the ability of the GPCR to predispose itself to nanodomains of enhanced signaling, these results may simply be reflecting the intrinsic ligand-receptor conformation signaling capacity, and not of the degree of plasma membrane-localized  $G\alpha_s$  that may potentially facilitate a ligand-induced GLP-1R internalization capacity.

Therefore, we next tested if inhibiting receptor internalization with M $\beta$ CD would impact G $\alpha_s$  recruitment to the plasma membrane in its entirety, therefore bypassing the membrane-localized GLP-1R lateral mobility detriment induced by M $\beta$ CD and thus quantifying the degree of global activation at the plasma membrane (Buenaventura *et al.*, 2019). However, upon ligand-induced activation of the GLP-1R, M $\beta$ CD pretreatment once again proportionally decreased the degree of G $\alpha_s$  recruitment by both ligands, however this time to the plasma membrane reflecting global activation in general (**Figure 27, E-F**).

Consequently, this data demonstrates that ligand-stimulated GLP-1R internalization was not decoupled from G $\alpha_s$  recruitment following M $\beta$ CD pretreatment, in that the proportional decrease in receptor internalization elicited by each ligand following internalization inhibitor pretreatment was also mirrored by a proportional decrease in maximal G $\alpha_s$  recruitment. Therefore, here we emphasize the association of ligand-induced G $\alpha_s$  recruitment efficacy in its association with GLP-1R internalization, indicating a potential point of control toward receptor internalization by MAR709 and Tirzepatide.

#### *MAR709 and Tirzepatide Differentially Recruit $\beta$ -arrestin 1/2 to the Plasma Membrane via the GLP-1R, but is Not A Determinant of Receptor Internalization*

The internalization of various GPCRs following ligand binding has been implicated in a number of consequences including resensitization of the GPCR, regulation of cell surface GPCR expression and cellular ligand responsiveness, and an initiation point for the intracellular trafficking and subcellular compartmentalization of the receptor (Ferguson, 2001). GPCR internalization typically revolves around clathrin-mediated or caveolin-mediated endocytosis. Clathrin-mediated endocytosis is initiated following ligand-binding and subsequent clustering of clathrin and AP2 on the inner-leaflet of the plasma membrane. Following ligand-induced GRK phosphorylation of the GPCR C-terminal tail and subsequent  $\beta$ -arrestin 1/2 binding, AP2 facilitates the movement of the plasma membrane-localized GPCR into clathrin coated pits by forming a tripartite connection between clathrin and the  $\beta$ -arrestin bound to the GPCR. Importantly,  $\beta$ -arrestin interaction within the GPCR not only facilitate CME, but also acts as a brake to ligand-induced signaling by sterically inhibiting further G $\alpha_s$  activation. The GLP-1R and GIPR have been evidenced to internalize via clathrin-mediated endocytosis (Ismail *et al.*, 2015; Marzook *et al.*, 2021). Although, GLP-1R endocytosis has also been suggested to internalize via a caveolin-dependent mechanism (Syme *et al.*, 2006). Additionally, GLP-1R has

also been evidenced to recruit both  $\beta$ -arrestin 1 and  $\beta$ -arrestin 2 isoforms (Jorgensen et al., 2005; Marzook *et al.*, 2021; Sonoda *et al.*, 2008). Therefore,  $\beta$ -arrestin is a lucrative aspect of pharmaceutical investigation, as it reflects on both GPCR signaling and receptor internalization. Interestingly, biased ligands that facilitate reduced receptor  $\beta$ -arrestin 1/2 recruitment have demonstrated prolonged signaling and therapeutic action (Gray et al., 2018; Jones *et al.*, 2021).

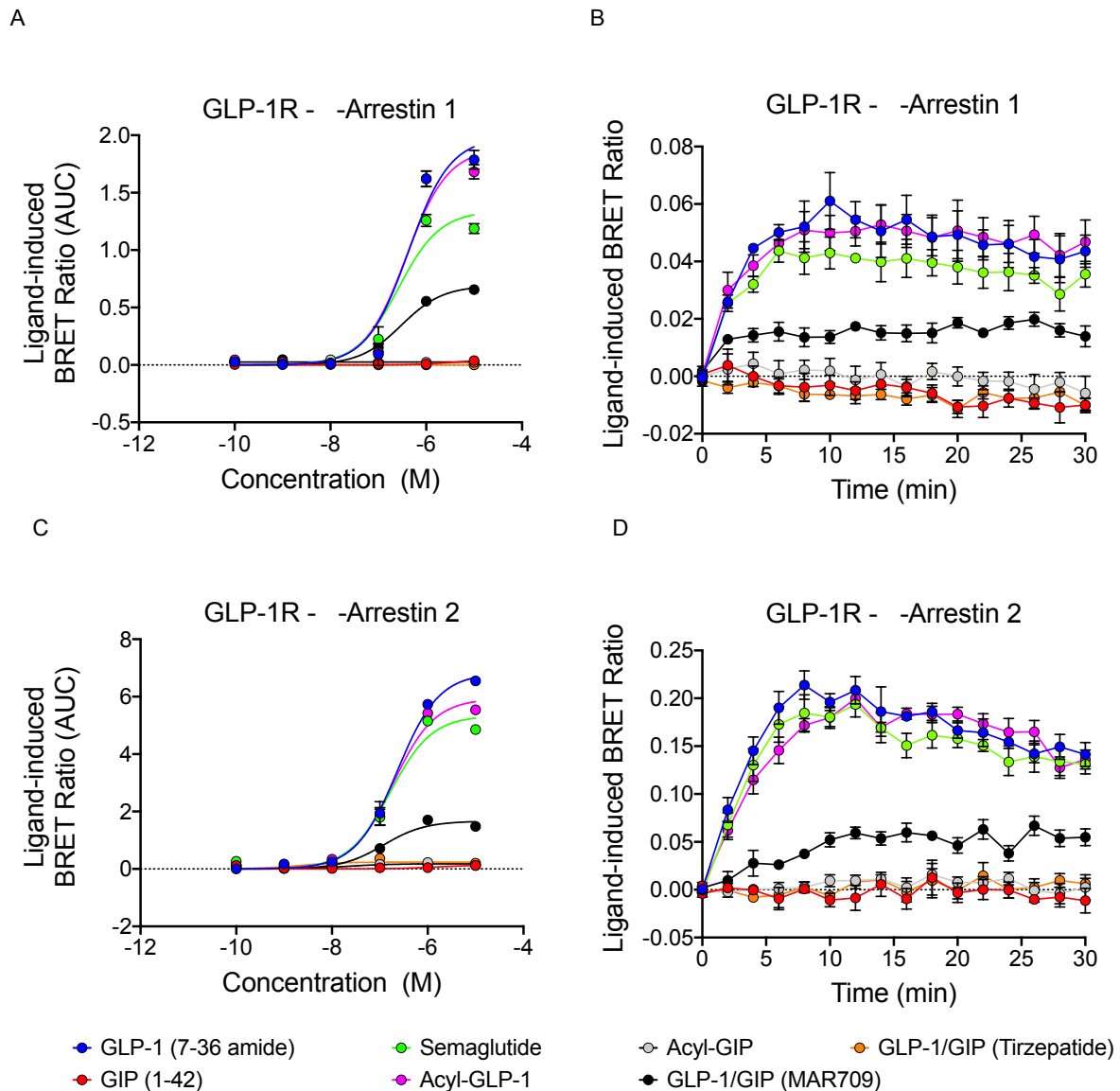


**Figure 28: Ligand-induced  $\beta$ -arrestin 1/2 recruitment to the GLP-1R.** Dose-response curves (A) and temporal resolution (1  $\mu$ M stimulation) (B) of ligand-induced BRET resulting from  $\beta$ arr1-Rluc8 recruitment to the GFP-tagged hGLP-1R. Dose-response curves (C) and temporal resolution (1  $\mu$ M stimulation) (D) of ligand-induced BRET resulting from  $\beta$ arr2-Rluc8 recruitment to the GFP-tagged hGLP-1R. +iAUC representation of vehicle- and baseline-corrected 30 min temporal responses to each agonist is expressed as mean  $\pm$  SEM. Three independent experiments were performed with at least two technical replicates per group. *Figure adapted from Novikoff et al. 2021 (Mol. Met.).*

Therefore, using HEK293T cells co-transfected with hGLP-1R-GFP and either isoform of  $\beta$ -arrestin-Rluc8, we aimed to identify ligand-specific effects on  $\beta$ -arrestin 1/2 recruitment and if differential recruitment may play a role in facilitating enhanced receptor internalization. The GLP-1R mono-agonist Semaglutide stimulated 67% and 78% of the  $\beta$ -arrestin 1 and  $\beta$ -arrestin 2  $E_{max}$  elicited by GLP-1 (7-36 amide), while potency between the two ligands was non-significantly different (**Figure 28, A-D; Table 2**). Acyl-GLP-1, also a mono-agonist for the GLP-1R, did not exhibit a significant difference in  $E_{max}$  to GLP-1 (7-36 amide) for  $\beta$ -arrestin 1, however did show a slight but significant 14% reduction for  $\beta$ -arrestin 2, without any significant differences in potency. Interestingly, the GLP-1/GIP dual-agonist MAR709 stimulated 35% of the  $\beta$ -arrestin 1  $E_{max}$  of GLP-1 (7-36 amide) and just 24% for  $\beta$ -arrestin 2, while Tirzepatide did not exhibit a quantifiable degree of recruitment for either  $\beta$ -arrestin 1 or  $\beta$ -arrestin 2. These results together demonstrate an interesting paradigm, in that despite full agonist profiles for cAMP production between Semaglutide, MAR709, and Tirzepatide at the GLP-1R, all three agonists elicit differential  $\beta$ -arrestin 1/2 recruitment profiles that may be implicative for sustained signaling.

Despite clear ligand-induced  $\beta$ -arrestin 1/2 recruitment at the GLP-1R, questions and debate remain whether GLP-1R co-internalizes with  $\beta$ -arrestin 1/2. Previous literature has demonstrated  $\beta$ -arrestin 2 to not co-internalize with GLP-1R upon ligand administration *in vitro*, as 30 minutes of ligand incubation only resulted in  $\beta$ -arrestin 2 retention at the plasma membrane, without presence in intracellular compartments (Al-Sabah *et al.*, 2014). However, in additional studies, the GLP-1R, upon ligand-stimulation, has been indirectly suggested to co-internalize with  $\beta$ -arrestin 2 in a tissue-specific manner (Nakashima *et al.*, 2018). If indeed the interaction of  $\beta$ -arrestin 2 with the GLP-1R is restrained to the plasma membrane, it is hypothesized that  $\beta$ -arrestin 2 recruitment quantified solely at the GLP-1R may be misleading due to differing extents of ligand-induced receptor internalization by the GLP-1R mono-agonists relative to MAR709 and Tirzepatide. As a consequence, the highly internalizing GLP-1R mono-agonists may be underrepresented in terms of  $\beta$ -arrestin 2 recruitment to the receptor, while the less internalizing, plasma membrane-localized GLP-1R effects of the GLP-1/GIP dual-agonists may be overrepresented. Therefore, to test for discrepancies in  $\beta$ -arrestin recruitment due to spatial localization differences of the GLP-1R following ligand stimulation, GLP-1R-mediated recruitment of  $\beta$ -arrestin 2 was measured as a function of colocalization



with the plasma membrane (Venus-KRAS) and early/late endosomal (Venus-Rab5/Venus-Rab7) compartments.

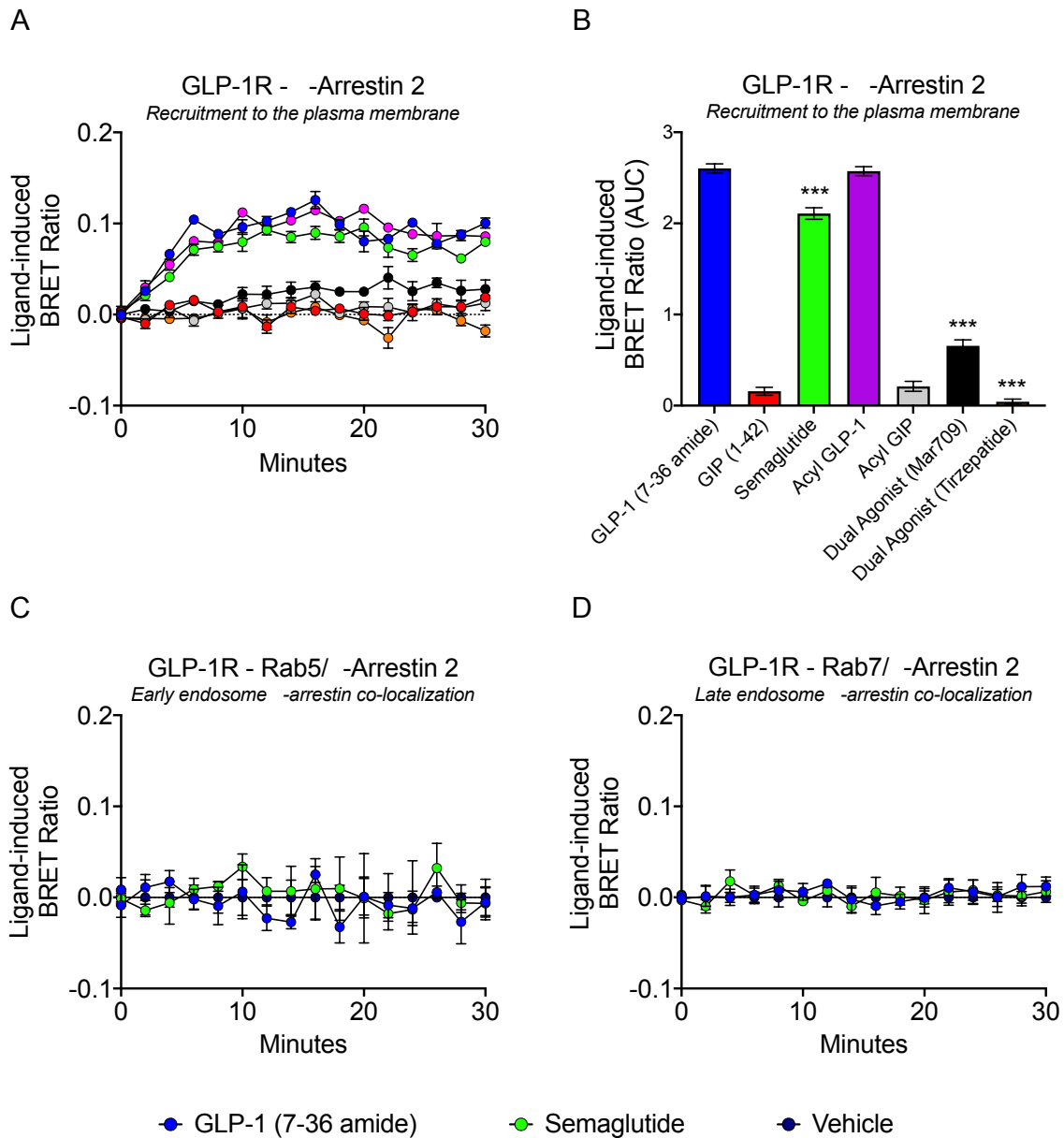


**Figure 29: Ligand-induced  $\beta$ -arrestin 2 recruitment to the plasma membrane and endosomal compartments as mediated by GLP-1R.** Temporal resolution (1  $\mu$ M stimulation) (A) and +iAUC (B) of ligand-induced BRET resulting from  $\beta$ arr2-Rluc8 recruitment to the plasma membrane marker Venus-KRAS as mediated by the untagged hGLP-1R. Temporal resolution (1  $\mu$ M stimulation) of  $\beta$ arr2-Rluc8 recruitment to hGLP-1R<sup>+</sup> Venus-Rab5<sup>+</sup> (C) and Venus-Rab7<sup>+</sup> (D) endosomes. +iAUC representation of vehicle- and baseline-corrected 30 min temporal responses to each agonist is expressed as mean  $\pm$  SEM. Three independent experiments were performed with at least two technical replicates per group.

Utilizing GLP-1R<sup>+</sup> HEK293T cells, 30 minutes of 1  $\mu$ M ligand incubation elicited a GLP-1R-mediated differential recruitment of  $\beta$ -arrestin 2 to the plasma membrane that was highly

reflective of recruitment to the GLP-1R itself (**Figure 29, A-B**). Semaglutide elicited a 20% decrease in  $\beta$ arr2 recruitment to the plasma membrane relative to GLP-1 (7-36 amide), which is reflective of the 22% decrease seen when colocalization between  $\beta$ arr2 and GLP-1R was assessed (**Figure 28, C-D**). There were no clear differences in  $\beta$ arr2 recruitment kinetics between Semaglutide and GLP-1 (7-36 amide) within the assay, nor in comparative aspects between GLP-1R-specific or plasma membrane-specific colocalization kinetics. Similarly, MAR709 elicited just 25% of the plasma membrane  $\beta$ arr2 AUC of GLP-1 (7-36 amide), while Tirzepatide again produced no distinct  $\beta$ arr 2 recruitment. We additionally checked for GLP-1R-mediated entry of  $\beta$ arr2 into Rab5<sup>+</sup> early endosomes and Rab7<sup>+</sup> late endosomes and found no meaningful colocalization of  $\beta$ arr2 within these compartments induced by any agonist (**Figure 29, C-D**). Taken together, these data indicate GLP-1R agonism by Semaglutide, MAR709, and Tirzepatide evoke a significantly reduced  $\beta$ arr2 recruitment response in comparison to GLP-1 (7-36 amide), and that this effect has specifically to do with the ligand-induced activation/conformational status of the GLP-1R and is not mischaracterized by spatiotemporal intracellular compartmentalization of the GLP-1R following ligand activation. Additionally, in this way the GLP-1 receptor is uniquely characterized as a class A type GPCR for  $\beta$ arr recruitment, while also exhibiting structural properties of a class B GPCR.

$\beta$ -arrestin 1/2 recruitment, as mentioned prior, may act to facilitate clathrin-mediated GPCR internalization through a tripartite linkage between the C-terminal tail of the GPCR and the  $\beta$ 2-subunit of the clathrin-bound AP2 at the plasma membrane. Therefore, questions remained whether chemically inhibiting  $\beta$ -arrestin 1/2 action would reduce GLP-1R internalization to a similar degree of that of M $\beta$ CD pretreatment. Barbadin is a small-molecule that has been previously shown to block internalization of the angiotensin-II type-1 receptor (AT1R),  $\beta$ 2AR, and V2R, by directly interfering in the interaction between the C-terminal portion of  $\beta$ -arrestin and the  $\beta$ 2-subunit of AP2 (Beautrait *et al.*, 2017). In this way, barbadin inhibits internalization at a site external to direct contact with the GPCR, thereby not interfering with the activation status of the GPCR as seen with M $\beta$ CD. Inhibition of ligand-induced GLP-1R internalization by barbadin would therefore indicate a critical role of the  $\beta$ -arrestin/AP2 machinery in mediating GLP-1R clathrin-dependent endocytosis, and may connect ligand bias for  $\beta$ -arrestin recruitment to GLP-1R internalization.

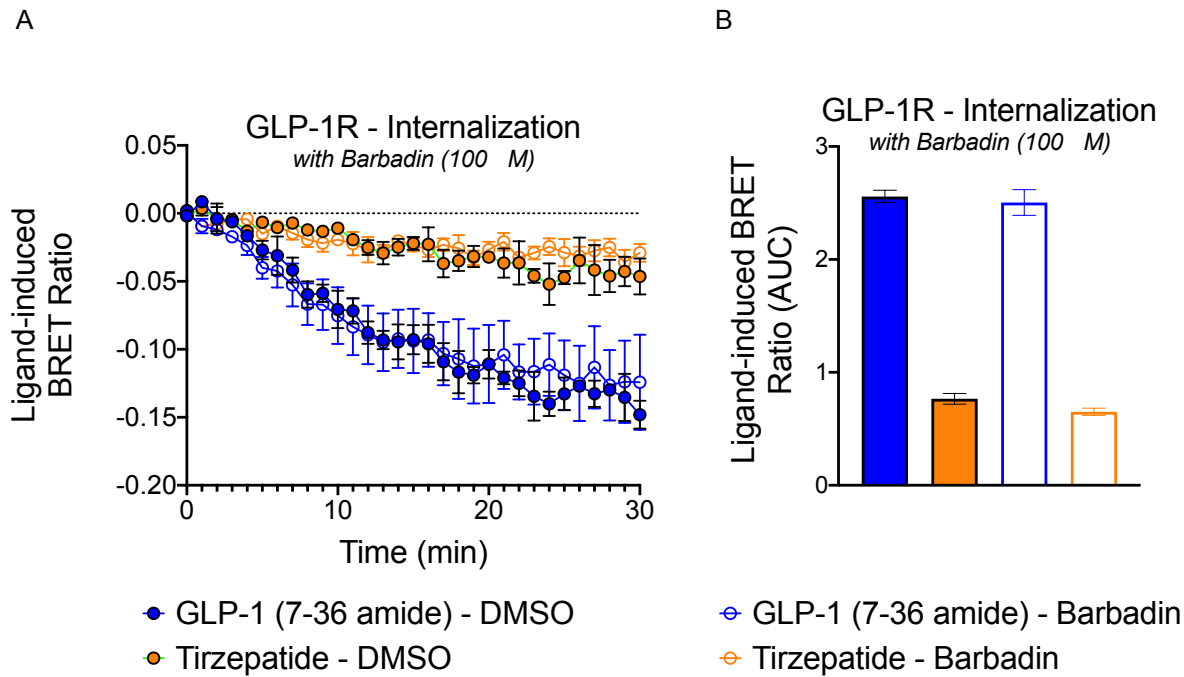


**Figure 30: Ligand-induced GLP-1R internalization within the context of  $\beta$ -arrestin inhibition.** Temporal resolution (1  $\mu$ M stimulation) (A) and -iAUC (B) of loss in BRET signal resulting from hGLP-1R-Rluc8 internalization and movement away from the plasma membrane marker Venus-KRAS within the context of barbadin pretreatment (100  $\mu$ M). -iAUC representation of vehicle- and baseline-corrected 30 min temporal responses to each agonist is expressed as mean  $\pm$  SEM. Three independent experiments were performed with at least two technical replicates per group.

In GLP-1R-Rluc8<sup>+</sup> HEK293T cells, we aimed to identify if the inhibition of the  $\beta$ -arrestin/AP2 interaction affected the degree of ligand-induced GLP-1R internalization by pre-treating cells with barbadin (100 $\mu$ M). The degree of GLP-1R internalization induced by GLP-1 (7-36 amide) was found to be almost identical between conditions of barbadin pretreatment and matched DMSO pretreatment (**Figure 30, A-B**). Similarly, the intrinsic low degree of GLP-1R internalization evoked by Tirzepatide was not differentially altered within conditions of DMSO pretreatment or barbadin pretreatment.

Previous literature has examined the necessity of  $\beta$ -arrestin in mediating GLP-1R internalization. Despite evidence of clathrin-mediated endocytosis of the GLP-1R,  $\beta$ -arrestin isoform deletion by CRISPR-Cas9 yielded no significant differences to the wild-type in terms of ligand-induced receptor internalization (Buenaventura *et al.*, 2019; Jones *et al.*, 2018a). It has been pointed out that within the C-terminal sequence of the GLP-1R is an AP2 binding motif which may facilitate direct binding of AP2 to the GLP-1R C-terminal tail, therefore side-stepping the necessity of  $\beta$ -arrestin recruitment to accumulate the receptor into clathrin-

coated pits for internalization (Buenaventura *et al.*, 2019; Huang *et al.*, 2013). Clathrin-mediated endocytosis of GLP-1R was found to be highly correlated with AP2 colocalization at the plasma membrane (Buenaventura *et al.*, 2019). Due to AP2 inhibition by barbadin, our data suggests that either GLP-1R internalization is independent of direct AP2  $\beta$ -subunit binding to the C-terminal tail of the GLP-1R, or that the established potency of barbadin to inhibit  $\beta$ -arrestin/AP2 interaction is less than the concentration required to inhibit direct binding of the GLP-1R AP2 motif to the AP2  $\beta$ -subunit. It is possible that the  $\mu$ 1 subunit of AP2 facilitates ligand-induced clathrin-mediated GLP-1R internalization (Huang *et al.*, 2013). Taken together, it seems evident that  $\beta$ -arrestin recruitment to the GLP-1R may be more relevant to steric hindrance of  $G\alpha_s$  recruitment rather than clathrin-mediated endocytosis, which uniquely positions MAR709 and Tirzepatide as full agonists for cAMP with minimal signal brake by  $\beta$ arr.

#### *The GIP Receptor Does Not Actively Recruit $\beta$ -arrestin 2 Following Ligand Stimulation*

The GIP receptor, like the GLP-1R, has similarly been demonstrated to undergo clathrin-mediated endocytosis (Syme *et al.*, 2006). Despite the  $\beta$ -arrestin and AP2-centric mechanisms behind clathrin-mediated endocytosis, the ability for GIPR to recruit  $\beta$ -arrestin has been debated. Multiple studies have indicated a distinct lack of  $\beta$ -arrestin 1 and 2 recruitment to the GIPR C-terminal tail following ligand stimulation, including a lack of preceding GRK recruitment and phosphorylation (Al-Sabah *et al.*, 2014; Ismail *et al.*, 2015; Jones *et al.*, 2021). On a similar note, the C-terminal tail of the GIPR has also been shown to be dispensable for GIPR internalization, thus trivializing the role of  $\beta$ -arrestins in GIPR clathrin-mediated endocytosis (Ismail *et al.*, 2015). On the other hand, various studies have demonstrated substantial ligand-induced  $\beta$ arr recruitment to the GIPR, and subsequent modulation on receptor desensitization (Gabe *et al.*, 2018; Willard *et al.*, 2020). To explain these discrepancies between literature, the *in vitro* presence of ligand-induced  $\beta$ -arrestin recruitment to a C-terminal fluorophore-tagged GIPR has been suggested to be a potential artifact. Commonly used linkers that connect the GIPR to a fluorophore for ratiometric quantification, or to extensions for enzymatically-driven colorimetric models, contain potential GRK phosphorylation motifs, which may facilitate artificial  $\beta$ arr recruitment to the synthetic linker (Al-Sabah *et al.*, 2020). In this way, the recruitment of  $\beta$ -arrestin to the GIPR can occur within a synthetic context, and may not reflect endogenous effect. However, we

investigated the effect of ligand-induced  $\beta$ arr2 recruitment at the GIPR, particularly as Tirzepatide has been previously evidenced to act as a full agonist for  $\beta$ arr2 to the GIPR, albeit with a slight shift in potency (Willard *et al.*, 2020).

In GIPR<sup>+</sup> HEK293T cells,  $\beta$ -arrestin 2 recruitment was quantified via the ligand-induced colocalization of  $\beta$ arr2-Rluc8 with hGIPR-GFP. Upon a dose-response analysis of ligand stimulation, MAR709 and Tirzepatide elicited a respective 36% and 35% response in comparison to that of the GIP (1-42)  $E_{\max}$  for  $\beta$ -arrestin 2 (**Figure 31, A; Table 2**). However, considering the poor assay resolution of temporal  $\beta$ -arrestin 2 recruitment to the GIPR and the incomplete dose-response curve fit for MAR709 and Tirzepatide, the differences between GIP (1-42), MAR709, and Tirzepatide are not assessed within the context of significance (**Figure 31, A-B**).

The validity of GIPR-mediated  $\beta$ -arrestin 2 is uncertain, but not disproven. However, the degree of  $\beta$ arr2 recruitment to the GLP-1R and GIPR following stimulation by 1  $\mu$ M of the respective endogenous ligand is largely discrepant, in which GLP-1 (7-36 amide) stimulated approximately 9-fold greater  $\beta$ arr2 recruitment to the GLP-1R relative to GIP (1-42) at the GIPR (**Figure 31, C**). Therefore, we next assessed if the small degree of GIPR-mediated  $\beta$ arr2 recruitment was real, or instead was a residual effect due to artificial GRK phosphorylation sites within the synthetic linker of the GIPR-GFP construct. The linker connecting the GIPR and GFP in this experiment contains serine residues, explicitly serine residues intrinsic to an XbaI restriction site, which have previously been demonstrated to artificially facilitate  $\beta$ -arrestin recruitment to the GIPR (**Figure 31, D**) (Al-Sabah *et al.*, 2020). Substitution of the SR sequence within the XbaI restriction site with the amino acid sequence GG has previously been shown to eliminate  $\beta$ -arrestin recruitment to the GIPR (Al-Sabah *et al.*, 2020). To control for the serine-involved artifact, ligand-induced  $\beta$ arr2-Rluc8 colocalization with the plasma membrane marker Venus-KRAS was measured. The Venus-KRAS construct does not harbor a linker nor serine phosphorylation sites, nor is directly interacting with the GLP-1R therefore, therefore ligand-induced  $\beta$ arr2-Rluc8 colocalization with Venus-KRAS was proposed to allow for an artifact-free indirect measurement of GIPR-mediated  $\beta$ -arrestin recruitment to the plasma membrane. However, ligand-induced GIPR-mediated  $\beta$ arr2 recruitment to the plasma membrane displayed an absolute lack of change in signal indicating a failure of GIPR to stimulate  $\beta$ arr2 colocalization from the cytosol to the plasma membrane (**Figure 31, E**).

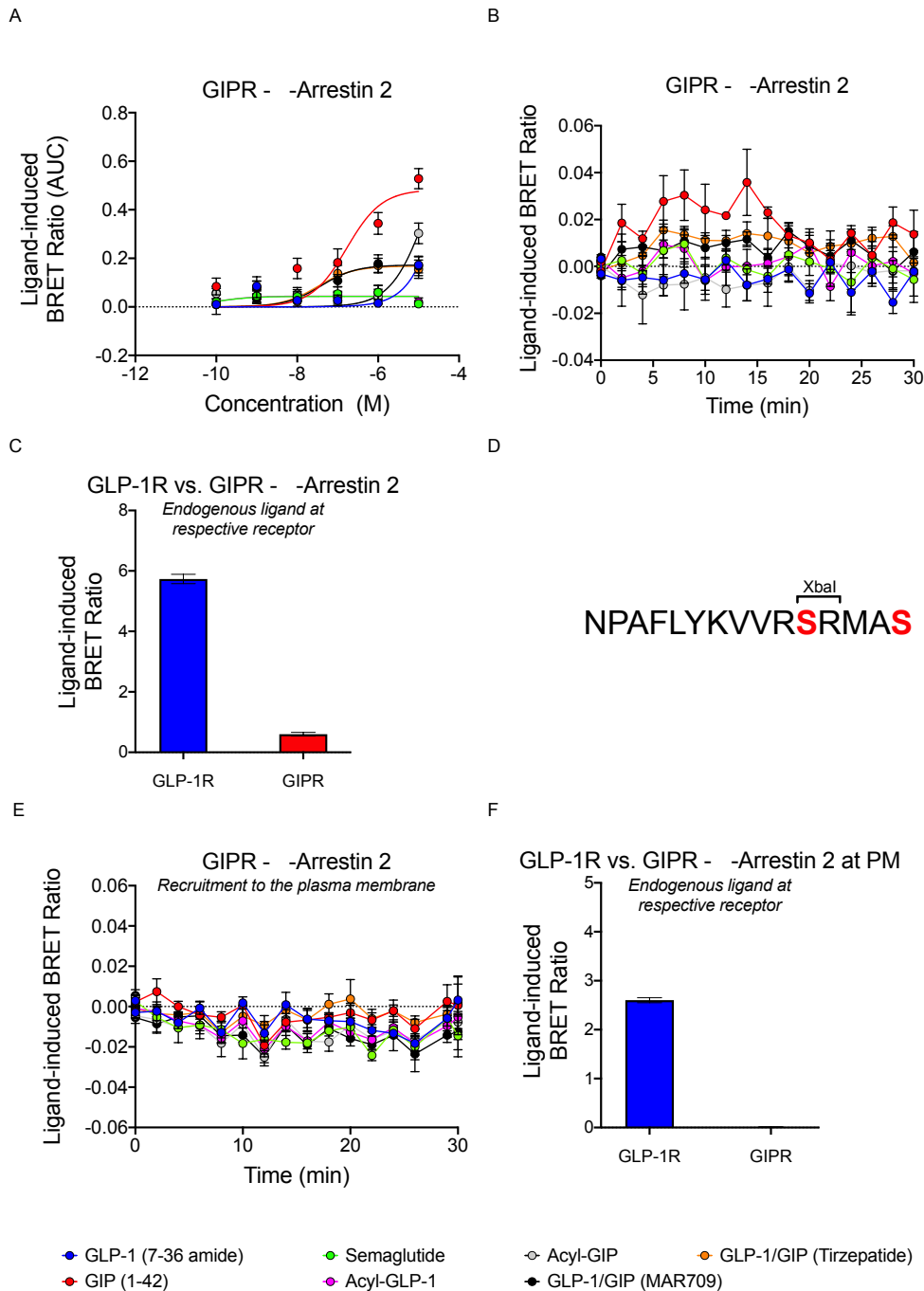


**Figure 31: The presence of  $\beta$ -arrestin recruitment to the GIPR is dependent on assay type.** Dose-response (A) and temporal resolution (1  $\mu$ M) (B) of the ligand-induced  $\beta$ arr2-Rluc8 response as measured by a gain in BRET signal following recruitment to the GFP-tagged hGIPR. Relative difference in the extent of ligand-induced (1  $\mu$ M)  $\beta$ arr2-Rluc8 recruitment to either GFP-tagged hGLP-1R or hGIPR by the respective native ligands GLP-1 (7-36 amide) or GIP (1-42) (C). Amino acid sequence of synthetic linker connecting hGIPR to the GFP fluorophore with serine residues highlighted in bold red (D). Untagged hGIPR-mediated  $\beta$ arr2-Rluc8 colocalization with plasma membrane marker Venus-KRAS following ligand stimulation (1  $\mu$ M) (E).  $\beta$ arr2-Rluc8 colocalization with plasma membrane marker Venus-KRAS as mediated by the untagged endogenous GLP-1R or GIPR sequences following ligand stimulation (1  $\mu$ M) (F). +iAUC representation of vehicle- and baseline-corrected 30 min temporal responses to each agonist is expressed as mean  $\pm$  SEM. Three independent experiments were performed with at least two technical replicates per group. *Figure adapted from Novikoff et al. 2021 (Mol. Met.).*

The previous GLP-1R and GIPR  $\beta$ arr2-Rluc8/Venus-KRAS assays have provided an adequate control for receptor functionality as it utilized an untagged form of either incretin receptor, both of which had been previously validated in cAMP experiments. When comparing 1  $\mu$ M ligand-induced receptor-mediated  $\beta$ arr2 recruitment to the plasma membrane between the GLP-1 and GIP receptor, the untagged endogenous sequence of hGLP-1R facilitated a high degree of  $\beta$ -arrestin recruitment to the plasma membrane while the untagged endogenous sequence of hGIPR failed to recruit any (**Figure 31, F**). Altogether, these data indicate that the GIPR does not effectively recruit  $\beta$ -arrestin upon ligand stimulation. However, new data has indicated that the ligand-induced recruitment of  $\beta$ arr to the GIPR may not fully capture all quantitative elements regarding the relationship of GIPR to  $\beta$ arr. It is possible that ligand-induced changes in  $\beta$ -arrestin conformational status, from inactive to active, regardless of recruitment to the ligand-bound GIPR, may play a functional role and provide another aspect that may help settle the discrepancy between GIPR  $\beta$ -arrestin activity across literature (Jones *et al.*, 2021).

#### *MAR709 and Tirzepatide Induce Weak Partial $G\alpha_q$ Recruitment at the GLP-1R but Strong Partial $G\alpha_q$ Recruitment at the GIPR*

$G\alpha_q$  is a G-protein subunit that has been previously demonstrated to couple with the GLP-1R, however its interaction with the GIPR remains unclear as multiple studies have produced conflicting results (Harris *et al.*, 2021; Jones *et al.*, 2020b; Oduori *et al.*, 2020).  $G\alpha_q$  has a wide range of downstream effectors, which include its canonical action on PLC $\beta$  and non-canonical activity, including activation of PI3K and inhibition of TRPM8 channels (Sánchez-Fernández *et al.*, 2014). In addition to the action of  $G\alpha_q$  on a variety of signaling effectors, it is also known to interact with cytoskeletal components resulting in the recruitment of tubulin to the plasma membrane, with action at filamentous actin (Sánchez-Fernández *et al.*, 2014). The actions of  $G\alpha_q$  with cytoskeletal machinery facilitate the assembly of plasma membrane signaling boundaries by organizing cholesterol, caveolin, and certain glycosphingolipids into the formation of lipid raft caveolae (Simons and Toomre, 2000). In particular, as opposed to  $G\alpha_s$  and  $G\alpha_i$  which target lipids rafts populated with GPI-anchored proteins,  $G\alpha_q$  localizes predominantly to lipid rafts rich in caveolin, which brings into questions the role of  $G\alpha_q$  in facilitating caveolae-dependent internalization of GLP-1R or GIPR (Sánchez-Fernández *et al.*, 2014). Interestingly, inhibition of  $G\alpha_q$  activity, but not  $G\alpha_s$  activity, at the GLP-1R has been

demonstrated to inhibit GLP-1R internalization and reflects a modulating role for  $G\alpha_q$  signaling in the process (Thompson and Kanamarlapudi, 2015). In particular, small-molecule GLP-1R agonists that selectively activate only the  $G\alpha_s$  pathway failed to induce GLP-1R internalization, indicating a potential for ligand bias within the  $G\alpha_q$  pathway to directly modulate the degree of receptor internalization (Thompson and Kanamarlapudi, 2015).

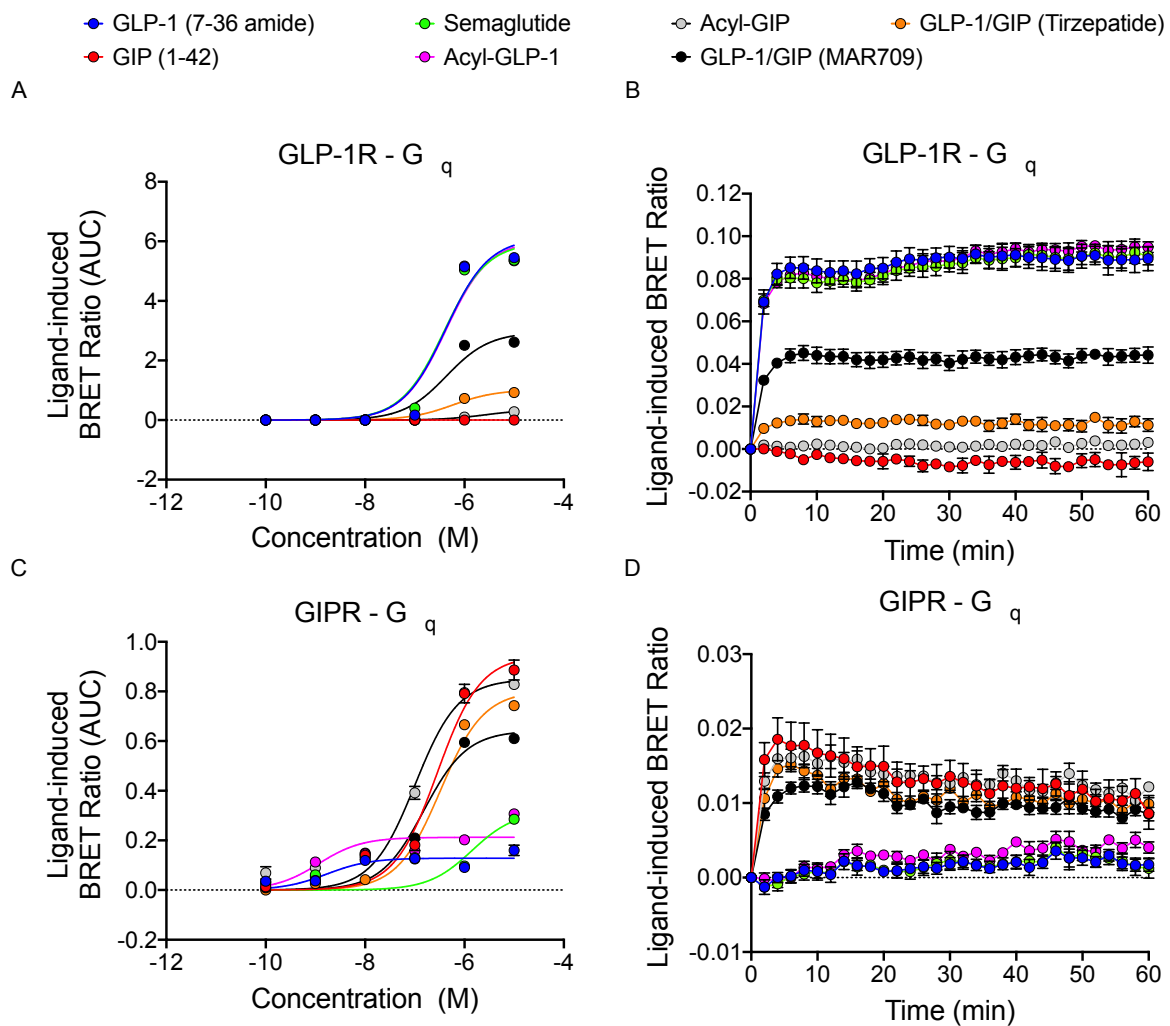


**Figure 32:  $G\alpha_q$  subunit recruitment to the GLP-1R or the GIPR.** Dose-response (A, C) and temporal resolution (1  $\mu$ M) (B, D) for Mini $G\alpha_q$ -Nluc recruitment to the GFP-tagged hGLP-1R or hGIPR. +iAUC representation of vehicle- and baseline-corrected 60 min temporal responses to each agonist is expressed as mean  $\pm$  SEM. Three independent experiments were performed with at least two technical replicates per group. *Figure adapted from Novikoff et al. 2021 (Mol. Met.).*

To understand how GLP-1R and GIPR internalization bias is reflected within  $G\alpha_q$  recruitment, hGLP-1R-GFP<sup>+</sup> or hGIPR-GFP<sup>+</sup> HEK293T cells were examined for ligand-induced mini $G\alpha_q$ -Nluc recruitment in both a dose-dependent and temporal scale. At the GLP-1R, mono-agonists



Semaglutide and Acyl-GLP-1 both stimulated 98% of the  $G\alpha_q$  recruitment  $E_{max}$  relative to GLP-1 (7-36 amide), which reflects the receptor internalization capacity of the respective ligands at the GLP-1R (**Figure 32, A-B; Table 2**). Interestingly, MAR709 and Tirzepatide recruited only 48% and 17% of the GLP-1 (7-36 amide)  $E_{max}$ , which is almost identical to the GLP-1R internalization properties of MAR709 and Tirzepatide (51% and 13%). There were no significant differences in potency between any ligand relevant at the GLP-1R (Table 2). Additionally, there were no fluctuating dynamics in  $G\alpha_q$  recruitment over the course of 60 minutes, therefore the dose-response effect of the GLP-1R relevant agonists was independent of time.

Surprisingly  $G\alpha_q$  recruitment to the GIPR was evident for all GIPR relevant agonists, albeit to a dramatically lesser magnitude than  $G\alpha_q$  to the GLP-1R (**Figure 32, C-D; Table 2**). These data demonstrate the capacity for GIPR to couple to  $G\alpha_q$ , thus contrary to the findings of a majority of studies (Jones *et al.*, 2020b; Oduori *et al.*, 2020). However, it is possible that ligand-induced mini $G\alpha_q$ -Nluc recruitment to the GIPR is an artifact linked to the lack of spatial restraint of the Mini $G\alpha$  constructs. Endogenous  $G\alpha_q$  is housed and membrane-bound specifically in plasma membrane caveolin-rich regions (Oh and Schnitzer, 2001). Indeed, the GIPR is found to internalize via clathrin-dependent endocytosis independently of caveolin (Ismail *et al.*, 2015). Therefore, it is possible that the GIPR does not interact with endogenous  $G\alpha_q$  due to the lack of colocalization of both receptor and  $G\alpha_q$  within plasma membrane caveolin-rich microdomains, while the mini $G\alpha_q$ -Nluc, which is freely localized within the cytosol at baseline, likely does not adhere to the caveolin-defined localization restrictions that endogenous  $G\alpha_q$  has. Nonetheless, it does seem that the ligand-induced conformational rearrangement of the GIPR is open to  $G\alpha_q$  binding regardless if endogenous  $G\alpha_q$  is spatially accessible on the plasma membrane. In that light, Acyl-GIP stimulated 90% of the  $G\alpha_q$  recruitment relative to the GIP (1-42)  $E_{max}$ , while MAR709 and Tirzepatide were significantly reduced in their capacity achieving a 68% and 85% relative response. In accordance with the GIP-centric design of Tirzepatide relative to the balanced design of MAR709, Tirzepatide was more effective in recruiting  $G\alpha_q$  to the GIPR. These results were also independent of time as evidenced by the 1  $\mu$ M ligand temporal response over 60 minutes.

*The Internalized GLP-1R is Primarily Trafficked Through Rab5<sup>+</sup>, Rab7<sup>+</sup>, and Rab11<sup>+</sup> Endosomes*

The endolysosomal system is a connected network of biosynthetic and endocytic vesicle transport, which ultimately facilitates the trafficking and sorting of transmembrane proteins to target compartments (Cullen and Steinberg, 2018). When particular GPCRs, such as the GLP-1R and GIPR, are ligand activated, the GPCRs are first trafficked laterally within the plasma membrane into invaginated microdomains enriched in either clathrin or caveolin. These budded invaginations are then liberated from the plasma membrane via dynamin recruitment and dynamin-mediated scission, thus accomplishing the endocytic process. Within the membrane of the newly liberated endosome are the internalized GPCRs, in which the destination of the GPCR is influenced by the unique properties of the ligand and receptor interaction (Rosciiglione *et al.*, 2014; Sutkeviciute and Vilardaga, 2020). The intracellular compartmental destination of ligand-induced GPCR trafficking can have profound impacts on cellular functionality, which includes facilitating cellular ligand desensitization via targeting of the GPCR to terminal lysosomal pathways, or cellular resensitization through ligand dissociation and GPCR recycling.

It is not only endosomal transport of the receptor that can modulate global responses within a cell, but also the presence of GPCR-mediated signaling localized within the internalized compartment. In terms of GPCR signaling, G $\alpha_s$  signaling is initiated at the plasma membrane and induces a first transient wave of global cAMP production, which is then followed by a lower but more sustained second wave of cAMP originating from endosomal G $\alpha_s$  action as mediated by the GPCR (Girada *et al.*, 2017). The dynamics of ligand-induced spatial and temporal localization of the endosomal GPCR signaling complex facilitates a phosphoproteomic response unique to the respective ligand interaction at the single receptor (Tsvetanova *et al.*, 2021). The unique pharmacological responses of these ligands toward receptor trafficking and intracellular compartmentalized signaling may have physiological relevance in clinical models.

In order to first better understand how the effect of GLP-1R and GIPR biased signaling affects receptor trafficking and endosomal signaling, an initial identificatory screen evaluating the presence of GLP-1R colocalization at a number of endosomal sites was performed (**Figure 33, A-H**), followed by a more in-depth temporal analysis of ligand-specific endosomal trafficking and signaling at selected sites.

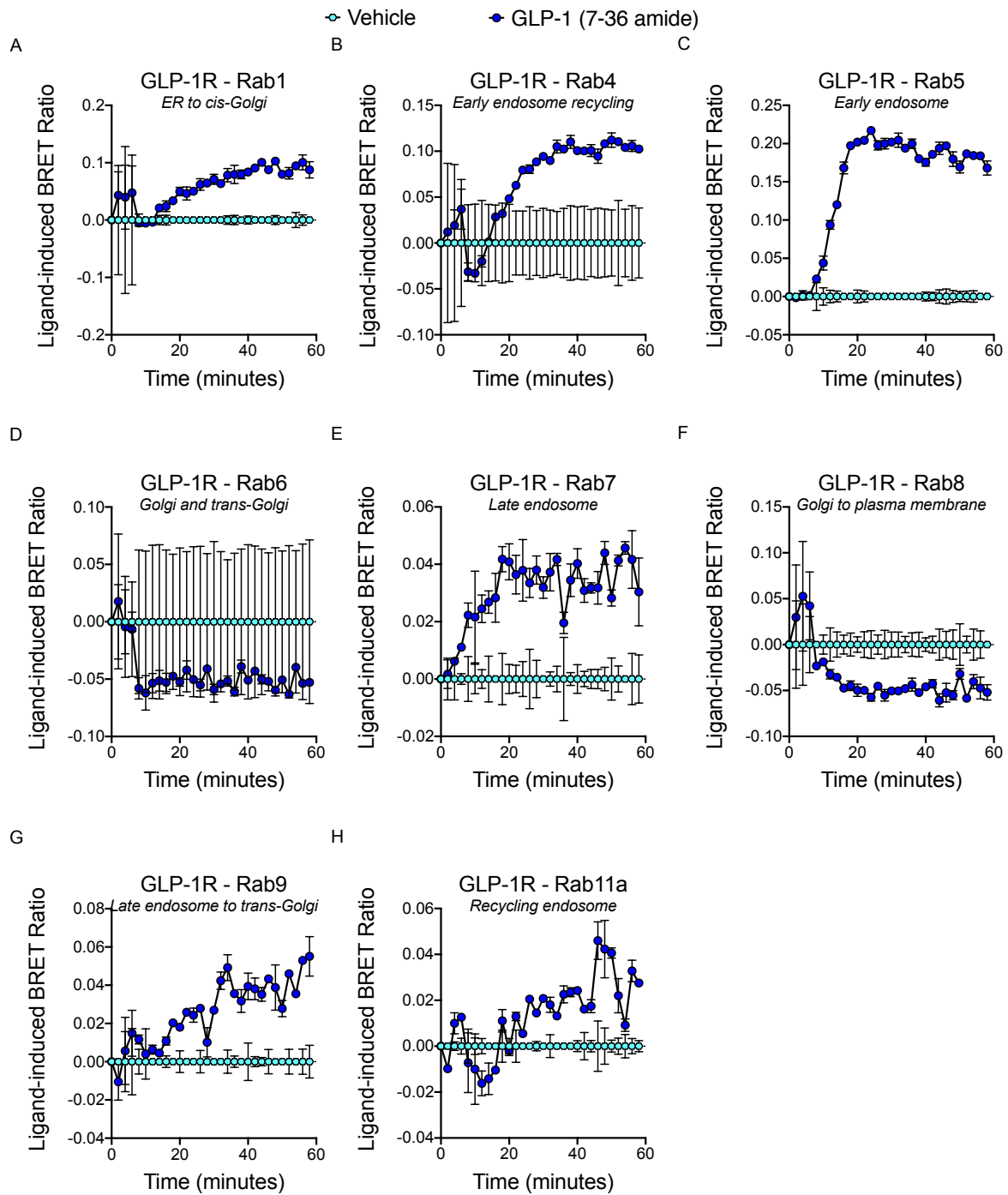


**Figure 33: Screen of ligand-induced hGLP-1R colocalization into various endolysosomal/biosynthetic pathways.** Temporal resolution of hGLP-1R-Rluc8 colocalization into Venus-tagged Rab1 (A), Rab4 (B), Rab 5 (C), Rab6 (D), Rab7 (E), Rab8 (F), Rab9 (G), Rab11a (H) -positive endosomal compartments following GLP-1 (7-36 amide) stimulation (1  $\mu$ M) over the course of 60 minutes. Three independent experiments were performed with at least two technical replicates per group.

In order to better understand spatiotemporal GLP-1R trafficking profile, hGLP-1R-Rluc8<sup>+</sup> HEK293T cells were screened for a preliminary assessment of potential intracellular

destinations in which the GLP-1R might be trafficked following 1  $\mu$ M GLP-1 (7-36 amide) ligand-induced internalization (**Figure 33, A-H**). This assessment was measured via the colocalization of GLP-1R-Rluc8 with various fluorescent endosomal Rab proteins and markers for intracellular organelles. Of particular relevance to the endocytic pathway, Rab4 (early endosome recycling), Rab5 (early endosomes), Rab7 (late endosomes), and Rab11 (recycling endosomes) all demonstrated substantial coherent signals. This finding indicates that the GLP-1R, following agonism by its endogenous ligand and internalization, is networked first into Rab5 endosomes and then distributed out into Rab4, Rab7, and Rab11-positive endosomes. This reflects a primary trafficking pattern of early endosomal incorporation of the GLP-1R upon agonism, which is then subsequently trafficked into degradation and recycling pathways. Substantial GLP-1R colocalization within Rab9<sup>+</sup> endosomes was demonstrated, indicating a divergent movement of the subgroup of receptor localized within the Rab7<sup>+</sup> late endosomal pathway towards the trans-Golgi. However, Rab9 among many other roles, has been also associated with lysosomal biogenesis, indicating the movement of the receptor may also indicate terminal degradation (Kucera et al., 2016). Rab1, which is associated with biosynthetic endosomal transport from the endoplasmic reticulum to the cis-Golgi network, was interestingly shown to strongly co-localize with GLP-1R following ligand stimulation (Saraste, 2016). These preliminary results suggest that ligand-induced activation of the GLP-1R at the plasma membrane somehow mediates an enhanced translocation of GLP-1R from the ER to the Golgi, indicating a paradigm of enhanced biosynthetic endosomal transport at the moment of ligand stimulation. Surprisingly, no study has investigated this further, and as this was outside the scope of the current study, was not further investigated.

Rab5, Rab7, and Rab11 are reflective of the primary dogmas of endocytic trafficking, that being receptor entry, degradation, and recycling (**Figure 34**). Therefore, we set out to identify how biased agonism at the GLP-1R or GIPR can influence receptor trafficking, and ultimately that of receptor degradation and resensitization through late endosomal and recycling endosomal transport. In addition to the trafficking profile of a ligand at a particular endosomal step, we simultaneously investigated the presence of continued GLP-1R or GIPR signaling within the endosomal compartment. Thereby, both receptor trafficking and the activation status of the respective receptor within the endosome were analyzed.

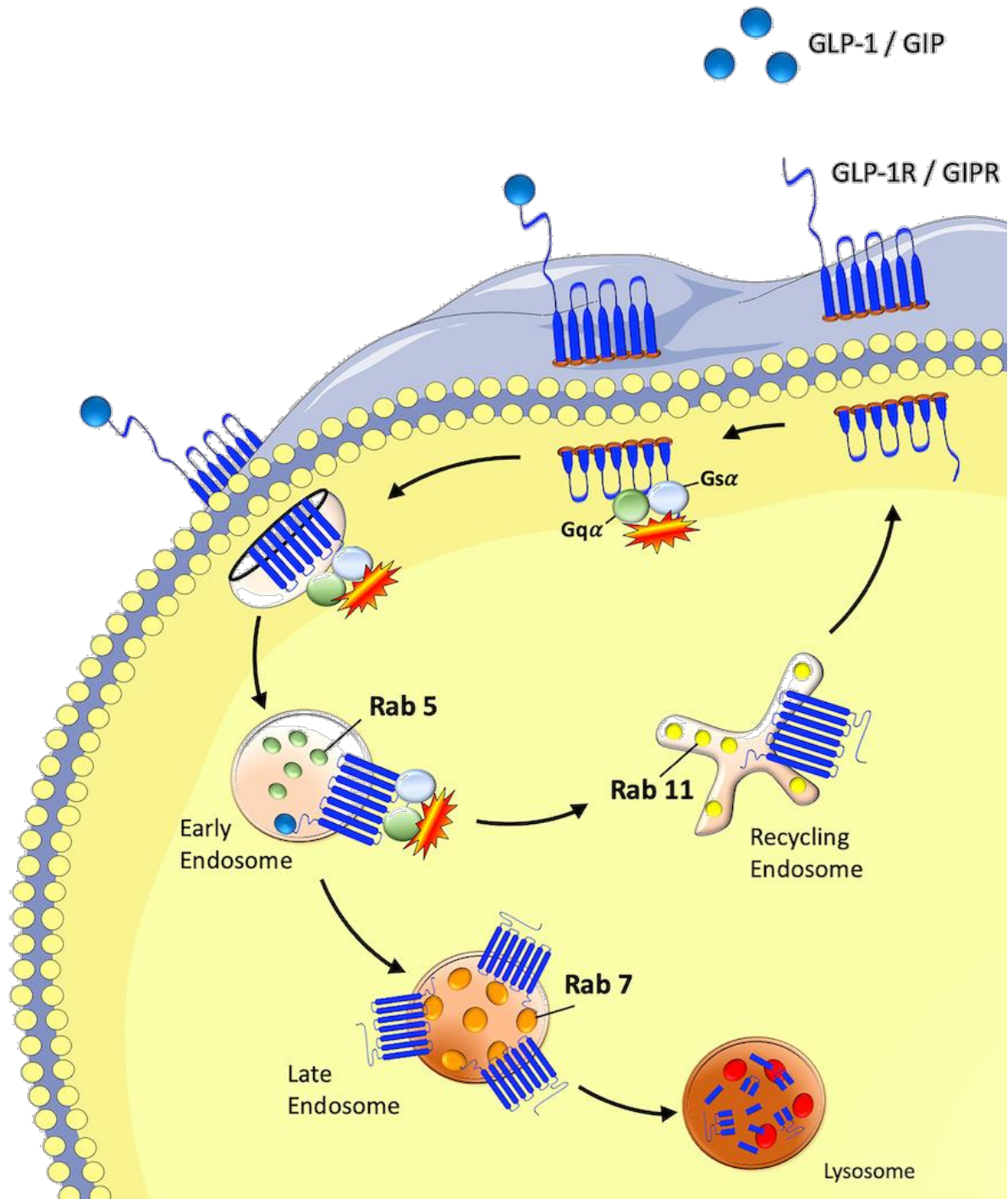


**Figure 34: Schematic of GLP-1R G $\alpha$  subunit signaling and subsequent endosomal trafficking.**  
*Figure adapted from Novikoff et al. 2021 (Mol. Met.).*

*Rab5-associated Endosomal GLP-1R and GIPR Trafficking and Signaling are Uniquely Modulated by MAR709 and Tirzepatide*

We evaluated the endosomal trafficking and signaling of ligand-receptor complexes by respectively assessing the colocalization of hGLP-1R-Rluc8 or MiniG $\alpha_s$ -Nluc (as mediated by hGLP-1R) with Venus-tagged endosomal markers in HEK293T cells and Min6 cells. Consistent with the evidenced reduction in GLP-1R internalization by the dual-agonists, MAR709 and Tirzepatide stimulated 68% and 13% of the total GLP-1R Rab5 colocalization elicited by GLP-1 (7-36 amide) following 60 minutes of agonist incubation (**Figure 35, A-C**). Semaglutide and Acyl-GLP-1 both similarly elicited hGLP-1R colocalization with Rab5<sup>+</sup> endosomes to that of GLP-1 (7-36 amide), with a 92% and 102% relative capacity. The signal for all GLP-1R relevant agonists plateaued within 20-30 minutes, indicating the observation to be independent of time. We next assessed if these receptor trafficking results in HEK293T cells were reflected in a mouse-specific  $\beta$ -cell Min6 cell line transfected with hGLP-1R-Rluc8. In Min6 cells, surprisingly, MAR709 was non-significantly different than GLP-1 (7-36 amide), Semaglutide, and Acyl-GLP-1 in eliciting GLP-1R colocalization with the early endosome marker Venus-Rab5 (**Figure 35, D-F**). This finding is opposed to the MAR709 GLP-1R internalization and Rab5 colocalization dynamics identified within HEK293T cells, and the GLP-1R internalization dynamics observed previously in  $\beta$ -cell Min6 cells (**Figure 23, A-C**). Tirzepatide-induced GLP-1R Rab5 colocalization maintained similar affect across both models demonstrating a 69% reduction in colocalization relative to GLP-1 (7-36 amide) within the  $\beta$ -cell Min6 cell line, an effect that was synonymous with its reduction in GLP-1 receptor internalization found in both HEK293T and Min6 cells. Therefore, ligand-induced GLP-1R Rab5 colocalization between HEK293T and Min6 cells was relatively preserved, except for the Min6-specific case of MAR709 which elicited a comparable degree of Rab5 colocalization to the GLP-1R mono-agonists despite having a lower Min6-specific GLP-1R internalization profile.

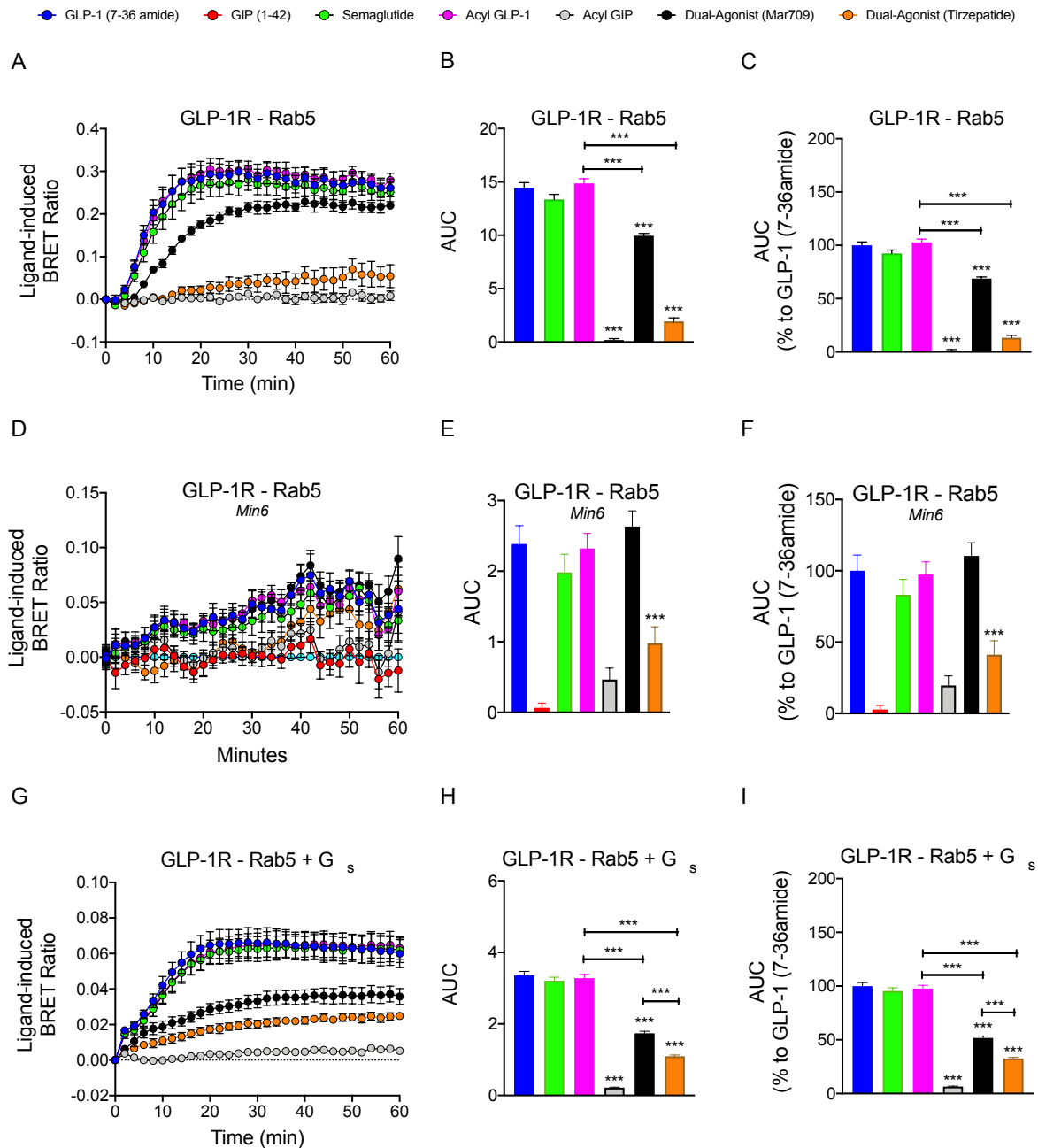


**Figure 35: GLP-1R colocalization and signaling within Rab5<sup>+</sup> early endosomes.** Temporal resolution, +iAUC, and % +iAUC normalized to GLP-1 (7-36 amide), of ligand-induced (1  $\mu$ M) hGLP-1R-Rluc8 colocalization into Venus-Rab5<sup>+</sup> endosomes in HEK293T (A-C) and Min6 (D-F) cell lines. MiniG $\alpha_s$  recruitment to Venus-Rab5<sup>+</sup> endosomes as mediated by the untagged hGLP-1R (G-I). The +iAUC representation of vehicle- and baseline-corrected 60 min response to each agonist is expressed as mean  $\pm$  SEM. Bonferroni's test, \*p < 0.05, \*\*p < 0.005, and \*\*\*p < 0.0005 using one-way ANOVA vs GLP-1 (7-36 amide), Semaglutide, and Acyl-GLP-1. Three independent experiments were performed with at least two technical replicates per group. *Figure adapted from Novikoff et al. 2021 (Mol. Met.).*

Despite ligand-dependent differences in both GLP-1R internalization and Rab5 colocalization, ligand-induced G $\alpha_s$  recruitment to the GLP-1R within Rab5<sup>+</sup> endosomes was assessed as a proxy for activated receptors localized within the early endosomal compartment in HEK293T

cells (**Figure 35, G-I**). Both GLP-1R mono-agonists Semaglutide and Acyl-GLP-1 had an almost identical capacity to recruit  $G\alpha_s$  into GLP-1R<sup>+</sup> Rab5<sup>+</sup> early endosomes relative to GLP-1 (7-36 amide), indicating that the endosome-localized receptor population was similarly sustained in its active conformation across all three GLP-1R mono-agonists. Interestingly, the stimulation of  $G\alpha_s$  recruitment to GLP-1R<sup>+</sup> Rab5<sup>+</sup> early endosomes by MAR709 and Tirzepatide reflected their ability to co-localize GLP-1R into Rab5<sup>+</sup> endosomes, achieving 51% and 32% of the GLP-1 (7-36 amide) endosomal  $G\alpha_s$  recruitment response. As the comparative hierarchical rankings between mono-agonists and dual-agonists persisted between GLP-1R Rab5 colocalization and GLP-1R-mediated Rab5<sup>+</sup> endosomal  $G\alpha_s$  signaling in HEK293T cells, it is suggested that, in comparison to the GLP-1R mono-agonists, the reduced  $G\alpha_s$  recruitment to the early endosomes by MAR709 and Tirzepatide is mediated by a reduction in GLP-1R population density at the endosome, and therefore is not simply an effect of greater ligand-dissociation following receptor incorporation into the early endosome.

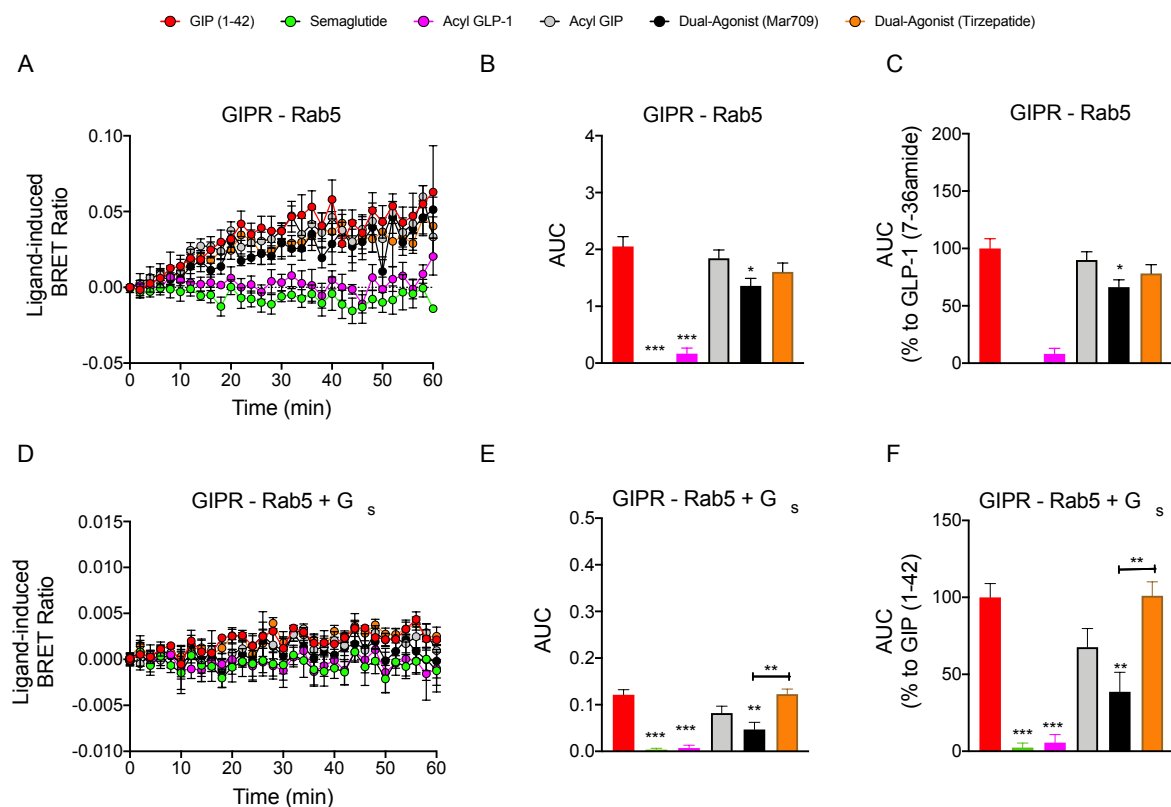


**Figure 36: GIPR colocalization and signaling within Rab5<sup>+</sup> early endosomes.** Temporal resolution, +iAUC, and % +iAUC normalized to GIP (1-42), of ligand-induced (1  $\mu$ M) hGIPR-Rluc8 colocalization into Venus-Rab5<sup>+</sup> endosomes in HEK293T cells (A-C). Mini $G\alpha_s$  recruitment to Venus-Rab5<sup>+</sup> endosomes as mediated by the untagged hGIPR (D-F). The +iAUC representation of vehicle- and baseline-corrected 60 min response to each agonist is expressed as mean  $\pm$  SEM. Bonferroni's test, \* $p$  < 0.05, \*\* $p$  < 0.005, and \*\*\* $p$  < 0.0005 using one-way ANOVA vs GIP (1-42) and Acyl-GIP. Three independent experiments were performed



with at least two technical replicates per group. *Figure adapted from Novikoff et al. 2021 (Mol. Met.).*

Next evaluated within HEK293T cells was ligand-induced hGIPR-Rluc8 colocalization into Rab5<sup>+</sup> endosomes following endocytosis, and the paralleled measurement of MiniG $\alpha_s$ -Nluc endosomal recruitment (as mediated by hGIPR). GIP (1-42) and Acyl-GIP similarly induced GIPR Rab5<sup>+</sup> colocalization, while MAR709 and Tirzepatide were demonstrated to elicit a 66% and 78% response relative to GIP (1-42) (**Figure 36, A-C**). Despite the magnitude of GIPR-mediated recruitment of G $\alpha_s$  to Rab5<sup>+</sup> endosomes being minimal, it however remained reflective to the GIPR Rab5 colocalization results (**Figure 36, D-F**). In general, there does not seem to be the same extent of Rab5<sup>+</sup> endosomal signaling seen with the GIPR as there is with the GLP-1R. This discrepancy between GLP-1R and GIPR endosomal signaling could be indicative of differential receptor internalization rates, GIPR-specific ligand dissociation rates within the early endosomes, a ligand-bound GIPR conformational change within the endosome that does not facilitate enhanced continued signaling, or structural compartmentalization of the GIPR within the endosome that precludes it from continued G-protein recruitment.

#### *Differential GLP-1R Endosomal Colocalization and Signaling Within Rab7<sup>+</sup> Endosomes By MAR709 and Tirzepatide, but Not at the GIPR*

Receptor entry into the late endosomal pathway is canonically associated with a step toward lysosomal trafficking and degradation. Using hGLP-1R-Rluc8<sup>+</sup> HEK293T cells co-expressing Venus-Rab7, incorporation of GLP-1R into the late endosomal pathway was assessed. Both GLP-1R mono-agonists Semaglutide and Acyl-GLP-1 were evidenced to be non-significantly different from GLP-1 (7-36 amide) in stimulating GLP-1R translocation into Rab7<sup>+</sup> endosomes (**Figure 37, A-C**). In accordance with the previous reductions in Rab5<sup>+</sup> endosome GLP-1R colocalization stimulated by MAR709 and Tirzepatide, both dual-agonists elicited 62% and 24% of GLP-1R colocalization into Rab7<sup>+</sup> endosomes relative to GLP-1 (7-36 amide), respectively. This data was not however recapitulated within the hGLP-1R-Rluc8<sup>+</sup> Min6 cell model in which no significant differences in GLP-1R Rab7<sup>+</sup> endosome colocalization between any agonists were found (**Figure 37, D-E**). This absence of signal in Min6 cells is viewed as a lack of coherent and robust temporal resolution, indicating either: a technological limitation of the system that requires unknown optimization, biological limitation in overexpression of

certain Rab endosomal compartment within Min6 cell lines, or simply a lack of signal due to a lack of trafficking of the GLP-1R into Rab7 endosomal compartments within Min6 cells. However, GLP-1R has been previously evidenced to co-localize with Rab7<sup>+</sup> endosomes, albeit to a low degree, in mouse pancreatic islets (Nakashima *et al.*, 2018).

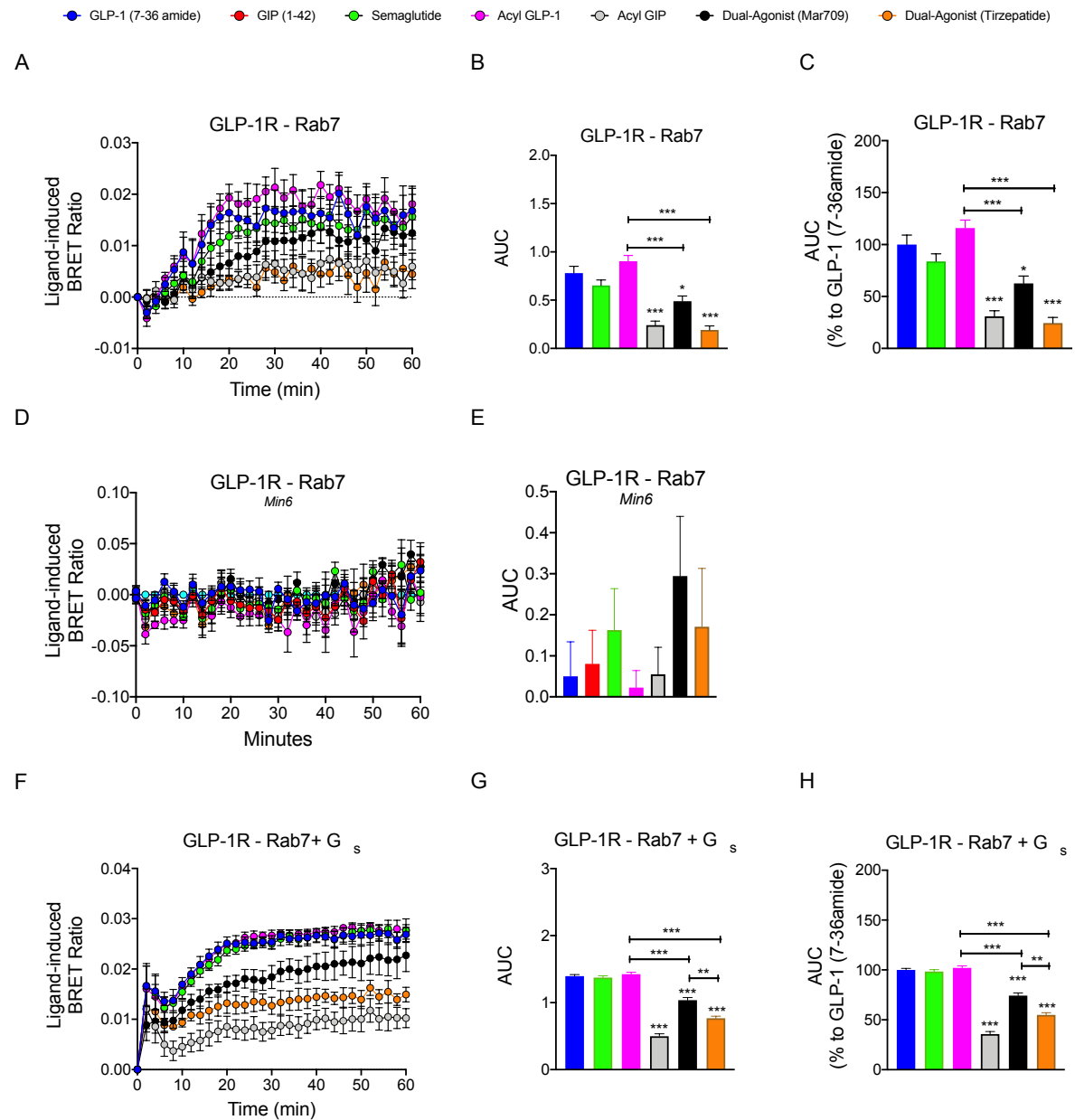


**Figure 37: GLP-1R colocalization and signaling within Rab7<sup>+</sup> late endosomes.** Temporal resolution, +iAUC, and % +iAUC normalized to GLP-1 (7-36 amide), of ligand-induced (1  $\mu$ M) hGLP-1R-Rluc8 colocalization into Venus-Rab7<sup>+</sup> endosomes in HEK293T (A-C) and Min6 (D-E) cell lines. MiniG $\alpha_s$  recruitment to Venus-Rab7<sup>+</sup> endosomes as mediated by the untagged hGLP-1R (F-H). The +iAUC representation of vehicle- and baseline-corrected 60 min response to each agonist is expressed as mean  $\pm$  SEM. Bonferroni's test, \* $p < 0.05$ , \*\* $p < 0.005$ , and \*\*\* $p < 0.0005$  using one-way ANOVA vs GLP-1 (7-36 amide), Semaglutide, and Acyl-GLP-1. Three independent experiments were performed with at least two technical replicates per group. *Figure adapted from Novikoff et al. 2021 (Mol. Met.).*

GPCR-mediated recruitment of  $G\alpha_s$  to Rab7<sup>+</sup> endosomes has not yet been identified as a phenomenon to naturally occur, however the Rab7 endosomal compartment itself is known to play a role in various alternative signaling cascades (Calebiro *et al.*, 2009; Flinn and Backer, 2010). Nonetheless GLP-1R-mediated Rab7<sup>+</sup> endosomal Mini $G\alpha_s$  recruitment was assessed as a function of endosomal signaling. GLP-1 (7-36 amide), Semaglutide, and Acyl-GLP-1 all produced substantial and comparably maximal Mini $G\alpha_s$  recruitment to GLP-1R<sup>+</sup> Rab7<sup>+</sup> endosomes (**Figure 37, F-H**). Relative to GLP-1 (7-36 amide), MAR709 and Tirzepatide elicited 74% and 54% of the endosomal  $G\alpha_s$  signal, indicating a retention of the partial signaling profile carried over from Rab5<sup>+</sup> endosomes. In order for the GLP-1 receptor to be open to  $G\alpha_s$  binding within the endosomal compartment, a correct ligand-bound conformational rearrangement of the receptor is needed. These results indicate that the respective ligands are still bound to the GLP-1R in Rab7<sup>+</sup> endosomes and elicit a ligand-specific conformation of the receptor to facilitate accessibility for Mini $G\alpha_s$  binding. However, these results while coherent, may be not reflect true signaling biology due to the artifact of the non-membrane bound nature of the Mini $G\alpha_s$  construct. Despite the ligand-bound open conformation of the receptor, it is not clearly understood if membrane-bound endogenous  $G\alpha_s$  is capable of localizing from Rab5<sup>+</sup> endosomes to Rab7<sup>+</sup> endosomes, as shown in previous literature (Calebiro *et al.*, 2009). Therefore, it is possible that the non-spatially restricted nature of cytosol-localized Mini $G\alpha_s$  proteins allows for binding to the ligand-induced open conformation of the GLP-1R within Rab7<sup>+</sup> endosomes, which would not be normally reachable by membrane-bound endogenous  $G\alpha_s$  subunits. Further, it is likely that the reduced Mini $G\alpha_s$  recruitment stimulated by MAR709 and Tirzepatide is due to a reduction in GLP-1R population within the Rab7<sup>+</sup> endosomes, as is reflected by similar findings with reduced GLP-1R internalization and Rab5<sup>+</sup>/ Rab7<sup>+</sup> GLP-1R colocalization, rather than by an enhanced ligand dissociation rate of MAR709 and Tirzepatide.

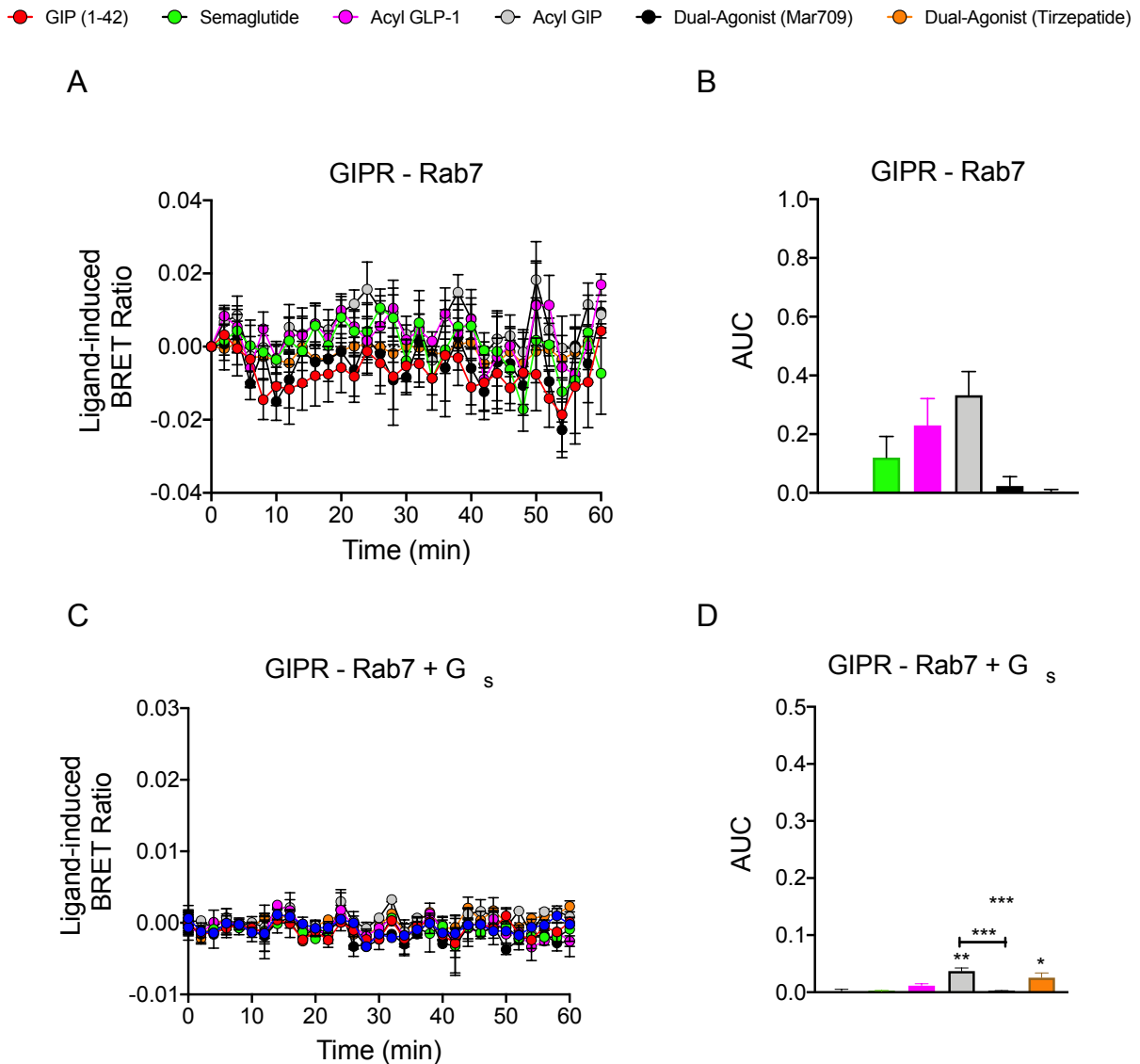


**Figure 38: GIPR colocalization and signaling within Rab7<sup>+</sup> late endosomes.** Temporal resolution and +iAUC of ligand-induced (1  $\mu$ M) hGIPR-Rluc8 colocalization into Venus-Rab7<sup>+</sup> endosomes in HEK293T cells (A-B). MiniG $\alpha_s$  recruitment to Venus-Rab7<sup>+</sup> endosomes as mediated by the untagged hGIPR (C-D). The +iAUC representation of vehicle- and baseline-corrected 60 min response to each agonist is expressed as mean  $\pm$  SEM. Bonferroni's test, \*p < 0.05, \*\*p < 0.005, and \*\*\*p < 0.0005 using one-way ANOVA vs GIP (1-42) and Acyl-GIP. Three independent experiments were performed with at least two technical replicates per group. *Figure adapted from Novikoff et al. 2021 (Mol. Met.).*

Similarly, ligand-induced GIPR-Rluc8 colocalization and GIPR-mediated endosomal G $\alpha_s$  recruitment were assessed at Rab7<sup>+</sup> endosomes. However, low to absent ligand-induced colocalization of GIPR into Rab7<sup>+</sup> endosomes with GIP (1-42) incubation indicated that upon stimulation with the endogenous ligand, Rab7<sup>+</sup> endosomes do not seem to be a primary destination for the GIPR (**Figure 38, A-B**). In line with this, GIPR-mediated MiniG $\alpha_s$  recruitment to the Rab7<sup>+</sup> endosomes was absent upon stimulation with the endogenous ligand GIP (1-42)

(Figure 38, C-D). In accordance with its relatively low degree of internalization and Rab5<sup>+</sup> endosome colocalization, it seems that GIPR intracellular trafficking is limited within the regard of Rab-based endosomal sorting.

#### *MAR709 and Tirzepatide Direct Less Terminal Lysosomal Colocalization of the GLP-1R*

The Rab7 late endosome pathway is associated with the transfer of cargo protein to terminal lysosomes, in which the cargo is then degraded through a mixture of acidification and proteases. As the GLP-1R was demonstrated to clearly co-localize into Rab7<sup>+</sup> endosomes, it was then next assessed if there was any deviation between agonists within the process of Rab7<sup>+</sup> endosome maturation into terminal lysosomes. An influencing factor to this result may be based on the number of endosomal pathways that potentially branch out from Rab7<sup>+</sup> endosomes towards a variety of intracellular destinations, including the trans-Golgi Network (Guerra and Bucci, 2016).

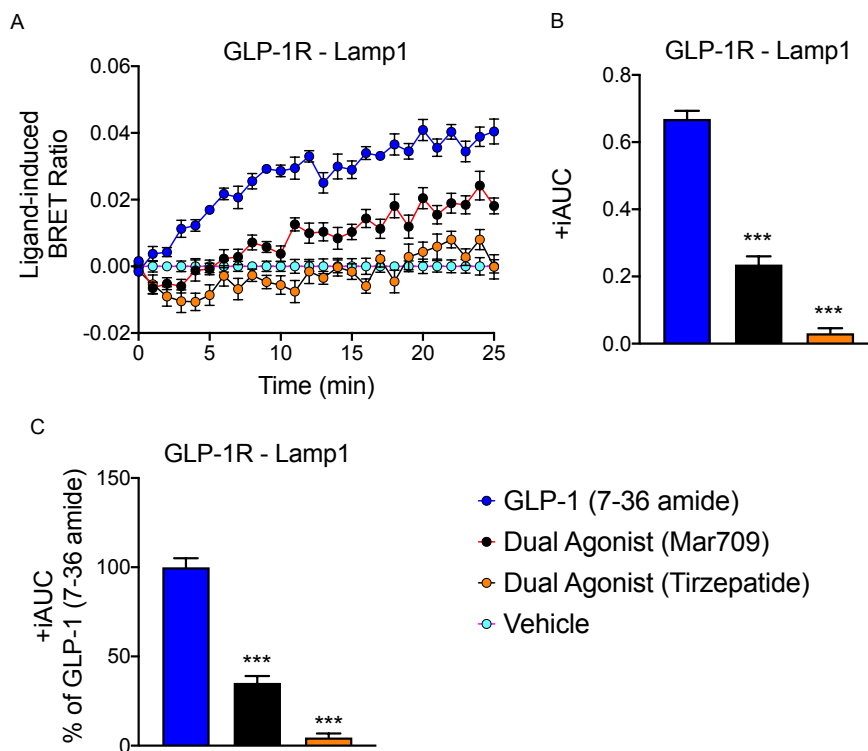


**Figure 39: GLP-1R colocalization into LAMP1<sup>+</sup> terminal lysosomes.** Temporal resolution, +iAUC, and % +iAUC normalized to GLP-1 (7-36 amide), of ligand-induced (1  $\mu$ M) hGLP-1R-Rluc8 colocalization into LAMP1-mNeonGreen<sup>+</sup> terminal lysosomes in HEK293T cells (A-C). The +iAUC representation of vehicle- and baseline-corrected 60 min response to each agonist is expressed as mean  $\pm$  SEM. Bonferroni's test, \* $p < 0.05$ , \*\* $p < 0.005$ , and \*\*\* $p < 0.0005$  using one-way ANOVA vs GLP-1 (7-36 amide), Semaglutide, and Acyl-GLP-1. Three independent experiments were performed with at least two technical replicates per group.

Ligand-induced receptor entry into terminal lysosomes was measured as hGLP-1R-Rluc8 colocalization with a mNeonGreen-tagged lysosomal-associated membrane protein 1 (LAMP-1) (Eskelinen, 2006). Here, the GLP-1/GIP dual-agonists MAR709 and Tirzepatide were compared to the native GLP-1 (7-36 amide) peptide (**Figure 39, A-C**). Similar to the results seen with GLP-1R internalization and Rab5/Rab7 colocalization, MAR709 and Tirzepatide demonstrated a 65% and 95% reduction in capacity to co-localize GLP-1R into terminal lysosomes relative to GLP-1 (7-36 amide). While the decrease in colocalization of the receptor with the lysosome is likely linked to the overall reduced rate in ligand-stimulated receptor internalization, it is a lucrative finding to consider the dual-agonists as full agonists for cAMP production yet with reduced propensity to localize GLP-1R into terminal lysosomes.

#### *MAR709 Comparatively Incorporates the GLP-1R into Rab11<sup>+</sup> Endosomes to that of GLP-1R Mono-agonists*

Outside cellular GPCR desensitization, and GPCR downregulation through the late endosomal/lysosomal pathway, the endosomal recycling pathway represents an opportunity for the return of ligand-free dephosphorylated GPCRs back to the plasma membrane to facilitate cellular resensitization and continued capacity for signaling (Li et al., 2008). To investigate the partitioning of GLP-1R and GIPR from Rab5<sup>+</sup> endosomes into the Rab11 recycling pathway, hGLP-1R-Rluc8 or hGIPR-Rluc8 was assessed for colocalization with Venus-Rab11 following ligand stimulation in HEK293T cells.

Both Semaglutide and Acyl-GLP-1 evoked similar GLP-1R colocalization into Rab11<sup>+</sup> endosomes to that of GLP-1 (7-36 amide) (**Figure 40, A-C**). The effect of maximal GLP-1R colocalization was attained at approximately 30 minutes following ligand stimulation, which is a degree slower than what is observed with Rab5 (10-15 minutes). In line with previous literature, this observation indicates a longer transitional process of receptor transport from the early endosomes into recycling endosomes (Li *et al.*, 2008). Surprisingly, ligand-induced differences in GLP-1R colocalization with Rab11-positive recycling endosomes were insignificant between treatments of MAR709 and GLP-1 (7-36 amide), in which MAR709 achieved approximately 106% of the relative GLP-1 (7-36 amide) response. Interestingly, Tirzepatide-induced GLP-1R recycling was reduced by 54% relative to GLP-1 (7-36 amide), which agrees with both the GLP-1R internalization and GLP-1R Rab5 colocalization profile of Tirzepatide. The non-significant difference between GLP-1 (7-36 amide) and MAR709 for GLP-

1R Rab11 colocalization, is the first clear deviation from the MAR709 partial agonist trafficking profile in HEK293T. Therefore, these data indicate that MAR709 not only induces less GLP-1R colocalization into Rab5 (early) and Rab7 (late) endosomes, but also maximally incorporates GLP-1R into Rab11<sup>+</sup> recycling endosomes in HEK293T cells. In hGLP-1R-Rluc8<sup>+</sup> Min6 cells, due to either a lack of BRET signals or the requirement for improved detection sensitivity, replication of coherent ligand-induced GLP-1R colocalization with Rab11-positive endosomes was not observable for any agonist (**Figure 40, D-E**).

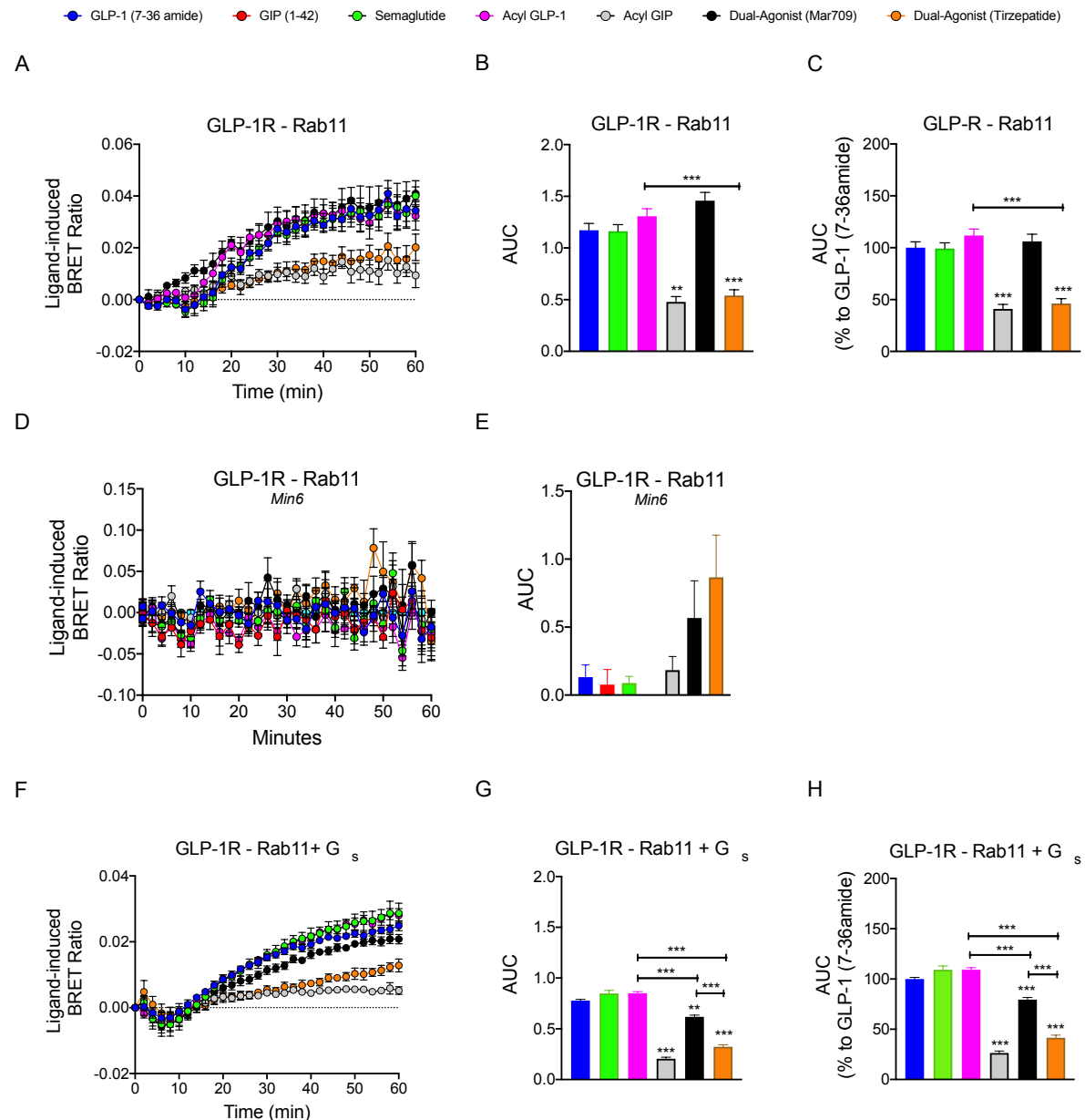


**Figure 40: GLP-1R colocalization and signaling within Rab11<sup>+</sup> recycling endosomes.** Temporal resolution, +iAUC, and % +iAUC normalized to GLP-1 (7-36 amide), of ligand-induced (1  $\mu$ M) hGLP-1R-Rluc8 colocalization into Venus-Rab11<sup>+</sup> recycling endosomes in HEK293T (A-C) and Min6 (D-E) cell lines. MiniG $\alpha_s$  recruitment to Venus-Rab11<sup>+</sup> endosomes as mediated by the untagged hGLP-1R (F-H). The +iAUC representation of vehicle- and baseline-corrected 60 min response to each agonist is expressed as mean  $\pm$  SEM. Bonferroni's test, \* $p$  < 0.05, \*\* $p$  < 0.005,

and  $***p < 0.0005$  using one-way ANOVA vs GLP-1 (7-36 amide), Semaglutide, and Acyl-GLP-1. Three independent experiments were performed with at least two technical replicates per group. *Figure adapted from Novikoff et al. 2021 (Mol. Met.).*

Rab11-associated endosomal signaling was evident with all relevant GLP-1R agonists in HEK293T cells. Semaglutide and Acyl-GLP-1 elicited non-significant differences in GLP-1R-mediated Rab11 endosomal  $G\alpha_s$  recruitment relative to GLP-1 (7-36 amide), while MAR709 and Tirzepatide stimulated a relative 79% and 41% response (**Figure 40, F-H**). Rab11 endosomes are not classically known to house continued  $G\alpha_s$  signaling, as the Rab11-associated GPCRs are considered ligand-free, dephosphorylated, and resensitized for insertion into the plasma membrane (Li *et al.*, 2008). However, as Mini $G\alpha_s$  recruitment was evidenced within the recycling endosomes, it is possible that this finding is due to an artifact attributable to the non-membrane bound property of the synthetic Mini $G\alpha_s$ . It is likely that a remnant of GLP-1 receptors within Rab11<sup>+</sup> endosomes are still ligand-bound, in which the resulting open GLP-1R conformation allows for continued access to Mini $G\alpha_s$  binding. However, the discrepant artifact may arrive from the inability of endogenous membrane-bound GDP- $G\alpha_s$  to physically transfer from Rab5<sup>+</sup> endosomes to Rab11<sup>+</sup> endosomes for conversion to GTP- $G\alpha_s$  by GLP-1R, while the non-membrane bound synthetic GDP-Mini $G\alpha_s$  is capable of localizing freely from the cytosol to the Rab11<sup>+</sup> endosome without physical restraint (Martin and Lambert, 2016; Wan *et al.*, 2018).

In hGIPR-Rluc8<sup>+</sup> HEK293T cells, ligand-induced receptor colocalization into Rab11<sup>+</sup> endosomes was assessed. Despite the coherence previously seen within GIPR colocalization into Rab5<sup>+</sup> endosomes, no meaningful colocalization of GIPR was evidenced with Rab11<sup>+</sup> endosomes (**Figure 41, A-B**). This is surprising as Rab5<sup>+</sup> endosomes containing GIPR do not seem to transfer their cargo into neither the late endosomal pathway nor the Rab11-associated recycling pathway. Similarly, no meaningful GIPR-mediated Mini $G\alpha_s$  colocalization was observed at the Rab11<sup>+</sup> endosomes (**Figure 41, C-D**). Together, contrary to the dynamics of the GLP-1R, these results indicate a physical lack of GIPR presence within Rab11<sup>+</sup> endosomes, and therefore a lack of endosomal signaling.



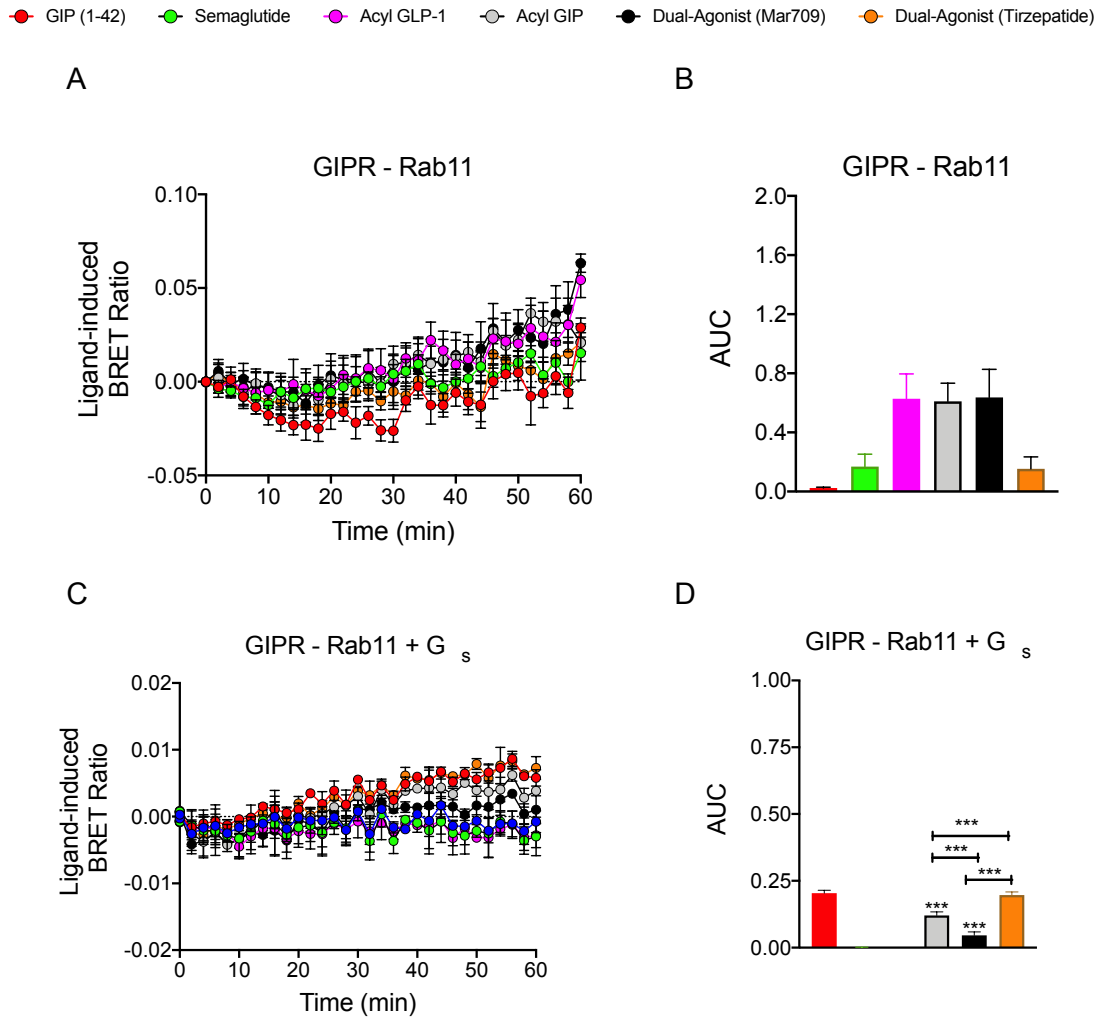


**Figure 41: GIPR colocalization and signaling within Rab11<sup>+</sup> recycling endosomes.** Temporal resolution and +iAUC of ligand-induced (1  $\mu$ M) hGIPR-Rluc8 colocalization into Venus-Rab11<sup>+</sup> endosomes in HEK293T cells (A-B). MiniG $\alpha_s$  recruitment to Venus-Rab11<sup>+</sup> endosomes as mediated by the untagged hGIPR (C-D). The +iAUC representation of vehicle- and baseline-corrected 60 min response to each agonist is expressed as mean  $\pm$  SEM. Bonferroni's test, \*p < 0.05, \*\*p < 0.005, and \*\*\*p < 0.0005 using one-way ANOVA vs GIP (1-42) and Acyl-GIP. Three independent experiments were performed with at least two technical replicates per group. *Figure adapted from Novikoff et al. 2021 (Mol. Met.).*

### *Maximally-induced GLP-1R Rab11 Colocalization by MAR709 Does Not Enhance Physical Recycling*

Between the hGLP-1R and hGIPR, the GLP-1 receptor was demonstrated to be involved in receptor recycling via the Rab11-associated endosomal recycling pathway. GPCR involvement in the endosomal recycling pathway is associated with physical reappearance of the sensitized GPCR at the plasma membrane. Therefore, we set out to measure the physical reappearance of the GLP-1R at the plasma membrane over time following maximal receptor internalization. This measurement was accomplished using the hGLP-1R-Rluc8 co-expressed with the non-

internalizing plasma membrane marker Venus-KRAS. Following initial ligand administration, the induced loss in BRET signal, represented as GLP-1R moving away from the plasma membrane, proceeded over the course of 20 minutes (**Figure 42, A-B**). Following the initial 20 minutes of ligand stimulation, ligand washout and subsequent incubation with the GLP-1R antagonist Jant-4 (9-39) was performed to prevent residual agonist binding (Patterson et al., 2011). Over the following 30 minutes with Jant-4 (9-39) incubation (10 $\mu$ M), the physical recycling of the internalized receptor back to the plasma membrane was assessed, a process represented as a positive gain in BRET signal (**Figure 42, B**). To provide a contrast to the degree of GLP-1R recycling, a separate sham washout was performed, in which following the initial 20 minutes of agonist-induced GLP-1R internalization and washout, the respective GLP-1R agonists were once again added, providing a negative control for the occurrence of GLP-1R recycling (**Figure 42, A**).

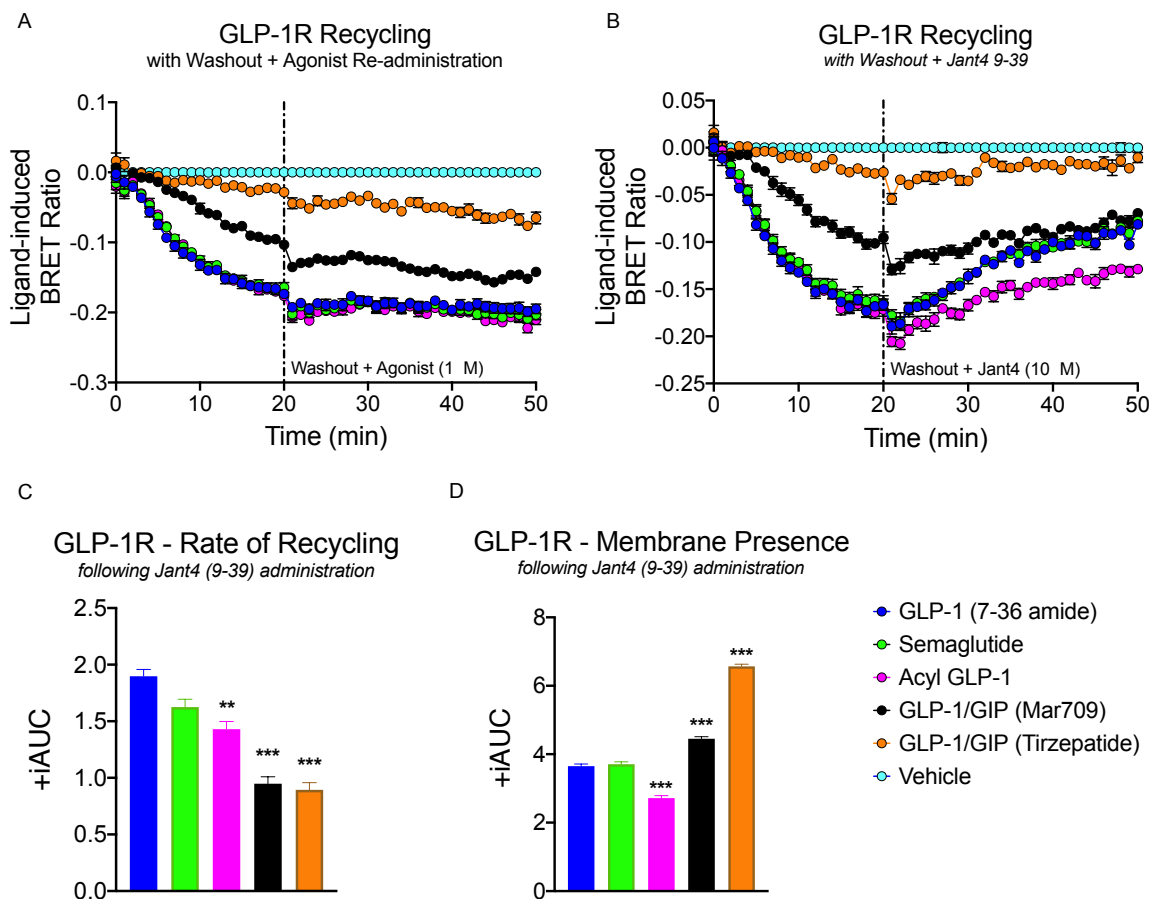


**Figure 42: Physical reappearance of GLP-1R at the plasma membrane following receptor internalization.** Temporal resolution of ligand-induced (1  $\mu$ M) changes in hGLP-1R-Rluc8 colocalization with the plasma membrane marker Venus-KRAS. Following 20 minutes of ligand-incubation, ligands were washed out and either re-administered ligands (A) or administered the GLP-1R antagonist Jant4 (9-39) (B), in which the resulting positive increases in BRET signal, indicative of hGLP-1R-Rluc8 return to the plasma membrane from the intracellular space, was measured over the course of the next 30 minutes. Pertaining to all

data points following JANT4 (9-39) administration, the rate of GLP-1R recycling was quantified using the +iAUC which had been normalized to the respective immediate post-washout measurement of each agonist (C). Again pertaining to all data points following JANT4 (9-39) administration, total GLP-1R presence at the plasma membrane was quantified via +AUC (not iAUC) by normalizing all ligand post-washout responses to a common minimal value (D). The iAUC and AUC representation of vehicle- and baseline-corrected 50 min response to each agonist is expressed as mean  $\pm$  SEM. Bonferroni's test, \* $p < 0.05$ , \*\* $p < 0.005$ , and \*\*\* $p < 0.0005$  using one-way ANOVA vs GLP-1 (7-36 amide), Semaglutide, and Acyl-GLP-1. Three independent experiments were performed with at least two technical replicates per group.

GLP-1 (7-36 amide), Semaglutide, and Acyl-GLP-1 were identical in terms of initial receptor internalization over the course of 20 minutes, and identical in terms of maximal degree of receptor internalization following washout and ligand re-administration over the next 30 minutes (**Figure 42, A**). MAR709 and Tirzepatide again recapitulated the partial GLP-1R internalization  $E_{max}$ , in which MAR709 exhibited approximately 50% the capacity to elicit GLP-1R internalization relative to GLP-1 (7-36 amide), while Tirzepatide faithfully demonstrated minimal induction of GLP-1R internalization. We next assessed the ligand-specific effects on GLP-1R recycling, and therefore following washout, GLP-1R antagonist Jant-4 (9-39) was administered (**Figure 42, B**). Following ligand washout and Jant-4 (9-39) addition, all GLP-1R relevant ligands experienced some degree of receptor recycling and re-appearance at the plasma membrane compared to the agonist re-administration control, as evidenced by an increasingly positive gain in signal over time post-washout. Surprisingly, both GLP-1 (7-36 amide) and Semaglutide demonstrated the highest rate of GLP-1R recycling to the plasma membrane over 30 minutes as quantified by the +iAUC using the value immediately following ligand washout at minute 20 as baseline (**Figure 42, B-C**). Despite Acyl-GLP-1 stimulating equal GLP-1R internalization to that of GLP-1 (7-36 amide) and Semaglutide through the first 20 minutes, Acyl-GLP-1 had a significantly lower rate of receptor recycling in comparison to GLP-1 (7-36 amide) (**Figure 42, C**). This difference between Acyl-GLP-1 and the other mono-agonists may be attributable to differential GLP-1R binding affinities, or  $K_{off}$  values, as a consequence of differences in peptide sequence or acylation properties. The GLP-1/GIP dual-agonists MAR709 and Tirzepatide demonstrated the lowest rates of physical receptor recycling, exhibiting a 5 % and 53% lower recycling rate relative to GLP-1 (7-36 amide). It is interesting to note that MAR709 and Acyl-GLP-1 share the same C16 mono-acylation property, which may be attributable to the reduced rate of physical receptor recycling, despite full incorporation of GLP-1R into Rab11<sup>+</sup> endosomes. Nonetheless, despite the reduced recycling

rate elicited by MAR709 and Tirzepatide, the total receptor presence at the membrane, as measured by the resultant physical GLP-1R localized to the plasma membrane following 30 minutes of ligand washout, was highest with MAR709 and Tirzepatide due to minimal initial receptor internalization (**Figure 42, D**). Acyl-GLP-1 evidenced the least amount of receptor localization at the plasma membrane following 30 minutes of ligand washout, which is an interesting development as it co-localized GLP-1R with Rab11<sup>+</sup> endosomes equally to that of GLP-1 (7-36 amide) and Semaglutide. It is possible that the same phenomenon driving the reduced physical recycling rate by Acyl-GLP-1, despite maximal preceding Rab11<sup>+</sup> endosomal colocalization, is also the cause for the high Rab11<sup>+</sup> endosome colocalization yet reduced physical receptor recycling rate of MAR709. It is suggested that extra-peptide structures, such as the C16 mono-acylation of the peptides, may in some way contribute to the prolonged involvement of the GLP-1R within Rab11 endosomes.

#### *GLP-1R Population at Endosomal Compartments is Positively Associated with the Degree of Endosomal G $\alpha_s$ Recruitment*

Certain GPCRs localized within the endosomal network traverse through the cytosol while retaining the ability to generate a G-protein specific signal. This intracellular compartmentalized signaling can selectively regulate cellular responses (Thomsen *et al.*, 2018). The GLP-1R was shown to, at minimum, have a subset of endosome-localized receptors within the active conformational state following ligand administration (**Figure 34; Figure 37; Figure 40**). Questions still remain regarding the relationship of the GLP-1R quantity co-localized within the endosomal compartment, and the associated extent of endosomal signaling in parallel. Primarily, we set out to clarify if there is a ligand-induced bias between endosomal receptor localization and signaling, or if the relationship between endosomal receptor occupation and signaling is simply a linearized effect. Therefore, the linear association of ligand-induced endosome-specific GLP-1R colocalization was assessed with GLP-1R-mediated G $\alpha_s$  recruitment at the specific endosomal compartment.

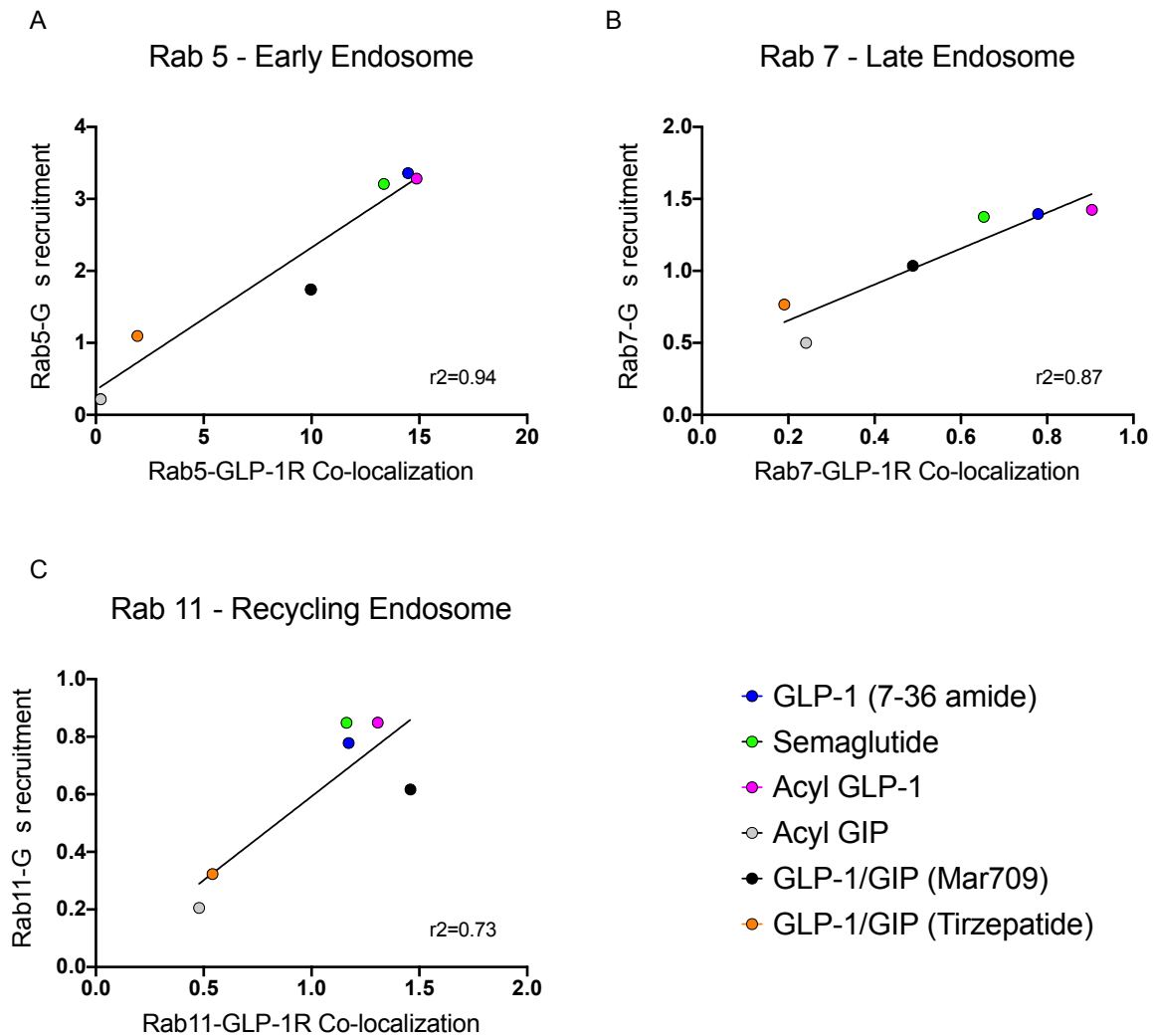


**Figure 43: Association of Rab-specific GLP-1R colocalization with the degree of GLP-1R mediated endosomal  $G\alpha_s$  recruitment.** Linear regression between Mini $G\alpha_s$ -Nluc recruitment and the physical colocalization of the hGLP-1R-Rluc8 into the Venus-tagged Rab endosomal compartments for Rab5 early endosomes (A), Rab7 late endosomes (B), and Rab11 recycling endosomes (C). *Figure adapted from Novikoff et al. 2021 (Mol. Met.).*

In GLP-1R<sup>+</sup> HEK293T cells, 1  $\mu$ M of respective ligands was incubated for 1 hour, in which either GLP-1R colocalization and GLP-1R mediated  $G\alpha_s$  recruitment to the specific endosomal compartments were assessed. The relationship between GLP-1R colocalization and GLP-1R-mediated  $G\alpha_s$  recruitment to the different endosomal compartments was assessed by taking the assay-specific AUC of the respective ligands and plotting into an XY linear regression plot. Within the early endosome Rab5 compartment, a linear association between GLP-1R endosomal colocalization and that of endosomal  $G\alpha_s$  recruitment was evident with a high fit to the regression model between ligands ( $r^2 = 0.94$ ) (**Figure 43, A**). Acyl-GIP represented the point with the least GLP-1R Rab5 endosomal colocalization and  $G\alpha_s$  recruitment, while GLP-1 (7-36 amide), Semaglutide, and Acyl-GLP-1 represented the highest values between both

respective assays. Interestingly, MAR709 and Tirzepatide retained the linear relationship, in which the hierarchical ranking of ligand-induced GLP-1R Rab5 colocalization also reflected that of GLP-1R-mediated Rab5  $G\alpha_s$  recruitment. Similarly, a tight linear association between ligand-induced GLP-1R colocalization into Rab7<sup>+</sup> endosomes and GLP-1R-mediated Rab7<sup>+</sup>  $G\alpha_s$  recruitment was evidenced (**Figure 43, B**). Both Tirzepatide and Acyl-GIP reflected the lowest degree of GLP-1R Rab7<sup>+</sup> endosomal colocalization and  $G\alpha_s$  recruitment, while all GLP-1R mono-agonist were located within the higher spectrum of the linear regression. At Rab11, a similar linear association was observed, however with exception of MAR709, which non-significantly deviated from the regression line due to higher induced GLP-1R colocalization into Rab11<sup>+</sup> endosomes (**Figure 43, C**). Therefore, it may be tentatively concluded that within these assays, the endosomal  $G\alpha_s$  signaling induced by a ligand is a direct product of the GLP-1R population density inside of the endosomal compartment. However at Rab11<sup>+</sup> endosomes, MAR709 seems to break away from this association, in which despite eliciting the highest GLP-1R endosome population density, its ability to recruit  $G\alpha_s$  was diminished, indicating a unidirectional ligand relationship, in which  $G\alpha_s$  endosomal recruitment is proportional or reduced in relation to GLP-1R endosomal colocalization, but not higher.

*The Transcriptional Response to GLP-1R Activation is Linked to the Degree of Receptor Internalization and Endosomal  $G\alpha_s$  Recruitment but not Global cAMP production*

Ligand-induced GPCR internalization and subsequent endosomal signaling facilitate a spatially compartmentalized cAMP signal within the intracellular space (Calebiro *et al.*, 2009). The intracellular span of the compartmentalized cAMP signal, that is the nanometer domain (nanodomain) reach of cAMP emanating from GPCR<sup>+</sup> endosomes, is critical in determining the transcriptional response of the ligand-activated GPCR (Tsvetanova and von Zastrow, 2014). In particular, the subcellular localization of the emanating cAMP nanodomain dictates the probability of locally-activated PKA catalytic subunits (PKAc<sub>at</sub>) successfully propagating across the micrometers-wide cytosolic landscape for entry into the nucleus (Peng *et al.*, 2021). The successful propagation of cAMP-activated PKAc<sub>at</sub> across the cytosolic space for entry into the nucleus connects the ligand-induced activation of the GPCR to nuclear transcription, which is ultimately mediated by PKAc<sub>at</sub> phosphorylative induction of nuclear CREB activity. Inhibition of ligand-bound GPCR internalization has minor detrimental effects on global cAMP production, yet has profound inhibitory effects on CRE/CREB target gene nuclear transcription

(Peng *et al.*, 2021). This inhibition of GPCR-mediated nuclear transcription by blocking GPCR internalization, is due to a lack of activated GPCR-containing endosomes colliding with and activating perinuclear-localized cytosolic PKA puncta (Peng *et al.*, 2021). By consequence, while blocking GPCR internalization, the activated plasma membrane-localized PKAcat likely exhibit decreased probability for traversing the entire cytosolic distance, from plasma membrane to nucleus, to evoke a transcriptional response. In short, internalized and trafficked GPCRs with parallel endosomal signaling activate PKAcat subunit populations that are localized closer the nucleus, thereby increasing the probability of nuclear entry by PKAcat. Therefore, it was hypothesized that despite equal global cAMP production at 1  $\mu$ M ligand stimulation, the differing internalization properties between GLP-1 (7-36 amide) and Tirzepatide, in which the former elicits a maximal degree of receptor internalization and endosomal signaling whereas the latter elicits the minimal, would correspond to differing extents of PKAcat propagation into the nucleus, ultimately resulting in differential degrees of nuclear transcription of the CRE/CREB-responsive target gene phosphoenolpyruvate carboxykinase 1 (PCK1) in HEK293T cells.

In a GLP-1R<sup>+</sup> HEK293T model, cells were incubated with either GLP-1 (7-36 amide), Tirzepatide, or vehicle for 3 hours at 1  $\mu$ M, in which following, relative qPCR quantification of the PCK1 transcript was assessed and then associated with the ligand-induced dynamics of receptor internalization, Rab5 endosomal signaling, and global cAMP production. Interestingly, GLP-1 (7-36 amide) was found to maximally stimulate PCK1 transcription, while Tirzepatide stimulated just 31% of the maximal response (**Figure 44, A**). The relationship of ligand-induced PCK1 transcription was found to have a strong linear association with the degree of ligand-induced GLP-1R internalization and GLP-1R-mediated Rab5<sup>+</sup> endosomal G $\alpha_s$  recruitment (**Figure 44, B-C**). However, as hypothesized, the relationship of ligand-induced PCK1 transcription was not clearly associated with the extent of global cAMP production (**Figure 44, D**). Therefore, despite similar global cAMP production and downstream PKAcat activity between GLP-1 (7-36 amide) and Tirzepatide (**Figure 44, D; Figure 18, C; Figure 21, A-B**), it is evident that ligand-induced GLP-1R G $\alpha_s$  recruitment, internalization, and endosomal colocalization coalesce to determine the spatiotemporal profile of endosomal signaling, which ultimately seems to dictate the extent of the GLP-1R-mediated resultant transcriptional response.

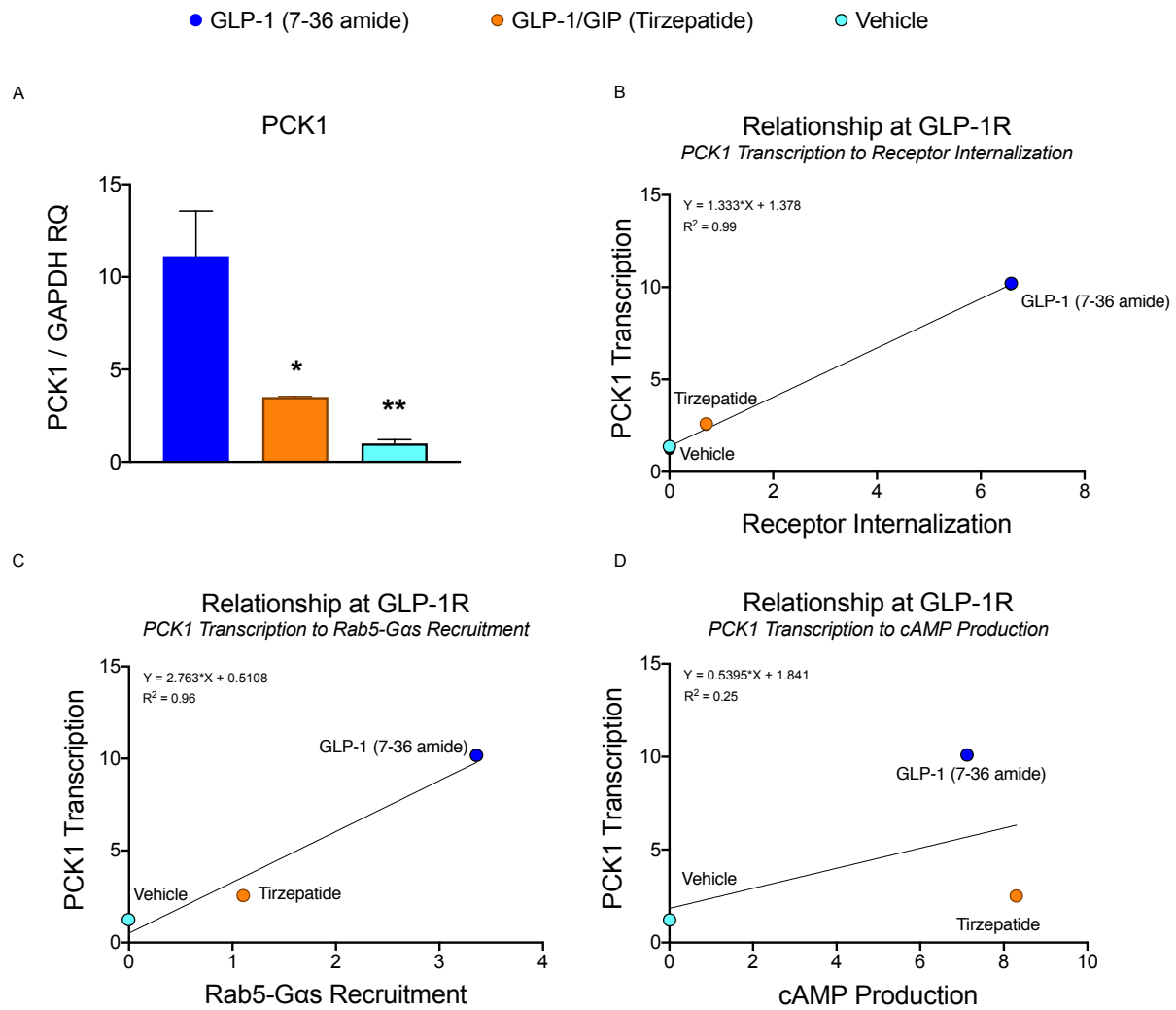


**Figure 44: The relationship of ligand-stimulated PCK1 transcription with GLP-1R internalization, Rab5<sup>+</sup> endosomal G $\alpha$ s signaling, and global cAMP production.** Ligand-induced hGLP-1R-mediated transcription of the cAMP-responsive gene PCK1 as normalized to vehicle (A). Linear regression between ligand-induced PCK1 transcription and hGLP-1R-Rluc8 internalization (B), hGLP-1R-mediated recruitment of miniG $\alpha_s$ -Nluc to Venus-Rab5<sup>+</sup> endosomal compartments (C), and cAMP production (D). Data is expressed as mean  $\pm$  SEM. Bonferroni's test, \* $p < 0.05$ , \*\* $p < 0.005$ , and \*\*\* $p < 0.0005$  using one-way ANOVA vs GLP-1 (7-36 amide). Four independent experiments were performed.



---

# CHAPTER 4: Discussion

---

---

## Discussion

The GLP-1 and GIP receptors are important pharmacological targets for the treatment of obesity and T2D. Despite large overlap in the signaling mechanisms between these two receptors, each has its own distinct biological characterizations in controlling hyperglycemia and food intake. The non-redundancy in action between the GLP-1 and GIP receptors has been evidenced to facilitate synergistic reductions in weight loss and food intake during co-administration of the respective receptor ligands (Finan *et al.*, 2013). The high similarity in amino acid sequence between GLP-1 (7-36 amide) and GIP (1-42) has allowed for capitalization in hybridizing the two sequences into unimolecular dual-agonists capable of activating both the GLP-1R and GIPR individually. The clinical relevance of these hybridized unimolecular dual-agonists for the treatment of obesity and T2D has recently expanded, joining Liraglutide and Semaglutide as state-of-the-art peptidic treatments (Bastin and Andreelli, 2019; Frías *et al.*, 2021). The development and clinical success of the unimolecular GLP-1/GIP dual-agonists MAR709 (Novo Nordisk, Copenhagen, Denmark) and Tirzepatide (Eli Lilly, Indianapolis, IN, USA) has highlighted the question whether the enhanced efficacy of these peptides is not solely due to dual-agonistic action, but also to altered interactions of the hybridized peptide sequence with the respective GPCR, conferring what is known as signal bias through distinct ligand-induced conformational profiles of the GPCR.

Signal bias is the phenomenon of a ligand differentially affecting a number of downstream signal transduction pathways relative to another ligand specific for the same receptor. Signal bias at the GLP-1R may play a beneficial role in enhancing insulin secretion and other therapeutic parameters, making it a lucrative endeavor to investigate (Jones *et al.*, 2018a; Jones *et al.*, 2020b). Although the basic ligand-induced GLP-1R and GIPR signaling cascades are well characterized, the unique signal bias that hybridized peptide sequences can confer onto the individual GLP-1 or GIP receptors is largely unknown. In addition to the potential of ligand-specific signaling biases to confer a degree of control in emphasizing particular therapeutic endpoints, the spatiotemporal dynamics of ligand-bound activated GPCR trafficking, recycling, and degradation, may also play a role in mediating long-term ligand therapeutic effectiveness (Marzook *et al.*, 2021).

To better understand the intracellular dynamics in both receptor signaling and trafficking elicited by the unimolecular GLP-1/GIP dual-agonists, we have utilized bioluminescence resonance energy transfer (BRET) in the form of BRET<sup>1</sup> (Rluc8 with GFP/YFP) or NanoBRET

(Nluc with GFP/YFP), to quantify the ligand efficacy, potency, and spatiotemporal aspects at a given intracellular event. Through this method, we were not only capable of quantifying and comparing the elicited ligand-induced signals at each intracellular event, but we could also evaluate if unique fluctuations in signaling and trafficking kinetics underlie these characterizations. Therefore, through BRET and live single cell HILO microscopy, we were able to thoroughly describe the intracellular dynamics of MAR709 and Tirzepatide at the GLP-1R and GIPR in both signaling and trafficking, in comparison to endogenous and clinically-relevant controls.

The ligands used within this study are represented as various approaches to control for assessing structure-function properties of the GLP-1/GIP dual-agonists MAR709 and Tirzepatide. GLP-1 (7-36 amide) and GIP (1-42) were used as the native peptide positive controls for comparative ligand characterization at their respective receptors, in which when applicable, the efficacy of various ligands were expressed as percentages to the positive control. Semaglutide (Novo Nordisk, Copenhagen, Denmark) is a clinically-relevant long-acting GLP-1R mono-agonist with 94% sequence homology to GLP-1 (7-36 amide) (Kalra and Sahay, 2020). The primary modifications to Semaglutide relative to GLP-1 (7-36 amide) are the Ala2Aib substitution to protect against DPP-IV cleavage, Arg27Lys substitution to facilitate post-peptide synthesis acylation at Lys20, and a C18 diacid acylation at Lys20 via an L- $\gamma$ -glutamic acid linker (Lau *et al.*, 2015). Semaglutide provides a relevant comparison to GLP-1 (7-36 amide), in which the high sequence homology between the two allows for assessing the effect of Aib2 and C18 diacid acylation. Tirzepatide is an imbalanced GLP-1/GIP dual-agonist initially described as favoring the GIPR over GLP-1R in terms of cAMP production (Coskun *et al.*, 2018). The synthesis of Tirzepatide is primarily designed as an eclectic interspersed hybridization of amino acids originating from the GLP-1 and GIP peptides, with the total sequence inclusion favoring GIP. Modifications specific to half-life extension on Tirzepatide include an Ala2Aib substitution, C20 diacid acylation at Lys20 via a L- $\gamma$ -glutamic acid linker, and a CEX-tail extension. MAR709, the first clinically relevant unimolecular GLP-1/GIP dual-agonist, was developed in 2013, and is a hybridized sequence with approximately equal inclusion of amino acid residues specific for GLP-1 (7-36 amide) and GIP (1-42), with balanced activity at the GLP-1 and GIP receptor (Finan *et al.*, 2013). Similar to Tirzepatide, MAR709 contains an Ala2Aib substitution and a CEX-tail extension, but differs in that it contains a Lys40 addition that facilitates a C-terminal C16 monoacid acylation. In this way, Tirzepatide and

MAR709 are closely comparable, differing in 7 amino acids and a repositioned fatty acid. We also included mono-agonist controls to MAR709 almost identical in sequence and acylation, but that contain the minimal changes required in order to induce receptor mono-agonism by deleting specificity for either the GLP-1 or GIP receptors. Therefore pharmacokinetically-matched “Acyl-GLP-1” and “Acyl-GIP” mono-agonist ligands were derived from the dual-agonist MAR709 sequence using double (Tyr1His, Tyr10Val) or single (Thr7Ile) point mutations, respectively.

The GLP-1 and GIP receptors are primarily coupled to the  $G\alpha_s$  signaling pathway, while the GLP-1R alone has demonstrated capacity to couple to  $G\alpha_q$ , albeit to a lesser extent (Montrose-Rafizadeh et al., 1999b; Oduori *et al.*, 2020; Weston et al., 2014).  $G\alpha_s$  connects the GLP-1R and GIPR to the cAMP/PKA pathway, which may play a major role in the amplification of  $\beta$ -cell insulin secretion (Oduori *et al.*, 2020). Therefore, within our BRET system, we first aimed to validate the G-protein recruitment specificity of the GLP-1R and GIPR, and additionally hypothesized that the unique hybridized sequences of MAR709 and Tirzepatide may confer additional “exotic” recruitment of G-protein subtypes to the individual receptors. GLP-1 (7-36 amide), Semaglutide, and Acyl-GLP-1 demonstrated equal efficacy for  $G\alpha_s$  and  $G\alpha_q$  at the GLP-1R, but did not evoke meaningful coupling to  $G\alpha_i$  and  $G\alpha_{12/13}$ , which aligns with previous BRET-based approaches in characterizing GLP-1 (7-36 amide)-induced G-protein recruitment (Jones *et al.*, 2021) (**Figure 15, A-D**). The GIPR mono-agonists, as expected, predominantly recruited  $G\alpha_s$  to the GIPR with little to no recruitment of other G-protein subunits (**Figure 16, A-D**). Both MAR709 and Tirzepatide stimulated  $G\alpha_s$  at the GLP-1R and GIPR, confirming the capacity for dual-agonism. Against the initial supposition, the unique sequences of MAR709 and Tirzepatide did not elicit an “exotic” G-protein subunit profile, as neither  $G\alpha_i$  nor  $G\alpha_{12/13}$  were differentially recruited by the dual-agonists.

Ligand-induced recruitment of  $G\alpha_s$  to either the GLP-1R or GIPR, as stimulated by the respective native peptides, revealed a 2-3 fold reduction in capacity for GIPR to recruit  $G\alpha_s$  relative to the GLP-1R (**Figure 17, A**). It has been suggested the GIPR may exhibit higher basal activity within the  $G\alpha_s$ -cAMP pathway relative to GLP-1R, as found in GIPR<sup>+</sup> and GLP-1R<sup>+</sup> HEK293T cells (Al-Sabah *et al.*, 2014). Therefore, as our resulting data is expressed as ligand-induced fold-change in signal from baseline within HEK293T cells, we assessed if the observed reduction in capacity for GIPR to recruit  $G\alpha_s$ , relative to the GLP-1R, was unduly influenced by higher starting baseline activity. The non-baseline corrected BRET values between  $G\alpha_s$  and the

GPCRs indicate lower basal  $G\alpha_s$  recruitment activity at the GIPR than at the GLP-1R (**Figure 17, B-C**). This confirms that the reduced ligand-stimulated capacity of the GIPR to recruit  $G\alpha_s$ , relative to the GLP-1R, is not an artifact of higher baseline activity. This analysis also suggests that relative to the GIPR, the GLP-1R intrinsically recruits a greater magnitude of  $G\alpha_s$  following ligand-stimulation.

As  $G\alpha_s$  recruitment following ligand binding to the GPCR is the first immediate step within the signal propagation cascade, it most closely reflects the fundamental degree of receptor activation elicited by a ligand, as it is without the confounding implications of signal amplification. The temporal and dose-dependent characterization of ligand-stimulated GLP-1R  $G\alpha_s$  recruitment revealed MAR709 and Tirzepatide to be partial agonists, in which relative to the  $E_{max}$  of GLP-1 (7-36 amide), achieved approximately 60% and 30% of the  $G\alpha_s$  recruitment response, respectively (**Figure 18, A-B; Table 2**). Partial  $G\alpha_s$  agonism by MAR709 and Tirzepatide may result from an altered physical interaction of the ligand amino acid sequence within the GLP-1R binding pocket. This altered binding may induce a unique GLP-1R conformational state not maximally conducive to  $G\alpha_s$  accessibility. Deviation in a ligand's amino acid composition from the native GLP-1 (7-36 amide) sequence may consequentially alter ligand interaction at the GLP-1R ECL2, and the membrane-proximal regions of ECL1 and ECL3. These particular alterations in receptor conformation have been demonstrated to influence ligand binding affinity and efficacy for  $G\alpha_s$ -cAMP pathway activation (Wootten *et al.*, 2016). Oxyntomodulin, a comparable endogenous GLP-1/Gcg dual-agonist peptide, with a similar amino acid sequence deviation from GLP-1 (7-36 amide), also binds to the GLP-1R in a manner fundamentally different than GLP-1 (7-36 amide), eliciting only partial  $G\alpha_s$  recruitment (Weston *et al.*, 2014; Wootten *et al.*, 2016). Interestingly, the MAR709 mono-agonist control Acyl-GLP-1 reconstituted full agonism for  $G\alpha_s$  recruitment, indicating the importance of His1 and Val10 in gating a maximally active GLP-1R conformational state. The minimal alteration required to induce partial  $G\alpha_s$  agonism in a GLP-1-based peptide amino acid sequence, is a single substitution of His1 with a phenolic amino acid (Jones *et al.*, 2018a; Lucey *et al.*, 2020). MAR709 and Tirzepatide both share a common phenolic Tyr1His substitution, potentially explaining the partial  $G\alpha_s$  agonism profiles. However, when comparing MAR709 and Tirzepatide, which have 100% sequence homology at positions 1–12, an additional 30% reduction in  $G\alpha_s$  recruitment efficacy is seen with Tirzepatide relative to MAR709. This indicates that the observed additional reduction in Tirzepatide efficacy

apparently results from sequence substitutions at positions 13-27, or from the size and location of the fatty acid.

At the GIP receptor, such dramatic differences in terms of partial  $G\alpha_s$  agonism associated with the dual-agonists were not evident. Tirzepatide acted as a full agonist for  $G\alpha_s$  recruitment at the GIPR, while MAR709 exhibited properties of a strong partial agonist achieving approximately 80% of the GIP (1-42)  $E_{max}$  (**Figure 20, A-B; Table 2**). Acyl-GIP, which consists of the MAR709 sequence with a Thr7Ile mutation, reconstituted full agonism. The N-terminus of the GIP sequence, and particularly that of Tyr1, is responsible for mediating the interaction between the ligand and three different transmembrane helices of the GIPR. This described ligand-receptor interaction is critical to achieving full agonism within the  $G\alpha_s$ -cAMP pathway (Gabe et al., 2020). Therefore, as both MAR709 and Tirzepatide share a common Tyr1, the dramatic partial agonism profile is not evident at the GIPR, as it is at the GLP-1R. However, as Tirzepatide has identical sequence homology to MAR709 at position 1-12, the 20% reduction in  $G\alpha_s$  efficacy by MAR709 is likely due to alternative sequence substitutions within the body of the peptide.

$G\alpha_s$ -mediated production of cAMP acts as a ubiquitous intracellular messenger to promote insulin secretion by increasing electrical activity,  $Ca^{2+}$  signaling, membrane recruitment of insulin containing granules, and priming of exocytic machinery. Much of the effects of cAMP may be attributable to PKA-mediated phosphorylation of the voltage-gated channels,  $IP_3$  receptors,  $K_{ATP}$  channels, and an enhancement in the mobility and  $Ca^{2+}$  responsiveness of the insulin-containing secretory vesicles (Tengholm, 2012). Therefore, based on the  $G\alpha_s$  partial agonism profile of MAR709 and Tirzepatide at the GLP-1R, it may be expected that the efficacy of these compounds in stimulating insulin secretion would be diminished. However, within Min6 and Ins1 pancreatic  $\beta$ -cell models, the GLP-1R specific ligand EX4-Phe1, which minimally recruits  $G\alpha_s$  upon stimulation, was capable of stimulating greater, if not equal, total insulin secretion in comparison to the  $G\alpha_s$  full agonist EX4-Asp3 (Jones et al., 2018a; Lucey et al., 2020). Therefore, it may be hypothesized that the mechanism underlying enhanced insulin secretion, despite minimal  $G\alpha_s$  recruitment, may result from a cellular capacity for amplification of the  $G\alpha_s$  signal into high levels of cAMP, without the associated GLP-1R desensitization. The signal amplification of a partial  $G\alpha_s$  agonist may mitigate any deleterious effects on insulin secretion that would be present if cAMP production was proportionally linked 1:1 with the  $G\alpha_s$  signal. A single GTP-bound  $G\alpha_s$  subunit, when interacting with

adenylate cyclase, can produce between 100-1000 cAMP molecules; similarly a single ligand-bound GPCR can activate multiple  $G\alpha_s$  subunits (Nelson, 2009). Additionally, stimulated increases in intracellular  $Ca^{2+}$ , as is seen with GLP-1R agonists, may further improve the magnitude of cAMP produced from a single  $G\alpha_s$ , by synergistically acting with  $G\alpha_s$  at AC (Sadana and Dessauer, 2009). Interestingly, a cell typically only has a few thousand activatable adenylate cyclases, but has approximately 100,000 copies of the  $G\alpha_s$  subunit. This indicates the AC component of the  $G\alpha_s$ -cAMP cascade to likely be saturable, and calls into question the minimal degree of partial agonism required to achieve saturation of the  $G\alpha_s$ -AC interaction (Alousi et al., 1991). We identified both MAR709 and Tirzepatide, along with all GLP-1R mono-agonists, to act as full agonists for cAMP production, with only Tirzepatide demonstrating a slight decrease in potency (**Figure 18, C; Table 2**). The full cAMP agonism demonstrated by MAR709 and Tirzepatide was confirmed to not be an artifact of sensor saturation (**Figure 19, A-C**). In addition, the full agonism properties of MAR709 and Tirzepatide, due to signal amplification, extended past cAMP production and continued into subsequent signaling events. 1  $\mu$ M stimulation of MAR709 or Tirzepatide stimulated equal PKA activation to that of GLP-1 (7-36 amide) (**Figure 21, A-B**). Therefore, the full cAMP and PKA agonism of MAR709 and Tirzepatide represent a unique departure from  $G\alpha_s$  partial agonism, and may initiate a branching of categorical affect, as cellular events may now be considered designated within (1) the signal amplification pathway, and (2) a non-signal amplification pathway, in which processes are more closely linked to the G-protein activation of the receptor than to cAMP or associated downstream kinase activity.

GIP (1-42), Acyl-GIP, MAR709, and Tirzepatide all demonstrated full agonism properties for cAMP production via the GIPR, albeit with differing potencies (**Figure 20, C; Table 2**). MAR709 and its GIPR mono-agonist control, Acyl-GIP, demonstrated similar improvements in potency relative to GIP (1-42). Tirzepatide was approximately 10-fold less potent than MAR709, however reason to the decrease in potency was not apparent.

It may be suggested that the high therapeutic efficacy of MAR709 and Tirzepatide may reside within the capacity of these ligands to minimally activate the GLP-1R, while still eliciting full agonism within the cAMP-PKA pathway. Interestingly, the degree of immediate ligand-induced GPCR activation, such as that with  $G\alpha_s$  recruitment, is positively correlated to the degree of receptor desensitization (Clark et al., 1999; Woolf and Linderman, 2003; Xu et al., 2017). Ligand-induced receptor desensitization can occur through a number of pathways,

including  $\beta$ -arrestin recruitment, receptor internalization, and receptor degradation (Clark *et al.*, 1999). A ligand's capacity to induce receptor desensitization is a key determinant of acute and chronic therapeutic efficacy (Rajagopal and Shenoy, 2018). Therefore, the ability of GLP-1R  $G\alpha_s$  partial agonists to minimally activate the receptor, while capitalizing on downstream signal amplification processes, may provide unique benefits in terms of achieving maximal cAMP-PKA pathway activation with a minimal degree of receptor desensitization. Interestingly, relative to all GLP-1R mono-agonists, MAR709 and Tirzepatide only partially induced GLP-1R internalization in HEK293T and Min6 cell lines (**Figure 22, A-C; Figure 23, A-C**). The extent of ligand-specific GLP-1R internalization was tightly correlated with the ligand-specific degree of  $G\alpha_s$  recruitment (**Figure 26, A-B**). This correlation between ligand-specific degree of  $G\alpha_s$  recruitment and GLP-1R internalization was persistent also during inhibition of receptor internalization (**Figure 27, A-E**).  $\beta$ -arrestin recruitment to a ligand-bound GPCR is another primary mode of receptor desensitization, as it sterically blocks G-protein accessibility to the receptor, terminates G-protein signal transduction, and acts as a linker to bridge the GRK-phosphorylated C-terminal end of the GPCR to endocytic machinery. The partial agonism profile of MAR709 and Tirzepatide, relative to all GLP-1R mono-agonists, was replicated within  $\beta$ -arrestin 1 and  $\beta$ -arrestin 2 recruitment to the GLP-1R (**Figure 28, A-D**). Interestingly, ligand-induced GLP-1R internalization was found to be independent of  $\beta$ -arrestin action at the GLP-1R, as pretreatment with barbadin (a selective  $\beta$ -arrestin/AP2 inhibitor) failed to negatively influence ligand-induced GLP-1R internalization (**Figure 30, A-B**). This indicates that the function of  $\beta$ -arrestin recruitment to the GLP-1R is more closely associated with termination of  $G\alpha_s$  signaling rather than receptor internalization, thereby aligning with previous literature that assessed ligand-induced GLP-1R internalization and cAMP production in  $\beta$ -arrestin-less HEK293T cells (Jones *et al.*, 2018a). Together, MAR709 and Tirzepatide elicit minimal  $\beta$ -arrestin recruitment and receptor internalization which thus, by consequence, minimizes inhibition on the continuation of signaling. This minimal ligand-induced receptor desensitization may be critical to the full cAMP and PKA agonism evidenced for the  $G\alpha_s$  partial agonists MAR709 and Tirzepatide. Although  $\beta$ -arrestin can function as part of its own endosomal signaling scaffold, it is not likely that endosomal  $\beta$ -arrestin signaling is a factor in GLP-1R agonism. We demonstrate a lack of GLP-1R colocalization with  $\beta$ -arrestin at Rab5<sup>+</sup> and Rab7<sup>+</sup> endosomal compartments (**Figure 29, C-D**). This finding highlights the spatial specificity



of  $\beta$ -arrestin interaction with GLP-1R to be localized to the plasma membrane (**Figure 29, A-B**).

Within previous literature, GIP receptor internalization has proven to be enigmatic. Studies using similar techniques have evidenced contrary conclusions regarding the presence of ligand-induced GIPR internalization. However, in general, accumulated evidence tends to point toward its occurrence (Ismail *et al.*, 2015; Roed *et al.*, 2015; Willard *et al.*, 2020). Using our BRET technique, which measures the change in resonance between a Rluc8-tagged GIPR and a fluorescent plasma membrane marker, we were able to directly quantify the physical presence of the GIPR at the membrane, and as a byproduct, the internalization of the receptor as assessed by a loss of a signal between GIPR and the plasma membrane markers. Only GIP (1-42) was found to stimulate GIP receptor internalization, with Acyl-GIP, MAR709 and Tirzepatide all failing to induce meaningful effect at the highest doses (**Figure 24, A-C; Table 2**). Our finding is in direct contrast to a recently published study, in which full GIPR internalization was induced by both GIP (1-42) and Tirzepatide (Willard *et al.*, 2020). We suggest that the discrepancy lies within the methodology used, in which Willard *et al.* (2020) initially label their N-terminal SNAP-tag GIPR using a non-membrane permeable SNAP-tag substrate, thereby restricting all receptor labeling to only the GIPR present at the plasma membrane at the time of baseline labeling. Following subsequent SNAP-tag substrate washout, and ligand incubation, GIPR receptor internalization is quantified as a relative change in FRET signal between the one-time labeled membrane-bound SNAP-tag GIPR, and that of an extracellular FRET partner (fluorescein-O'-acetic acid). The relevant difference between our BRET-based method and this FRET-based method is that all GIPR present within the cell, both plasma membrane-bound and cytosol-localized, are tagged and used within the quantification of the BRET-based method. Therefore, the BRET assay is bidirectional in the fact that it can quantify receptor internalization, as a loss in BRET signal between the plasma membrane-bound GIPR and the plasma membrane marker (**Figure 11**), and receptor recruitment to the plasma membrane, as a gain in BRET signal due to GIPR translocation from the cytosol into the plasma membrane. Using the BRET method, we identified a surprising phenomenon, in which GIPR agonism simultaneously causes both receptor departure from and recruitment to the plasma membrane, representing a parabolic-like kinetic in which receptor departure is out paced by receptor recruitment within the first 5 minutes of ligand-stimulation (**Figure 25, A-C**). Following the initial recruitment of GIPR to the plasma

membrane, the rate of receptor internalization is quantified against the rate of receptor recruitment. We find that GIP (1-42) is able to overcome the extent of GIPR recruitment to the plasma membrane in a time-dependent manner, in which following 30 minutes, a net negative signal is achieved indicating that more receptor has been internalized than has been recruited to the plasma membrane. With Tirzepatide, a higher degree of GIPR recruitment to the plasma membrane within the first 5 minutes of ligand incubation was evident, relative to GIP (1-42). However, over the course of thirty minutes, Tirzepatide was not able to achieve a net negative signal, indicating that ligand-stimulated GIPR internalization and plasma membrane recruitment were approximately equal. Therefore, an -iAUC quantification would evidence the receptor internalization capacity of Tirzepatide as approximately 0, yet hidden in that is the dynamic of receptor internalization counterbalanced by receptor recruitment. The discrepancy in findings between our BRET-based experiments and previous literature is that the FRET-based method used within Willard et al. (2020) quantifies pure receptor internalization due to one-time labeling of plasma membrane-bound GIPR, while our BRET-based method quantifies both GIPR internalization and plasma membrane recruitment. It was unclear, however, within our BRET-based method, if the enhanced GIPR internalization by GIP (1-42) relative to Tirzepatide was due to a higher rate of GIPR internalization or a lower rate of GIPR recruitment to the plasma membrane. Therefore in an additional experiment, we evaluated total GIPR recruitment to the plasma membrane by inhibiting receptor internalization with sucrose pretreatment. We found that GIP (1-42) and Tirzepatide stimulate roughly equal GIPR recruitment to the plasma membrane when receptor internalization was inhibited (**Figure 25, D-E**). This suggests that GIP (1-42) and Tirzepatide do not internalize equally; that given their equal capacity to recruit GIPR to the membrane, GIP (1-42) stimulates a higher rate of receptor internalization than that of Tirzepatide. Therefore, examining ligand-induced GIPR internalization via BRET has provided a first look at ligand-stimulated GIPR recruitment to the plasma membrane. To our understanding, this phenomenon has not yet been reported.

GIPR, notwithstanding a chance for enigmatic characterization, has also been at the center of controversy regarding GIPR-mediated  $\beta$ -arrestin recruitment. Several studies indicate an absence of ligand-induced GRK phosphorylation and  $\beta$ arr 1/2 recruitment at the C-terminal tail of the GIPR (Al-Sabah *et al.*, 2014; Ismail *et al.*, 2015; Jones *et al.*, 2021). We identified only GIP (1-42) to produce meaningful, albeit minimal,  $\beta$ arr2 recruitment to the GIPR (**Figure 31,**

**A-B, Table 2).** On the contrary, other studies have evidenced substantial GIP (1-42) and Tirzepatide-induced  $\beta$ -arrestin recruitment to the GIPR (Gabe *et al.*, 2018; Kizilkaya *et al.*, 2021; Willard *et al.*, 2020). It has been recently identified that commonly used linkers that connect the GIPR to a fluorophore for ratiometric quantification, or to extensions for enzymatically-driven colorimetric models, may contain potential GRK phosphorylation motifs capable of facilitating artificial  $\beta$ -arrestin recruitment (Al-Sabah *et al.*, 2020). We identified our own hGIPR-Rluc8 construct to contain a serine-based GRK phosphorylation motif (XbaI restriction site) (**Figure 31, D**). Therefore, we controlled for this artifact by utilizing an endogenous hGIPR without a linker sequence to quantify ligand-induced  $\beta$ arr2 to the plasma membrane. In this assay following ligand stimulation,  $\beta$ arr2-Rluc8 would be recruited to, and BRET with, the plasma membrane marker Venus-KRAS. This approach had faithfully replicated the earlier results of  $\beta$ arr2 recruitment directly to the GLP-1R (**Figure 28, C-D; Figure 29, A-B**). However, when utilizing this same approach with the GIPR, ligand-induced recruitment of  $\beta$ arr2 to the plasma membrane was non-existent for any agonist (**Figure 31, E-F**). Therefore, we have determined that the GIPR has no meaningful  $\beta$ -arrestin 2 recruitment, which may be relevant to the  $G\alpha_s$  signaling cascade of the GIPR.

The actualization of acute or chronic GPCR desensitization within a cell reflects the balance in GPCR trafficking through degradation and recycling endosomal pathways. Rab7<sup>+</sup> endosomes, and LAMP1<sup>+</sup> terminal lysosomes, destine the receptor to degradation and ultimately have the potential to desensitize the cell to further ligand stimulation. GPCR colocalization into Rab11<sup>+</sup> endosomal compartments is associated with receptor recycling and cellular resensitization to ligands in the extracellular environment (Ferguson, 2001). Pharmaceutical ligands that preferentially localize the respective GPCR into the recycling pathway, and away from degradation, typically are associated with less tolerance development and higher therapeutic efficacy over prolonged periods of treatment. Entry into the endolysosomal system following receptor internalization begins with trafficking of the receptor into Rab5<sup>+</sup> early endosomes. Ligand-induced colocalization of the GLP-1R into Rab5<sup>+</sup> endosomes, as expected, mirrored that of ligand-induced GLP-1R internalization, in which MAR709 and Tirzepatide only partially co-localized, relative to GLP-1 (7-36 amide) (**Figure 35, A-F**). Following early endosome incorporation, MAR709 and Tirzepatide, relative to the GLP-1R mono-agonists, also stimulated reduced GLP-1R colocalization into the Rab7<sup>+</sup> late endosomal pathway (**Figure 37, A-E**). In addition, reduced Rab7 colocalization by MAR709 and Tirzepatide subsequently

translated to minimal GLP-1R entry into Lamp1<sup>+</sup> terminal lysosomes (**Figure 39, A-C**). Contrarily, GLP-1 (7-36 amide), Semaglutide, and Acyl-GLP-1 induced maximal GLP-1R incorporation into the late endosome/lysosomal pathway. The minimal movement of the GLP-1R into the degradation endosomal pathway, as stimulated by MAR709 and Tirzepatide, likely reflects prior trafficking disparities at the point of endosomal entry, such as receptor internalization and Rab5<sup>+</sup> endosome colocalization. It cannot, however, be entirely ruled out that the unique sequences of MAR709 and Tirzepatide independently influence the trafficking of the GLP-1R. Nonetheless, the minimal incorporation of the GLP-1R into the late endosomal/lysosomal pathway by MAR709 and Tirzepatide, accompanied with the full agonist cAMP profile, may suggest a lucrative pharmacological profile at the GLP-1R (Pickford et al., 2021).

Surprisingly, despite stimulating minimal GLP-1R internalization and Rab5<sup>+</sup> early endosome entry, MAR709 stimulated equal GLP-1R colocalization into Rab11<sup>+</sup> recycling endosomes relative to that of the fully-internalizing GLP-1R mono-agonists (**Figure 40, A-E**). This indicates a disproportionate flow of MAR709-stimulated receptor movement towards the recycling pathway, rather than toward degradation. Therefore, it seems MAR709 alone facilitates an enhanced GLP-1R recycling response as measured by endosomal colocalization, adding to a unique profile of biased dynamics at the GLP-1R. We next evaluated if the high colocalization of GLP-1R into Rab11<sup>+</sup> recycling endosomes by MAR709 conferred greater physical reappearance of the receptor at the plasma membrane following ligand washout. Following ligand incubation, washout, and then incubation with the GLP-1R antagonist Jant-4 (9-39), GLP-1 (7-36 amide) and Semaglutide surprisingly demonstrated the highest rate of physical receptor return to the plasma membrane over the course of 30 minutes finishing with a receptor population at the plasma membrane equal to that of MAR709 (**Figure 42, B-C**). Therefore, MAR709 does not seem to enhance the rate of physical GLP-1R recycling, despite the high degree of GLP-1R colocalization into Rab11<sup>+</sup> recycling endosomes. Interestingly, Acyl-GLP-1, the MAR709 GLP-1R mono-agonist control, similarly displayed a discrepancy in terms of exhibiting a lower rate of physical GLP-1R recycling back to the membrane despite high Rab11<sup>+</sup> endosomal colocalization. Together, these findings of MAR709 and Acyl-GLP-1 hint at a structure-function relationship which seems to predispose the GLP-1R to maximal Rab11 colocalization without an enhancement in physical recycling of the receptor. The phenomenon may be due to ligand sequence or acylation status, or alternative preferential

routes for endocytic receptor recycling by GLP-1 (7-36 amide) and Semaglutide that may not be captured within this study.

Trafficking of the GIP receptor was not as elegantly characterized within the endolysosomal pathway. Previously we had evidenced ligand-specific differential rates of GIPR internalization as determined by a stimulated balance between GIP receptor internalization and recruitment to the plasma membrane. GIP receptor internalization was further confirmed with evidence of substantial ligand-induced GIPR incorporation into Rab5<sup>+</sup> early endosomes. GIPR colocalization into Rab5<sup>+</sup> early endosomes by MAR709 and Tirzepatide achieved 66% and 78% of the response of GIP (1-42), respectively (**Figure 36, A-C**). Interestingly, ligand-stimulated GIPR colocalization into subsequent endosomal compartments, such as Rab7<sup>+</sup> and Rab11<sup>+</sup>, was non-coherent and minimal (**Figure 38, A-B; Figure 41, A-B**). GIPR colocalization to Rab7<sup>+</sup> or Rab11<sup>+</sup> has not been robustly evidenced in previous literature (Ismail *et al.*, 2015). Therefore, the question arises as to where the GIPR is trafficked following internalization and Rab5<sup>+</sup> endosomal colocalization. It may be suggested that GIPR is rapidly shuttled back to the plasma membrane following receptor internalization, which may partially explain GIPR recruitment to the plasma membrane evidenced to accompany GIPR internalization.

Following receptor internalization, an alternative form of G $\alpha_s$ -mediated signaling can occur at the GPCR, in which the receptor remains ligand-bound and active within the endosomal compartment resulting in a phenomenon known as endosomal signaling. The continuation of G $\alpha_s$  activation within the endosomal compartment confers the advantage of sustained intracellular cAMP signaling regardless of changes in extracellular ligand concentrations (Calebiro *et al.*, 2009). The GLP-1R has previously been demonstrated to take advantage of this phenomenon, in which endosomal G $\alpha_s$  action at the endosomal membrane facilitates sustained cAMP production (Girada *et al.*, 2017). Relative to the GLP-1R mono-agonists, both MAR709 and Tirzepatide produced partial G $\alpha_s$  recruitment to Rab5<sup>+</sup>, Rab7<sup>+</sup>, and Rab11<sup>+</sup> endosomes, as mediated by GLP-1R (**Figure 35, G-I; Figure 37, F-H; Figure 40, F-H**). This partial endosomal G $\alpha_s$  recruitment by MAR709 and Tirzepatide may be due to: minimized receptor density within the endosomal compartments as a product of reduced receptor internalization, intrinsic differences in ligand capacity to induce G $\alpha_s$  recruitment at the GLP-1R, or both. Interestingly, it has been evidenced that endosomal G $\alpha_s$  is critical to early endosome formation and post-endocytic sorting, indicating the possibility of ligand-induced G $\alpha_s$  recruitment as a potential determinant of lysosomal GPCR degradation (Beas *et al.*, 2012;

Buenaventura *et al.*, 2018a; Rosciglione *et al.*, 2014). Regarding the GIP receptor,  $G\alpha_s$  recruitment to GIPR<sup>+</sup> Rab5<sup>+</sup> early endosomes was minimal, however GIP (1-42), Acyl-GIP, and Tirzepatide all stimulated maximal degrees of endosomal  $G\alpha_s$  recruitment, while MAR709 was found to be only partially efficacious (**Figure 36, D-F**). GIPR-mediated endosomal  $G\alpha_s$  recruitment at Rab7<sup>+</sup> and Rab11<sup>+</sup> endosomes was non-existent, emphasizing the unique trafficking nature of the GIPR (**Figure 38, C-D; Figure 41, C-D**).

The degree of ligand-induced GLP-1R colocalization into endosomal compartments was found to be linearly and positively associated to the degree of ligand-induced GLP-1R-mediated  $G\alpha_s$  recruitment at the endosomal compartments (**Figure 43, A-C**). The unique ability of a ligand to elicit concomitant endosomal GPCR trafficking and  $G\alpha_s$  signaling is a key component in facilitating spatially compartmentalized intercellular cAMP signaling (Calebiro *et al.*, 2009). The presence and location of the endosomal cAMP signal, which emanates from the endosome within a nanometer scale (nanodomain), is critical in determining the transcriptional response of an activated GPCR (Tsvetanova and von Zastrow, 2014). In general, for a transcriptional response to occur via GPCR-mediated cAMP production, cAMP-activated cytosolic PKA catalytic subunits (PKAcat) translocate over a micrometer-wide distance into the nucleus, where it then phosphorylates CREB and induces nuclear transcriptional activity. The micrometer range of PKAcat signal transduction across the cytosol largely acts as semiconductor to extend the nanometer reach of the cAMP gradient (Peng *et al.*, 2021). In order to improve the probability of successful PKAcat activation and propagation into the nucleus, endosomal transport of the GPCR-mediated cAMP nanodomain is critical, as the physical movement of the endosome over large distances within the intracellular space allows for activation and exposure of spatially-compartmentalized PKA puncta to a locally concentrated cAMP source. Inhibition of ligand-induced GPCR internalization, therefore, consequently inhibits the movement of the endosomal cAMP nanodomain into proximity of intracellular PKA puncta, and thus results in a strong reduction in the GPCR-mediated CREB transcriptional response (Peng *et al.*, 2021). We therefore hypothesized that Tirzepatide, with its full agonist cAMP profile, yet relative absence of GLP-1 receptor internalization, endosomal trafficking, and endosomal  $G\alpha_s$  recruitment, would induce minimal nuclear transcription of the CREB-responsive target gene phosphoenolpyruvate carboxykinase 1 (PCK1). Contrarily, GLP-1 (7-36 amide), which has displayed equal cAMP production with maximal receptor internalization, endosomal trafficking, and endosomal  $G\alpha_s$  recruitment properties, would

maximally stimulate PCK1 transcription. Tirzepatide was found to stimulate just 31% of the PCK1 transcriptional response, relative to GLP-1 (7-36 amide) (**Figure 44, A**). The ligand-specific PCK1 transcriptional response was highly correlated with degree of ligand-induced receptor internalization and Rab5-G $\alpha_s$  recruitment, but not with global cAMP production (**Figure 44, B-D**). Here, we exemplify a novel ligand-specific regulation on the cAMP-induced transcriptional response, in which GLP-1 receptor internalization and endosomal G $\alpha_s$  signaling seem to be primary determinants. This differential regulation is present despite equal global cAMP production. It is unknown if this ligand-specific transcriptional effect translates to improved therapeutic value *in vivo*. Nonetheless, the unique spatiotemporal signaling and trafficking profile of Tirzepatide seems to differentiate the CREB-mediated nuclear transcriptional response from GLP-1 (7-36 amide).

In conclusion, we have identified unique spatiotemporal receptor signaling and trafficking characteristics elicited by the GLP-1/GIP dual-agonists MAR709 and Tirzepatide, relative to endogenous, clinical, and sequence-matched peptide mono-agonists at the respective GLP-1 and GIP receptors. Simply, we suggest that intracellular receptor signaling and trafficking characterizations can be grouped within *signal amplification* and *non-signal amplification* pathways. Within the signal amplification pathway, we identify that all relevant agonists at the GLP-1R and GIPR are full agonists for both cAMP production and PKA activity. This finding sets the stage for equivalent ligand-induced, cAMP-mediated, insulinotropic properties with respect to the individual receptors. However, within the preceding step to cAMP production, G $\alpha_s$  recruitment to the receptor represents the most intrinsic depiction of GLP-1R and GIPR activation. In accordance with partial GLP-1R activation at the G-protein level by MAR709 and Tirzepatide, we identify  $\beta$ -arrestin recruitment, receptor internalization, receptor trafficking into Rab5<sup>+</sup> and Rab7<sup>+</sup> endosomes, lysosomal incorporation, and transcription of nuclear targets, to achieve partial induction as well. Partial agonism within the non-signal amplification pathway may minimize ligand-induced desensitization of the GLP-1R, and therefore may be a key therapeutic component when coupled with full agonism for cAMP production. In addition to localizing less GLP-1R into the Rab7<sup>+</sup>/LAMP1<sup>+</sup> degradation pathway, MAR709 co-localized GLP-1R into Rab11<sup>+</sup> recycling endosomes to the same extent as the GLP-1R mono-agonists. However, this did not directly translate to a higher rate of physical receptor recycling. With respect to the GIP receptor, Tirzepatide acted as a full G $\alpha_s$  agonist, while MAR709 was evidenced to be a strong partial agonist at most intracellular events. All

respective ligands evidenced a lack of  $\beta$ -arrestin recruitment to the GIPR, and achieved only minimal  $G\alpha_s$  recruitment to Rab5<sup>+</sup> endosomes, which is implicative of fundamental GIPR biology. Additionally, we provided evidence to the presence of ligand-induced GIPR internalization, and novel resolution into the differences behind ligand-specific rates of GIPR internalization between GIP (1-42) and Tirzepatide.

Collectively, the data provided here establishes new insights into the biological mechanisms at the individual receptors underlying the therapeutic efficacy of the unimolecular hybridized GLP-1/GIP dual-agonist MAR709 and Tirzepatide. These characterized receptor signaling and trafficking aspects found attributable to MAR709 and Tirzepatide may be seen as lucrative developmental targets in the improved pharmacotherapy of diabetes and obesity.



## References

- Adelhorst, K., Hedegaard, B.B., Knudsen, L.B., and Kirk, O. (1994). Structure-activity studies of glucagon-like peptide-1. *J Biol Chem* *269*, 6275-6278.
- Adriaenssens, A.E., Biggs, E.K., Darwish, T., Tadross, J., Sukthankar, T., Girish, M., Poley-Wolf, J., Lam, B.Y., Zvetkova, I., Pan, W., et al. (2019). Glucose-Dependent Insulinotropic Polypeptide Receptor-Expressing Cells in the Hypothalamus Regulate Food Intake. *Cell Metab* *30*, 987-996.e986. 10.1016/j.cmet.2019.07.013.
- Ahima, R.S., and Antwi, D.A. (2008). Brain regulation of appetite and satiety. *Endocrinology and metabolism clinics of North America* *37*, 811-823. 10.1016/j.ecl.2008.08.005.
- Ahmann, A.J., Capehorn, M., Charpentier, G., Dotta, F., Henkel, E., Lingvay, I., Holst, A.G., Annett, M.P., and Aroda, V.R. (2018). Efficacy and Safety of Once-Weekly Semaglutide Versus Exenatide ER in Subjects With Type 2 Diabetes (SUSTAIN 3): A 56-Week, Open-Label, Randomized Clinical Trial. *Diabetes Care* *41*, 258-266. 10.2337/dc17-0417.
- Al-Sabah, S. (2016). Molecular Pharmacology of the Incretin Receptors. *Medical principles and practice : international journal of the Kuwait University, Health Science Centre* *25 Suppl 1*, 15-21. 10.1159/000433437.
- Al-Sabah, S., Adi, L., Bünemann, M., and Krasel, C. (2020). The Effect of Cell Surface Expression and Linker Sequence on the Recruitment of Arrestin to the GIP Receptor. *Frontiers in pharmacology* *11*, 1271. 10.3389/fphar.2020.01271.
- Al-Sabah, S., Al-Fulaij, M., Shaaban, G., Ahmed, H.A., Mann, R.J., Donnelly, D., Bünemann, M., and Krasel, C. (2014). The GIP receptor displays higher basal activity than the GLP-1 receptor but does not recruit GRK2 or arrestin3 effectively. *PLoS One* *9*, e106890. 10.1371/journal.pone.0106890.
- Alousi, A.A., Jasper, J.R., Insel, P.A., and Motulsky, H.J. (1991). Stoichiometry of receptor-Gs-adenylate cyclase interactions. *FASEB journal : official publication of the Federation of American Societies for Experimental Biology* *5*, 2300-2303. 10.1096/fasebj.5.9.1650314.
- Ansell, T.B., Song, W., and Sansom, M.S.P. (2020). The Glycosphingolipid GM3 Modulates Conformational Dynamics of the Glucagon Receptor. *Biophysical journal* *119*, 300-313. 10.1016/j.bpj.2020.06.009.
- Aquila, H., Link, T.A., and Klingenberg, M. (1985). The uncoupling protein from brown fat mitochondria is related to the mitochondrial ADP/ATP carrier. Analysis of sequence homologies and of folding of the protein in the membrane. *The EMBO journal* *4*, 2369-2376.
- Baggio, L.L., and Drucker, D.J. (2014). Glucagon-like peptide-1 receptors in the brain: controlling food intake and body weight. *J Clin Invest* *124*, 4223-4226. 10.1172/jci78371.
- Baggio, L.L., Huang, Q., Brown, T.J., and Drucker, D.J. (2004). A recombinant human glucagon-like peptide (GLP)-1-albumin protein (albugon) mimics peptidergic activation of GLP-1 receptor-dependent pathways coupled with satiety, gastrointestinal motility, and glucose homeostasis. *Diabetes* *53*, 2492-2500. 10.2337/diabetes.53.9.2492.
- Baraboi, E.D., St-Pierre, D.H., Shooner, J., Timofeeva, E., and Richard, D. (2011). Brain activation following peripheral administration of the GLP-1 receptor agonist exendin-4. *American journal of physiology. Regulatory, integrative and comparative physiology* *301*, R1011-1024. 10.1152/ajpregu.00424.2010.
- Basith, S., Cui, M., Macalino, S.J.Y., Park, J., Clavio, N.A.B., Kang, S., and Choi, S. (2018). Exploring G Protein-Coupled Receptors (GPCRs) Ligand Space via Cheminformatics Approaches: Impact on Rational Drug Design. *Frontiers in pharmacology* *9*, 128. 10.3389/fphar.2018.00128.

- Bastin, M., and Andreelli, F. (2019). Dual GIP-GLP1-Receptor Agonists In The Treatment Of Type 2 Diabetes: A Short Review On Emerging Data And Therapeutic Potential. *Diabetes Metab Syndr Obes* 12, 1973-1985. 10.2147/dms0.S191438.
- Baver, S.B., Hope, K., Guyot, S., Bjørbaek, C., Kaczorowski, C., and O'Connell, K.M. (2014). Leptin modulates the intrinsic excitability of AgRP/NPY neurons in the arcuate nucleus of the hypothalamus. *The Journal of neuroscience : the official journal of the Society for Neuroscience* 34, 5486-5496. 10.1523/jneurosci.4861-12.2014.
- Bazarsuren, A., Grauschopf, U., Wozny, M., Reusch, D., Hoffmann, E., Schaefer, W., Panzner, S., and Rudolph, R. (2002). In vitro folding, functional characterization, and disulfide pattern of the extracellular domain of human GLP-1 receptor. *Biophysical chemistry* 96, 305-318. 10.1016/s0301-4622(02)00023-6.
- Beas, A.O., Taupin, V., Teodorof, C., Nguyen, L.T., Garcia-Marcos, M., and Farquhar, M.G. (2012). Gαs promotes EEA1 endosome maturation and shuts down proliferative signaling through interaction with GIV (Girdin). *Molecular biology of the cell* 23, 4623-4634. 10.1091/mbc.E12-02-0133.
- Beautrait, A., Paradis, J.S., Zimmerman, B., Giubilaro, J., Nikolajev, L., Armando, S., Kobayashi, H., Yamani, L., Namkung, Y., Heydenreich, F.M., et al. (2017). A new inhibitor of the β-arrestin/AP2 endocytic complex reveals interplay between GPCR internalization and signalling. *Nat Commun* 8, 15054. 10.1038/ncomms15054.
- Benmerah, A. (2004). Endocytosis: signaling from endocytic membranes to the nucleus. *Current biology : CB* 14, R314-316. 10.1016/j.cub.2004.03.053.
- Bergmann, N.C., Lund, A., Gasbjerg, L.S., Meessen, E.C.E., Andersen, M.M., Bergmann, S., Hartmann, B., Holst, J.J., Jessen, L., Christensen, M.B., et al. (2019). Effects of combined GIP and GLP-1 infusion on energy intake, appetite and energy expenditure in overweight/obese individuals: a randomised, crossover study. *Diabetologia* 62, 665-675. 10.1007/s00125-018-4810-0.
- Bos, J.L., Rehmann, H., and Wittinghofer, A. (2007). GEFs and GAPs: critical elements in the control of small G proteins. *Cell* 129, 865-877. 10.1016/j.cell.2007.05.018.
- Botos, E., Turi, A., Müllner, N., Kovalszky, I., Tátrai, P., and Kiss, A.L. (2007). Regulatory role of kinases and phosphatases on the internalisation of caveolae in HepG2 cells. *Micron (Oxford, England : 1993)* 38, 313-320. 10.1016/j.micron.2006.03.012.
- Broide, E., Bloch, O., Ben-Yehudah, G., Cantrell, D., Shirin, H., and Rapoport, M.J. (2013). GLP-1 receptor is expressed in human stomach mucosa: analysis of its cellular association and distribution within gastric glands. *The journal of histochemistry and cytochemistry : official journal of the Histochemistry Society* 61, 649-658. 10.1369/0022155413497586.
- Bucci, C., Thomsen, P., Nicoziani, P., McCarthy, J., and van Deurs, B. (2000). Rab7: a key to lysosome biogenesis. *Molecular biology of the cell* 11, 467-480. 10.1091/mbc.11.2.467.
- Buenaventura, T., Bitsi, S., Laughlin, W.E., Burgoyne, T., Lyu, Z., Oqua, A.I., Norman, H., McGlone, E.R., Klymchenko, A.S., Corrêa, I.R., Jr., et al. (2019). Agonist-induced membrane nanodomain clustering drives GLP-1 receptor responses in pancreatic beta cells. *PLoS Biol* 17, e3000097. 10.1371/journal.pbio.3000097.
- Buenaventura, T., Kanda, N., Douzenis, P.C., Jones, B., Bloom, S.R., Chabosseu, P., Corrêa, I.R., Jr., Bosco, D., Piemonti, L., Marchetti, P., et al. (2018a). A Targeted RNAi Screen Identifies Endocytic Trafficking Factors That Control GLP-1 Receptor Signaling in Pancreatic β-Cells. *Diabetes* 67, 385-399. 10.2337/db17-0639.
- Buenaventura, T., Laughlin, W., Bitsi, S., Burgoyne, T., Lyu, Z., Oqua, A., Norman, H., McGlone, E., Klymchenko, A., Corrêa, I., et al. (2018b). Agonist binding affinity determines

- palmitoylation of the glucagon-like peptide-1 receptor and its functional interaction with plasma membrane nanodomains in pancreatic beta cells. *bioRxiv*.
- Bünemann, M., Gerhardstein, B.L., Gao, T., and Hosey, M.M. (1999). Functional regulation of L-type calcium channels via protein kinase A-mediated phosphorylation of the beta(2) subunit. *J Biol Chem* 274, 33851-33854. 10.1074/jbc.274.48.33851.
- Calebiro, D., and Jobin, M.L. (2019). Hot spots for GPCR signaling: lessons from single-molecule microscopy. *Current opinion in cell biology* 57, 57-63. 10.1016/j.ceb.2018.11.003.
- Calebiro, D., Koszegi, Z., Lanoiselée, Y., Miljus, T., and O'Brien, S. (2021). G protein-coupled receptor-G protein interactions: a single-molecule perspective. *Physiological reviews* 101, 857-906. 10.1152/physrev.00021.2020.
- Calebiro, D., Nikolaev, V.O., Gagliani, M.C., de Filippis, T., Dees, C., Tacchetti, C., Persani, L., and Lohse, M.J. (2009). Persistent cAMP-signals triggered by internalized G-protein-coupled receptors. *PLoS Biol* 7, e1000172. 10.1371/journal.pbio.1000172.
- Cali, J.J., Zwaagstra, J.C., Mons, N., Cooper, D.M., and Krupinski, J. (1994). Type VIII adenylyl cyclase. A Ca<sup>2+</sup>/calmodulin-stimulated enzyme expressed in discrete regions of rat brain. *J Biol Chem* 269, 12190-12195.
- Campbell, J.E. (2021). Targeting the GIPR for obesity: To agonize or antagonize? Potential mechanisms. *Mol Metab* 46, 101139. 10.1016/j.molmet.2020.101139.
- Campbell, J.E., and Newgard, C.B. (2021). Mechanisms controlling pancreatic islet cell function in insulin secretion. *Nat Rev Mol Cell Biol* 22, 142-158. 10.1038/s41580-020-00317-7.
- Capehorn, M.S., Catarig, A.M., Furberg, J.K., Janez, A., Price, H.C., Tadayon, S., Vergès, B., and Marre, M. (2020). Efficacy and safety of once-weekly semaglutide 1.0mg vs once-daily liraglutide 1.2mg as add-on to 1-3 oral antidiabetic drugs in subjects with type 2 diabetes (SUSTAIN 10). *Diabetes & metabolism* 46, 100-109. 10.1016/j.diabet.2019.101117.
- Chabenne, J., Chabenne, M.D., Zhao, Y., Levy, J., Smiley, D., Gelfanov, V., and Dimarchi, R. (2014). A glucagon analog chemically stabilized for immediate treatment of life-threatening hypoglycemia. *Mol Metab* 3, 293-300. 10.1016/j.molmet.2014.01.006.
- Chaloux, B., Caron, A.Z., and Guillemette, G. (2007). Protein kinase A increases the binding affinity and the Ca<sup>2+</sup> release activity of the inositol 1,4,5-trisphosphate receptor type 3 in RINm5F cells. *Biology of the cell* 99, 379-388. 10.1042/bc20060121.
- Chang-Chen, K.J., Mullur, R., and Bernal-Mizrachi, E. (2008). Beta-cell failure as a complication of diabetes. *Reviews in endocrine & metabolic disorders* 9, 329-343. 10.1007/s11154-008-9101-5.
- Clark, R.B., Knoll, B.J., and Barber, R. (1999). Partial agonists and G protein-coupled receptor desensitization. *Trends in pharmacological sciences* 20, 279-286. 10.1016/s0165-6147(99)01351-6.
- Cocucci, E., Gaudin, R., and Kirchhausen, T. (2014). Dynamin recruitment and membrane scission at the neck of a clathrin-coated pit. *Molecular biology of the cell* 25, 3595-3609. 10.1091/mbc.E14-07-1240.
- Cone, R.D., Cowley, M.A., Butler, A.A., Fan, W., Marks, D.L., and Low, M.J. (2001). The arcuate nucleus as a conduit for diverse signals relevant to energy homeostasis. *Int J Obes Relat Metab Disord* 25 Suppl 5, S63-67. 10.1038/sj.ijo.0801913.
- Coskun, T., Sloop, K.W., Loghin, C., Alsina-Fernandez, J., Urva, S., Bokvist, K.B., Cui, X., Briere, D.A., Cabrera, O., Roell, W.C., et al. (2018). LY3298176, a novel dual GIP and GLP-1 receptor agonist for the treatment of type 2 diabetes mellitus: From discovery to clinical proof of concept. *Mol Metab* 18, 3-14. 10.1016/j.molmet.2018.09.009.

- Costa-Neto, C.M., Parreiras, E.S.L.T., and Bouvier, M. (2016). A Pluridimensional View of Biased Agonism. *Mol Pharmacol* *90*, 587-595. 10.1124/mol.116.105940.
- Cowley, M.A., Smart, J.L., Rubinstein, M., Cerdán, M.G., Diano, S., Horvath, T.L., Cone, R.D., and Low, M.J. (2001). Leptin activates anorexigenic POMC neurons through a neural network in the arcuate nucleus. *Nature* *411*, 480-484. 10.1038/35078085.
- Cullen, P.J., and Steinberg, F. (2018). To degrade or not to degrade: mechanisms and significance of endocytic recycling. *Nat Rev Mol Cell Biol* *19*, 679-696. 10.1038/s41580-018-0053-7.
- Da Silva Xavier, G. (2018). The Cells of the Islets of Langerhans. *J Clin Med* *7*. 10.3390/jcm7030054.
- Dahl, D., Onishi, Y., Norwood, P., Huh, R., Patel, H., and Rodríguez, Á. (2021). 80-LB: Tirzepatide, a Dual GIP/GLP-1 Receptor Agonist, Is Effective and Safe When Added to Basal Insulin for Treatment of Type 2 Diabetes (SURPASS-5). *Diabetes* *70*, 80-LB. 10.2337/db21-80-LB.
- Dawaliby, R., Trubbia, C., Delporte, C., Masureel, M., Van Antwerpen, P., Kobilka, B.K., and Govaerts, C. (2016). Allosteric regulation of G protein-coupled receptor activity by phospholipids. *Nat Chem Biol* *12*, 35-39. 10.1038/nchembio.1960.
- Day, J.W., Ottaway, N., Patterson, J.T., Gelfanov, V., Smiley, D., Gidda, J., Findeisen, H., Bruemmer, D., Drucker, D.J., Chaudhary, N., et al. (2009). A new glucagon and GLP-1 co-agonist eliminates obesity in rodents. *Nat Chem Biol* *5*, 749-757. 10.1038/nchembio.209.
- Deacon, C.F., Johnsen, A.H., and Holst, J.J. (1995a). Degradation of glucagon-like peptide-1 by human plasma in vitro yields an N-terminally truncated peptide that is a major endogenous metabolite in vivo. *J Clin Endocrinol Metab* *80*, 952-957. 10.1210/jcem.80.3.7883856.
- Deacon, C.F., Nauck, M.A., Meier, J., Hücking, K., and Holst, J.J. (2000). Degradation of endogenous and exogenous gastric inhibitory polypeptide in healthy and in type 2 diabetic subjects as revealed using a new assay for the intact peptide. *J Clin Endocrinol Metab* *85*, 3575-3581. 10.1210/jcem.85.10.6855.
- Deacon, C.F., Nauck, M.A., Toft-Nielsen, M., Pridal, L., Willms, B., and Holst, J.J. (1995b). Both subcutaneously and intravenously administered glucagon-like peptide I are rapidly degraded from the NH<sub>2</sub>-terminus in type II diabetic patients and in healthy subjects. *Diabetes* *44*, 1126-1131. 10.2337/diab.44.9.1126.
- DeFronzo, R.A. (2004). Pathogenesis of type 2 diabetes mellitus. *The Medical clinics of North America* *88*, 787-835, ix. 10.1016/j.mcna.2004.04.013.
- DeFronzo, R.A., and Tripathy, D. (2009). Skeletal muscle insulin resistance is the primary defect in type 2 diabetes. *Diabetes care* *32 Suppl 2*. 10.2337/dc09-S302.
- Delmeire, D., Flamez, D., Hinke, S.A., Cali, J.J., Pipeleers, D., and Schuit, F. (2003). Type VIII adenylyl cyclase in rat beta cells: coincidence signal detector/generator for glucose and GLP-1. *Diabetologia* *46*, 1383-1393. 10.1007/s00125-003-1203-8.
- Dhanasekaran, N., and Dermott, J.M. (1996). Signaling by the G12 class of G proteins. *Cell Signal* *8*, 235-245. 10.1016/0898-6568(96)00048-4.
- Dillon, J.S., Tanizawa, Y., Wheeler, M.B., Leng, X.H., Ligon, B.B., Rabin, D.U., Yoo-Warren, H., Permutt, M.A., and Boyd, A.E., 3rd (1993). Cloning and functional expression of the human glucagon-like peptide-1 (GLP-1) receptor. *Endocrinology* *133*, 1907-1910. 10.1210/endo.133.4.8404634.
- Dodson, G., and Steiner, D. (1998). The role of assembly in insulin's biosynthesis. *Current opinion in structural biology* *8*, 189-194. 10.1016/s0959-440x(98)80037-7.

- Domingue, B.W., Belsky, D.W., Harris, K.M., Smolen, A., McQueen, M.B., and Boardman, J.D. (2014). Polygenic risk predicts obesity in both white and black young adults. *PLoS One* *9*, e101596. 10.1371/journal.pone.0101596.
- Doyle, M.E., and Egan, J.M. (2007). Mechanisms of action of glucagon-like peptide 1 in the pancreas. *Pharmacology & therapeutics* *113*, 546-593. 10.1016/j.pharmthera.2006.11.007.
- Doyle, M.E., Theodorakis, M.J., Holloway, H.W., Bernier, M., Greig, N.H., and Egan, J.M. (2003). The importance of the nine-amino acid C-terminal sequence of exendin-4 for binding to the GLP-1 receptor and for biological activity. *Regulatory peptides* *114*, 153-158. 10.1016/s0167-0115(03)00120-4.
- Drake, M.T., Shenoy, S.K., and Lefkowitz, R.J. (2006). Trafficking of G protein-coupled receptors. *Circ Res* *99*, 570-582. 10.1161/01.RES.0000242563.47507.ce.
- Dresner, A., Laurent, D., Marcucci, M., Griffin, M.E., Dufour, S., Cline, G.W., Slezak, L.A., Andersen, D.K., Hundal, R.S., Rothman, D.L., et al. (1999). Effects of free fatty acids on glucose transport and IRS-1-associated phosphatidylinositol 3-kinase activity. *J Clin Invest* *103*, 253-259. 10.1172/jci5001.
- Drucker, D.J. (2003). Glucagon-like peptide-1 and the islet beta-cell: augmentation of cell proliferation and inhibition of apoptosis. *Endocrinology* *144*, 5145-5148. 10.1210/en.2003-1147.
- Drucker, D.J., Philippe, J., Mojsov, S., Chick, W.L., and Habener, J.F. (1987). Glucagon-like peptide I stimulates insulin gene expression and increases cyclic AMP levels in a rat islet cell line. *Proc Natl Acad Sci U S A* *84*, 3434-3438. 10.1073/pnas.84.10.3434.
- Dupre, J., Ross, S.A., Watson, D., and Brown, J.C. (1973). Stimulation of insulin secretion by gastric inhibitory polypeptide in man. *J Clin Endocrinol Metab* *37*, 826-828. 10.1210/jcem-37-5-826.
- Ehses, J.A., Pelech, S.L., Pederson, R.A., and McIntosh, C.H. (2002). Glucose-dependent insulinotropic polypeptide activates the Raf-Mek1/2-ERK1/2 module via a cyclic AMP/cAMP-dependent protein kinase/Rap1-mediated pathway. *J Biol Chem* *277*, 37088-37097. 10.1074/jbc.M205055200.
- Eichel, K., and von Zastrow, M. (2018). Subcellular Organization of GPCR Signaling. *Trends in pharmacological sciences* *39*, 200-208. 10.1016/j.tips.2017.11.009.
- Eknoyan, G. (2021). Adolphe Quetelet (1796–1874)—the average man and indices of obesity. *Nephrology Dialysis Transplantation* *23*, 47-51. 10.1093/ndt/gfm517.
- Elahi, D., McAloon-Dyke, M., Fukagawa, N.K., Meneilly, G.S., Sclater, A.L., Minaker, K.L., Habener, J.F., and Andersen, D.K. (1994). The insulinotropic actions of glucose-dependent insulinotropic polypeptide (GIP) and glucagon-like peptide-1 (7-37) in normal and diabetic subjects. *Regulatory peptides* *51*, 63-74. 10.1016/0167-0115(94)90136-8.
- Elkin, S.R., Lakoduk, A.M., and Schmid, S.L. (2016). Endocytic pathways and endosomal trafficking: a primer. *Wiener medizinische Wochenschrift (1946)* *166*, 196-204. 10.1007/s10354-016-0432-7.
- Elks, C.E., Hoed, M.d., Zhao, J.H., Sharp, S.J., Wareham, N.J., Loos, R.J.F., and Ong, K.K. (2012). Variability in the Heritability of Body Mass Index: A Systematic Review and Meta-Regression.
- Elrick, H., Stimmler, L., Hlad, C.J., Jr., and Arai, Y. (1964). PLASMA INSULIN RESPONSE TO ORAL AND INTRAVENOUS GLUCOSE ADMINISTRATION. *J Clin Endocrinol Metab* *24*, 1076-1082. 10.1210/jcem-24-10-1076.
- Elvert, R., Bossart, M., Herling, A.W., Weiss, T., Zhang, B., Kannt, A., Wagner, M., Haack, T., Evers, A., Dudda, A., et al. (2018). Team Players or Opponents: Coadministration of Selective

- Glucagon and GLP-1 Receptor Agonists in Obese Diabetic Monkeys. *Endocrinology* 159, 3105-3119. 10.1210/en.2018-00399.
- Eng, J., Kleinman, W.A., Singh, L., Singh, G., and Raufman, J.P. (1992). Isolation and characterization of exendin-4, an exendin-3 analogue, from *Heloderma suspectum* venom. Further evidence for an exendin receptor on dispersed acini from guinea pig pancreas. *J Biol Chem* 267, 7402-7405.
- English, A.R., and Voeltz, G.K. (2013). Endoplasmic reticulum structure and interconnections with other organelles. *Cold Spring Harbor perspectives in biology* 5, a013227. 10.1101/cshperspect.a013227.
- Eskelinen, E.L. (2006). Roles of LAMP-1 and LAMP-2 in lysosome biogenesis and autophagy. *Mol Aspects Med* 27, 495-502. 10.1016/j.mam.2006.08.005.
- Fang, Z., Chen, S., Manchanda, Y., Bitsi, S., Pickford, P., David, A., Shchepinova, M.M., Corrêa, I.R., Jr., Hodson, D.J., Broichhagen, J., et al. (2020). Ligand-Specific Factors Influencing GLP-1 Receptor Post-Endocytic Trafficking and Degradation in Pancreatic Beta Cells. *International journal of molecular sciences* 21. 10.3390/ijms21218404.
- Fehmann, H.C., and Habener, J.F. (1991). Functional receptors for the insulinotropic hormone glucagon-like peptide-I(7-37) on a somatostatin secreting cell line. *FEBS letters* 279, 335-340. 10.1016/0014-5793(91)80182-3.
- Ferguson, S.S. (2001). Evolving concepts in G protein-coupled receptor endocytosis: the role in receptor desensitization and signaling. *Pharmacol Rev* 53, 1-24.
- Ferrandon, S., Feinstein, T.N., Castro, M., Wang, B., Bouley, R., Potts, J.T., Gardella, T.J., and Vilardaga, J.P. (2009). Sustained cyclic AMP production by parathyroid hormone receptor endocytosis. *Nat Chem Biol* 5, 734-742. 10.1038/nchembio.206.
- Fillion, D., Devost, D., Sleno, R., Inoue, A., and Hébert, T.E. (2019). Asymmetric Recruitment of  $\beta$ -Arrestin1/2 by the Angiotensin II Type I and Prostaglandin F<sub>2</sub> $\alpha$  Receptor Dimer. *Front Endocrinol (Lausanne)* 10, 162. 10.3389/fendo.2019.00162.
- Finan, B., Ma, T., Ottaway, N., Müller, T.D., Habegger, K.M., Heppner, K.M., Kirchner, H., Holland, J., Hembree, J., Raver, C., et al. (2013). Unimolecular dual incretins maximize metabolic benefits in rodents, monkeys, and humans. *Science translational medicine* 5. 10.1126/scitranslmed.3007218.
- Finan, B., Muller, T.D., Clemmensen, C., Perez-Tilve, D., DiMarchi, R.D., and Tschop, M.H. (2016). Reappraisal of GIP Pharmacology for Metabolic Diseases. *Trends Mol Med* 22, 359-376. 10.1016/j.molmed.2016.03.005.
- Finan, B., Yang, B., Ottaway, N., Smiley, D.L., Ma, T., Clemmensen, C., Chabenne, J., Zhang, L., Habegger, K.M., Fischer, K., et al. (2015). A rationally designed monomeric peptide triagonist corrects obesity and diabetes in rodents. *Nat Med* 21, 27-36. 10.1038/nm.3761.
- Finlay, D.B., Duffull, S.B., and Glass, M. (2020). 100 years of modelling ligand-receptor binding and response: A focus on GPCRs. *Br J Pharmacol* 177, 1472-1484. 10.1111/bph.14988.
- Flinn, R.J., and Backer, J.M. (2010). mTORC1 signals from late endosomes: taking a TOR of the endocytic system. *Cell Cycle* 9, 1869-1870. 10.4161/cc.9.10.11679.
- Flint, A., Raben, A., Astrup, A., and Holst, J.J. (1998). Glucagon-like peptide 1 promotes satiety and suppresses energy intake in humans. *J Clin Invest* 101, 515-520. 10.1172/jci990.
- Flock, T., Hauser, A.S., Lund, N., Gloriam, D.E., Balaji, S., and Babu, M.M. (2017). Selectivity determinants of GPCR-G-protein binding. *Nature* 545, 317-322. 10.1038/nature22070.
- Flock, T., Ravarani, C.N.J., Sun, D., Venkatakrishnan, A.J., Kayikci, M., Tate, C.G., Veprintsev, D.B., and Babu, M.M. (2015). Universal allosteric mechanism for Galpha activation by GPCRs. *Nature* 524, 173-179. 10.1038/nature14663.

- Frias, J.P., Bastyr, E.J., 3rd, Vignati, L., Tschöp, M.H., Schmitt, C., Owen, K., Christensen, R.H., and DiMarchi, R.D. (2017). The Sustained Effects of a Dual GIP/GLP-1 Receptor Agonist, NNC0090-2746, in Patients with Type 2 Diabetes. *Cell Metab* 26, 343-352.e342. 10.1016/j.cmet.2017.07.011.
- Frías, J.P., Davies, M.J., Rosenstock, J., Pérez Manghi, F.C., Fernández Landó, L., Bergman, B.K., Liu, B., Cui, X., and Brown, K. (2021). Tirzepatide versus Semaglutide Once Weekly in Patients with Type 2 Diabetes. *N Engl J Med* 385, 503-515. 10.1056/NEJMoa2107519.
- Frias, J.P., Nauck, M.A., Van, J., Kutner, M.E., Cui, X., Benson, C., Urva, S., Gimeno, R.E., Milicevic, Z., Robins, D., and Haupt, A. (2018). Efficacy and safety of LY3298176, a novel dual GIP and GLP-1 receptor agonist, in patients with type 2 diabetes: a randomised, placebo-controlled and active comparator-controlled phase 2 trial. *Lancet (London, England)* 392. 10.1016/S0140-6736(18)32260-8.
- Fu, Z., Gilbert, E.R., and Liu, D. (2013). Regulation of insulin synthesis and secretion and pancreatic Beta-cell dysfunction in diabetes. *Current diabetes reviews* 9, 25-53.
- Gabe, M.B.N., Sparre-Ulrich, A.H., Pedersen, M.F., Gasbjerg, L.S., Inoue, A., Bräuner-Osborne, H., Hartmann, B., and Rosenkilde, M.M. (2018). Human GIP(3-30)NH(2) inhibits G protein-dependent as well as G protein-independent signaling and is selective for the GIP receptor with high-affinity binding to primate but not rodent GIP receptors. *Biochem Pharmacol* 150, 97-107. 10.1016/j.bcp.2018.01.040.
- Gabe, M.B.N., van der Velden, W.J.C., Smit, F.X., Gasbjerg, L.S., and Rosenkilde, M.M. (2020). Molecular interactions of full-length and truncated GIP peptides with the GIP receptor – A comprehensive review. *Peptides* 125, 170224. <https://doi.org/10.1016/j.peptides.2019.170224>.
- Galsgaard, K.D., Pedersen, J., Knop, F.K., Holst, J.J., and Wewer Albrechtsen, N.J. (2019). Glucagon Receptor Signaling and Lipid Metabolism. *Front Physiol* 10, 413. 10.3389/fphys.2019.00413.
- Gao, Z., Young, R.A., Trucco, M.M., Greene, S.R., Hewlett, E.L., Matschinsky, F.M., and Wolf, B.A. (2002). Protein kinase A translocation and insulin secretion in pancreatic beta-cells: studies with adenylate cyclase toxin from *Bordetella pertussis*. *The Biochemical journal* 368, 397-404. 10.1042/bj20020999.
- Gasbjerg, L.S., Helsted, M.M., Hartmann, B., Jensen, M.H., Gabe, M.B.N., Sparre-Ulrich, A.H., Veedfald, S., Stensen, S., Lanng, A.R., Bergmann, N.C., et al. (2019). Separate and Combined Glucometabolic Effects of Endogenous Glucose-Dependent Insulinotropic Polypeptide and Glucagon-like Peptide 1 in Healthy Individuals. *Diabetes* 68, 906-917. 10.2337/db18-1123.
- Geary, N. (1990). Pancreatic glucagon signals postprandial satiety. *Neuroscience and biobehavioral reviews* 14, 323-338. 10.1016/s0149-7634(05)80042-9.
- Gervasi, N., Hepp, R., Tricoire, L., Zhang, J., Lambolez, B., Paupardin-Tritsch, D., and Vincent, P. (2007). Dynamics of protein kinase A signaling at the membrane, in the cytosol, and in the nucleus of neurons in mouse brain slices. *The Journal of neuroscience : the official journal of the Society for Neuroscience* 27, 2744-2750. 10.1523/jneurosci.5352-06.2007.
- Gilleron, J., Gerdes, J.M., and Zeigerer, A. (2019). Metabolic regulation through the endosomal system. *Traffic (Copenhagen, Denmark)* 20, 552-570. 10.1111/tra.12670.
- Girada, S.B., Kuna, R.S., Bele, S., Zhu, Z., Chakravarthi, N.R., DiMarchi, R.D., and Mitra, P. (2017). Gas regulates Glucagon-Like Peptide 1 Receptor-mediated cyclic AMP generation at Rab5 endosomal compartment. *Mol Metab* 6, 1173-1185. 10.1016/j.molmet.2017.08.002.
- González-Muniesa, P., Garcia-Gerique, L., Quintero, P., Arriaza, S., Lopez-Pascual, A., and Martinez, J.A. (2015). Effects of Hyperoxia on Oxygen-Related Inflammation with a Focus on Obesity. *Oxidative medicine and cellular longevity* 2015, 8957827. 10.1155/2016/8957827.

- Goossens, G.H., and Blaak, E.E. (2012). Adipose tissue oxygen tension: implications for chronic metabolic and inflammatory diseases. *Current opinion in clinical nutrition and metabolic care* 15. 10.1097/MCO.0b013e328358fa87.
- Gray, D.L., Allen, J.A., Mente, S., O'Connor, R.E., DeMarco, G.J., Efremov, I., Tierney, P., Volfson, D., Davoren, J., Guilmette, E., et al. (2018). Impaired  $\beta$ -arrestin recruitment and reduced desensitization by non-catechol agonists of the D1 dopamine receptor. *Nat Commun* 9, 674. 10.1038/s41467-017-02776-7.
- Graziano, M.P., Hey, P.J., Borkowski, D., Chicchi, G.G., and Strader, C.D. (1993). Cloning and functional expression of a human glucagon-like peptide-1 receptor. *Biochemical and biophysical research communications* 196, 141-146. 10.1006/bbrc.1993.2226.
- Grespan, E., Giorgino, T., Natali, A., Ferrannini, E., and Mari, A. (2021). Different mechanisms of GIP and GLP-1 action explain their different therapeutic efficacy in type 2 diabetes. *Metabolism: clinical and experimental* 114, 154415. 10.1016/j.metabol.2020.154415.
- Gribble, F.M., Williams, L., Simpson, A.K., and Reimann, F. (2003). A novel glucose-sensing mechanism contributing to glucagon-like peptide-1 secretion from the GLUTag cell line. *Diabetes* 52, 1147-1154. 10.2337/diabetes.52.5.1147.
- Gromada, J., Franklin, I., and Wollheim, C.B. (2007). Alpha-cells of the endocrine pancreas: 35 years of research but the enigma remains. *Endocrine reviews* 28, 84-116. 10.1210/er.2006-0007.
- Grundmann, M., Merten, N., Malfacini, D., Inoue, A., Preis, P., Simon, K., Rüttiger, N., Ziegler, N., Benkel, T., Schmitt, N.K., et al. (2018). Lack of beta-arrestin signaling in the absence of active G proteins. *Nat Commun* 9, 341. 10.1038/s41467-017-02661-3.
- Guenifi, A., Portela-Gomes, G.M., Grimelius, L., Efendić, S., and Abdel-Halim, S.M. (2000). Adenylyl cyclase isoform expression in non-diabetic and diabetic Goto-Kakizaki (GK) rat pancreas. Evidence for distinct overexpression of type-8 adenylyl cyclase in diabetic GK rat islets. *Histochem Cell Biol* 113, 81-89. 10.1007/s004180050010.
- Guerra, F., and Bucci, C. (2016). Multiple Roles of the Small GTPase Rab7. *Cells* 5. 10.3390/cells5030034.
- Guo, S., Zhang, X., Zheng, M., Zhang, X., Min, C., Wang, Z., Cheon, S.H., Oak, M.H., Nah, S.Y., and Kim, K.M. (2015). Selectivity of commonly used inhibitors of clathrin-mediated and caveolae-dependent endocytosis of G protein-coupled receptors. *Biochimica et biophysica acta* 1848, 2101-2110. 10.1016/j.bbamem.2015.05.024.
- Habegger, K.M., Heppner, K.M., Geary, N., Bartness, T.J., DiMarchi, R., and Tschöp, M.H. (2010). The metabolic actions of glucagon revisited. *Nat Rev Endocrinol* 6, 689-697. 10.1038/nrendo.2010.187.
- Hager, M.V., Clydesdale, L., Gellman, S.H., Sexton, P.M., and Wootten, D. (2017). Characterization of signal bias at the GLP-1 receptor induced by backbone modification of GLP-1. *Biochem Pharmacol* 136, 99-108. 10.1016/j.bcp.2017.03.018.
- Hager, M.V., Johnson, L.M., Wootten, D., Sexton, P.M., and Gellman, S.H. (2016).  $\beta$ -Arrestin-Biased Agonists of the GLP-1 Receptor from  $\beta$ -Amino Acid Residue Incorporation into GLP-1 Analogues. *J Am Chem Soc* 138, 14970-14979. 10.1021/jacs.6b08323.
- Hällbrink, M., Holmqvist, T., Olsson, M., Ostenson, C.G., Efendic, S., and Langel, U. (2001). Different domains in the third intracellular loop of the GLP-1 receptor are responsible for Galpha(s) and Galpha(i)/Galpha(o) activation. *Biochimica et biophysica acta* 1546, 79-86. 10.1016/s0167-4838(00)00270-3.
- Hansen, K.B., Vilsbøll, T., Bagger, J.I., Holst, J.J., and Knop, F.K. (2010). Reduced glucose tolerance and insulin resistance induced by steroid treatment, relative physical inactivity,



- and high-calorie diet impairs the incretin effect in healthy subjects. *J Clin Endocrinol Metab* **95**, 3309-3317. 10.1210/jc.2010-0119.
- Hansen, L., Deacon, C.F., Orskov, C., and Holst, J.J. (1999). Glucagon-like peptide-1-(7-36)amide is transformed to glucagon-like peptide-1-(9-36)amide by dipeptidyl peptidase IV in the capillaries supplying the L cells of the porcine intestine. *Endocrinology* **140**, 5356-5363. 10.1210/endo.140.11.7143.
- Harada, N., and Inagaki, N. (2017). Role of GIP receptor signaling in  $\beta$ -cell survival. *Diabetol Int* **8**, 137-138. 10.1007/s13340-017-0317-z.
- Harada, N., Yamada, Y., Tsukiyama, K., Yamada, C., Nakamura, Y., Mukai, E., Hamasaki, A., Liu, X., Toyoda, K., Seino, Y., and Inagaki, N. (2008). A novel GIP receptor splice variant influences GIP sensitivity of pancreatic beta-cells in obese mice. *Am J Physiol Endocrinol Metab* **294**, E61-68. 10.1152/ajpendo.00358.2007.
- Harris, M., Mackie, D.I., Pawlak, J.B., Carvalho, S., Truong, T.T., Safitri, D., Yeung, H.Y., Routledge, S., Harper, M.T., Al-Zaid, B., et al. (2021). RAMPs regulate signalling bias and internalisation of the GIPR. *bioRxiv*, 2021.2004.2008.436756. 10.1101/2021.04.08.436756.
- Hausdorff, W.P., Campbell, P.T., Ostrowski, J., Yu, S.S., Caron, M.G., and Lefkowitz, R.J. (1991). A small region of the beta-adrenergic receptor is selectively involved in its rapid regulation. *Proc Natl Acad Sci U S A* **88**, 2979-2983. 10.1073/pnas.88.8.2979.
- Hauser, A.S., Attwood, M.M., Rask-Andersen, M., Schiöth, H.B., and Gloriam, D.E. (2017). Trends in GPCR drug discovery: new agents, targets and indications. *Nature reviews. Drug discovery* **16**, 829-842. 10.1038/nrd.2017.178.
- Hayes, M.R. (2012). Neuronal and intracellular signaling pathways mediating GLP-1 energy balance and glycemic effects. *Physiol Behav* **106**, 413-416. 10.1016/j.physbeh.2012.02.017.
- Haynes, W.G., Morgan, D.A., Djalali, A., Sivitz, W.I., and Mark, A.L. (1999). Interactions between the melanocortin system and leptin in control of sympathetic nerve traffic. *Hypertension (Dallas, Tex. : 1979)* **33**, 542-547. 10.1161/01.hyp.33.1.542.
- Heaney, J. (2013). Energy: Expenditure, Intake, Lack of. In *Encyclopedia of Behavioral Medicine*, M.D. Gellman, and J.R. Turner, eds. (Springer New York), pp. 699-700. 10.1007/978-1-4419-1005-9\_454.
- Heng, B.C., Aubel, D., and Fussenegger, M. (2013). An overview of the diverse roles of G-protein coupled receptors (GPCRs) in the pathophysiology of various human diseases. *Biotechnology advances* **31**, 1676-1694. 10.1016/j.biotechadv.2013.08.017.
- Henley, J.R., Krueger, E.W., Oswald, B.J., and McNiven, M.A. (1998). Dynamin-mediated internalization of caveolae. *J Cell Biol* **141**, 85-99. 10.1083/jcb.141.1.85.
- Himsworth, H.P. (1936). Diabetes Mellitus: Its differentiation into insulin-sensitive and insulin-insensitive types. *The Lancet* **227**, 127-130. 10.1016/S0140-6736(01)36134-2.
- Hinke, S.A., Manhart, S., Speck, M., Pederson, R.A., Demuth, H.U., and McIntosh, C.H. (2004). In depth analysis of the N-terminal bioactive domain of gastric inhibitory polypeptide. *Life sciences* **75**, 1857-1870. 10.1016/j.lfs.2004.03.024.
- Hjorth, S.A., Adelhorst, K., Pedersen, B.B., Kirk, O., and Schwartz, T.W. (1994). Glucagon and glucagon-like peptide 1: selective receptor recognition via distinct peptide epitopes. *J Biol Chem* **269**, 30121-30124.
- Højberg, P.V., Vilsbøll, T., Rabøl, R., Knop, F.K., Bache, M., Krarup, T., Holst, J.J., and Madsbad, S. (2009). Four weeks of near-normalisation of blood glucose improves the insulin response to glucagon-like peptide-1 and glucose-dependent insulinotropic polypeptide in patients with type 2 diabetes. *Diabetologia* **52**, 199-207. 10.1007/s00125-008-1195-5.
- Holford, N. (2017). Pharmacodynamic principles and the time course of immediate drug effects. *Translational and clinical pharmacology* **25**, 157-161. 10.12793/tcp.2017.25.4.157.

- Holst, J.J., Knop, F.K., Vilsbøll, T., Krarup, T., and Madsbad, S. (2011). Loss of incretin effect is a specific, important, and early characteristic of type 2 diabetes. *Diabetes Care* *34 Suppl 2*, S251-257. 10.2337/dc11-s227.
- Holst, J.J., Orskov, C., Nielsen, O.V., and Schwartz, T.W. (1987). Truncated glucagon-like peptide I, an insulin-releasing hormone from the distal gut. *FEBS letters* *211*, 169-174. 10.1016/0014-5793(87)81430-8.
- Holst, J.J., and Rosenkilde, M.M. (2020). GIP as a Therapeutic Target in Diabetes and Obesity: Insight From Incretin Co-agonists. *J Clin Endocrinol Metab* *105*, e2710-2716. 10.1210/clinem/dgaa327.
- Holz, G.G. (2004). New insights concerning the glucose-dependent insulin secretagogue action of glucagon-like peptide-1 in pancreatic beta-cells. *Hormone and metabolic research = Hormon- und Stoffwechselforschung = Hormones et métabolisme* *36*, 787-794. 10.1055/s-2004-826165.
- Hruby, A., Manson, J.E., Qi, L., Malik, V.S., Rimm, E.B., Sun, Q., Willett, W.C., and Hu, F.B. (2016). Determinants and Consequences of Obesity. *Am J Public Health* *106*, 1656-1662. 10.2105/ajph.2016.303326.
- Huang, X., Dai, F.F., Gaisano, G., Giglou, K., Han, J., Zhang, M., Kittanakom, S., Wong, V., Wei, L., Showalter, A.D., et al. (2013). The identification of novel proteins that interact with the GLP-1 receptor and restrain its activity. *Mol Endocrinol* *27*, 1550-1563. 10.1210/me.2013-1047.
- Huang, Y., Wilkinson, G.F., and Willars, G.B. (2010). Role of the signal peptide in the synthesis and processing of the glucagon-like peptide-1 receptor. *Br J Pharmacol* *159*, 237-251. 10.1111/j.1476-5381.2009.00517.x.
- Huising, M.O. (2020). Paracrine regulation of insulin secretion. *Diabetologia* *63*, 2057-2063. 10.1007/s00125-020-05213-5.
- Iizuka, K., Tomita, R., Suwa, T., Horikawa, Y., and Takeda, J. (2012). Normalization of fasting hyperglycemia is beneficial for successful introduction of small amount of the GLP-1 analog liraglutide in an obese patient with type 2 diabetes mellitus. *Diabetology International* *3*, 61-64. 10.1007/s13340-011-0052-9.
- Imeryüz, N., Yeğen, B.C., Bozkurt, A., Coşkun, T., Villanueva-Peñacarrillo, M.L., and Ulusoy, N.B. (1997). Glucagon-like peptide-1 inhibits gastric emptying via vagal afferent-mediated central mechanisms. *Am J Physiol* *273*, G920-927. 10.1152/ajpgi.1997.273.4.G920.
- Iozzo, P., Pratipanawat, T., Pijl, H., Vogt, C., Kumar, V., Pipek, R., Matsuda, M., Mandarino, L.J., Cusi, K.J., and DeFronzo, R.A. (2001). Physiological hyperinsulinemia impairs insulin-stimulated glycogen synthase activity and glycogen synthesis. *American journal of physiology. Endocrinology and metabolism* *280*. 10.1152/ajpendo.2001.280.5.E712.
- Ismail, S., Dubois-Vedrenne, I., Laval, M., Tikhonova, I.G., D'Angelo, R., Sanchez, C., Clerc, P., Gherardi, M.J., Gigoux, V., Magnan, R., and Fourmy, D. (2015). Internalization and desensitization of the human glucose-dependent-insulinotropic receptor is affected by N-terminal acetylation of the agonist. *Mol Cell Endocrinol* *414*, 202-215. 10.1016/j.mce.2015.07.001.
- Iyengar, R., Rich, K.A., Herberg, J.T., Premont, R.T., and Codina, J. (1988). Glucagon receptor-mediated activation of Gs is accompanied by subunit dissociation. *J Biol Chem* *263*, 15348-15353.
- Jean-Charles, P.Y., Kaur, S., and Shenoy, S.K. (2017). G Protein-Coupled Receptor Signaling Through  $\beta$ -Arrestin-Dependent Mechanisms. *Journal of cardiovascular pharmacology* *70*, 142-158. 10.1097/fjc.0000000000000482.

- Jiang, L.I., Collins, J., Davis, R., Lin, K.M., DeCamp, D., Roach, T., Hsueh, R., Rebres, R.A., Ross, E.M., Taussig, R., et al. (2007). Use of a cAMP BRET sensor to characterize a novel regulation of cAMP by the sphingosine 1-phosphate/G13 pathway. *J Biol Chem* 282, 10576-10584. 10.1074/jbc.M609695200.
- Jones, B. (2021). The therapeutic potential of GLP-1 receptor biased agonism. *Br J Pharmacol*. 10.1111/bph.15497.
- Jones, B., Buenaventura, T., Kanda, N., Chabosseau, P., Owen, B.M., Scott, R., Goldin, R., Angkathunyakul, N., Corrêa, I.R., Bosco, D., et al. (2018a). Targeting GLP-1 receptor trafficking to improve agonist efficacy. *Nature communications* 9. 10.1038/s41467-018-03941-2.
- Jones, B., Buenaventura, T., Kanda, N., Chabosseau, P., Owen, B.M., Scott, R., Goldin, R., Angkathunyakul, N., Correa, I.R., Jr., Bosco, D., et al. (2018b). Targeting GLP-1 receptor trafficking to improve agonist efficacy. *Nat Commun* 9, 1602. 10.1038/s41467-018-03941-2.
- Jones, B., McGlone, E.R., Fang, Z., Pickford, P., Corrêa, I.R., Jr., Oishi, A., Jockers, R., Inoue, A., Kumar, S., Görlitz, F., et al. (2021). Genetic and biased agonist-mediated reductions in  $\beta$ -arrestin recruitment prolong cAMP signaling at glucagon family receptors. *J Biol Chem* 296, 100133. 10.1074/jbc.RA120.016334.
- Jones, B., McGlone, E.R., Fang, Z., Pickford, P., Corrêa, I.R., Kumar, S., Görlitz, F., Dunsby, C., French, P.M.W., Rutter, G.A., et al. (2020a). Impact of N-terminally substituted glucagon family receptor agonists on signal bias, trafficking and downstream responses. *bioRxiv*, 2020.2004.2026.062372. 10.1101/2020.04.26.062372.
- Jones, B., McGlone, E.R., Fang, Z., Pickford, P., Corrêa, I.R., Oishi, A., Jockers, R., Inoue, A., Kumar, S., Görlitz, F., et al. (2020b). Signal bias at glucagon family receptors: rationale and downstream impacts. *bioRxiv*, 2020.2004.2026.062372. 10.1101/2020.04.26.062372.
- Jones, J.R., Caul, W.F., and Hill, J.O. (1992). The effects of amphetamine on body weight and energy expenditure. *Physiol Behav* 51, 607-611. 10.1016/0031-9384(92)90187-7.
- Jorgensen, R., Martini, L., Schwartz, T.W., and Elling, C.E. (2005). Characterization of glucagon-like peptide-1 receptor beta-arrestin 2 interaction: a high-affinity receptor phenotype. *Mol Endocrinol* 19, 812-823. 10.1210/me.2004-0312.
- Kaihara, K.A., Dickson, L.M., Jacobson, D.A., Tamarina, N., Roe, M.W., Philipson, L.H., and Wicksteed, B. (2013).  $\beta$ -Cell-specific protein kinase A activation enhances the efficiency of glucose control by increasing acute-phase insulin secretion. *Diabetes* 62, 1527-1536. 10.2337/db12-1013.
- Kaksonen, M., and Roux, A. (2018). Mechanisms of clathrin-mediated endocytosis. *Nat Rev Mol Cell Biol* 19, 313-326. 10.1038/nrm.2017.132.
- Kalra, S., and Sahay, R. (2020). A Review on Semaglutide: An Oral Glucagon-Like Peptide 1 Receptor Agonist in Management of Type 2 Diabetes Mellitus. *Diabetes therapy : research, treatment and education of diabetes and related disorders* 11, 1965-1982. 10.1007/s13300-020-00894-y.
- Karra, E., Chandarana, K., and Batterham, R.L. (2009). The role of peptide YY in appetite regulation and obesity. *The Journal of physiology* 587, 19-25. 10.1113/jphysiol.2008.164269.
- Katritch, V., Cherezov, V., and Stevens, R.C. (2012). Diversity and modularity of G protein-coupled receptor structures. *Trends in pharmacological sciences* 33, 17-27. 10.1016/j.tips.2011.09.003.
- Kelly, T., Yang, W., Chen, C., Reynolds, K., and He, J. (2008). Global burden of obesity in 2005 and projections to 2030. *International Journal of Obesity* 32, 1431-1437. doi:10.1038/ijo.2008.102.

- Khera, A.V., Chaffin, M., Wade, K.H., Zahid, S., Brancale, J., Xia, R., Distefano, M., Senol-Cosar, O., Haas, M.E., Bick, A., et al. (2019). Polygenic prediction of weight and obesity trajectories from birth to adulthood. *Cell*.
- Kieffer, T.J., McIntosh, C.H., and Pederson, R.A. (1995). Degradation of glucose-dependent insulinotropic polypeptide and truncated glucagon-like peptide 1 in vitro and in vivo by dipeptidyl peptidase IV. *Endocrinology* *136*, 3585-3596. 10.1210/endo.136.8.7628397.
- Killion, E.A., Wang, J., Yie, J., Shi, S.D., Bates, D., Min, X., Komorowski, R., Hager, T., Deng, L., Atangan, L., et al. (2018). Anti-obesity effects of GIPR antagonists alone and in combination with GLP-1R agonists in preclinical models. *Sci Transl Med* *10*. 10.1126/scitranslmed.aat3392.
- Kitaguchi, T., Oya, M., Wada, Y., Tsuboi, T., and Miyawaki, A. (2013). Extracellular calcium influx activates adenylate cyclase 1 and potentiates insulin secretion in MIN6 cells. *The Biochemical journal* *450*, 365-373. 10.1042/bj20121022.
- Kizilkaya, H.S., Sørensen, K.V., Kibsgaard, C.J., Gasbjerg, L.S., Hauser, A.S., Sparre-Ulrich, A.H., Grarup, N., and Rosenkilde, M.M. (2021). Loss of Function Glucose-Dependent Insulinotropic Polypeptide Receptor Variants Are Associated With Alterations in BMI, Bone Strength and Cardiovascular Outcomes. *Frontiers in cell and developmental biology* *9*. 10.3389/fcell.2021.749607.
- Knudsen, L.B., Hastrup, S., Underwood, C.R., Wulff, B.S., and Fleckner, J. (2012). Functional importance of GLP-1 receptor species and expression levels in cell lines. *Regulatory peptides* *175*, 21-29. 10.1016/j.regpep.2011.12.006.
- Knudsen, L.B., and Lau, J. (2019). The Discovery and Development of Liraglutide and Semaglutide. *Front Endocrinol (Lausanne)* *10*, 155. 10.3389/fendo.2019.00155.
- Kong, W., Stanley, S., Gardiner, J., Abbott, C., Murphy, K., Seth, A., Connoley, I., Ghatei, M., Stephens, D., and Bloom, S. (2003). A role for arcuate cocaine and amphetamine-regulated transcript in hyperphagia, thermogenesis, and cold adaptation. *FASEB journal : official publication of the Federation of American Societies for Experimental Biology* *17*, 1688-1690. 10.1096/fj.02-0805fje.
- Koole, C., Wootten, D., Simms, J., Valant, C., Sridhar, R., Woodman, O.L., Miller, L.J., Summers, R.J., Christopoulos, A., and Sexton, P.M. (2010). Allosteric ligands of the glucagon-like peptide 1 receptor (GLP-1R) differentially modulate endogenous and exogenous peptide responses in a pathway-selective manner: implications for drug screening. *Mol Pharmacol* *78*, 456-465. 10.1124/mol.110.065664.
- Koster, J.C., Permutt, M.A., and Nichols, C.G. (2005). Diabetes and insulin secretion: the ATP-sensitive K<sup>+</sup> channel (K ATP) connection. *Diabetes* *54*, 3065-3072. 10.2337/diabetes.54.11.3065.
- Kovtun, O., Dickson, V.K., Kelly, B.T., Owen, D.J., and Briggs, J.A.G. (2020). Architecture of the AP2/clathrin coat on the membranes of clathrin-coated vesicles. *Science advances* *6*, eaba8381. 10.1126/sciadv.aba8381.
- Kreymann, B., Williams, G., Ghatei, M.A., and Bloom, S.R. (1987). Glucagon-like peptide-1 7-36: a physiological incretin in man. *Lancet* *2*, 1300-1304. 10.1016/s0140-6736(87)91194-9.
- Krumm, B., and Roth, B.L. (2020). A Structural Understanding of Class B GPCR Selectivity and Activation Revealed. *Structure (London, England : 1993)* *28*, 277-279. 10.1016/j.str.2020.02.004.
- Kucera, A., Bakke, O., and Progidia, C. (2016). The multiple roles of Rab9 in the endolysosomal system. *Commun Integr Biol* *9*, e1204498. 10.1080/19420889.2016.1204498.
- Kuna, R.S., Girada, S.B., Asalla, S., Vallentyne, J., Maddika, S., Patterson, J.T., Smiley, D.L., DiMarchi, R.D., and Mitra, P. (2013). Glucagon-like peptide-1 receptor-mediated endosomal

- cAMP generation promotes glucose-stimulated insulin secretion in pancreatic  $\beta$ -cells. *Am J Physiol Endocrinol Metab* 305, E161-170. 10.1152/ajpendo.00551.2012.
- Kurzchalia, T.V., and Parton, R.G. (1999). Membrane microdomains and caveolae. *Curr Opin Cell Biol* 11, 424-431. 10.1016/s0955-0674(99)80061-1.
- Kwik, J., Boyle, S., Fooksman, D., Margolis, L., Sheetz, M.P., and Edidin, M. (2003). Membrane cholesterol, lateral mobility, and the phosphatidylinositol 4,5-bisphosphate-dependent organization of cell actin. *Proc Natl Acad Sci U S A* 100, 13964-13969. 10.1073/pnas.2336102100.
- Lakadamyali, M., Rust, M.J., and Zhuang, X. (2006). Ligands for clathrin-mediated endocytosis are differentially sorted into distinct populations of early endosomes. *Cell* 124, 997-1009. 10.1016/j.cell.2005.12.038.
- Lan, T.H., Kuravi, S., and Lambert, N.A. (2011). Internalization Dissociates  $\beta$ 2-Adrenergic Receptors. *PLoS One* 6. 10.1371/journal.pone.0017361.
- Lau, J., Bloch, P., Schäffer, L., Pettersson, I., Spetzler, J., Kofoed, J., Madsen, K., Knudsen, L.B., McGuire, J., Steensgaard, D.B., et al. (2015). Discovery of the Once-Weekly Glucagon-Like Peptide-1 (GLP-1) Analogue Semaglutide. *Journal of medicinal chemistry* 58, 7370-7380. 10.1021/acs.jmedchem.5b00726.
- Lee, A., Cardel, M., and Donahoo, W.T. (2019). Social and Environmental Factors Influencing Obesity. <https://www.ncbi.nlm.nih.gov/books/NBK278977/>.
- Lee, H., Park, D.S., Wang, X.B., Scherer, P.E., Schwartz, P.E., and Lisanti, M.P. (2002). Src-induced phosphorylation of caveolin-2 on tyrosine 19. Phospho-caveolin-2 (Tyr(P)19) is localized near focal adhesions, remains associated with lipid rafts/caveolae, but no longer forms a high molecular mass hetero-oligomer with caveolin-1. *J Biol Chem* 277, 34556-34567. 10.1074/jbc.M204367200.
- Lee, J., and Pilch, P.F. (1994). The insulin receptor: structure, function, and signaling. *Am J Physiol* 266, C319-334. 10.1152/ajpcell.1994.266.2.C319.
- Lee, S.M., Booe, J.M., and Pioszak, A.A. (2015). Structural insights into ligand recognition and selectivity for classes A, B, and C GPCRs. *European journal of pharmacology* 763, 196-205. 10.1016/j.ejphar.2015.05.013.
- Lefkowitz, R.J. (1998). G protein-coupled receptors. III. New roles for receptor kinases and beta-arrestins in receptor signaling and desensitization. *J Biol Chem* 273, 18677-18680. 10.1074/jbc.273.30.18677.
- Li, H., Li, H.F., Felder, R.A., Periasamy, A., and Jose, P.A. (2008). Rab4 and Rab11 coordinately regulate the recycling of angiotensin II type I receptor as demonstrated by fluorescence resonance energy transfer microscopy. *J Biomed Opt* 13, 031206. 10.1117/1.2943286.
- Liberini, C.G., Koch-Laskowski, K., Shaulson, E., McGrath, L.E., Lipsky, R.K., Lhamo, R., Ghidewon, M., Ling, T., Stein, L.M., and Hayes, M.R. (2019). Combined Amylin/GLP-1 pharmacotherapy to promote and sustain long-lasting weight loss. *Scientific reports* 9, 8447. 10.1038/s41598-019-44591-8.
- Liggett, S.B. (2011). Phosphorylation barcoding as a mechanism of directing GPCR signaling. *Science signaling* 4, pe36. 10.1126/scisignal.2002331.
- Lin, F.T., Chen, W., Shenoy, S., Cong, M., Exum, S.T., and Lefkowitz, R.J. (2002). Phosphorylation of beta-arrestin2 regulates its function in internalization of beta(2)-adrenergic receptors. *Biochemistry* 41, 10692-10699. 10.1021/bi025705n.
- Lin, F.T., Daaka, Y., and Lefkowitz, R.J. (1998). beta-arrestins regulate mitogenic signaling and clathrin-mediated endocytosis of the insulin-like growth factor I receptor. *J Biol Chem* 273, 31640-31643. 10.1074/jbc.273.48.31640.

- Lin, F.T., Miller, W.E., Luttrell, L.M., and Lefkowitz, R.J. (1999). Feedback regulation of beta-arrestin1 function by extracellular signal-regulated kinases. *J Biol Chem* 274, 15971-15974. 10.1074/jbc.274.23.15971.
- Lingvay, I., Hansen, T., Macura, S., Marre, M., Nauck, M.A., de la Rosa, R., Woo, V., Yildirim, E., and Wilding, J. (2020). Superior weight loss with once-weekly semaglutide versus other glucagon-like peptide-1 receptor agonists is independent of gastrointestinal adverse events. *BMJ open diabetes research & care* 8. 10.1136/bmjdr-2020-001706.
- Liu, J., and Pang, Z.P. (2016). Glucagon-like peptide-1 drives energy metabolism on the synaptic highway. *The FEBS journal* 283, 4413-4423. 10.1111/febs.13785.
- Liu, X., Xu, X., Hilger, D., Aschauer, P., Tiemann, J.K.S., Du, Y., Liu, H., Hirata, K., Sun, X., Guixà-González, R., et al. (2019). Structural Insights into the Process of GPCR-G Protein Complex Formation. *Cell* 177, 1243-1251.e1212. 10.1016/j.cell.2019.04.021.
- Longo, M., Zatterale, F., Naderi, J., Parrillo, L., Formisano, P., Raciti, G.A., Beguinot, F., and Miele, C. (2019). Adipose Tissue Dysfunction as Determinant of Obesity-Associated Metabolic Complications. *International journal of molecular sciences* 20. 10.3390/ijms20092358.
- Lønsmann, I., and Bak, L.K. (2020). Potential role of adenylyl cyclase 8 signaling complexes in regulating insulin secretion from pancreatic beta cells. *Cell Signal* 72, 109635. 10.1016/j.cellsig.2020.109635.
- Lu, J., and Willars, G.B. (2019). Endothelin-converting enzyme-1 regulates glucagon-like peptide-1 receptor signalling and resensitisation. *The Biochemical journal* 476, 513-533. 10.1042/bcj20180853.
- Lucey, M., Pickford, P., Bitsi, S., Minnion, J., Ungewiss, J., Schoeneberg, K., Rutter, G.A., Bloom, S.R., Tomas, A., and Jones, B. (2020). Disconnect between signalling potency and in vivo efficacy of pharmacokinetically optimised biased glucagon-like peptide-1 receptor agonists. *Mol Metab* 37, 100991. 10.1016/j.molmet.2020.100991.
- Ludvik, B., Giorgino, F., Jodar, E., Frias, J.P., Lando, L.F., Brown, K., Bray, R., and Rodríguez, Á. (2021). 78-LB: Efficacy and Safety of Tirzepatide, a Dual GIP/GLP-1 Receptor Agonist, Compared with Insulin Degludec in Patients with Type 2 Diabetes (SURPASS-3). *Diabetes* 70, 78-LB. 10.2337/db21-78-LB.
- Luttrell, L.M., Daaka, Y., Della Rocca, G.J., and Lefkowitz, R.J. (1997). G protein-coupled receptors mediate two functionally distinct pathways of tyrosine phosphorylation in rat 1a fibroblasts. Shc phosphorylation and receptor endocytosis correlate with activation of Erk kinases. *J Biol Chem* 272, 31648-31656. 10.1074/jbc.272.50.31648.
- Lutz, T.A. (2005). Pancreatic amylin as a centrally acting satiating hormone. *Current drug targets* 6, 181-189. 10.2174/1389450053174596.
- MacDonald, P.E., El-Kholy, W., Riedel, M.J., Salapatek, A.M., Light, P.E., and Wheeler, M.B. (2002). The multiple actions of GLP-1 on the process of glucose-stimulated insulin secretion. *Diabetes* 51 Suppl 3, S434-442. 10.2337/diabetes.51.2007.s434.
- MacDonald, P.E., Wang, X., Xia, F., El-kholy, W., Targonsky, E.D., Tsushima, R.G., and Wheeler, M.B. (2003). Antagonism of rat beta-cell voltage-dependent K<sup>+</sup> currents by exendin 4 requires dual activation of the cAMP/protein kinase A and phosphatidylinositol 3-kinase signaling pathways. *J Biol Chem* 278, 52446-52453. 10.1074/jbc.M307612200.
- Madsbad, S. (2016). Review of head-to-head comparisons of glucagon-like peptide-1 receptor agonists. *Diabetes Obes Metab* 18, 317-332. 10.1111/dom.12596.
- Madugula, V., and Lu, L. (2016). A ternary complex comprising transportin1, Rab8 and the ciliary targeting signal directs proteins to ciliary membranes. *Journal of cell science* 129, 3922-3934. 10.1242/jcs.194019.

- Mahammad, S., and Parmryd, I. (2015). Cholesterol depletion using methyl- $\beta$ -cyclodextrin. *Methods Mol Biol* 1232, 91-102. 10.1007/978-1-4939-1752-5\_8.
- Makki, K., Froguel, P., and Wolowczuk, I. (2013). Adipose Tissue in Obesity-Related Inflammation and Insulin Resistance: Cells, Cytokines, and Chemokines. *ISRN Inflammation* 2013. <https://doi.org/10.1155/2013/139239>.
- Marks, M.S., Woodruff, L., Ohno, H., and Bonifacino, J.S. (1996). Protein targeting by tyrosine- and di-leucine-based signals: evidence for distinct saturable components. *J Cell Biol* 135, 341-354. 10.1083/jcb.135.2.341.
- Martin, B.R., and Lambert, N.A. (2016). Activated G Protein G $\alpha$ s Samples Multiple Endomembrane Compartments. *J Biol Chem* 291, 20295-20302. 10.1074/jbc.M116.729731.
- Marzook, A., Tomas, A., and Jones, B. (2021). The Interplay of Glucagon-Like Peptide-1 Receptor Trafficking and Signalling in Pancreatic Beta Cells. *Front Endocrinol (Lausanne)* 12, 678055. 10.3389/fendo.2021.678055.
- Matschinsky, F.M. (2002). Regulation of pancreatic beta-cell glucokinase: from basics to therapeutics. *Diabetes* 51 Suppl 3, S394-404. 10.2337/diabetes.51.2007.s394.
- Maxfield, F.R., and McGraw, T.E. (2004). Endocytic recycling. *Nat Rev Mol Cell Biol* 5, 121-132. 10.1038/nrm1315.
- Mayor, S., Parton, R.G., and Donaldson, J.G. (2014). Clathrin-independent pathways of endocytosis. *Cold Spring Harbor perspectives in biology* 6. 10.1101/cshperspect.a016758.
- McClean, P.L., Irwin, N., Cassidy, R.S., Holst, J.J., Gault, V.A., and Flatt, P.R. (2007). GIP receptor antagonism reverses obesity, insulin resistance, and associated metabolic disturbances induced in mice by prolonged consumption of high-fat diet. *Am J Physiol Endocrinol Metab* 293, E1746-1755. 10.1152/ajpendo.00460.2007.
- McCudden, C.R., Hains, M.D., Kimple, R.J., Siderovski, D.P., and Willard, F.S. (2005). G-protein signaling: back to the future. *Cellular and Molecular Life Sciences* 62, 551-577. 10.1007/s00018-004-4462-3.
- McCulloch, L.J., van de Bunt, M., Braun, M., Frayn, K.N., Clark, A., and Gloyn, A.L. (2011). GLUT2 (SLC2A2) is not the principal glucose transporter in human pancreatic beta cells: implications for understanding genetic association signals at this locus. *Molecular genetics and metabolism* 104, 648-653. 10.1016/j.ymgme.2011.08.026.
- McIntyre, N., Holdsworth, C.D., and Turner, D.S. (1964). NEW INTERPRETATION OF ORAL GLUCOSE TOLERANCE. *Lancet* 2, 20-21. 10.1016/s0140-6736(64)90011-x.
- Mehta, S., Zhang, Y., Roth, R.H., Zhang, J.F., Mo, A., Tenner, B., Haganir, R.L., and Zhang, J. (2018). Single-fluorophore biosensors for sensitive and multiplexed detection of signalling activities. *Nat Cell Biol* 20, 1215-1225. 10.1038/s41556-018-0200-6.
- Meier, J.J. (2012). GLP-1 receptor agonists for individualized treatment of type 2 diabetes mellitus. *Nature reviews. Endocrinology* 8, 728-742. 10.1038/nrendo.2012.140.
- Meier, J.J., Gallwitz, B., Kask, B., Deacon, C.F., Holst, J.J., Schmidt, W.E., and Nauck, M.A. (2004). Stimulation of insulin secretion by intravenous bolus injection and continuous infusion of gastric inhibitory polypeptide in patients with type 2 diabetes and healthy control subjects. *Diabetes* 53 Suppl 3, S220-224. 10.2337/diabetes.53.suppl\_3.s220.
- Meier, J.J., and Nauck, M.A. (2010). Is the diminished incretin effect in type 2 diabetes just an epi-phenomenon of impaired beta-cell function? *Diabetes* 59, 1117-1125. 10.2337/db09-1899.
- Mettlen, M., Chen, P.H., Srinivasan, S., Danuser, G., and Schmid, S.L. (2018). Regulation of Clathrin-Mediated Endocytosis. *Annual review of biochemistry* 87, 871-896. 10.1146/annurev-biochem-062917-012644.

- Milligan, G., and Kostenis, E. (2006). Heterotrimeric G-proteins: a short history. *Br J Pharmacol* *147 Suppl 1*, S46-55. 10.1038/sj.bjp.0706405.
- Min, T., and Bain, S.C. (2021). The Role of Tirzepatide, Dual GIP and GLP-1 Receptor Agonist, in the Management of Type 2 Diabetes: The SURPASS Clinical Trials. *Diabetes Ther* *12*, 143-157. 10.1007/s13300-020-00981-0.
- Mizuno, N., and Itoh, H. (2009). Functions and regulatory mechanisms of Gq-signaling pathways. *Neurosignals* *17*, 42-54. 10.1159/000186689.
- Mohammad, S., Patel, R.T., Bruno, J., Panhwar, M.S., Wen, J., and McGraw, T.E. (2014). A naturally occurring GIP receptor variant undergoes enhanced agonist-induced desensitization, which impairs GIP control of adipose insulin sensitivity. *Molecular and cellular biology* *34*, 3618-3629. 10.1128/mcb.00256-14.
- Mohammad, S., Ramos, L.S., Buck, J., Levin, L.R., Rubino, F., and McGraw, T.E. (2011). Gastric inhibitory peptide controls adipose insulin sensitivity via activation of cAMP-response element-binding protein and p110 $\beta$  isoform of phosphatidylinositol 3-kinase. *J Biol Chem* *286*, 43062-43070. 10.1074/jbc.M111.289009.
- Mojsov, S., Heinrich, G., Wilson, I.B., Ravazzola, M., Orci, L., and Habener, J.F. (1986). Preproglucagon gene expression in pancreas and intestine diversifies at the level of post-translational processing. *J Biol Chem* *261*, 11880-11889.
- Mojsov, S., Weir, G.C., and Habener, J.F. (1987). Insulinotropin: glucagon-like peptide I (7-37) co-encoded in the glucagon gene is a potent stimulator of insulin release in the perfused rat pancreas. *J Clin Invest* *79*, 616-619. 10.1172/jci112855.
- Montrose-Rafizadeh, C., Avdonin, P., Garant, M.J., Rodgers, B.D., Kole, S., Yang, H., Levine, M.A., Schwindinger, W., and Bernier, M. (1999a). Pancreatic glucagon-like peptide-1 receptor couples to multiple G proteins and activates mitogen-activated protein kinase pathways in Chinese hamster ovary cells. *Endocrinology* *140*, 1132-1140. 10.1210/endo.140.3.6550.
- Montrose-Rafizadeh, C., Avdonin, P., Garant, M.J., Rodgers, B.D., Kole, S., Yang, H., Levine, M.A., Schwindinger, W., and Bernier, M. (1999b). Pancreatic Glucagon-Like Peptide-1 Receptor Couples to Multiple G Proteins and Activates Mitogen-Activated Protein Kinase Pathways in Chinese Hamster Ovary Cells\*. *Endocrinology* *140*, 1132-1140. 10.1210/endo.140.3.6550.
- Moon, M.J., Park, S., Kim, D.K., Cho, E.B., Hwang, J.I., Vaudry, H., and Seong, J.Y. (2012). Structural and Molecular Conservation of Glucagon-Like Peptide-1 and Its Receptor Confers Selective Ligand-Receptor Interaction. *Front Endocrinol (Lausanne)* *3*. 10.3389/fendo.2012.00141.
- Moore, C.A., Milano, S.K., and Benovic, J.L. (2007). Regulation of receptor trafficking by GRKs and arrestins. *Annual review of physiology* *69*, 451-482. 10.1146/annurev.physiol.69.022405.154712.
- Moorthy, B.S., Gao, Y., and Anand, G.S. (2011). Phosphodiesterases catalyze hydrolysis of cAMP-bound to regulatory subunit of protein kinase A and mediate signal termination. *Mol Cell Proteomics* *10*, M110.002295. 10.1074/mcp.M110.002295.
- Moran, T.H., and Kinzig, K.P. (2004). Gastrointestinal satiety signals II. Cholecystokinin. *American journal of physiology. Gastrointestinal and liver physiology* *286*, G183-188. 10.1152/ajpgi.00434.2003.
- Muller, T.D., Clemmensen, C., Finan, B., DiMarchi, R.D., and Tschop, M.H. (2018). Anti-Obesity Therapy: from Rainbow Pills to Polyagonists. *Pharmacol Rev* *70*, 712-746. 10.1124/pr.117.014803.



- Müller, T.D., Finan, B., Clemmensen, C., DiMarchi, R.D., and Tschöp, M.H. (2017). The New Biology and Pharmacology of Glucagon. *Physiological reviews* 97, 721-766. 10.1152/physrev.00025.2016.
- Mullershausen, F., Zecri, F., Cetin, C., Billich, A., Guerini, D., and Seuwen, K. (2009). Persistent signaling induced by FTY720-phosphate is mediated by internalized S1P1 receptors. *Nat Chem Biol* 5, 428-434. 10.1038/nchembio.173.
- Muscelli, E., Mari, A., Casolaro, A., Camastra, S., Seghieri, G., Gastaldelli, A., Holst, J.J., and Ferrannini, E. (2008). Separate impact of obesity and glucose tolerance on the incretin effect in normal subjects and type 2 diabetic patients. *Diabetes* 57, 1340-1348. 10.2337/db07-1315.
- Myers, M.G., and Leibel, R.L. (2015). Lessons From Rodent Models of Obesity. <https://www.ncbi.nlm.nih.gov/books/NBK279123/>.
- Nakashima, K., Kaneto, H., Shimoda, M., Kimura, T., and Kaku, K. (2018). Pancreatic alpha cells in diabetic rats express active GLP-1 receptor: Endosomal co-localization of GLP-1/GLP-1R complex functioning through intra-islet paracrine mechanism. *Scientific reports* 8, 3725. 10.1038/s41598-018-21751-w.
- NamKoong, C., Kim, M.S., Jang, B.T., Lee, Y.H., Cho, Y.M., and Choi, H.J. (2017). Central administration of GLP-1 and GIP decreases feeding in mice. *Biochemical and biophysical research communications* 490, 247-252. 10.1016/j.bbrc.2017.06.031.
- Nauck, M., Stöckmann, F., Ebert, R., and Creutzfeldt, W. (1986). Reduced incretin effect in type 2 (non-insulin-dependent) diabetes. *Diabetologia* 29, 46-52. 10.1007/bf02427280.
- Nauck, M.A., Bartels, E., Orskov, C., Ebert, R., and Creutzfeldt, W. (1993a). Additive insulinotropic effects of exogenous synthetic human gastric inhibitory polypeptide and glucagon-like peptide-1-(7-36) amide infused at near-physiological insulinotropic hormone and glucose concentrations. *J Clin Endocrinol Metab* 76, 912-917. 10.1210/jcem.76.4.8473405.
- Nauck, M.A., Heimesaat, M.M., Orskov, C., Holst, J.J., Ebert, R., and Creutzfeldt, W. (1993b). Preserved incretin activity of glucagon-like peptide 1 [7-36 amide] but not of synthetic human gastric inhibitory polypeptide in patients with type-2 diabetes mellitus. *The Journal of clinical investigation* 91. 10.1172/JCI116186.
- Nauck, M.A., Heimesaat, M.M., Orskov, C., Holst, J.J., Ebert, R., and Creutzfeldt, W. (1993c). Preserved incretin activity of glucagon-like peptide 1 [7-36 amide] but not of synthetic human gastric inhibitory polypeptide in patients with type-2 diabetes mellitus. *J Clin Invest* 91, 301-307. 10.1172/jci116186.
- Nauck, M.A., and Meier, J.J. (2016). The incretin effect in healthy individuals and those with type 2 diabetes: physiology, pathophysiology, and response to therapeutic interventions. *The lancet. Diabetes & endocrinology* 4, 525-536. 10.1016/s2213-8587(15)00482-9.
- Neary, N.M., Small, C.J., Druce, M.R., Park, A.J., Ellis, S.M., Semjonous, N.M., Dakin, C.L., Filipsson, K., Wang, F., Kent, A.S., et al. (2005). Peptide YY3-36 and glucagon-like peptide-17-36 inhibit food intake additively. *Endocrinology* 146, 5120-5127. 10.1210/en.2005-0237.
- Nelson, J. (2009). *Structure and function in cell signalling* (Wiley).
- Nicholls, D.G., and Locke, R.M. (1984). Thermogenic mechanisms in brown fat. *Physiological reviews* 64, 1-64. 10.1152/physrev.1984.64.1.1.
- Nielsen, M.D., Chan, G.C., Poser, S.W., and Storm, D.R. (1996). Differential regulation of type I and type VIII Ca<sup>2+</sup>-stimulated adenylyl cyclases by Gi-coupled receptors in vivo. *J Biol Chem* 271, 33308-33316. 10.1074/jbc.271.52.33308.
- Novikoff, A., O'Brien, S.L., Bernecker, M., Grandl, G., Kleinert, M., Knerr, P.J., Stemmer, K., Klingenspor, M., Zeigerer, A., DiMarchi, R., et al. (2021). Spatiotemporal GLP-1 and GIP

- receptor signaling and trafficking/recycling dynamics induced by selected receptor mono- and dual-agonists. *Mol Metab* 49, 101181. 10.1016/j.molmet.2021.101181.
- Nyberg, J., Anderson, M.F., Meister, B., Alborn, A.M., Ström, A.K., Brederlau, A., Illerskog, A.C., Nilsson, O., Kieffer, T.J., Hietala, M.A., et al. (2005). Glucose-dependent insulinotropic polypeptide is expressed in adult hippocampus and induces progenitor cell proliferation. *J Neurosci* 25, 1816-1825. 10.1523/jneurosci.4920-04.2005.
- Oakley, R.H., Laporte, S.A., Holt, J.A., Caron, M.G., and Barak, L.S. (2000). Differential affinities of visual arrestin, beta arrestin1, and beta arrestin2 for G protein-coupled receptors delineate two major classes of receptors. *J Biol Chem* 275, 17201-17210. 10.1074/jbc.M910348199.
- Oduori, O.S., Murao, N., Shimomura, K., Takahashi, H., Zhang, Q., Dou, H., Sakai, S., Minami, K., Chanclon, B., Guida, C., et al. (2020). Gs/Gq signaling switch in  $\beta$  cells defines incretin effectiveness in diabetes. *J Clin Invest* 130, 6639-6655. 10.1172/jci140046.
- Oh, P., and Schnitzer, J.E. (2001). Segregation of heterotrimeric G proteins in cell surface microdomains. G(q) binds caveolin to concentrate in caveolae, whereas G(i) and G(s) target lipid rafts by default. *Molecular biology of the cell* 12, 685-698. 10.1091/mbc.12.3.685.
- Ohtake, N., Saito, M., Eto, M., and Seki, K. (2014). Exendin-4 promotes the membrane trafficking of the AMPA receptor GluR1 subunit and ADAM10 in the mouse neocortex. *Regulatory peptides* 190-191, 1-11. 10.1016/j.regpep.2014.04.003.
- Okamoto, Y., Ninomiya, H., Miwa, S., and Masaki, T. (2000). Cholesterol oxidation switches the internalization pathway of endothelin receptor type A from caveolae to clathrin-coated pits in Chinese hamster ovary cells. *J Biol Chem* 275, 6439-6446. 10.1074/jbc.275.9.6439.
- Oldham, W.M., and Hamm, H.E. (2008). Heterotrimeric G protein activation by G-protein-coupled receptors. *Nat Rev Mol Cell Biol* 9, 60-71. 10.1038/nrm2299.
- Orskov, C., Rabenhøj, L., Wettergren, A., Kofod, H., and Holst, J.J. (1994). Tissue and plasma concentrations of amidated and glycine-extended glucagon-like peptide I in humans. *Diabetes* 43, 535-539. 10.2337/diab.43.4.535.
- Ouchi, N., Parker, J.L., Lugus, J.J., and Walsh, K. (2011). Adipokines in inflammation and metabolic disease. *Nature reviews. Immunology* 11. 10.1038/nri2921.
- Owen, D.J., and Evans, P.R. (1998). A structural explanation for the recognition of tyrosine-based endocytotic signals. *Science* 282, 1327-1332. 10.1126/science.282.5392.1327.
- Owens, D.R., Monnier, L., and Bolli, G.B. (2013). Differential effects of GLP-1 receptor agonists on components of dysglycaemia in individuals with type 2 diabetes mellitus. *Diabetes & metabolism* 39, 485-496. 10.1016/j.diabet.2013.09.004.
- Pan, D.A., Lillioja, S., Kriketos, A.D., Milner, M.R., Baur, L.A., Bogardus, C., Jenkins, A.B., and Storlien, L.H. (1997). Skeletal muscle triglyceride levels are inversely related to insulin action. *Diabetes* 46. 10.2337/diab.46.6.983.
- Parker, J.A., McCullough, K.A., Field, B.C., Minnion, J.S., Martin, N.M., Ghatei, M.A., and Bloom, S.R. (2013). Glucagon and GLP-1 inhibit food intake and increase c-fos expression in similar appetite regulating centres in the brainstem and amygdala. *Int J Obes (Lond)* 37, 1391-1398. 10.1038/ijo.2012.227.
- Patterson, J.T., Ottaway, N., Gelfanov, V.M., Smiley, D.L., Perez-Tilve, D., Pfluger, P.T., Tschöp, M.H., and Dimarchi, R.D. (2011). A novel human-based receptor antagonist of sustained action reveals body weight control by endogenous GLP-1. *ACS Chem Biol* 6, 135-145. 10.1021/cb1002015.
- Peng, G.E., Pessino, V., Huang, B., and von Zastrow, M. (2021). Spatial decoding of endosomal cAMP signals by a metastable cytoplasmic PKA network. *Nat Chem Biol* 17, 558-566. 10.1038/s41589-021-00747-0.

- Perley, M.J., and Kipnis, D.M. (1967). Plasma insulin responses to oral and intravenous glucose: studies in normal and diabetic subjects. *J Clin Invest* 46, 1954-1962. 10.1172/jci105685.
- Pickford, P., Lucey, M., Rujan, R.-M., McGlone, E.R., Bitsi, S., Ashford, F.B., Corrêa, I.R., Hodson, D.J., Tomas, A., Deganutti, G., et al. (2021). Partial agonism improves the anti-hyperglycaemic efficacy of an oxyntomodulin-derived GLP-1R/GCGR co-agonist. *Molecular Metabolism* 51, 101242. <https://doi.org/10.1016/j.molmet.2021.101242>.
- Pierce, K.L., and Lefkowitz, R.J. (2001). Classical and new roles of beta-arrestins in the regulation of G-protein-coupled receptors. *Nature reviews. Neuroscience* 2, 727-733. 10.1038/35094577.
- Porrello, E.R., Pflieger, K.D., Seeber, R.M., Qian, H., Oro, C., Abogadie, F., Delbridge, L.M., and Thomas, W.G. (2011). Heteromerization of angiotensin receptors changes trafficking and arrestin recruitment profiles. *Cellular signalling* 23. 10.1016/j.cellsig.2011.06.011.
- Prasad-Reddy, L., and Isaacs, D. (2015). A clinical review of GLP-1 receptor agonists: efficacy and safety in diabetes and beyond. *Drugs Context* 4, 212283. 10.7573/dic.212283.
- Pratley, R.E., Aroda, V.R., Lingvay, I., Lüdemann, J., Andreassen, C., Navarria, A., and Viljoen, A. (2018). Semaglutide versus dulaglutide once weekly in patients with type 2 diabetes (SUSTAIN 7): a randomised, open-label, phase 3b trial. *The lancet. Diabetes & endocrinology* 6, 275-286. 10.1016/s2213-8587(18)30024-x.
- Quoyer, J., Longuet, C., Broca, C., Linck, N., Costes, S., Varin, E., Bockaert, J., Bertrand, G., and Dalle, S. (2010). GLP-1 mediates antiapoptotic effect by phosphorylating Bad through a beta-arrestin 1-mediated ERK1/2 activation in pancreatic beta-cells. *J Biol Chem* 285, 1989-2002. 10.1074/jbc.M109.067207.
- Rahmouni, K., Haynes, W.G., Morgan, D.A., and Mark, A.L. (2003). Role of melanocortin-4 receptors in mediating renal sympathoactivation to leptin and insulin. *The Journal of neuroscience : the official journal of the Society for Neuroscience* 23, 5998-6004. 10.1523/jneurosci.23-14-05998.2003.
- Rajagopal, S., and Shenoy, S.K. (2018). GPCR desensitization: Acute and prolonged phases. *Cell Signal* 41, 9-16. 10.1016/j.cellsig.2017.01.024.
- Rajan, S., Dickson, L.M., Mathew, E., Orr, C.M., Ellenbroek, J.H., Philipson, L.H., and Wicksteed, B. (2015). Chronic hyperglycemia downregulates GLP-1 receptor signaling in pancreatic  $\beta$ -cells via protein kinase A. *Mol Metab* 4, 265-276. 10.1016/j.molmet.2015.01.010.
- Rask-Madsen, C., and King, G.L. (2013). Vascular complications of diabetes: mechanisms of injury and protective factors. *Cell Metab* 17, 20-33. 10.1016/j.cmet.2012.11.012.
- Reimann, F., and Gribble, F.M. (2002). Glucose-sensing in glucagon-like peptide-1-secreting cells. *Diabetes* 51, 2757-2763. 10.2337/diabetes.51.9.2757.
- Roed, S.N., Nøhr, A.C., Wismann, P., Iversen, H., Bräuner-Osborne, H., Knudsen, S.M., and Waldhoer, M. (2015). Functional consequences of glucagon-like peptide-1 receptor cross-talk and trafficking. *J Biol Chem* 290, 1233-1243. 10.1074/jbc.M114.592436.
- Roger, B., Papin, J., Vacher, P., Raoux, M., Mulot, A., Dubois, M., Kerr-Conte, J., Voy, B.H., Pattou, F., Charpentier, G., et al. (2011). Adenylyl cyclase 8 is central to glucagon-like peptide 1 signalling and effects of chronically elevated glucose in rat and human pancreatic beta cells. *Diabetologia* 54, 390-402. 10.1007/s00125-010-1955-x.
- Rosciglione, S., Thériault, C., Boily, M.O., Paquette, M., and Lavoie, C. (2014). Gas regulates the post-endocytic sorting of G protein-coupled receptors. *Nat Commun* 5, 4556. 10.1038/ncomms5556.

- Rosenstock, J., Wysham, C., Frías, J.P., Kaneko, S., Lee, C.J., Fernández Landó, L., Mao, H., Cui, X., Karanikas, C.A., and Thieu, V.T. (2021). Efficacy and safety of a novel dual GIP and GLP-1 receptor agonist tirzepatide in patients with type 2 diabetes (SURPASS-1): a double-blind, randomised, phase 3 trial. *Lancet* *398*, 143-155. 10.1016/s0140-6736(21)01324-6.
- Ross, E.M. (2008). Coordinating speed and amplitude in G-protein signaling. *Current biology* : *CB* *18*, R777-r783. 10.1016/j.cub.2008.07.035.
- Ross, E.M. (2014). G Protein-coupled receptors: Multi-turnover GDP/GTP exchange catalysis on heterotrimeric G proteins. *Cellular logistics* *4*, e29391. 10.4161/cl.29391.
- Runge, S., Wulff, B.S., Madsen, K., Bräuner-Osborne, H., and Knudsen, L.B. (2003). Different domains of the glucagon and glucagon-like peptide-1 receptors provide the critical determinants of ligand selectivity. *Br J Pharmacol* *138*, 787-794. 10.1038/sj.bjp.0705120.
- Rupprecht, L.E., Mietlicki-Baase, E.G., Zimmer, D.J., McGrath, L.E., Olivos, D.R., and Hayes, M.R. (2013). Hindbrain GLP-1 receptor-mediated suppression of food intake requires a PI3K-dependent decrease in phosphorylation of membrane-bound Akt. *Am J Physiol Endocrinol Metab* *305*, E751-759. 10.1152/ajpendo.00367.2013.
- Sadana, R., and Dessauer, C.W. (2009). Physiological roles for G protein-regulated adenylyl cyclase isoforms: insights from knockout and overexpression studies. *Neurosignals* *17*, 5-22. 10.1159/000166277.
- Salahpour, A., Espinoza, S., Masri, B., Lam, V., Barak, L.S., and Gainetdinov, R.R. (2012). BRET biosensors to study GPCR biology, pharmacology, and signal transduction. *Front Endocrinol (Lausanne)* *3*, 105. 10.3389/fendo.2012.00105.
- Salem, V., Izz-Engbeaya, C., Coello, C., Thomas, D.B., Chambers, E.S., Comninou, A.N., Buckley, A., Win, Z., Al-Nahas, A., Rabiner, E.A., et al. (2016). Glucagon increases energy expenditure independently of brown adipose tissue activation in humans. *Diabetes Obes Metab* *18*, 72-81. 10.1111/dom.12585.
- Salera, M., Giacomoni, P., Pironi, L., Cornia, G., Capelli, M., Marini, A., Benfenati, F., Miglioli, M., and Barbara, L. (1982). Gastric inhibitory polypeptide release after oral glucose: relationship to glucose intolerance, diabetes mellitus, and obesity. *J Clin Endocrinol Metab* *55*, 329-336. 10.1210/jcem-55-2-329.
- Samms, R.J., Sloop, K.W., Gribble, F.M., Reimann, F., and Adriaenssens, A.E. (2021). GIPR Function in the Central Nervous System: Implications and Novel Perspectives for GIP-Based Therapies in Treating Metabolic Disorders. *Diabetes*. 10.2337/dbi21-0002.
- Sánchez-Fernández, G., Cabezudo, S., García-Hoz, C., Benincá, C., Aragay, A.M., Mayor, F., Jr., and Ribas, C. (2014). Gαq signalling: the new and the old. *Cell Signal* *26*, 833-848. 10.1016/j.cellsig.2014.01.010.
- Saraste, J. (2016). Spatial and Functional Aspects of ER-Golgi Rabs and Tethers. *Frontiers in cell and developmental biology* *4*, 28. 10.3389/fcell.2016.00028.
- Schelshorn, D., Joly, F., Mutel, S., Hampe, C., Breton, B., Mutel, V., and Lütjens, R. (2012). Lateral allosterism in the glucagon receptor family: glucagon-like peptide 1 induces G-protein-coupled receptor heteromer formation. *Mol Pharmacol* *81*, 309-318. 10.1124/mol.111.074757.
- Secher, A., Jelsing, J., Baquero, A.F., Hecksher-Sørensen, J., Cowley, M.A., Dalbøge, L.S., Hansen, G., Grove, K.L., Pyke, C., Raun, K., et al. (2014). The arcuate nucleus mediates GLP-1 receptor agonist liraglutide-dependent weight loss. *J Clin Invest* *124*, 4473-4488. 10.1172/jci75276.
- Seed Ahmed, M., Kovoov, A., Nordman, S., Abu Seman, N., Gu, T., Efendic, S., Brismar, K., Östenson, C.G., and Gu, H.F. (2012). Increased expression of adenylyl cyclase 3 in pancreatic

- islets and central nervous system of diabetic Goto-Kakizaki rats: a possible regulatory role in glucose homeostasis. *Islets* 4, 343-348. 10.4161/isl.22283.
- Seino, S. (2012). Cell signalling in insulin secretion: the molecular targets of ATP, cAMP and sulfonylurea. *Diabetologia* 55, 2096-2108. 10.1007/s00125-012-2562-9.
- Seino, Y., Fukushima, M., and Yabe, D. (2010). GIP and GLP-1, the two incretin hormones: Similarities and differences. *Journal of diabetes investigation* 1, 8-23. 10.1111/j.2040-1124.2010.00022.x.
- Sharma, D.K., Choudhury, A., Singh, R.D., Wheatley, C.L., Marks, D.L., and Pagano, R.E. (2003). Glycosphingolipids internalized via caveolar-related endocytosis rapidly merge with the clathrin pathway in early endosomes and form microdomains for recycling. *J Biol Chem* 278, 7564-7572. 10.1074/jbc.M210457200.
- Sheff, D.R., Daro, E.A., Hull, M., and Mellman, I. (1999). The receptor recycling pathway contains two distinct populations of early endosomes with different sorting functions. *J Cell Biol* 145, 123-139. 10.1083/jcb.145.1.123.
- Simons, K., and Toomre, D. (2000). Lipid rafts and signal transduction. *Nat Rev Mol Cell Biol* 1, 31-39. 10.1038/35036052.
- Simonsen, L., Holst, J.J., Madsen, K., and Deacon, C.F. (2013). The C-terminal extension of exendin-4 provides additional metabolic stability when added to GLP-1, while there is minimal effect of truncating exendin-4 in anaesthetized pigs. *Regulatory peptides* 181, 17-21. 10.1016/j.regpep.2012.12.012.
- Smith, J.S., and Rajagopal, S. (2016). The  $\beta$ -Arrestins: Multifunctional Regulators of G Protein-coupled Receptors. *J Biol Chem* 291, 8969-8977. 10.1074/jbc.R115.713313.
- Smrcka, A.V. (2008). G protein  $\beta\gamma$  subunits: central mediators of G protein-coupled receptor signaling. *Cellular and molecular life sciences : CMLS* 65, 2191-2214. 10.1007/s00018-008-8006-5.
- Snel, M., Jonker, J.T., Schoones, J., Lamb, H., de Roos, A., Pijl, H., Smit, J.W., Meinders, A.E., and Jazet, I.M. (2012). Ectopic fat and insulin resistance: pathophysiology and effect of diet and lifestyle interventions. *International journal of endocrinology* 2012. 10.1155/2012/983814.
- Song, W.-J., Seshadri, M., Ashraf, U., Mdluli, T., Mondal, P., Keil, M., Azevedo, M., Kirschner, Lawrence S., Stratakis, Constantine A., and Hussain, Mehboob A. (2011). Snapin Mediates Incretin Action and Augments Glucose-Dependent Insulin Secretion. *Cell Metabolism* 13, 308-319. <https://doi.org/10.1016/j.cmet.2011.02.002>.
- Song, W.J., Mondal, P., Li, Y., Lee, S.E., and Hussain, M.A. (2013). Pancreatic  $\beta$ -cell response to increased metabolic demand and to pharmacologic secretagogues requires EPAC2A. *Diabetes* 62, 2796-2807. 10.2337/db12-1394.
- Sönnichsen, B., De Renzis, S., Nielsen, E., Rietdorf, J., and Zerial, M. (2000). Distinct membrane domains on endosomes in the recycling pathway visualized by multicolor imaging of Rab4, Rab5, and Rab11. *J Cell Biol* 149, 901-914. 10.1083/jcb.149.4.901.
- Sonoda, N., Imamura, T., Yoshizaki, T., Babendure, J.L., Lu, J.C., and Olefsky, J.M. (2008). Beta-Arrestin-1 mediates glucagon-like peptide-1 signaling to insulin secretion in cultured pancreatic beta cells. *Proc Natl Acad Sci U S A* 105, 6614-6619. 10.1073/pnas.0710402105.
- Sorkin, A., and von Zastrow, M. (2009). Endocytosis and signalling: intertwining molecular networks. *Nat Rev Mol Cell Biol* 10, 609-622. 10.1038/nrm2748.
- Sparre-Ulrich, A.H., Hansen, L.S., Svendsen, B., Christensen, M., Knop, F.K., Hartmann, B., Holst, J.J., and Rosenkilde, M.M. (2016). Species-specific action of (Pro3)GIP - a full agonist at human GIP receptors, but a partial agonist and competitive antagonist at rat and mouse GIP receptors. *Br J Pharmacol* 173, 27-38. 10.1111/bph.13323.

- Speliotes, E.K., Willer, C.J., Berndt, S.I., Monda, K.L., Thorleifsson, G., Jackson, A.U., Lango Allen, H., Lindgren, C.M., Luan, J., Mägi, R., et al. (2010). Association analyses of 249,796 individuals reveal 18 new loci associated with body mass index. *Nature genetics* *42*, 937-948. 10.1038/ng.686.
- Spillmann, M., Thurner, L., Romantini, N., Zimmermann, M., Meger, B., Behe, M., Waldhoer, M., Schertler, G.F.X., and Berger, P. (2020). New Insights into Arrestin Recruitment to GPCRs. *International journal of molecular sciences* *21*. 10.3390/ijms21144949.
- Sriram, K., and Insel, P.A. (2018). G Protein-Coupled Receptors as Targets for Approved Drugs: How Many Targets and How Many Drugs? *Mol Pharmacol* *93*, 251-258. 10.1124/mol.117.111062.
- Sungkaworn, T., Jobin, M.L., Burnecki, K., Weron, A., Lohse, M.J., and Calebiro, D. (2017). Single-molecule imaging reveals receptor-G protein interactions at cell surface hot spots. *Nature* *550*, 543-547. 10.1038/nature24264.
- Sutkeviciute, I., and Vilardaga, J.P. (2020). Structural insights into emergent signaling modes of G protein-coupled receptors. *J Biol Chem* *295*, 11626-11642. 10.1074/jbc.REV120.009348.
- Syme, C.A., Zhang, L., and Bisello, A. (2006). Caveolin-1 regulates cellular trafficking and function of the glucagon-like Peptide 1 receptor. *Mol Endocrinol* *20*, 3400-3411. 10.1210/me.2006-0178.
- Syrovatkina, V., Alegre, K.O., Dey, R., and Huang, X.Y. (2016). Regulation, Signaling, and Physiological Functions of G-Proteins. *J Mol Biol* *428*, 3850-3868. 10.1016/j.jmb.2016.08.002.
- Taghon, G.J., Rowe, J.B., Kapolka, N.J., and Isom, D.G. (2021). Predictable cholesterol binding sites in GPCRs lack consensus motifs. *Structure (London, England : 1993)* *29*, 499-506.e493. 10.1016/j.str.2021.01.004.
- Talchai, C., Xuan, S., Lin, H.V., Sussel, L., and Accili, D. (2012). Pancreatic  $\beta$  cell dedifferentiation as a mechanism of diabetic  $\beta$  cell failure. *Cell* *150*. 10.1016/j.cell.2012.07.029.
- Tan, T.M., Field, B.C., McCullough, K.A., Troke, R.C., Chambers, E.S., Salem, V., Gonzalez Maffe, J., Baynes, K.C., De Silva, A., Viardot, A., et al. (2013). Coadministration of glucagon-like peptide-1 during glucagon infusion in humans results in increased energy expenditure and amelioration of hyperglycemia. *Diabetes* *62*, 1131-1138. 10.2337/db12-0797.
- Tang-Christensen, M., Larsen, P.J., Göke, R., Fink-Jensen, A., Jessop, D.S., Møller, M., and Sheikh, S.P. (1996). Central administration of GLP-1-(7-36) amide inhibits food and water intake in rats. *Am J Physiol* *271*, R848-856. 10.1152/ajpregu.1996.271.4.R848.
- Taussig, R., Iñiguez-Lluhi, J.A., and Gilman, A.G. (1993). Inhibition of adenylyl cyclase by Gi alpha. *Science* *261*, 218-221. 10.1126/science.8327893.
- Tengholm, A. (2012). Cyclic AMP dynamics in the pancreatic  $\beta$ -cell. *Ups J Med Sci* *117*, 355-369. 10.3109/03009734.2012.724732.
- Thompson, A., and Kanamarlapudi, V. (2015). Agonist-induced internalisation of the glucagon-like peptide-1 receptor is mediated by the G $\alpha$ q pathway. *Biochem Pharmacol* *93*, 72-84. 10.1016/j.bcp.2014.10.015.
- Thomsen, A.R.B., Jensen, D.D., Hicks, G.A., and Bunnett, N.W. (2018). Therapeutic Targeting of Endosomal G-Protein-Coupled Receptors. *Trends in pharmacological sciences* *39*, 879-891. 10.1016/j.tips.2018.08.003.
- Thorens, B. (1992). Expression cloning of the pancreatic beta cell receptor for the gluco-incretin hormone glucagon-like peptide 1. *Proc Natl Acad Sci U S A* *89*, 8641-8645. 10.1073/pnas.89.18.8641.
- Tilg, H., and Moschen, A.R. (2008). Inflammatory mechanisms in the regulation of insulin resistance. *Molecular medicine (Cambridge, Mass.)* *14*, 222-231. 10.2119/2007-00119.Tilg.

- Tiulpakov, A., White, C.W., Abhayawardana, R.S., See, H.B., Chan, A.S., Seeber, R.M., Heng, J.I., Dedov, I., Pavlos, N.J., and Pflieger, K.D. (2016a). Mutations of Vasopressin Receptor 2 Including Novel L312S Have Differential Effects on Trafficking. *Mol Endocrinol* 30, 889-904. 10.1210/me.2016-1002.
- Tiulpakov, A., White, C.W., Abhayawardana, R.S., See, H.B., Chan, A.S., Seeber, R.M., Heng, J.I., Dedov, I., Pavlos, N.J., and Pflieger, K.D.G. (2016b). Mutations of Vasopressin Receptor 2 Including Novel L312S Have Differential Effects on Trafficking. *Mol Endocrinol* 30, 889-904. 10.1210/me.2016-1002.
- Todkar, K., Chikhi, L., and Germain, M. (2019). Mitochondrial interaction with the endosomal compartment in endocytosis and mitochondrial transfer. *Mitochondrion* 49, 284-288. 10.1016/j.mito.2019.05.003.
- Traub, L.M. (2009). Tickets to ride: selecting cargo for clathrin-regulated internalization. *Nat Rev Mol Cell Biol* 10, 583-596. 10.1038/nrm2751.
- Traub, L.M. (2011). Regarding the amazing choreography of clathrin coats. *PLoS Biol* 9, e1001037. 10.1371/journal.pbio.1001037.
- Trevaskis, J.L., Sun, C., Athanacio, J., D'Souza, L., Samant, M., Tatarkiewicz, K., Griffin, P.S., Wittmer, C., Wang, Y., Teng, C.H., et al. (2015). Synergistic metabolic benefits of an exenatide analogue and cholecystokinin in diet-induced obese and leptin-deficient rodents. *Diabetes Obes Metab* 17, 61-73. 10.1111/dom.12390.
- Trivedi, P.C., Bartlett, J.J., and Pulinilkunnil, T. (2020). Lysosomal Biology and Function: Modern View of Cellular Debris Bin. *Cells* 9. 10.3390/cells9051131.
- Trümper, A., Trümper, K., Trusheim, H., Arnold, R., Göke, B., and Hörsch, D. (2001). Glucose-dependent insulinotropic polypeptide is a growth factor for beta (INS-1) cells by pleiotropic signaling. *Mol Endocrinol* 15, 1559-1570. 10.1210/mend.15.9.0688.
- Tschöp, M., Smiley, D.L., and Heiman, M.L. (2000). Ghrelin induces adiposity in rodents. *Nature* 407, 908-913. 10.1038/35038090.
- Tschöp, M.H., Speakman, J.R., Arch, J.R., Auwerx, J., Brüning, J.C., Chan, L., Eckel, R.H., Farese, R.V., Jr., Galgani, J.E., Hambly, C., et al. (2011). A guide to analysis of mouse energy metabolism. *Nature methods* 9, 57-63. 10.1038/nmeth.1806.
- Tsvetanova, N.G., Trester-Zedlitz, M., Newton, B.W., Peng, G.E., Johnson, J.R., Jimenez-Morales, D., Kurland, A.P., Krogan, N.J., and von Zastrow, M. (2021). Endosomal cAMP production broadly impacts the cellular phosphoproteome. *J Biol Chem* 297, 100907. 10.1016/j.jbc.2021.100907.
- Tsvetanova, N.G., and von Zastrow, M. (2014). Spatial encoding of cyclic AMP signaling specificity by GPCR endocytosis. *Nat Chem Biol* 10, 1061-1065. 10.1038/nchembio.1665.
- Tu, Y., Zhao, L., Billadeau, D.D., and Jia, D. (2020). Endosome-to-TGN Trafficking: Organelle-Vesicle and Organelle-Organelle Interactions. *Frontiers in cell and developmental biology* 8, 163. 10.3389/fcell.2020.00163.
- Turton, M.D., O'Shea, D., Gunn, I., Beak, S.A., Edwards, C.M., Meeran, K., Choi, S.J., Taylor, G.M., Heath, M.M., Lambert, P.D., et al. (1996). A role for glucagon-like peptide-1 in the central regulation of feeding. *Nature* 379. 10.1038/379069a0.
- van Bloemendaal, L., Ten Kulve, J.S., la Fleur, S.E., Ijzerman, R.G., and Diamant, M. (2014). Effects of glucagon-like peptide 1 on appetite and body weight: focus on the CNS. *The Journal of endocrinology* 221, T1-16. 10.1530/joe-13-0414.
- van Gastel, J., Hendrickx, J.O., Leysen, H., Santos-Otte, P., Luttrell, L.M., Martin, B., and Maudsley, S. (2018).  $\beta$ -Arrestin Based Receptor Signaling Paradigms: Potential Therapeutic Targets for Complex Age-Related Disorders. *Frontiers in pharmacology* 9, 1369. 10.3389/fphar.2018.01369.

- van Keulen, S.C., and Rothlisberger, U. (2017). Exploring the inhibition mechanism of adenylyl cyclase type 5 by n-terminal myristoylated Gai1. *PLoS Comput Biol* *13*, e1005673. 10.1371/journal.pcbi.1005673.
- Vauquelin, G., and Mentzer, B.V. (2008). G Protein-coupled Receptors Molecular Pharmacology.
- Wacker, D., Stevens, R.C., and Roth, B.L. (2017). How Ligands Illuminate GPCR Molecular Pharmacology. *Cell* *170*, 414-427. 10.1016/j.cell.2017.07.009.
- Wan, Q., Okashah, N., Inoue, A., Nehmé, R., Carpenter, B., Tate, C.G., and Lambert, N.A. (2018). Mini G protein probes for active G protein-coupled receptors (GPCRs) in live cells. *J Biol Chem* *293*, 7466-7473. 10.1074/jbc.RA118.001975.
- Wang, Y., Montrose-Rafizadeh, C., Adams, L., Raygada, M., Nadiv, O., and Egan, J.M. (1996). GIP regulates glucose transporters, hexokinases, and glucose-induced insulin secretion in RIN 1046-38 cells. *Mol Cell Endocrinol* *116*, 81-87. 10.1016/0303-7207(95)03701-2.
- Ward, Z.J., Bleich, S.N., Cradock, A.L., Barrett, J.L., Giles, C.M., Flax, C., Long, M.W., and Gortmaker, S.L. (2019). Projected U.S. State-Level Prevalence of Adult Obesity and Severe Obesity. <https://doi.org/10.1056/NEJMsa1909301>. NJ201912193812509.
- Watts, M., Ha, J., Kimchi, O., and Sherman, A. (2016). Paracrine regulation of glucagon secretion: the  $\beta/\alpha/\delta$  model. *Am J Physiol Endocrinol Metab* *310*, E597-e611. 10.1152/ajpendo.00415.2015.
- Wayman, G.A., Impey, S., Wu, Z., Kinsvogel, W., Prichard, L., and Storm, D.R. (1994). Synergistic activation of the type I adenylyl cyclase by  $Ca^{2+}$  and Gs-coupled receptors in vivo. *J Biol Chem* *269*, 25400-25405.
- Wenzel, E.M., Schultz, S.W., Schink, K.O., Pedersen, N.M., Nähse, V., Carlson, A., Brech, A., Stenmark, H., and Raiborg, C. (2018). Concerted ESCRT and clathrin recruitment waves define the timing and morphology of intraluminal vesicle formation. *Nat Commun* *9*, 2932. 10.1038/s41467-018-05345-8.
- Weston, C., Poyner, D., Patel, V., Dowell, S., and Ladds, G. (2014). Investigating G protein signalling bias at the glucagon-like peptide-1 receptor in yeast. *Br J Pharmacol* *171*, 3651-3665. 10.1111/bph.12716.
- Wettergren, A., Pridal, L., Wøjdemann, M., and Holst, J.J. (1998). Amidated and non-amidated glucagon-like peptide-1 (GLP-1): non-pancreatic effects (cephalic phase acid secretion) and stability in plasma in humans. *Regulatory peptides* *77*, 83-87. 10.1016/s0167-0115(98)00044-5.
- Wettschureck, N., and Offermanns, S. (2005). Mammalian G proteins and their cell type specific functions. *Physiological reviews* *85*, 1159-1204. 10.1152/physrev.00003.2005.
- Wheeler, M.B., Lu, M., Dillon, J.S., Leng, X.H., Chen, C., and Boyd, A.E., 3rd (1993). Functional expression of the rat glucagon-like peptide-I receptor, evidence for coupling to both adenylyl cyclase and phospholipase-C. *Endocrinology* *133*, 57-62. 10.1210/endo.133.1.8391428.
- Whitaker, G.M., Lynn, F.C., McIntosh, C.H., and Accili, E.A. (2012). Regulation of GIP and GLP1 receptor cell surface expression by N-glycosylation and receptor heteromerization. *PLoS One* *7*, e32675. 10.1371/journal.pone.0032675.
- WHO | Obesity. (2020). <https://www.who.int/topics/obesity/en/>.
- Widmann, C., Dolci, W., and Thorens, B. (1997). Internalization and homologous desensitization of the GLP-1 receptor depend on phosphorylation of the receptor carboxyl tail at the same three sites. *Molecular endocrinology (Baltimore, Md.)* *11*. 10.1210/mend.11.8.9959.
- Willard, F.S., Douros, J.D., Gabe, M.B.N., Showalter, A.D., Wainscott, D.B., Suter, T.M., Capozzi, M.E., van der Velden, W.J.C., Stutsman, C., Cardona, G.R., et al. (2020). Tirzepatide



- is an imbalanced and biased dual GIP and GLP-1 receptor agonist. *JCI insight*. 10.1172/jci.insight.140532.
- Willoughby, D., and Cooper, D.M. (2008). Live-cell imaging of cAMP dynamics. *Nature methods* 5, 29-36. 10.1038/nmeth1135.
- Woodman, P.G. (2000). Biogenesis of the sorting endosome: the role of Rab5. *Traffic (Copenhagen, Denmark)* 1, 695-701. 10.1034/j.1600-0854.2000.010902.x.
- Wolf, P.J., and Linderman, J.J. (2003). Untangling ligand induced activation and desensitization of G-protein-coupled receptors. *Biophysical journal* 84, 3-13. 10.1016/s0006-3495(03)74828-0.
- Wootten, D., Reynolds, C.A., Smith, K.J., Mobarec, J.C., Koole, C., Savage, E.E., Pabreja, K., Simms, J., Sridhar, R., Furness, S.G.B., et al. (2016). The Extracellular Surface of the GLP-1 Receptor Is a Molecular Trigger for Biased Agonism. *Cell* 165, 1632-1643. 10.1016/j.cell.2016.05.023.
- Wright, S.C., Lukashova, V., Le Gouill, C., Kobayashi, H., Breton, B., Mailhot-Larouche, S., Blondel-Tepaz, É., Antunes Vieira, N., Costa-Neto, C., Héroux, M., et al. (2021). BRET-based effector membrane translocation assay monitors GPCR-promoted and endocytosis-mediated G(q) activation at early endosomes. *Proc Natl Acad Sci U S A* 118. 10.1073/pnas.2025846118.
- Wu, B., Wei, S., Petersen, N., Ali, Y., Wang, X., Bacaj, T., Rorsman, P., Hong, W., Südhof, T.C., and Han, W. (2015). Synaptotagmin-7 phosphorylation mediates GLP-1-dependent potentiation of insulin secretion from  $\beta$ -cells. *Proc Natl Acad Sci U S A* 112, 9996-10001. 10.1073/pnas.1513004112.
- Xiao, K., and Sun, J. (2018). Elucidating structural and molecular mechanisms of beta-arrestin-biased agonism at GPCRs via MS-based proteomics. *Cell Signal* 41, 56-64. 10.1016/j.cellsig.2017.09.013.
- Xu, G., Kaneto, H., Laybutt, D.R., Duvivier-Kali, V.F., Trivedi, N., Suzuma, K., King, G.L., Weir, G.C., and Bonner-Weir, S. (2007). Downregulation of GLP-1 and GIP receptor expression by hyperglycemia: possible contribution to impaired incretin effects in diabetes. *Diabetes* 56, 1551-1558. 10.2337/db06-1033.
- Xu, W., Wang, X., Tocker, A.M., Huang, P., Reith, M.E., Liu-Chen, L.Y., Smith, A.B., 3rd, and Kortagere, S. (2017). Functional Characterization of a Novel Series of Biased Signaling Dopamine D3 Receptor Agonists. *ACS Chem Neurosci* 8, 486-500. 10.1021/acchemneuro.6b00221.
- Xu, Y., and Xie, X. (2009). Glucagon receptor mediates calcium signaling by coupling to G alpha q/11 and G alpha i/o in HEK293 cells. *J Recept Signal Transduct Res* 29, 318-325. 10.3109/10799890903295150.
- Yang, D., de Graaf, C., Yang, L., Song, G., Dai, A., Cai, X., Feng, Y., Reedtz-Runge, S., Hanson, M.A., Yang, H., et al. (2016). Structural Determinants of Binding the Seven-transmembrane Domain of the Glucagon-like Peptide-1 Receptor (GLP-1R). *J Biol Chem* 291, 12991-13004. 10.1074/jbc.M116.721977.
- Yang, Y., Choi, P.P., Smith, W.W., Xu, W., Ma, D., Corder, Z.A., Liang, N.C., and Moran, T.H. (2017). Exendin-4 reduces food intake via the PI3K/AKT signaling pathway in the hypothalamus. *Scientific reports* 7, 6936. 10.1038/s41598-017-06951-0.
- Yaqub, T., Tikhonova, I.G., Lättig, J., Magnan, R., Laval, M., Escrieut, C., Boulègue, C., Hewage, C., and Fourmy, D. (2010). Identification of determinants of glucose-dependent insulinotropic polypeptide receptor that interact with N-terminal biologically active region of the natural ligand. *Mol Pharmacol* 77, 547-558. 10.1124/mol.109.060111.
- Yarwood, R.E., Imlach, W.L., Lieu, T., Veldhuis, N.A., Jensen, D.D., Klein Herenbrink, C., Aurelio, L., Cai, Z., Christie, M.J., Poole, D.P., et al. (2017). Endosomal signaling of the

- receptor for calcitonin gene-related peptide mediates pain transmission. *Proc Natl Acad Sci U S A* *114*, 12309-12314. 10.1073/pnas.1706656114.
- Yen, H.Y., Hoi, K.K., Liko, I., Hedger, G., Horrell, M.R., Song, W., Wu, D., Heine, P., Warne, T., Lee, Y., et al. (2018). PtdIns(4,5)P(2) stabilizes active states of GPCRs and enhances selectivity of G-protein coupling. *Nature* *559*, 423-427. 10.1038/s41586-018-0325-6.
- Yip, R.G., Boylan, M.O., Kieffer, T.J., and Wolfe, M.M. (1998). Functional GIP receptors are present on adipocytes. *Endocrinology* *139*, 4004-4007. 10.1210/endo.139.9.6288.
- Yip, R.G., and Wolfe, M.M. (2000). GIP biology and fat metabolism. *Life sciences* *66*, 91-103. 10.1016/s0024-3205(99)00314-8.
- Yuliantie, E., Darbalaei, S., Dai, A., Zhao, P., Yang, D., Sexton, P.M., Wang, M.W., and Wootten, D. (2020). Pharmacological characterization of mono-, dual- and tri-peptidic agonists at GIP and GLP-1 receptors. *Biochemical pharmacology* *177*. 10.1016/j.bcp.2020.114001.
- Yusta, B., Baggio, L.L., Estall, J.L., Koehler, J.A., Holland, D.P., Li, H., Pipeleers, D., Ling, Z., and Drucker, D.J. (2006). GLP-1 receptor activation improves beta cell function and survival following induction of endoplasmic reticulum stress. *Cell Metab* *4*, 391-406. 10.1016/j.cmet.2006.10.001.
- Zalyapin, E.A., Bouley, R., Hasler, U., Vilardaga, J.P., Lin, H.Y., Brown, D., and Ausiello, D.A. (2008). Effects of the renal medullary pH and ionic environment on vasopressin binding and signaling. *Kidney international* *74*, 1557-1567. 10.1038/ki.2008.412.
- Zamboni, M., Rossi, A., Fantin, F., Zamboni, G., Chirumbolo, S., Zoico, E., and Mazzali, G. (2014). Adipose tissue, diet and aging. *Mechanisms of ageing and development* *136-137*. 10.1016/j.mad.2013.11.008.
- Zerial, M., and McBride, H. (2001). Rab proteins as membrane organizers. *Nat Rev Mol Cell Biol* *2*, 107-117. 10.1038/35052055.
- Zhang, J.F., Liu, B., Hong, I., Mo, A., Roth, R.H., Tenner, B., Lin, W., Zhang, J.Z., Molina, R.S., Drobizhev, M., et al. (2021a). An ultrasensitive biosensor for high-resolution kinase activity imaging in awake mice. *Nat Chem Biol* *17*, 39-46. 10.1038/s41589-020-00660-y.
- Zhang, M., Hu, T., Zhang, S., and Zhou, L. (2015). Associations of Different Adipose Tissue Depots with Insulin Resistance: A Systematic Review and Meta-analysis of Observational Studies. *Scientific reports* *5*, 18495. 10.1038/srep18495.
- Zhang, Q., Delessa, C.T., Augustin, R., Bakhti, M., Colldén, G., Drucker, D.J., Feuchtinger, A., Caceres, C.G., Grandl, G., Harger, A., et al. (2021b). The glucose-dependent insulinotropic polypeptide (GIP) regulates body weight and food intake via CNS-GIPR signaling. *Cell Metab* *33*, 833-844.e835. 10.1016/j.cmet.2021.01.015.
- Zhang, Y., Parajuli, K.R., Fava, G.E., Gupta, R., Xu, W., Nguyen, L.U., Zakaria, A.F., Fonseca, V.A., Wang, H., Mauvais-Jarvis, F., et al. (2019). GLP-1 Receptor in Pancreatic  $\alpha$ -Cells Regulates Glucagon Secretion in a Glucose-Dependent Bidirectional Manner. *Diabetes* *68*, 34-44. 10.2337/db18-0317.
- Zhao, L.H., Ma, S., Sutkeviciute, I., Shen, D.D., Zhou, X.E., de Waal, P.W., Li, C.Y., Kang, Y., Clark, L.J., Jean-Alphonse, F.G., et al. (2019). Structure and dynamics of the active human parathyroid hormone receptor-1. *Science* *364*, 148-153. 10.1126/science.aav7942.

# Letter of Approval – Molecular Metabolism, Volume 49, July 2021, 101181

**Permissions Helpdesk** Inbox - Google 30. August 2021 at 08:40 PH

Re: Re-using figures published in Molecular Metabolism for thesis [210827-005809]  
 To: anovikoff1@gmail.com,  
 Reply-To: Permissions Helpdesk

---

Dear Aaron Novikoff,

We hereby grant you permission to reprint the material below at no charge in your thesis subject to the following conditions:

1. If any part of the material to be used (for example, figures) has appeared in our publication with credit or acknowledgement to another source, permission must also be sought from that source. If such permission is not obtained then that material may not be included in your publication/copies.
2. Suitable acknowledgment to the source must be made, either as a footnote or in a reference list at the end of your publication, as follows: "This article was published in Publication title, Vol number, Author(s), Title of article, Page Nos, Copyright Elsevier (or appropriate Society name) (Year)."
3. Your thesis may be submitted to your institution in either print or electronic form.
4. Reproduction of this material is confined to the purpose for which permission is hereby given
5. This permission is granted for non-exclusive world English rights only. For other languages please reapply separately for each one required. Permission excludes use in an electronic form other than submission. Should you have a specific electronic project in mind please reapply for permission.
6. Should your thesis be published commercially, please reapply for permission.

This includes permission for the Library and Archives of Canada to supply single copies, on demand, of the complete thesis. Should your thesis be published commercially, please reapply for permission- Canada  
 This includes permission for UMI to supply single copies, on demand, of the complete thesis. Should your thesis be published commercially, please reapply for permission-ROW

7. Posting of the full article online is not permitted. You may post an abstract with a link to the Elsevier website [www.elsevier.com](http://www.elsevier.com), or to the article on ScienceDirect if it is available on that platform.
8. Article can used be in the University library if it is embedded in the thesis and not used commercially.

Kind regards,

**Anita Mercy Vethakkan**  
 Senior Copyrights Coordinator  
 ELSEVIER | HCM - Health Content Management

---

**From:** Aaron Novikoff  
**Date:** Thursday, August 26, 2021 09:01 PM GMT

Hello, is it possible to re-use the images within my published paper for inclusion into my PhD thesis? I have an open-access paper published in Molecular Metabolism, and I have read the "author rights" table, and it states that I can " Re-use portions, excerpts, and their own figures or tables in other works." I believe this unequivocally translates to that I can indeed use the figures I created within the publication for my own PhD thesis. But I am hoping to get an official confirmation. Is this possible?

---

This email is for use by the intended recipient and contains information that may be confidential. If you are not the intended recipient, please notify the sender by return email and delete this email from your inbox. Any unauthorized use or distribution of this email, in whole or in part, is strictly prohibited and may be unlawful. Any price quotes contained in this email are merely indicative and will not result in any legally binding or enforceable obligation. Unless explicitly designated as an intended e-contract, this email does not constitute a contract offer, a contract amendment, or an acceptance of a contract offer.

Elsevier Limited. Registered Office: The Boulevard, Langford Lane, Kidlington, Oxford, OX5 1GB, United Kingdom, Registration No. 1982084, Registered in England and Wales. [Privacy Policy](#)

## List of Publications

### *Submitted or Published*

Douros J.\*,...**Novikoff A.**, et al. (2022) The incretin co-agonist tirzepatide requires the GIPR for hormone secretion from human islets. *Nature Metabolism*. (Submitted, in review)

Grandl G.\*, Colldén G.\*, **Novikoff A.**, et al (2022) Global, neuronal, and beta-cell specific deletion of insulin inhibitors receptor (inceptor) improves glucose homeostasis in diet-induced obese mice. *Nature Metabolism*. (Submitted, in revision)

Sekar R.\*, Motzler K.\*, Kwon Y., **Novikoff A.**, et al (2022). Vps37a regulates hepatic glucose production by controlling glucagon receptor localization to endosomes. *Cell Metabolism*, 34.

Quarta C.\*, Stemmer K.\*, **Novikoff A.\***, et al (2022). GLP-1-mediated delivery of Tesaglitazar improves obesity and glucose metabolism in male mice. *Nature Metabolism*, 4.

**Novikoff A.\***, et al (2021). Spatiotemporal GLP-1 and GIP receptor signaling and trafficking/recycling dynamics induced by selected receptor mono- and dual-agonists. *Molecular Metabolism*, 49.

Sekar R.\*, et al (2021). Vps37a Regulates Hepatic Glucose Production by Controlling Glucagon Receptor Localization to Endosomes. *Nature Metabolism*. (Submitted, In Review)

Jall S.\*, et al (2020) Pharmacological targeting of  $\alpha 3\beta 4$  nicotinic receptors improves peripheral insulin sensitivity in mice with diet-induced obesity. *Diabetologia*, 63.

Grandl G.\*, Novikoff A., et al (2020). Gut Peptide Agonism in the Treatment of Obesity and Diabetes. *Comprehensive Physiology*, 10.

### *In Preparation*

Akindehin S., ... Novikoff A.\*\*\*, Müller T.\*\* (2022). The involvement of Liraglutide and Semaglutide acylation status in modulating GLP-1R intracellular signaling and trafficking. (Manuscript in preparation)

Coupland C., ... Novikoff A.\*\*\*, Müller T.\*\* (2022). Intracellular signaling, trafficking, and estradiol liberation dynamics of the GLP-1/E2 nuclear hormone conjugate. (Manuscript in preparation)

Novikoff A., et al (2022). BAT-specific BMP8b upregulation and subsequent vascularization mediates the energy expenditure enhancements of glucagon in DIO mice. (Manuscript in preparation)

Novikoff A., et al (2023). GLP-1R/GIPR/GcgR Triple KO mice are uniquely protected from diet-induced obesity. (Manuscript in preparation).

## Bibliometrics:

ORCID: 0000-0002-4838-001X

Peer Reviewed 1<sup>st</sup> author Articles: 2

Number of Citations: 36

## Presentations:

24.01.2019 – 26.01.2019

Third EASD Incretin Study Group Meeting | Bochum, Germany